University of Bath

PHD

Applications of iontophoresis in sports medicine

Sylvestre, Jean-Philippe

Award date:
2007

Awarding institution:
University of Bath

APPLICATIONS OF IONTOPHORESIS IN SPORTS MEDICINE

JEAN-PHILIPPE SYLVESTRE

A thesis submitted for the degree of Doctor of Philosophy

University of Bath
Department of Pharmacy and Pharmacology
November 2007

Table of contents

Acknowledgments

I would like to thank my supervisors Prof. Richard Guy and Dr. Begoña Delgado-Charro for their guidance and constant support throughout my doctoral studies.

I gratefully acknowledge Prof. Véronique Préat and Prof. Rex Tyrrell for accepting to evaluate this work.

I would like to thank Dr. Camille Bouissou for her active collaboration to the amino acids project, and Cristina Díaz-Marín for her contribution to the tape-stripping experiments of the dexamethasone project.

I thank all the volunteers for their participation in the experiments and their patience.

I also whish to thank my friends and colleagues, past and present, from the Skin & Nail group for their moral and technical support.

I acknowledge Universities UK, BIJAB, FQRNT and NSERC for financial support.

Finally, I thank my family for their moral support and my wife, Stéphanie, for her patience and encouragement at all times.

Abstract

In this thesis, two potential applications of transdermal iontophoresis in the field of sports medicine were studied: (1) the local delivery of dexamethasone phosphate (Dex-Phos), a corticosteroid used to treat musculoskeletal inflammation, and (2) the extraction of systemic amino acids (AAs), potential biological markers of fatigue in athletes.

The iontophoretic delivery of Dex-Phos was studied, *in vitro*, in order to evaluate the effects of competing ions and electroosmosis, and identify the optimal conditions for its delivery. The iontophoretic extraction of AAs from the skin was first studied *in vitro*, before evaluating the method in a group of human volunteers.

Dex-Phos was best delivered by iontophoresis from the cathode in absence of background electrolyte in the drug solution. In this situation, the delivery of Dex-Phos is limited principally by the competition with counter-ions (mainly Na^+) present subdermally and the small mobility of the drug inside the membrane. The accumulation of Cl^-, released by the Ag/AgCl cathode in the drug solution during current passage, can also reduce Dex-Phos delivery.

The extraction of zwitterionic AAs from the skin during iontophoresis was highly influenced by their presence in the outermost layer of the skin, the stratum corneum (SC). In the pig skin model, the amount of the AAs extracted during a short extraction period (1 hour) correlated with their abundance in the SC. Once this 'reservoir' was emptied (after ~3 hours of iontophoresis), the subdermal compartment could be sampled, suggesting that the method could be used to monitor systemic levels of AAs. The experiments in human volunteers revealed, however, that a 4-hour iontophoretic extraction period was insufficient to deplete the AAs SC 'reservoir'. It follows that the method can be used to evaluate the abundance of AAs in the SC, but is unpractical for the clinical monitoring of their systemic levels.

List of abbreviations

AA(s)	Amino acid(s)
Ala	Alanine
Asn	Asparagine
BCAAs	Branched-chain amino acids
Dex	Dexamethasone
Dex-Phos	Dexamethasone phosphate
Dex-H_2-Phos	Dexamethasone dihydrogen phosphate
Dex-Na_2-Phos	Dexamethasone disodium phosphate
Gly	Glycine
His	Histidine
HPLC	High performance liquid chromatography
IC	Ion chromatography
Ile	Isoleucine
IPAD	Integrated pulsed amperometric detection
Leu	Leucine
Met	Methionine
NSAIDs	Non-steroidal anti-inflammatory drugs
NMF	Natural moisturising factor
Phe	Phenylalanine
Pro	Proline
Ser	Serine
SC	Stratum corneum
TEWL	Transepidermal water loss
Thr	Threonine
Tyr	Tyrosine
Trp	Tryptophan
Val	Valine

Introduction

Sports medicine is the branch of medicine that oversees the medical care of the exercising individual. It is a wide-range discipline that includes: the prevention, diagnosis, treatment and rehabilitation of injury and illness; the enhancement of performance through training, nutrition and psychology; and ethical issues, such as the problem of drug abuse in sport [1]. This underlies the need for medical methods for both treatment and diagnosis of injury and illness. On one hand, methods to treat locally musculoskeletal injury-related pain and/or inflammation would certainly be welcomed by clinicians and athletes. On the other hand, non-invasive clinical monitoring tools could help, for example, either the athletes to maintain optimal physical fitness by following the level of biological markers of fatigue, or the sporting regulator agencies to detect the presence of prohibited substances in athletes.

Iontophoresis is a minimally-invasive technique that enhances the transport of charged and polar molecules across the skin by the application of a mild electrical current (resulting usually in a current density <0.5 mA/cm^2) [2]. The symmetrical nature of iontophoresis makes it useful for the delivery of therapeutic molecules in the body through the skin [3] or inversely (often called 'reverse iontophoresis' in that context), for the transdermal extraction of endogenous substances of clinical relevance [4].

Sports medicine could, therefore, strongly benefit from iontophoresis to both deliver drugs and monitor endogenous substances across the skin in a minimally-invasive manner. This research project concerns the development and optimization of iontophoresis in the field of sports medicine. Some examples of possible applications of iontophoresis in this field are summarized in Table 1. From these potential uses of iontophoresis in sports medicine, two are more specifically the subject of this thesis: (1) the optimization of local delivery of corticosteroids to inflamed joints using iontophoresis, and (2) the

evaluation of reverse iontophoresis as a clinical monitoring tool of biological markers of overtraining.

Table 1. Examples of possible applications of iontophoresis in the field of sports medicine.

Drug delivery	Clinical monitoring
Pain management - Reduce injury-related pain with local administration of: + NSAIDs[a] (piroxicam, diclofenac...) + Local anesthetics (lidocaine) - Reduce post-operative pain with systemic administration of: + Opioids (fentanyl, morphine…)	**Prevention of overtraining** - Monitor overtraining biological markers - Non-invasive method - Many potential markers: lactate, cortisol, testosterone, glutamine, tryptophan, branched-chain amino acids…
Treatment of soft tissue inflammation - Treatment of musculoskeletal injuries - Local administration limiting side-effects - Wide range of possible drugs: + Corticosteroids (cortisone, prednisolone, dexamethasone…) + NSAIDs[a] (ketoprofen, diclofenac...)	**Anti-doping control** - Control of prohibited substances - Systemic concentration and skin reservoir - Many potentially detectable doping agents: caffeine, ephedrine, anabolic steroids...

[a]NSAIDs stands for non-steroidal anti-inflammatory drugs

1. Iontophoresis of corticosteroids

Corticosteroids are commonly used for the treatment of musculoskeletal injuries [1, 5-9]. The rationale of its use is to reduce pain and inflammation sufficiently to allow the commencement of a strengthening program. Local administration of corticosteroids by injection maximizes the clinical effect of the drug at the site of injury and minimizes the systemic side effects associated with the administration via the oral route [1, 6-10]. While the delivery of corticosteroids by injection is generally considered safe, the use of a needle is the source of

disadvantages and risks of complications. Indeed, corticosteroid injections are commonly the cause of postinjection pain and flares. As any invasive method, there is also a risk of infection at the site of injection. Furthermore, the efficiency of the treatment relies on the accuracy of the needle placement and an experienced health-care professional is required to perform the injection [1, 6, 10].

Iontophoresis represents an alternative to the needle to deliver locally corticosteroids [11-13]. Amongst the corticosteroids available, dexamethasone phosphate (Dex-Phos, MW: 472.4), a phosphorylated prodrug of dexamethasone (Dex), has undoubtedly been the most studied corticosteroid for iontophoretic delivery [12]. Dex-Phos is a potent corticosteroid (equivalent potency 25-fold higher than hydrocortisone and ~6-fold higher than prednisolone), meaning that a smaller amount needs to be delivered to obtain a clinical effect [6]. Furthermore, Dex-Phos is available in the form of a disodium salt, dexamethasone sodium phosphate (MW 516.4) which is water soluble, and at physiological pH is essentially doubly negatively charged (pK_as: 1.9 and 6.4). Many clinical studies have been conducted to evaluate iontophoresis of Dex-Phos for the treatment of a variety of musculoskeletal problems [14-26]. A majority of these studies report at least subjective positive outcome [14-24]. However, improvement in the patient's condition is not always seen [25, 26]. Moreover, the design of some of these clinical studies is questionable, preventing the true causes of the clinical outcomes to be identified [11]. The limited evidence supporting the iontophoretic delivery of Dex-Phos for the management of inflammatory musculoskeletal conditions is possibly the principal reason that the method has not yet been generally adopted by clinicians to replace the injection of corticosteroids. From a drug delivery perspective, it can be observed that a variety of iontophoretic conditions are employed in these studies. Indeed, the formulation of the drug solution and even the polarity of the electrode chosen for delivery vary from one study to another. Clearly, the optimal conditions for Dex-Phos iontophoretic delivery have not been identified and this could, at least partially, explain the results obtained in clinical studies. While the assessment of the effectiveness of the

method will ultimately require additional, better-designed clinical studies, it seems logical to determine the optimal delivery conditions beforehand.

Hence, there is a need to find the optimal conditions for Dex-Phos iontophoresis that is addressed in this thesis. The goal is to better understand the effects of: (1) the ions present in the formulation and/or subdermally that are competing with Dex-Phos for the transport of current, and (2) the electroosmotic flow which normally occurs in the anode-to-cathode direction; that is against the electromigration of Dex-Phos delivered from the negative electrode (cathode).

2. Reverse iontophoresis of markers of overtraining

The other potential use of iontophoresis in sports medicine explored in this thesis is the monitoring of biological markers of overtraining. The overtraining syndrome can be defined as a state of prolonged fatigue and underperformance caused by the failure to recover from hard training and competition [1, 27]. It is most common in endurance athletes, touching, for example, as many as 10 to 20% of elite swimmers per year [27]. Unfortunately, there is no single test that can detect overtraining in the athlete, but rather a number of clinical and laboratory parameters, which in combination can be used for the prevention of overtraining [1].

Variations in the blood levels of some molecules have been linked to overtraining in athletes: lactate, cortisol, testosterone, glutamine, tryptophan and the branched-chain amino acids (BCAAs: isoleucine, leucine and valine) are examples of such overtraining biomarkers [1, 27-29]. Blood lactate increases exponentially as exercise intensity is increased. The lactate production during exercise is principally due to the anaerobic production of adenosine triphosphate (ATP), the chemical energy used in muscle, from glycogen [30]. In overtrained athletes, decreased blood lactate concentrations at maximal work rate have been observed [1, 31]. Cortisol and testosterone are hormones associated respectively with catabolic and anabolic activity. A decrease in the free blood testosterone to cortisol ratio is therefore an indication that the training load is too intensive to allow sufficient recovery (insufficient anabolic acitivity) and have been suggested as a marker of overtraining [1, 29].

Glutamine is the most abundant amino acid in plasma and is used as a substrate by the cells of the immune system. When the body is placed under a catabolic stress, like during illness or exercise, the glutamine stores may be depleted. Indeed, a decrease in plasma glutamine has been observed in overtrained athletes and is proposed as a marker of fatigue in athletes [1, 27, 29, 32].

Tryptophan and the BCAAs (isoleucine, leucine and valine) are other primary amino acids that are linked with overtraining. Indeed, it has been suggested that overtraining can result in chronically diminished levels of BCAAs and increased free tryptophan plasma levels. During prolonged exercise, BCAAs are metabolized in skeletal muscles to generate energy and their plasma levels decrease as a result. The increase in free tryptophan plasma levels during sustained exercise originates indirectly from an increase in blood levels of free fatty acids (FFAs), used as a source of energy by the muscles, as the glycogen stores are depleted. As both tryptophan and FFAs are competing for the same binding sites on the protein albumin, some of the albumin-bound tryptophan is therefore released. Serotonin is a neurotransmitter metabolized in the brain directly from tryptophan and an increase in its concentration in the brain is believed to result in central fatigue. Since the transport of tryptophan across the blood-barrier is in competition with the transport of large neutral amino acids (BCAAs, phenylalanine and tyrosine), an increase in the free tryptophan-BCAAs concentration ratio in blood facilitates the entry of tryptophan into the brain. The free tryptophan to BCAAs ratio is therefore proposed as a marker of overtraining (or central fatigue) in athletes [1, 29, 33, 34].

To be really efficient, these biomarkers should be monitored on a regular basis in individual athletes, before and after exercise, because variation in levels, rather than absolute levels, gives an indication of overtraining [1, 29]. This is where an iontophoretic device capable of extracting non-invasively (and eventually analysing *in situ*) a biological marker of overtraining could be very practical. Indeed, the frequent blood samples would be avoided. The use of this transdermal technique to monitor biological markers of overtraining represents a novel application at the stage of evaluation and development. To date, the only work related to the subject, to the best of our knowledge, is a preliminary study on the monitoring of lactate by reverse iontophoresis, where it was

demonstrated that reverse iontophoresis could be used to extract lactate *in vitro* and *in vivo* [35]. However, considerable more research is required to evaluate this technique as a tool for the monitoring of biological markers of overtraining.

In this thesis, the reverse iontophoresis of amino acids (AAs) in general is evaluated. As previously mentioned, glutamine, tryptophan and the BCAAs are all AAs that could be potential biological markers of overtraining. Central fatigue being present in other conditions than overtraining, a tool to monitor the free tryptophan to BCAAs ratio could find applications in other spheres of medicine. For example, it could be useful to follow patients after a surgery [36]. Furthermore, the similitude between many signs and symptoms of central fatigue observed in overtrained athletes and in patients suffering from clinical depression suggests that patients followed for depression could also benefit from the method to monitor their free tryptophan to BCAAs ratio [37, 38]. Since AAs fulfill a multitude of other functions essential to life [39], their clinical monitoring could find even more applications outside sports medicine. For example, hereditary metabolic diseases, such as phenylketonuria which concerns specifically the metabolism of phenylalanine, can result in mental retardation and early death if left untreated [39, 40]. Screening for these metabolic diseases in neonates currently requires a blood sample to be collected invasively, which could be avoided with a method like reverse iontophoresis [41, 42].

Moreover, iontophoresis being a transdermal method, the AAs present inside the skin are also expected to be extracted during current passage. It is well documented that AAs are essential for skin's health. Indeed, AAs and their derivatives are the main constituents of natural moisturizing factors (NMF), a mixture of highly hydroscopic molecules present in the stratum corneum (SC) to ensure that it retains an appropriate level of hydration [43-45]. Reduced levels of NMF in the SC are associated with diseased or abnormally dry and scaly skin [43, 46-48]. It follows that information from skin's condition could also be obtained by reverse iontophoresis of AAs. On the other hand, it is also essential to verify if this expected 'reservoir' of AAs in the skin compromises the possibility of using reverse iontophoresis to monitor their systemic levels.

This thesis aims at evaluating reverse iontophoresis for the clinical monitoring of AAs with *in vitro* and *in vivo* studies. The *in vitro* experiments are

necessary to verify that iontophoresis can extract detectable amounts of the AAs in a reasonable period of time and that the iontophoretic fluxes correlate with the subdermal concentration. The effect of the skin reservoir on the extraction fluxes can also be determined. Then, *in vivo* experiments are performed to confirm that the findings obtained in the *in vitro* study are applicable in human.

3. Organization of the thesis

In the first chapter, the literature on transdermal iontophoresis pertinent to the two applications studied here is reviewed.

Chapters 2 and 3 concern the *in vitro* experiments performed to optimize and better understand the delivery of Dex-Phos by iontophoresis.

In Chapters 4 and 5, the *in vitro* study evaluating reverse iontophoresis as a clinical monitoring tool of AAs is presented. First, in Chapter 4, the AAs 'reservoir' in the SC is quantified and the possibility to use reverse iontophoresis to sample it is explored. Then, the possibility to correlate the extraction fluxes of AAs with their concentration in the subdermal compartment is evaluated in Chapter 5. The effect of the SC 'reservoir' previously characterized on the AA extraction fluxes is also investigated.

Finally, reverse iontophoresis is evaluated for the extraction of AAs in human volunteers in Chapter 6. Again, the SC 'reservoir' in AAs is quantified in order to determine its effect on the iontophoretic extraction of endogenous AAs.

4. References

1. Brukner, P., Khan, K., *Clinical sports medicine*. 3dr ed. 2007, Sydney: McGraw-Hill. 1032.
2. Delgado-Charro, M.B., Guy, R.H., *Transdermal iontophoresis for controlled drug delivery and non-invasive monitoring.* S.T.P. Pharma Sciences, 2001. **11**(6): p. 403-414.
3. Kalia, Y.N., et al., *Iontophoretic drug delivery.* Adv Drug Deliv Rev, 2004. **56**(5): p. 619-58.

4. Leboulanger, B., R.H. Guy, and M.B. Delgado-Charro, *Reverse iontophoresis for non-invasive transdermal monitoring.* Physiol Meas, 2004. **25**(3): p. R35-50.
5. Harmon, K.G. and C. Hawley, *Physician prescribing patterns of oral corticosteroids for musculoskeletal injuries.* J Am Board Fam Pract, 2003. **16**(3): p. 209-12.
6. Ines, L.P. and J.A. da Silva, *Soft tissue injections.* Best Pract Res Clin Rheumatol, 2005. **19**(3): p. 503-27.
7. Bell, A.D. and D. Conaway, *Corticosteroid injections for painful shoulders.* Int J Clin Pract, 2005. **59**(10): p. 1178-86.
8. Schumacher, H.R. and L.X. Chen, *Injectable corticosteroids in treatment of arthritis of the knee.* Am J Med, 2005. **118**(11): p. 1208-14.
9. Goodyear-Smith, F. and B. Arroll, *What can family physicians offer patients with carpal tunnel syndrome other than surgery? A systematic review of nonsurgical management.* Ann Fam Med, 2004. **2**(3): p. 267-73.
10. Cole, B.J. and H.R. Schumacher, Jr., *Injectable corticosteroids in modern practice.* J Am Acad Orthop Surg, 2005. **13**(1): p. 37-46.
11. Hamann, H., M. Hodges, and B. Evans, *Effectiveness of iontophoresis of anti-inflammatory medications in the treatment of common musculoskeletal inflammatory conditions: a systematic review.* Physical Therapy Reviews, 2006. **11**: p. 190-194.
12. Banga, A.K. and P.C. Panus, *Clinical Applications of Iontophoretic Devices in Rehabilitation Medicine.* Critical Reviews in Physical and Rehabilitation Medicine, 1998. **10**(2): p. 147-179.
13. Petelenz, T.J., et al., *Iontophoresis of Dexamethasone - Laboratory Studies.* Journal of Controlled Release, 1992. **20**(1): p. 55-66.
14. Harris, P.R., *Iontophoresis: Clinical Research in Musculoskeletal Inflammatory Conditions.* The Journal of Orthopaedic and Sports Physical Therapy, 1982. **4**(2): p. 109-112.
15. Bertolucci, L.E., *Introduction of Antiinflammatory Drugs by Iontophoresis: Double Blind Study.* The Journal of Orthopaedic and Sports Physical Therapy, 1982. **4**(2): p. 103-108.

16. Pellecchia, G.L., H. Hamel, and P. Behnke, *Treatement of Infrapatellar Tendinitis: A Combination of Modalities and Transverse Friction Massage Versus Iontophoresis.* Journal of Sport Rehabilitation, 1994. **3**: p. 135-145.
17. Banta, C.A., *A Prospective, Nonrandomized Study of Iontophoresis, Wrist Splinting, and Antiinflammatory Medication in the Treatment of Early-Mild Carpal-Tunnel Syndrome.* Journal of Occupational and Environmental Medicine, 1994. **36**(2): p. 166-173.
18. Schiffman, E.L., B.L. Braun, and B.R. Lindgren, *Temporomandibular joint iontophoresis: a double-blind randomized clinical trial.* J Orofac Pain, 1996. **10**(2): p. 157-65.
19. Hasson, S.M., et al., *Dexamethasone Iontophoresis: Effect on Delayed Muscle Soreness and Muscle Function.* Canadian Journal of Sport Sciences-Revue Canadienne Des Sciences Du Sport, 1992. **17**(1): p. 8-13.
20. Neeter, C., et al., *Iontophoresis with or without dexamethazone in the treatment of acute Achilles tendon pain.* Scand J Med Sci Sports, 2003. **13**(6): p. 376-82.
21. Nirschl, R.P., et al., *Iontophoretic administration of dexamethasone sodium phosphate for acute epicondylitis. A randomized, double-blinded, placebo-controlled study.* The American Journal of Sports Medicine, 2003. **31**(2): p. 189-195.
22. Gokoglu, F., et al., *Evaluation of iontophoresis and local corticosteroid injection in the treatment of carpal tunnel syndrome.* American Journal of Physical Medicine & Rehabilitation, 2005. **84**(2): p. 92-96.
23. Li, L.C., et al., *The efficacy of dexamethasone iontophoresis for the treatment of rheumatoid arthritic knees: a pilot study.* Arthritis Care and Research, 1996. **9**(2): p. 126-132.
24. Gudeman, S.D., et al., *Treatment of plantar fasciitis by Iontophoresis of 0.4% dexamethasone - A randomized, double-blind, placebo-controlled study.* The American Journal of Sports Medicine, 1997. **25**(3): p. 312-316.

25. Reid, K.I., et al., *Evaluation of iontophoretically applied dexamethasone for painful pathologic temporomandibular joints.* Oral Surg Oral Med Oral Pathol, 1994. **77**(6): p. 605-9.
26. Runeson, L. and E. Haker, *Iontophoresis with cortisone in the treatment of lateral epicondylalgia (tennis elbow)--a double-blind study.* Scand J Med Sci Sports, 2002. **12**(3): p. 136-42.
27. Budgett, R., Castell, L., Newsholme, E.A., *The overtraining syndrome*, in *Oxford Textbook of Sports Medicine*, M. Harris, Williams, C., Stanish, W.D., Micheli, L.J., Editor. 1998, Oxford Medical Publications: Oxford. p. 367-377.
28. Lac, G. and F. Maso, *Biological markers for the follow-up of athletes throughout the training season.* Pathol Biol (Paris), 2004. **52**(1): p. 43-9.
29. Petibois, C., et al., *Biochemical aspects of overtraining in endurance sports: a review.* Sports Med, 2002. **32**(13): p. 867-78.
30. Hargreaves, M., Spriet, L., ed. *Exercise Metabolism*. 2nd ed. 2006, Human Kinetics, Inc.: Champaign. 301.
31. Bosquet, L., L. Leger, and P. Legros, *Blood lactate response to overtraining in male endurance athletes.* Eur J Appl Physiol, 2001. **84**(1-2): p. 107-14.
32. Rowbottom, D.G., D. Keast, and A.R. Morton, *The emerging role of glutamine as an indicator of exercise stress and overtraining.* Sports Med, 1996. **21**(2): p. 80-97.
33. Blomstrand, E., *Amino acids and central fatigue.* Amino Acids, 2001. **20**(1): p. 25-34.
34. Davis, J.M., N.L. Alderson, and R.S. Welsh, *Serotonin and central nervous system fatigue: nutritional considerations.* Am J Clin Nutr, 2000. **72**(2 Suppl): p. 573S-8S.
35. Nixon, S., et al., *Reverse iontophoresis of L-lactate: In vitro and in vivo studies.* J Pharm Sci, 2007.
36. McGuire, J., et al., *Biochemical markers for post-operative fatigue after major surgery.* Brain Res Bull, 2003. **60**(1-2): p. 125-30.
37. Armstrong, L.E. and J.L. VanHeest, *The unknown mechanism of the overtraining syndrome: clues from depression and psychoneuroimmunology.* Sports Med, 2002. **32**(3): p. 185-209.

38. Bell, C., J. Abrams, and D. Nutt, *Tryptophan depletion and its implications for psychiatry.* Br J Psychiatry, 2001. **178**: p. 399-405.
39. Murray, R.K., Granner, D.K., Mayes, P.A., Rodwell, V.W., *Harper's Biochemistry*. 25th ed. 2000, Stamford, CT: Appleton&Lange. 927.
40. Bender, D.A., *Amino Acid Metabolism*. 2nd ed. ed. 1985, Chichester: John Wiley & Sons. 263.
41. Merino, V., et al., *Noninvasive sampling of phenylalanine by reverse iontophoresis.* J Control Release, 1999. **61**(1-2): p. 65-9.
42. Yan, G., et al., *Correlation of transdermal iontophoretic phenylalanine and mannitol transport: test of the internal standard concept under DC iontophoresis and constant resistance AC iontophoresis conditions.* J Control Release, 2004. **98**(1): p. 127-38.
43. Rawlings, A.V., et al., *Stratum corneum moisturization at the molecular level.* J Invest Dermatol, 1994. **103**(5): p. 731-41.
44. Rawlings, A.V. and P.J. Matts, *Stratum corneum moisturization at the molecular level: an update in relation to the dry skin cycle.* J Invest Dermatol, 2005. **124**(6): p. 1099-110.
45. Rawlings, A.V., *Sources and Role of Stratum Corneum Hydration*, in *Skin Barrier*, P.M. Elias, Feingold, K.R., Editor. 2006, Taylor & Francis. p. 399-425.
46. Marstein, S., E. Jellum, and L. Eldjarn, *The concentration of pyroglutamic acid (2-pyrrolidone-5-carboxylic acid) in normal and psoriatic epidermis, determined on a microgram scale by gas chromatography.* Clin Chim Acta, 1973. **49**(3): p. 389-95.
47. Horii, I., et al., *Stratum corneum hydration and amino acid content in xerotic skin.* Br J Dermatol, 1989. **121**(5): p. 587-92.
48. Denda, M., et al., *Stratum corneum sphingolipids and free amino acids in experimentally-induced scaly skin.* Arch Dermatol Res, 1992. **284**(6): p. 363-7.

Chapter 1. Transdermal iontophoresis for drug delivery and clinical monitoring: a review

Transdermal iontophoresis for drug delivery and clinical monitoring: a review

1. Introduction

Iontophoresis generally refers to the use of an electric field to transfer charged and neutral, polar molecules through a biological membrane [1-4]. While the technique has been applied for ocular, buccal, tympanic and nail drug delivery [4-8], it is most commonly used for transdermal applications. Since the applications of iontophoresis in sports medicine considered in this thesis are related to the electrotransport of compounds across the skin, it is specifically transdermal iontophoresis that is covered in this review. More precisely, the objective of this chapter is to understand how transdermal iontophoresis can be used in sports medicine for the management of injury-related pain and tissue inflammation, and to monitor, without the use of a needle, compounds of interest in athletes such as markers of overtraining or doping agents.

First, the transdermal route is described. Then, the theoretical basis of transdermal iontophoresis and some practical considerations are covered. Examples of iontophoretic drug delivery for the management of pain and treatment of inflammation follows and includes an overview of previous experimental research attempting to quantify the iontophoretic delivery of corticosteroids. Finally, the use of reverse iontophoresis for clinical monitoring is reviewed.

2. The transdermal route

2.1. Structure and function of the skin

The skin is the largest organ of the body with an area of approximately 2 m^2 and accounts for more than 10% of body mass [9, 10]. As illustrated in Figure 1, the skin consists of three distinct layers, the hypodermis (or subcutaneous tissue), the dermis and the epidermis, and several associated appendages: hair follicles and their associated sebaceous glands, eccrine sweat glands, apocrine sweat

glands and nails. The deepest layer of the skin is the subcutaneous tissue and is constituted of fat cells arranged in lobules and linked to the dermis by collagen and elastin fibres. In addition to the fat cells, the hypordermis also contains fibroblasts and macrophages. The principal functions of the subcutaneous tissue are to act as an insulator, a shock absorber, an energy storage region and to carry the vascular and neural systems for the skin [10].

The dermis is made up of connective tissue elements and forms the bulk of the skin. Dermis is highly vascular and includes dermal adipose cells, nerve endings as well as sebaceous and sweat gland. It plays an important role in the regulation of temperature, pressure and pain, and provides nutritive and immune support to the epidermis [9, 10].

The overlaying, avascular epidermis is composed essentially of keratinocytes (~95%), but also contains melanocytes, Langerhans cells and Merkel cells. The total thickness of the epidermis is ~100 to 150 μm and is constituted of four distinct layers (Figure 2). The keratinocytes originate from a layer called stratum basale, located at the interface between the dermis and the epidermis, and undergo continuous differentiation during the course of migration upward through the layers of spinosum and granulosum.

Finally, the outermost layer of the epidermis, called the stratum corneum (SC), is composed of corneocytes (terminally differentiated keratinocytes) and the secreted contents of the lamellar bodies (elaborated by the keratinocytes). The epidermis has, above all, a function of protection, which covers physical, chemical (including water loss), immune, pathogen, UV radiation and free radical defences. It is the stratum corneum, and more precisely the highly tortuous path (due to its brick-and-mortar organization) through which substances have to traverse in order to cross it, that is the most efficient barrier against chemical penetration in the body and water loss from the skin [9, 10].

The barrier function of the SC is further facilitated by the continuous desquamation of its top layer, resulting in a total turnover every 2-3 weeks. The controlled loss of corneocytes from the surface of the skin is regulated by the water content of the SC. Critical in maintaining the SC hydrated despite the desiccating action of the environment are the natural moisturizing factors (NMFs). NMF is exclusively found in the SC and comprises water soluble and

hydroscopic compounds capable of retaining water (Table 1). As it can be observed in Table 1, the principal constituents of NMF are the free amino acids (AAs) and their derivatives (pyrrolidone carboxylic acid and urocanic acid). These AAs are derived from a protein precursor system: the profilaggrin-filaggrin system [11-13]. As seen in Figure 2, the profilaggrin is first expressed in the stratum granulosum as a large highly phosphorylated protein (>500 kDa) composed of multiple filaggrin repeats linked by short hydrophobic peptides. As the keratinocytes mature into corneocytes and form the SC, the profilaggrin is dephosphorylayed in filaggrin (37 kDa), which is itself proteolyzed to NMF within the corneocytes [11-13].

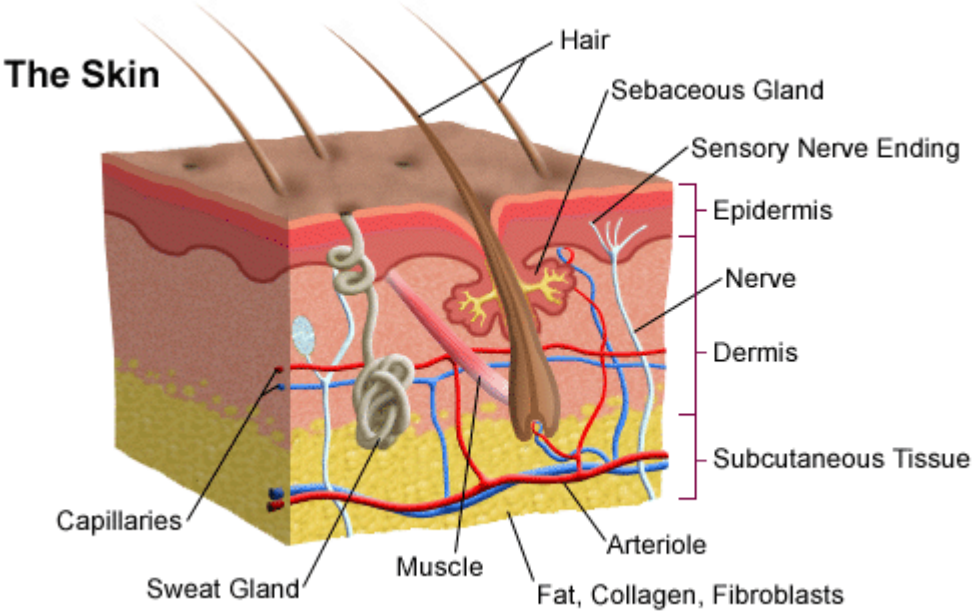

Figure 1. Illustration of the principal structures of the skin (http://www.healthsystem.virginia.edu/uvahealth/adult_derm/images/ei_0390.gif).

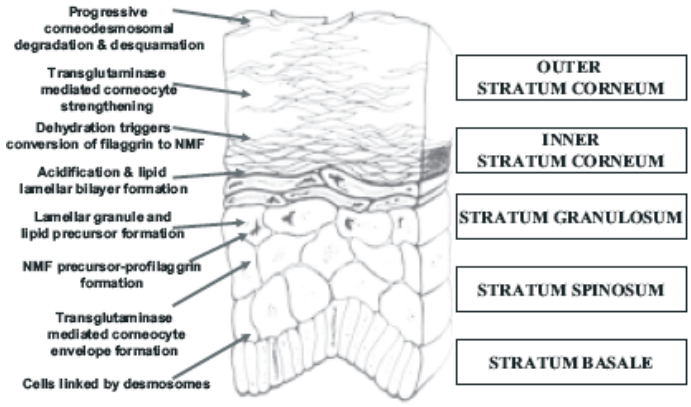

Figure 2. Illustration of the epidermis [12].

Table 1. Chemical composition of natural moisturizing factor [13].

Chemical	Composition (%)
Free amino acids	40
Pyrrolidone carboxylic acid	12
Lactate	12
Sugars	8.5
Urea	7
Chloride	6
Sodium	5
Potassium	4
Ammonia, uric acid, glucosamine and creatine	1.5
Calcium	1.5
Magnesium	1.5
Phosphate	0.5
Citrate and formate	0.5

2.2. Advantages and limitations of the transdermal route

It follows that trying to deliver or extract compounds from the skin in a minimally-invasive manner is against the very nature of this formidable barrier and represents, therefore, a real challenge. In the case of clinical monitoring, transdermal extraction relying exclusively on passive diffusion is not sufficiently efficient for practicable use unless the barrier is compromised [14, 15]. For a limited number of very potent drugs, with appropriate physicochemical properties (MW < 500 Da, aqueous solubility > 1 mg/mL and $10 < K_{o/w} < 1000$), it is possible to rely only on passive diffusion for their transdermal delivery [16].

Transdermal drug delivery is accompanied with many advantages: avoidance of first-pass effect and/or gastro-intestinal metabolism or degradation, easy access, non-invasive and consequently improved patient acceptance and compliance [16].

2.3. Pig skin as a model of human skin

As excised human skin is often difficult to obtain, animal skin is extensively used as a model, with pig skin being the most reliable [17]. Indeed, porcine skin is a well-established model of human skin and is often used to assess transdermal transport either *in vivo*, or *in vitro* [18, 19]. The skin model remains representative of the *in vivo* situation even if it was kept frozen before use [20]. Recently, it was demonstrated that pig skin could also be used as an *in vitro* model for its *in vivo* human counterpart during tape-stripping procedure, either to assess drug permeability in this membrane or its barrier function [21, 22]. Again, storage of the skin in the freezer until its use had no apparent detrimental effect on the tape-stripping procedure [23, 24].

Pig skin is also an established model of human skin for iontophoresis studies. For example, the transport fluxes of lithium measured with the pig skin *in vitro* model could be directly used to predict those observed *in vivo* in man [25]. Furthermore, the pig skin model is a cation-permselective membrane as its human counterpart (with a similar pI), meaning that it can also be used to model the electrotransport of neutral molecules by electroosmosis [26].

3. Transdermal iontophoresis

3.1. Description of iontophoresis

Iontophoresis is one of many methods that have been developed in order to improve the efficiency of transdermal delivery and expand the range of compounds that could be transported through the skin. Most of these methods (chemical enhancers, microneedles, needless injections, sonophoresis etc.) increase the permeability of the skin via direct effects on the skin barrier itself, such as the disruption or the extraction of SC lipids for example [27, 28]. In iontophoresis, an electrical field is applied across the skin, generally via a mild

constant current (≤0.5 mA/cm^2), in order to act principally on the molecules themselves rather than on the skin's barrier [1-4]. Indeed, the major perturbations of the SC observed after application of iontophoresis are limited to an increase in hydration and a moderate disorganisation of the lipid bilayers (not always observed [29]), which are hardly modifying the barrier function of the skin [30]. Furthermore, the viable skin is also minimally affected during current application as evidenced by only mild erythema and fast skin recovery usually observed after iontophoresis [30, 31]. In summary, when used correctly, iontophoresis is considered as a safe and minimally-invasive technique. Iontophoresis should not be confused with electroporation, another electrically-assisted transdermal technique that applies high voltage (>100 V) pulses of short duration (μs-ms) in order to increase the skin's permeability [32].

The principal advantage of iontophoresis is to open the way to the transdermal transport of polar and/or charged molecules whose passive skin permeation is severely restricted [16]. Other advantages include the possibility to control the extent of transdermal passage by simple adjustment of current intensity, and to limit the effect of skin's condition on its efficiency [1-4, 33, 34].

3.2. The electrical circuit of iontophoresis

A basic iontophoretic system is composed of a power supply and two electrodes placed on the skin via a conducting electrolytic medium (Figure 3). The electrical current passed in the circuit determines how much of the charged species are carried across the skin. The electrochemistry occurring at the electrode/electrolyte interface permits the transition from a current of electrons, in the external circuit, to a current of ions in the electrolyte and the skin. There are two types of electrodes: non-consumable and consumable [35]. When non-consumable electrodes, made of inert materials (e.g., platinum, glassy carbon, stainless steel), are used in an aqueous electrolyte solution, electrolysis of water is likely to occur. The respective electrochemical reactions at the anode and cathode are:

$$anode: \quad 2H_2O_{(l)} \rightarrow 4H^+_{(aq)} + O_{2(g)} + 4e^- \qquad (eq.1)$$

$$cathode: \quad 2H_2O_{(l)} + 2e^- \rightarrow 2OH^-_{(aq)} + H_{2(g)} \qquad (eq.2)$$

As it can be seen from eq.1 and 2 respectively, each electron flowing in the circuit generates a proton at the anode and a hydroxyl ion at the cathode. This can lead to pH shifts during iontophoresis unless the solutions are sufficiently buffered. Furthermore, the gases generated can accumulate on the electrode or skin surface and may interfere with the uniformity of current distribution [35]. In order to avoid reaction of water at the electrodes, materials with lower redox potential can be used. Ag/AgCl is an example of consumable electrode very popular for iontophoresis due to its biocompatibility, its reversability and the fact that pH shifts are avoided [35, 36]. The electrochemical reactions of Ag/AgCl at the anode and cathode are respectively:

$$anode: \quad Ag_{(M)} + Cl^-_{(aq)} \rightarrow AgCl_{(s)} + e^- \qquad (eq.3)$$

$$cathode: \quad AgCl_{(s)} + e^- \rightarrow Ag_{(M)} + Cl^-_{(aq)} \qquad (eq.4)$$

As one chloride is consumed at the anode for each electron flowing in the circuit, the electrolyte in contact with this electrode needs to have sufficient chloride for the duration of the experiment. Otherwise, Ag^+ are released in the anodal compartment and can lead to competition with the delivery of cationic drugs and apparition of stains on the skin. At the cathode, one chloride is released for each electron. The flux of anionic drugs delivered from the cathode may therefore decrease progressively due to the increasing chloride concentration in the donor solution [35, 37-40].

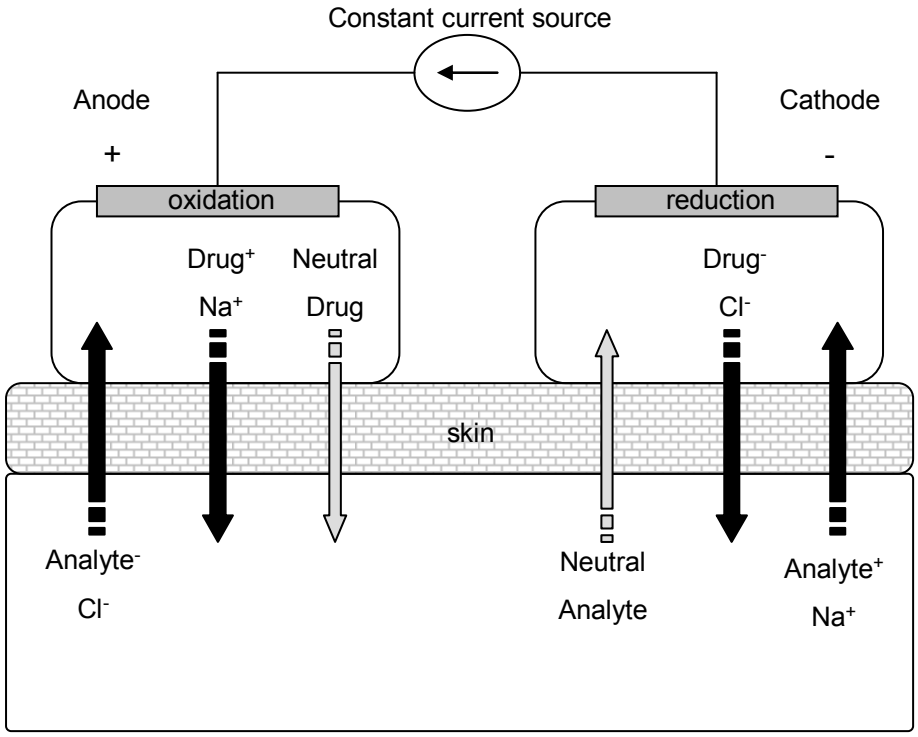

Figure 3. Schematic diagram of molecular transport during iontophoresis. Electromigration is represented by the thick black arrows and the electroosmotic flow by the grey arrows (inspired from [1]).

3.3. Mechanisms of transport

Three mechanisms can contribute to the transport of a molecule across the skin during iontophresis: (1) the direct interaction of the (charged) molecule with the electrical field (electromigration), (2) the convective transport due to the solvent flow (electroosmosis), and (3) the diffusion related to a concentration gradient (passive diffusion) [3]. The total flux of a molecule being transported transdermally (J_{tot}) is therefore the sum of these three contributions:

$$J_{tot} = J_{EM} + J_{EO} + J_P \qquad (eq.5)$$

where J_{EM} represents the flux attributable to electromigration, J_{EO}, that obtained by electroosmosis, and, J_P, the contribution of passive diffusion. For many compounds, however, passive diffusion can be neglected and the two main mechanisms of transport are electromigration and/or electroosmosis [1, 2].

Electromigration can be thought of as the repulsion of solute ions by an electrode of like charge and their migration towards an electrode of opposite

charge (Figure 3). The reality is slightly more complicated and is a direct result of the application of an electrical. As seen previously, the electrical current imposed through the electrodes results in electrochemical reactions at the surface of the electrodes resulting in the release or consumption of charges species. Ionic transport occurs through the skin in order to maintain electroneutrality in the electrode compartments. The speed of migration of an ion is determined by its physicochemical characteristics and the properties of the media through which the ion is progressing. The sum of the electrical current carried by each ion must equal to the electrical current supplied by the power source. Practically, as far as drug delivery is concerned, this means that the drug will compete for the current delivery with all the other ions present in the system [41]. The efficiency of transport, or in other words the fraction of the total charge transported by a given drug, can be evaluated by determining its transport number, t_d:

$$t_d = \frac{c_d z_d \mu_d}{\sum_i c_i z_i \mu_i} \qquad (eq.\,6)$$

where c, z and μ refer respectively to the concentration, valence and mobility inside the skin of either the drug (d) or ion (i) [41]. It can be seen from this equation that a small ionic (highly mobile) drug will have a higher transport number than a larger (less mobile) one. Electromigration is thus considered to be an efficient mechanism of transport for relatively small ions. Experimentally, the transport number of the drug can be deduced from the measurement of the ionic flux of the drug, J_d, using the relation:

$$J_d = \frac{I \cdot t_d}{F \cdot z_d} \qquad (eq.\,7)$$

where I is the electrical current passed, F, the Faraday's constant and z_d, the valence of the drug [20].

Electroosmosis has its origin in the fact that the skin is a negatively charged membrane at physiological pH. When an electrical potential is applied across a membrane containing fixed charge, a bulk flow of solution (volume flow) occurs in the direction of the counter-ion flow [42]. This means that for the negatively charged skin, the electoosmotic flow is oriented in the direction of the cations, in the anode-to-cathode direction (Figure 3). This will have as an effect

to assist the transport of cations and retard that of anions. This flow of solvent will carry through the skin any dissolved solute and is therefore the mechanism enhancing the transdermal delivery of neutral, but polar, molecules. The electroosmotic flow is proportional, at least in first approximation, to the concentration of the solute and is the dominant mechanism of transport for the delivery of larger molecules [1]. The pH and the ionic strength are the main parameters of the formulation that can be used to modulate electroosmosis by, respectively, modifying and screening the skin's charge (the isoelectric point is ~4.8 for human skin) [26, 43].

3.3. Pathways of transport

The electric current follows the routes of least resistance and the presence of appendages in the skin (i.e. hair follicles and sweat glands) raises the question whether ionic transport is localized in these natural 'pores' during iontophoresis [44]. Many techniques have been used in order to identify the principal routes of ionic transport across the skin. A method, involving the scanning of the skin surface with a vibrating probe electrode, revealed that the current is highly localized in structures related with skin appendages [45]. This was further confirmed with scanning electrochemical microscopy (SECM) during iontophoresis of ionized and neutral compounds, suggesting that significant transport during both electromigration and electroosmosis is associated with appendageal pathways [46-50]. Another technique proposed to evaluate the contribution of the appendageal routes is the skin sandwich, which consists in the superposition of two pieces of epidermis and virtually ensures that appendages of the two layers do not superpose [51, 52]. The transport or ionic and neutral compounds across the skin sandwich was importantly decreased compared to the transport measured in the single-epidermis case, suggesting that the 'shunts' in the skin are important pathways during iontophoresis [51, 52]. On the other hand, X-ray microanalysis after iontophoresis of mercuric chloride demonstrated that the mercuric ions are also transported through the intercellular route [53]. Confocal microscopy analysis of the skin, after the delivery of fluorescent compounds, also confirmed the appendageal and

intercellular routes, and suggests that their role is dependant on the physico-chemical properties of the compound being delivered [54-56].

3.4. Parameters affecting iontophoresis

The iontophoresis of a compound across the skin is affected by its physicochemical properties, the electrical parameters applied and the composition of the electrode compartments. The charge, the molecular weight, the mobility and the lipophilicity of a compound are physicochemical properties of great importance in iontophoresis. The charge determines the amplitude and direction of electrostatic force acting on the molecule and higher fluxes are usually observed for charged compounds. Due to the cationic permselectivity of the skin, cations are usually better transported during iontophoresis [38]. The iontophoretic fluxes of charged molecules have been shown to decrease rapidly with molecular weight and aqueous mobility [4, 57]. For neutral compounds transported mainly by electroosmosis, the fluxes are only slightly affected by the molecular weight at least for compounds in the range 60-400 Daltons [58]. An increase in lipophilicity usually results in a decrease of the iontophoretic flux [4].

From equation 7, it can be seen that the iontophoretic flux of a compound is proportional to the intensity of current applied and this has been verified for many charged compounds [3, 59]. Similar comportment has also been observed for electroosmosis [43, 60]. The current intensity that can be applied is however limited by the maximal current density that is tolerable in human (~0.5 mA/cm^2) [31]. Obviously, the quantity of a compound transported through the skin will also be linearly proportional to the time of current application.

Finally, the ionic composition of the electrode compartment can have an important effect on the iontophoretic transport. In the case of delivery of a charged drug, the inclusion in the donor of co-ions usually results in decreased efficiency in its transport due to competition [1, 2]. In presence of co-ions, the flux of the drug is increased by increasing its concentration (molar fraction) in the donor [59, 61]. In absence of co-ions, however, increase of drug concentration has usually no significant effect [59, 61]. Increase in ionic strength of the donor also results in decreased transport of neutral compounds from the

anode due to a reduction of the solvent flow [42, 43]. Similarly, the extraction efficiency of a neutral analyte at the cathode also decreases with an increase in ionic strength of the extraction solution for the same reason. The pH is another parameter of importance. Firstly, the pH of the solution may have an effect on the charge of the molecule iontophoresed (dependant of the pK_a of the compound). Moreover, the pH can change the charge of the skin, which can result in a modification of its permselectivity and the amplitude (and direction) of the net electroosmotic flow [26, 42, 43].

4. Transdermal iontophoretic drug delivery

Iontophoresis has been used to deliver across the skin a wide range of compounds including peptides and proteins [62, 63], oligonucleotides [64, 65], anti-Parkinson drugs [59, 66, 67], anti-viral agents [68-70] and pilocarpine (for the diagnosis of cystic fibrosis) [71]. The following sections will focus on the drug delivery for the management of pain and inflammation.

4.1. Iontophoresis for administration of local anesthetics

Local anesthetics are used to locally inhibit sensation. Lidocaine is a positively charged local anesthetic that has been successfully delivered by iontophoresis prior a variety of invasive interventions, e.g. insertion of a needle, catheter or cannula, laser surgery and shave biopsy [72-76]. The delivery of lidocaine by iontophoresis was compared to its topical application and subcutaneous infiltration. It was found that iontophoresis was more efficient than topical application and resulted in a quicker onset of action in addition to a longer duration and improved depth of anesthesia [77, 78]. Anesthesia induced by iontophoresis was of slightly shorter duration than that obtained by subcutaneous injection, but was better tolerated than the latter by patients [78, 79]. Pharmacokinetics studies in weanling pigs showed that the addition of a vasoconstrictor (e.g., epinephrine, norepinephrine) in the lidocaine donor solution resulted in increased residence time at the site of delivery and a lower systemic delivery [80, 81]. This conclusion was supported by an *in vivo* study in

human showing that the addition of epinephrine increased the duration of anesthesia [82].

These positive results led to commercialization of devices designed to deliver mixtures of lidocaine and epinephrine. The first FDA approved iontophoretic delivery system for lidocaine/epinephrine has been the IONTOCAINE® from IOMED (Salt Lake City, UT), which consists in a gel electrode that requires to be filled with a solution of the drugs before iontophoresis with IOMED's Phoresor® drug delivery system. Vyteris (Fair Lawn, NJ) now commercializes a recently FDA approved, disposable pre-filled electrode system that is used with a reusable power supply (Figure 4).

Figure 4. The LidoSite™ iontophoretic system for topical delivery of lidocaine (http://www.vyteris.com/home/Our_Products/Lidosite.php)

Recently, the specific use of lidocaine iontophoresis for the pain management of (sport-related) soft tissue injuries has been considered [83, 84]. One prospective study found that the iontophoreis of lidocaine was more effective than the oral administration of non-steroidal anti-inflammatory medication for the pain management of acute soft tissue injuries in the emergency department setting [83]. Another study, where the iontophoresis of lidocaine was part of larger treatment algorithm for five patients with 'tennis elbow', showed clinical improvement of the patients over time [84]. While the results of these prospective studies are encouraging, more studies are required to substantiate the use of lidocaine iontophoresis for such applications.

4.2. Iontophoresis for systemic administration of opioids

Opioids are a class of molecules (MW 300-500) with analgesic properties that are administered systemically to alleviate acute pain, such as post-operative pain. Surgery has an important role to play in the management of both acute and overuse sport-related injuries [85]. The iontophoretic delivery of opiods is therefore relevant to sports medicine. The size, positive charge under physiological conditions and relatively high potency makes these molecules good candidates for systemic delivery by iontophoresis. The iontophoretic delivery of hydromorphone, morphine, buprenorphine, nalbuphine, sufentanil and fentanyl has been studied [86-92].

The pharmacokinetics of fentanyl have been investigate extensively, as a function of the current intensity and profile, the dosing regiment, the site of application and demographics (sex, age, race and weight) of the patient, using an iontophoretic delivery platform developed by ALZA Corporation (Mountain View, CA), the E-TRANS® [34, 93-97]. The results showed that the plasma concentration increased continuously during the fentanyl delivery by iontophoresis over a 24-hour period, and that the maximum plasma concentration of the drug increased in direct proportion with the intensity of the current applied [93]. Furthermore, when the iontophoretic system was used in the intermittent mode to deliver fentanyl during 20 minutes at the beginning of each hour over a 24-hour period, the plasma profiles obtained for iontophoresis paralleled those obtained with intravenous (IV) infusion (Figure 5) [93]. Moreover, the dose administered was found to be linearly related with the intensity of current applied and independent of the patient's demographics, such as age, bodyweight, race and sex, and whether the device was placed on the chest or the outside of the upper arm [95, 96]. It was also found that the equivalent dose obtained from a single 10 minutes current application was independent of the frequency and total number of doses applied [97]. The safety and efficacy of the delivery system were also assessed in clinical trials. The device was well tolerated, and importantly, it was more efficient than placebo and of equivalent efficiency than the on-demand intravenous infusion of morphine for the management of post-surgery pain [98, 99].

These positive results led to the recent commercialization of a device based on the E-TRANS® platform: the IONSYS™ (Janssen-Cilag), an FDA approved needle-free, patient-controlled, iontophoresis fentanyl delivery system (Figure 6). The device, of the size of a credit card, is installed on intact skin of the upper outer arm or chest of hospitalized patients for their pain management. By pressing twice on the 'on-demand button', the patient receives a 40µg dose of fentanyl delivered over a 10 minutes period, a process that can be repeated 80 times over a 24 hours period [http://www.ionsys.net].

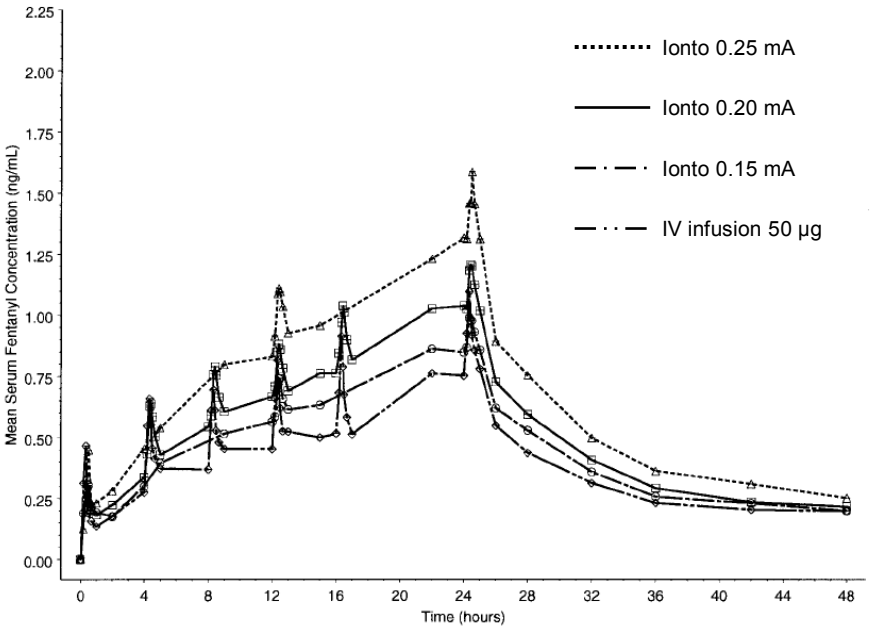

Figure 5. Mean serum concentration of fentanyl as a function of time for three iontophoretic currents applied for 20 minutes at the beginning of each hour for 24h, compared to the IV infusion of 50 µg (per 20 minutes application period) of the drug using an identical delivery regiment [93].

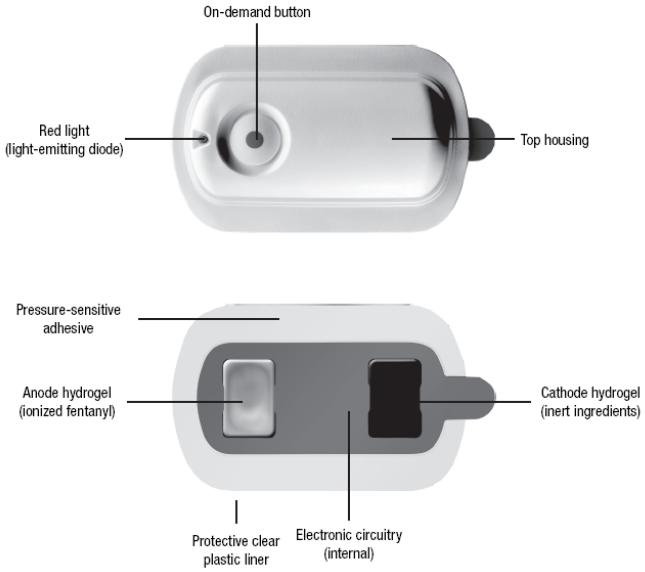

Figure 6. IONSYS^{TM} iontophoresis fentanyl delivery system [92].

4.3. Iontophoresis for local administration of NSAIDs

Non-steroidal anti-inflammatory drugs (NSAIDs) are pharmacologic agents with analgesic, antipyretic and anti-inflammatory effects that are widely used in the treatment of sporting injuries [85]. Most of these drugs, when administered orally, provoke adverse effects in the gastrointestinal tract, which may result in ulceration of the mucosa and bleeding. The rationale of using iontophoresis is therefore to deliver directly the molecules at the target (inflamed) site, while limiting the systemic side effects of the drug. As these compounds are acidic and usually negatively charged under physiological conditions, it is expected that iontophoresis from the cathode can result in an increased delivery compared to passive diffusion [2, 100].

This hypothesis was tested for numerous NSAIDs in both *in vitro* and *in vivo* studies [39, 40, 101-109]. In the case of piroxicam, a 6-hours iontophoresis period from solutions or gels of the drug, *in vitro,* resulted in a 100-1000 fold increase of its transdermal delivery compared to passive diffusion [39]. In an *in vivo* study in man, it was found that iontophoresis also enhanced the amount of piroxicam present in the stratum corneum compared to passive diffusion [101]. The *in vitro* iontophoresis of ketorolac from the cathode, using current densities ranging from 0.11 to 0.5 mA/cm^2, through rat skin was also found to be much more efficient (10-100 fold increase) than its passive delivery [102]. A study in

rats, using two microdialysis probes located respectively in the dermis and subcutaneous tissue underneath the delivery electrode (cathode), demonstrated that 15 minutes of current application (0.4 mA/cm^2) was sufficient to deliver a high amount of flurbiprofen in the dermis and underlying tissue while maintaining a low plasma concentration [103]. Deep (3-4 mm) penetration of salicylic acid in rats underneath the donor electrode was also attributed to its direct cathodic delivery (0.38 mA/cm^2, 120 minutes), while deeper penetration (>3-4 mm) was due to systemic redistribution of the drug [104]. Ketoprofen was also delivered more efficiently from the cathode than by passive diffusion [105]. Furthermore, ketoprofen was present in the venous blood collected close to the delivery site after iontophoresis in human and rat, demonstrating that the drug was delivered transcutaneously [105-107]. The local transcutaneous delivery was further demonstrated in an *in vivo* study in pig where the drug was quantified in the skin and underlying muscles after iontophoresis [108]. The transdermal delivery of the sodium, potassium and ammonium salts of diclofenac from the cathode were also more efficient than their respective passive delivery [109]. The local increase in concentration after iontophoresis of underlying tissues (as deep as muscle) was also demonstrated for sodium diclofenac administered to rabbits [40].

The efficiency of iontophoretic delivery of NSAIDs to treat musculoskeletal conditions has been evaluated in clinical studies in man. Table 2 (updated from [100]) summarizes the delivery conditions and clinical outcome for the treatment of articulation dysfunctions using iontophoresis of NSAIDs. All of the clinical investigations demonstrated at least subjective positive clinical outcome.

Table 2. Clinical investigations of NSAIDs iontophoresis [100, 110-115].

Dysfunction	Delivery electrode	Current dose (mA·min)	NSAID	Number of treatments	Outcome
Joint or tendon inflammation	Cathode	?	Diclofenac	10	Clinical improvement [110]
Upper extremity periarthritis	Cathode	100-240	Diclofenac	20	Subjective pain relief [111]
Upper extremity periarthritis	Cathode	100-240	Pirprofen	10	Subjective pain relief [112]
Rheumatic dysfunction	Cathode	41	Pirprofen or Lys-aspirin[a]	10	Subjective pain relief [113]
Rheumatic dysfunction	Cathode	40	Ketorolac	5	Subjective pain relief [114]
Lateral epicondylitis	Cathode	120-220	Diclofenac or salicylic acid	18	Subjective pain relief [115]

[a] Lysine soluble aspirin

4.4. Iontophoresis for local administration of corticosteroids

Corticosteroids are another type of drugs with anti-inflammatory effect and are also commonly used in the treatment of musculoskeletal injuries [85]. The rationale behind the use of iontophoresis for the delivery of these pharmacological agents is the same than that discussed for NSAIDs: local delivery of the drug at the inflamed site to obtain an anti-inflammatory effect with minimal systemic exposition of the drug, therefore limiting the adverse effects. While corticosteroids are chemically neutral molecules at physiological pH, it is possible to chemically modify them in order to form prodrugs containing an acidic group (e.g., sulphate or phosphate) that are negatively charged in physiological conditions. For example, dexamethasone phosphate (Dex-Phos) is a prodrug of the corticosteroid dexamethasone (Dex) and is essentially doubly charged at physiological pH (pK_as: 1.9 and 6.4). Iontophoresis from the cathode is therefore expected to increase the delivery of these anionic prodrugs. In the two following sections, the clinical studies performed to evaluate iontophoresis of corticosteroids for the treatment of musculoskeletal

conditions and the experimental studies carried to quantify their transcutaneous delivery are reviewed.

4.4.1. Clinical studies

Many studies have been conducted in human to evaluate the clinical relevance of corticosteroid iontophoresis to treat acute soft tissue inflammation (e.g. bursitis, tendonitis, carpal tunnel syndrome). The iontophoretic conditions used in these studies are summarized in Table 3 together with the clinical outcome obtained. It can be observed that the clinical outcome was not always positive. Moreover, a variety of iontophoretic conditions were used (and in some cases were not clearly described), strongly suggesting that the optimal conditions have not been clearly identified yet.

Table 3. Clinical studies of corticosteroid iontophoresis [100, 116-129].

Dysfunction	Delivery electrode	Current dose (mA·min)	Drug formulation	R_X[a]	Outcome
Musculoskeletal inflammation	Anode	85	Dex/Lido[b]	1-3	Subjective pain relief [117]
Tendinitis inflammation	?	45	Dex/Lido[b]	4	Subjective & objective improvements [118]
Musculoskeletal dysfunction	Anode	3-7	Triam-Ace[c]	11	56% subjects pain relief [116]
Muscle soreness	Anode	65	Dex/Lido[b]	1	Subjective improvement [119]
Infrapatellar tendinitis	?	40-80	Dex/Lido[b]	6	Subjective & objective improvements [120]
Carpal tunnel syndrome	?	40-45	Dex/Lido[b]	3	58% subjective & objective improvements [121]
TMJ[d] dysfunction	Cathode	40	Dex/Lido[b]	3	No improvement from iontophoresis [122]
Rheumatic knee	Cathode	80	Dex-Phos 0.2%[e]	3	Subjective improvement [123]
TMJ[d] dysfunction	?	40	Dex/Lido[b]	3	Objective improvement, but no pain relief [124]
Plantar fasciitis	Cathode	40	Dex-Phos 0.4%[e]	6	Enhanced rehabilitation [125]
Lateral epicondylalgia	Cathode	40	Dex-Phos 0.4%[e]	4	No improvement from iontophoresis [126]
Achilles tendon pain	?	?	Dex[f]	4	Subjective improvement [127]
Acute epicondylitis	Cathode	40	Dex-Phos 0.4%[e]	6	Subjective improvement [128]
Carpal tunnel syndrome	Cathode	40-45	Dex-Phos 0.4%[e]	3	Subjective improvement [129]

[a]R_X, number of treatments

[b]Dex/Lido, mixture of injectable Dex-Phos 0.4% in citrate:lidocaine HCl (1:2)

[c]Triam-Ace, Triamcinolone-acetonide (Kenacort-A)

[d]TMJ, temporomandibular joint

[e]Dex-Phos solution, the presence of other ionic species is unknown

[f]Solution of unknown composition

4.4.2. Quantitative Studies

Quantitative studies have been performed in order to evaluate the actual amount of corticosteroids delivered during iontophoresis and to optimize the iontophoretic conditions. Similarly to clinical studies, most quantitative studies were carried with Dex-Phos with only few studies performed with different corticosteroids. One study looked at a variety of commercially available water-soluble corticosteroids (including triamcinolone-acetonide, prednisolone sodium tetrahydrophthalate, hydrocortisone sodium succinate, dexamethasone sodium phosphate, prednisolone sodium succinate and methylprednisolone sodium succinate) and failed to demonstrate the transcutaneous migration during iontophoresis of the corticosteroids using an *in vitro* model [116]. This result is in contradiction with another study performed in human with a donor solution of radiolabeled prednisolone sodium phosphate delivered from the anode. It was found that the plasma concentration of the drug 15 minutes after the treatment was about one third than that obtained after the oral administration of 10 mg of prednisolone [130]. A reservoir of the drug was also found in the epidermis, most likely situated in the SC, as evidence by the presence of the drug in this tissue even 24 hours after the iontophoretic treatment [130]. The transcutaneous delivery from the anode of the neutral hydrocortisone by the electroosmotic flow was enhanced compared to passive diffusion or delivery from the cathode, and increased linearly with current density [131, 132]. The following studies all concern the iontophoretic delivery of Dex-Phos.

An early study performed over five joints of a single monkey established that iontophoresis from the positive electrode (5 mA, 20 minutes) of a mixture of 0.4% radiolabeled dexamethasone sodium phosphate and 4% lidocaine HCl resulted in local tissue concentrations of Dex-Phos (in the μg/g range) higher than those that would be obtained by systemic therapy, but lower than would be obtained by local injection [133]. These results should be interpreted with care however, firstly because the current density used in this study (0.94 mA/cm^2) was much higher than the accepted maximal value (0.5 mA/cm^2) used in human, and second, because the hairs were clipped before the experiment, two possible sources of barrier alteration. On the other hand, the use of the anode (positive electrode) as the electrode for delivery is questionable considering that

Dex-Phos is negatively charged. A later *in vitro* study, using hairless mouse skin, demonstrated that the delivery of Dex-Phos from the cathode was indeed slightly more effective than from the anode [134].

Two subsequent *in vivo* studies, the first one in horse tibiotorsal joint [135], the other in human wrist [136], were conducted to quantify the amount of Dex-Phos delivered with iontophoresis from the cathode. The end-points of the studies were the Dex-Phos concentration in the synovium of the joint and in the plasma of local venous blood for the study in horse, and the concentration of Dex-Phos in plasma of local venous blood for the study in human. Both studies used clinically relevant current densities and the concentration of Dex-Phos and Dex (measured in order to account for the possible dephosphorylation of the pro-drug in vivo) were assayed using HPLC. Both studies failed to demonstrate the presence of Dex-Phos in the fluids analyzed, a fact due, perhaps, to the insufficient sensitivity of the analytical method (HPLC, ~0.2 μg/ml). This seems a plausible explanation when we look at the serum concentration of Dex-Phos one hour after iontophoresis obtained in another study performed in the patellar tendon of rabbits (~6 ng/ml) [137]. The latter study also confirmed the presence of Dex-Phos in the patellar tendon one hour and 24 hours after the application of the current. Another study using iontophoresis to administer Dex-Phos, from a 10 mg/ml drug donor, into tarsocrural joint in 5 horses found a mean concentration of ~1 ng/ml in the synovial fluid 30 minutes after the treatment [138]. The drug was undetectable in the plasma in this condition. When the concentration of the donor solution was reduced to 4 mg/ml, the Dex-Phos was undetectable in the synovial fluid [138]. In all these four studies however, it is not clear if the Dex-Phos solution was prepared in pure water or in buffered electrolyte, so the possibility of co-ions in the formulation cannot be completely discarded.

Finally, two more studies aimed at the optimization of the delivery of Dex-Phos were performed [139, 140]. The first suggests that for a given current dose, a low current administered over a longer period seems to result in deeper penetration of the drug than a higher current applied for a shorter period [139]. This is based on results obtained in an *in vitro* study where the amount of Dex-Phos delivered through an artificial membrane (cellulose ultrafiltration

membrane), into an agarose gel, was quantified as a function of the distance in the gel, and an *in vivo* study were the temperature at the surface of the skin was measured to give an indication of the vasoconstriction occurring due to the presence of Dex-Phos in local tissue. Both results must be regarded with great care: *in vitro*, because the artificial membrane allows for a non-negligible amount of passive diffusion to occur, so a longer period will just allow for more drug to diffuse passively; *in vivo*, due to the fact that erythema (a sign of vasodilatation) will be more important at higher electrical current, and this may mask the antagonist effect (vasoconstriction) of the drug being measured. Nevertheless, the result is in good agreement with previous studies showing that the main effect of iontophoresis is to enhance the transport of molecules through the epidermis (the barrier of the skin), and from there, it is mainly passive diffusion (together with the microcirculation *in vivo*) that is the main mechanism of distribution [4]. Finally, an *in vitro* study (with an artificial membrane again) reported that the absence of background electrolyte in the drug formulation resulted in a drug flux four-fold higher than when citrate anions were present [140]. The quantity of Dex-Phos delivered *in vivo* was approximated (1.4 mg) by measuring the concentration of the drug in the donor solution before and after the treatment (80 mA·min over a 24h period). Here again, the methodology used (artificial membrane for the *in vitro* study and quantification method for in vivo study) is questionable.

In summary, therefore, the optimal iontophoretic delivery conditions for Dex-Phos have not yet been clearly identified.

5. Reverse iontophoresis for clinical monitoring

The symmetrical nature of iontophoresis means that ions and polar molecules are not only delivered from the electrode compartments into the body, but can also be extracted from the skin into these compartments (Figure 3). In this latter situation, the method is generally referred to as ‘reverse iontophoresis’. The method can be used to monitor, in a minimally-invasive manner, endogenous molecules or drugs present in the subdermal compartment [141].

5.1. Monitoring of endogenous substances

Glucose is the endogenous molecule that has received the most attention due to the obvious benefit that a minimally-invasive method to monitor blood sugar would bring to diabetics. The proof-of-concept to use reverse iontophoresis to extract subdermal glucose was established in preliminary *in vitro* and *in vivo* studies [142, 143], and led to the development of the GlucoWatch® Biographer (Animas Corporation, West Chester, PA). The biographer is a wristwatch device (Figure 7) capable of sampling glucose using reverse iontophoresis and detecting it *in situ* using an on-board amperometric detector. The device requires one conventional 'finger-stick' blood sample to be taken for its calibration. Once this calibration is performed, blood glucose can be monitored in a nearly continuous manner (up to 6 readings per hour for the second generation of the device) for up to 13 hours. Clinical studies have demonstrated the efficiency of the device to track changes in the blood sugar levels of diabetics over the entire range of glycemia (Figure 8) [144]. The system was the first device based on reverse iontophoresis to be approved by the FDA.

Figure 7. The GlucoWatch® Biographer [144].

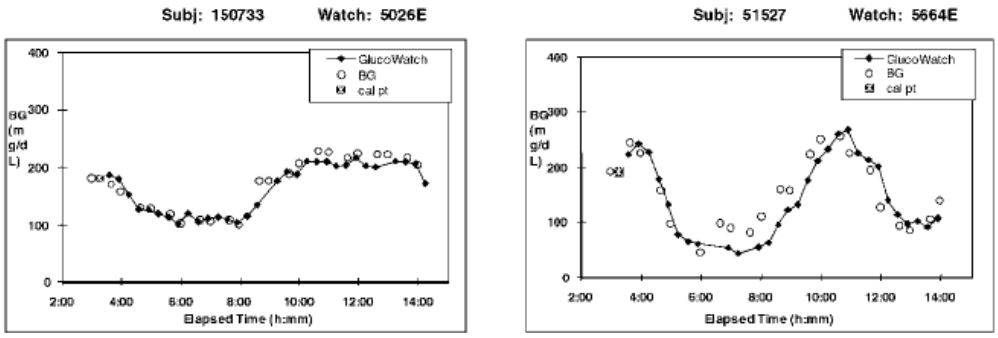

Figure 8. Representative results obtained in two subjects with the GlucoWatch biographer (filled symbols) compared to blood glucose measurements (empty symbols) [144].

Another endogenous substance that was extracted by reverse iontophoresis is prostaglandin E2 (PGE_2). The negatively charged PGE_2 was extracted from the skin of hairless guinea pigs, at the anode, following the application of several skin irritants. It was found that the amount extracted of PGE_2 correlated with the intensity of skin irritation observed [145]. The extraction, at the cathode, of the zwitterionic amino acid phenylalanine, a molecule of interest for the detection of phenylketonuria, was also investigated *in vitro*. The method showed promise as the fluxes correlated with the subdermal concentration, but the range of concentrations explored (1-10 mM) was higher than the usual *in vivo* levels for this molecule [146]. Very recently, the reverse iontophoresis of lactate, a marker of the tissue distress in critically ill patients and of sport performance in athletes was investigated. The *in vitro* experiments demonstrated a linear relationship between subdermal levels and extraction fluxes. The *in vivo* results were also encouraging as the fluxes followed the blood concentrations in some subjects, but as this was not the case in all volunteers more research is necessary to facilitate the interpretation of the data [147]. Finally, the extraction of urea and potassium, interesting to diagnose chronic kidney diseases, was evaluated *in vitro*, and again the extraction fluxes correlated with the subdermal concentrations [148].

5.2. Monitoring of therapeutic drugs

Some drugs have a narrow therapeutic window and reverse iontophoresis could be use to monitor their systemic levels in order to adjust the dose accurately [141]. The potential of the method was fist explored with caffeine and theophylline using tape-stripped pig skin as a model of the underdeveloping SC found in premature neonates. While the extraction across an intact membrane of the two compounds was increased by iontophoresis compared to passive diffusion, this was not the case for the stripped skin. The results suggest that the reverse iontophoresis of neutral compounds could be of interest in infants with a fully-developed SC, but not in premature neonates [15].

The reverse iontophoresis of two anti-convulsant drugs, valproate and phenytoin, known to be approximately 90% protein-bound in plasma, was investigated. As the complex drug-protein is expected to be too large to be extracted efficiently, extraction fluxes are expected to reflect the free-form of the drugs. The results indicated that the extractions fluxes were indeed dependant on the concentration of the free-fraction of the drugs [149, 150].

Finally, lithium is a drug commonly used in bipolar disorders. *In vitro* and *in vivo* studies demonstrated that reverse iontophoresis can be used to extract this small cation in a concentration dependant manner [151, 152].

5.3. Skin reservoir

Reverse iontophoresis being a transdermal method, the presence of the analyte of interest in the skin can affect the extraction fluxes, more so if the 'skin reservoir' is important. This reservoir should be emptied before a linear correlation between the extracted fluxes and the plasma concentration can be obtained. The GlucoWatch® Biographer, for example, requires a 'warm up' period of 2 hours to deplete the skin content before reporting on the glycemia [143]. The extraction of lithium in bipolar patients required a 30 minutes period before reliable information from the systemic level of the drug could be obtained, a fact attributed to a reservoir of drug 'stored' in the skin [152]. Recent studies investigating the reverse iontophoresis of lactate and urea, two compounds present in high concentration in the SC (Table 1), further demonstrated the interfering effect of the reservoir on the fluxes [147, 148, 153].

The extraction flux of a compound abundant in the SC, such as urea (Figure 9), is higher at the beginning of current passage and decreases to achieve a stable value. As amino acids are known to be abundant in the SC (Table 1), a similar effect can therefore be expected during the reverse iontophoresis of these molecules.

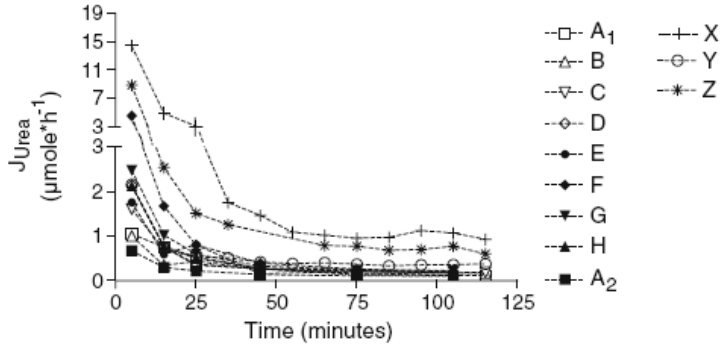

Figure 9. Reverse iontophoresis extraction fluxes as a function of time obtained in healthy volunteers (A-H) and patients with chronic kidney disease (X,Y and Z) [153].

5.4. Internal standard

As previously mentioned, the GlucoWatch® Biographer requires one conventional blood sample to be obtained in order to calibrate the device, a step that has been perceived as an inconvenient. The concept of internal standard has been developed to avoid this invasive procedure. During reverse iontophoresis, ions and small neutral molecules (including the compound of interest) are extracted non-specifically. The internal standard concept is based on the simultaneous detection of two compounds: the molecule of interest, the temporal change in whose concentration is of interest, and a second one, with known and essentially fixed physiological concentration [154]. Assuming that the iontophoretic transport of the analyte (A) and the latter internal standard (IS) are independent one another, the ratio of their fluxes (J_A/J_{IS}) should therefore follow the relationship:

$$\frac{J_A}{J_{IS}} = K\frac{[A]}{[IS]} \qquad (eq.\,8)$$

where $[A]$ and $[IS]$ are the concentrations in the blood of the analyte and the internal standard respectively and K is a proportionality constant.

This concept was validated *in vitro* for glucose with Na^+, sucrose, mannitol, glycerol and urea as internal standards [58, 154]. An *in vivo* study, however, indicated that Na^+ was not a suitable internal standard for glucose and that an electroosmotically-extracted internal standard should be identified in order to avoid the need for blood sampling [155]. The neutral urea was tested in another study for that purpose and performed reasonably well as an internal standard, but more research is required to better understand the inter-individual variability observed [156].

The validity of the internal concept was further validated in a variety of situations *in vitro*. Sodium was found to be a good internal standard for lithium [151], acetate for phenytoin [150], mannitol for phenylalanine [157], and glutamate for valproate [149]. Finally, when sodium was used as the internal standard during the extraction of lithium in man, increased precision on the predicted serum values of the drug could be obtained [152].

6. References

1. Delgado-Charro, M.B., Guy, R.H., *Transdermal iontophoresis for controlled drug delivery and non-invasive monitoring.* S.T.P. Pharma Sciences, 2001. **11**(6): p. 403-414.
2. Kalia, Y.N., et al., *Iontophoretic drug delivery.* Adv Drug Deliv Rev, 2004. **56**(5): p. 619-58.
3. Singh, P. and H.I. Maibach, *Iontophoresis: an alternative to the use of carriers in cutaneous drug delivery.* Advanced Drug Delivery Reviews, 1996. **18**(3): p. 379-394.
4. Roberts, M.S., Lai, P.M., Cross, S.E., Yoshida, N.H., *Solute Structure as a Determinant of Iontophoresic Transport*, in *Mechanisms of Transdermal Drug Delivery*, R.O. Potts, Guy, R.H., Editor. 1997, Marcel Dekker Inc.: New York. p. 291-349.
5. Eljarrat-Binstock, E. and A.J. Domb, *Iontophoresis: a non-invasive ocular drug delivery.* J Control Release, 2006. **110**(3): p. 479-89.

6. Puapichartdumrong, P., H. Ikeda, and H. Suda, *Facilitation of iontophoretic drug delivery through intact and caries-affected dentine.* Int Endod J, 2003. **36**(10): p. 674-81.
7. Christodoulou, P., et al., *Transtympanic iontophoresis of gadopentetate dimeglumine: Preliminary results.* Otolaryngol Head Neck Surg, 2003. **129**(4): p. 408-13.
8. Narasimha Murthy, S., D.E. Wiskirchen, and C.P. Bowers, *Iontophoretic drug delivery across human nail.* J Pharm Sci, 2007. **96**(2): p. 305-11.
9. Menon, G.K., *New insights into skin structure: scratching the surface.* Advanced Drug Delivery Reviews, 2002. **54**(Supplement 1): p. S3-S17.
10. Walters, K.A., Roberts, M.S., *The Structure and Function of Skin*, in *Dermatological and Transdermal Formulations*, K.A. Walters, Editor. 2002, Marcel Dekker Inc.: New York. p. 1-39.
11. Rawlings, A.V., et al., *Stratum corneum moisturization at the molecular level.* J Invest Dermatol, 1994. **103**(5): p. 731-41.
12. Rawlings, A.V. and P.J. Matts, *Stratum corneum moisturization at the molecular level: an update in relation to the dry skin cycle.* J Invest Dermatol, 2005. **124**(6): p. 1099-110.
13. Rawlings, A.V., *Sources and Role of Stratum Corneum Hydration*, in *Skin Barrier*, P.M. Elias, Feingold, K.R., Editor. 2006, Taylor & Francis. p. 399-425.
14. Pellett, M.A., J. Hadgraft, and M.S. Roberts, *The back diffusion of glucose across human skin in vitro.* International Journal of Pharmaceutics, 1999. **193**(1): p. 27-35.
15. Sekkat, N., et al., *Reverse iontophoretic monitoring in premature neonates: feasibility and potential.* Journal of Controlled Release, 2002. **81**(1-2): p. 83-89.
16. Naik, A., Y.N. Kalia, and R.H. Guy, *Transdermal drug delivery: overcoming the skin's barrier function.* Pharm Sci Technolo Today, 2000. **3**(9): p. 318-326.
17. Hadgraft, J., *Skin deep.* Eur J Pharm Biopharm, 2004. **58**(2): p. 291-9.

18. Simon, G.A. and H.I. Maibach, *The pig as an experimental animal model of percutaneous permeation in man: qualitative and quantitative observations--an overview.* Skin Pharmacol Appl Skin Physiol, 2000. **13**(5): p. 229-34.
19. Dick, I.P. and R.C. Scott, *Pig ear skin as an in-vitro model for human skin permeability.* J Pharm Pharmacol, 1992. **44**(8): p. 640-5.
20. Herkenne, C., et al., *Ibuprofen transport into and through skin from topical formulations: in vitro-in vivo comparison.* J Invest Dermatol, 2007. **127**(1): p. 135-42.
21. Herkenne, C., et al., *Pig ear skin ex vivo as a model for in vivo dermatopharmacokinetic studies in man.* Pharm Res, 2006. **23**(8): p. 1850-6.
22. Sekkat, N., Y.N. Kalia, and R.H. Guy, *Biophysical study of porcine ear skin in vitro and its comparison to human skin in vivo.* J Pharm Sci, 2002. **91**(11): p. 2376-81.
23. Trichard, L., et al., *Novel Beads Made of Alpha-cyclodextrin and Oil for Topical Delivery of a Lipophilic Drug.* Pharm Res, 2007.
24. Alvarez-Roman, R., et al., *Enhancement of topical delivery from biodegradable nanoparticles.* Pharm Res, 2004. **21**(10): p. 1818-25.
25. Mudry, B., R.H. Guy, and M. Begona Delgado-Charro, *Prediction of iontophoretic transport across the skin.* J Control Release, 2006. **111**(3): p. 362-7.
26. Marro, D., R.H. Guy, and M.B. Delgado-Charro, *Characterization of the iontophoretic permselectivity properties of human and pig skin.* J Control Release, 2001. **70**(1-2): p. 213-7.
27. Williams, A.C. and B.W. Barry, *Penetration enhancers.* Advanced Drug Delivery Reviews, 2004. **56**(5): p. 603-618.
28. Brown, M.B., et al., *Dermal and transdermal drug delivery systems: current and future prospects.* Drug Deliv, 2006. **13**(3): p. 175-87.
29. Fatouros, D.G., et al., *Visualization studies of human skin in vitro/in vivo under the influence of an electrical field.* Eur J Pharm Sci, 2006. **29**(2): p. 160-70.

30. Jadoul, A., J. Bouwstra, and V. Preat, *Effects of iontophoresis and electroporation on the stratum corneum - Review of the biophysical studies.* Advanced Drug Delivery Reviews, 1999. **35**(1): p. 89-105.
31. Ledger, P.W., *Skin biological issues in electrically enhanced transdermal delivery.* Advanced Drug Delivery Reviews, 1992. **9**(2-3): p. 289-307.
32. Banga, A.K., S. Bose, and T.K. Ghosh, *Iontophoresis and electroporation: comparisons and contrasts.* International Journal of Pharmaceutics, 1999. **179**(1): p. 1-19.
33. Sekkat, N., Y.N. Kalia, and R.H. Guy, *Porcine ear skin as a model for the assessment of transdermal drug delivery to premature neonates.* Pharm Res, 2004. **21**(8): p. 1390-7.
34. Gupta, S.K., et al., *Reproducible fentanyl doses delivered intermittently at different time intervals from an electrotransport system.* J Pharm Sci, 1999. **88**(8): p. 835-41.
35. Scott, E.R., Phipps, B., Gyory, R., Padmanabhan, R.V., *Electrotransport System for Transdermal Delivery: A Practical Implementation of Iontophoresis*, in *Handbook of Pharmaceutical Controlled Release Technology*, D.L. Wise, Editor. 2000, Marcel Dekker: New York. p. 617-659.
36. Cullander, C., Rao, G., Guy, R.H., ed. *Why silver/silver chloride? Criteria for iontophoresis electrodes*. Prediction of Percutaneous Penetration, ed. V.J.J. K.R. Brain, K.A. Walters. Vol. 3b. 1993, STS Publishing: Cardiff. 381-390.
37. Green, P.G., et al., *Iontophoretic delivery of amino acids and amino acid derivatives across the skin in vitro.* Pharm Res, 1991. **8**(9): p. 1113-20.
38. Green, P.G., et al., *Iontophoretic delivery of a series of tripeptides across the skin in vitro.* Pharm Res, 1991. **8**(9): p. 1121-7.
39. Gay, C.L., et al., *Iontophoretic delivery of piroxicam across the skin in vitro.* Journal of Controlled Release, 1992. **22**(1): p. 57-67.
40. Hui, X., et al., *Pharmacokinetic and local tissue disposition of [14C]sodium diclofenac following iontophoresis and systemic administration in rabbits.* J Pharm Sci, 2001. **90**(9): p. 1269-76.
41. Phipps, J.B., Gyory, J. R., *Transdermal ion migration.* Adv Drug Deliv Rev, 1992. **9**: p. 137-176.

42. Pikal, M.J., *The role of electroosmotic flow in transdermal iontophoresis.* Adv Drug Deliv Rev, 2001. **46**(1-3): p. 281-305.
43. Santi, P. and R.H. Guy, *Reverse iontophoresis -- Parameters determining electroosmotic flow: I. pH and ionic strength.* Journal of Controlled Release, 1996. **38**(2-3): p. 159-165.
44. Cullander, C., *What are the pathways of iontophoretic current flow through mammalian skin?* Advanced Drug Delivery Reviews, 1992. **9**(2-3): p. 119-135.
45. Cullander, C. and R.H. Guy, *Sites of iontophoretic current flow into the skin: identification and characterization with the vibrating probe electrode.* J Invest Dermatol, 1991. **97**(1): p. 55-64.
46. Scott, E.R., et al., *Transport of ionic species in skin: contribution of pores to the overall skin conductance.* Pharm Res, 1993. **10**(12): p. 1699-709.
47. Scott, E.R., J.B. Phipps, and H.S. White, *Direct imaging of molecular transport through skin.* J Invest Dermatol, 1995. **104**(1): p. 142-5.
48. Bath, B.D., et al., *Scanning electrochemical microscopy of iontophoretic transport in hairless mouse skin. Analysis of the relative contributions of diffusion, migration, and electroosmosis to transport in hair follicles.* J Pharm Sci, 2000. **89**(12): p. 1537-49.
49. Bath, B.D., H.S. White, and E.R. Scott, *Visualization and analysis of electroosmotic flow in hairless mouse skin.* Pharm Res, 2000. **17**(4): p. 471-5.
50. Uitto, O.D. and H.S. White, *Electroosmotic pore transport in human skin.* Pharm Res, 2003. **20**(4): p. 646-52.
51. Barry, B.W., *Drug delivery routes in skin: a novel approach.* Adv Drug Deliv Rev, 2002. **54 Suppl 1**: p. S31-40.
52. Essa, E.A., M.C. Bonner, and B.W. Barry, *Human skin sandwich for assessing shunt route penetration during passive and iontophoretic drug and liposome delivery.* J Pharm Pharmacol, 2002. **54**(11): p. 1481-90.
53. Monteiro-Riviere, N.A., A.O. Inman, and J.E. Riviere, *Identification of the pathway of iontophoretic drug delivery: light and ultrastructural studies using mercuric chloride in pigs.* Pharm Res, 1994. **11**(2): p. 251-6.

54. Turner, N.G. and R.H. Guy, *Iontophoretic transport pathways: dependence on penetrant physicochemical properties.* J Pharm Sci, 1997. **86**(12): p. 1385-9.
55. Turner, N.G., et al., *Iontophoresis of poly-L-lysines: the role of molecular weight?* Pharm Res, 1997. **14**(10): p. 1322-31.
56. Regnier, V. and V. Preat, *Localization of a FITC-labeled phosphorothioate oligodeoxynucleotide in the skin after topical delivery by iontophoresis and electroporation.* Pharm Res, 1998. **15**(10): p. 1596-602.
57. Mudry, B., et al., *Quantitative structure-permeation relationship for iontophoretic transport across the skin.* J Control Release, 2007. **122**(2): p. 165-72.
58. Sieg, A., R.H. Guy, and M.B. Delgado-Charro, *Electroosmosis in transdermal iontophoresis: implications for noninvasive and calibration-free glucose monitoring.* Biophys J, 2004. **87**(5): p. 3344-50.
59. Luzardo-Alvarez, A., M.B. Delgado-Charro, and J. Blanco-Mendez, *Iontophoretic delivery of ropinirole hydrochloride: effect of current density and vehicle formulation.* Pharm Res, 2001. **18**(12): p. 1714-20.
60. Delgado-Charro, M.B. and R.H. Guy, *Characterization of convective solvent flow during iontophoresis.* Pharm Res, 1994. **11**(7): p. 929-35.
61. Marro, D., et al., *Contributions of electromigration and electroosmosis to iontophoretic drug delivery.* Pharm Res, 2001. **18**(12): p. 1701-8.
62. Hirvonen, J., Y.N. Kalia, and R.H. Guy, *Transdermal delivery of peptides by iontophoresis.* Nat Biotechnol, 1996. **14**(13): p. 1710-3.
63. Green, P.G., *Iontophoretic delivery of peptide drugs.* Journal of Controlled Release, 1996. **41**(1-2): p. 33-48.
64. van der Geest, R., et al., *Iontophoresis of bases, nucleosides, and nucleotides.* Pharm Res, 1996. **13**(4): p. 553-8.
65. Brand, R.M., A. Wahl, and P.L. Iversen, *Effects of size and sequence on the iontophoretic delivery of oligonucleotides.* J Pharm Sci, 1998. **87**(1): p. 49-52.
66. van der Geest, R., M. Danhof, and H.E. Bodde, *Iontophoretic delivery of apomorphine. I: In vitro optimization and validation.* Pharm Res, 1997. **14**(12): p. 1798-803.

67. van der Geest, R., et al., *Iontophoretic delivery of apomorphine. II: An in vivo study in patients with Parkinson's disease.* Pharm Res, 1997. **14**(12): p. 1804-10.

68. Oh, S.Y., et al., *Enhanced transdermal delivery of AZT (Zidovudine) using iontophoresis and penetration enhancer.* Journal of Controlled Release, 1998. **51**(2-3): p. 161-168.

69. Volpato, N.M., et al., *In vitro acyclovir distribution in human skin layers after transdermal iontophoresis.* Journal of Controlled Release, 1998. **50**(1-3): p. 291-296.

70. Stagni, G., M.E. Ali, and D. Weng, *Pharmacokinetics of acyclovir in rabbit skin after IV-bolus, ointment, and iontophoretic administrations.* International Journal of Pharmaceutics, 2004. **274**(1-2): p. 201-211.

71. Gibson, L.E. and R.E. Cooke, *A test for concentration of electrolytes in sweat in cystic fibrosis of the pancreas utilizing pilocarpine by iontophoresis.* Pediatrics, 1959. **23**(3): p. 545-9.

72. Galinkin, J.L., et al., *Lidocaine Iontophoresis Versus Eutectic Mixture of Local Anesthetics (EMLA(R)) for IV Placement in Children.* Anesth Analg, 2002. **94**(6): p. 1484-1488.

73. Rose, J.B., et al., *A Study of Lidocaine Iontophoresis for Pediatric Venipuncture.* Anesth Analg, 2002. **94**(4): p. 867-871.

74. DeCou, J.M., et al., *Iontophoresis: A needle-free, electrical system of local anesthesia delivery for pediatric surgical office procedures.* Journal of Pediatric Surgery, 1999. **34**(6): p. 946-949.

75. Nunez, M., et al., *Iontophoresis for anesthesia during pulsed dye laser treatment of port-wine stains.* Pediatr Dermatol, 1997. **14**(5): p. 397-400.

76. Zempsky, W.T. and T.M. Parkinson, *Lidocaine Iontophoresis for Local Anesthesia Before Shave Biopsy.* Dermatologic Surgery, 2003. **29**(6): p. 627-630.

77. Irsfeld, S., W. Klement, and P. Lipfert, *DERMAL ANAESTHESIA: COMPARISON OF EMLA CREAM WITH IONTOPHORETIC LOCAL ANAESTHESIA.* Br. J. Anaesth., 1993. **71**(3): p. 375-378.

78. Russo, J., Jr., et al., *Lidocaine anesthesia: comparison of iontophoresis, injection, and swabbing.* Am J Health Syst Pharm, 1980. **37**(6): p. 843-847.

79. Zeltzer, L., et al., *Iontophoresis versus subcutaneous injection: a comparison of two methods of local anesthesia delivery in children.* Pain, 1991. **44**(1): p. 73-78.
80. J. E. Riviere, B. Sage, and P.L. Williams, *Effects of vasoactive drugs on transdermal lidocaine iontophoresis.* Journal of Pharmaceutical Sciences, 1991. **80**(7): p. 615-620.
81. Riviere, J.E., N.A. Monteiro-Riviere, and A.O. Inman, *Determination of lidocaine concentrations in skin after transdermal iontophoresis: effects of vasoactive drugs.* Pharm Res, 1992. **9**(2): p. 211-4.
82. Bezzant, J.L., et al., *Painless cauterization of spider veins with the use of iontophoretic local anesthesia.* J Am Acad Dermatol, 1988. **19**(5 Pt 1): p. 869-75.
83. Bailey, D.C., et al., *A Comparison of the Use of Iontophoresis and Oral Non-steroidal Anti-inflammatory Medication in the Pain Management of Acute Soft Tissue Injuries in the Emergency Department Setting.* Acad Emerg Med, 2003. **10**(5): p. 470-a-.
84. Yarrobino, T.E., et al., *Lidocaine iontophoresis mediates analgesia in lateral epicondylalgia treatment.* Physiother Res Int, 2006. **11**(3): p. 152-60.
85. Brukner, P., Khan, K., *Clinical sports medicine*. 3dr ed. 2007, Sydney: McGraw-Hill. 1032.
86. Padmanabhan, R.V., et al., *In vitro and in vivo evaluation of transdermal iontophoretic delivery of hydromorphone.* Journal of Controlled Release, 1990. **11**(1-3): p. 123-135.
87. Ashburn, M.A., et al., *Iontophoretic delivery of for postoperative analgesia.* Journal of Pain and Symptom Management, 1992. **7**(1): p. 27-33.
88. Bose, S., et al., *Electrically-assisted transdermal delivery of buprenorphine.* Journal of Controlled Release, 2001. **73**(2-3): p. 197-203.
89. Fang, J.Y., et al., *The effects of iontophoresis and electroporation on transdermal delivery of buprenorphine from solutions and hydrogels.* Journal of Pharmacy and Pharmacology, 2002. **54**: p. 1329-1337.

90. Sung, K.C., J.-Y. Fang, and O. Yoa-Pu Hu, *Delivery of nalbuphine and its prodrugs across skin by passive diffusion and iontophoresis.* Journal of Controlled Release, 2000. **67**(1): p. 1-8.
91. Thysman, S. and V. Preat, *In vivo iontophoresis of fentanyl and sufentanil in rats: pharmacokinetics and acute antinociceptive effects.* Anesth Analg, 1993. **77**(1): p. 61-6.
92. Sinatra, R., *The fentanyl HCl patient-controlled transdermal system (PCTS): an alternative to intravenous patient-controlled analgesia in the postoperative setting.* Clin Pharmacokinet, 2005. **44 Suppl 1**: p. 1-6.
93. Gupta, S.K., et al., *Effect of current density on pharmacokinetics following continuous or intermittent input from a fentanyl electrotransport system.* J Pharm Sci, 1998. **87**(8): p. 976-81.
94. Gupta, S.K., et al., *Fentanyl delivery from an electrotransport system: delivery is a function of total current, not duration of current.* J Clin Pharmacol, 1998. **38**(10): p. 951-8.
95. Sathyan, G., et al., *Characterisation of the Pharmacokinetics of the Fentanyl HCl Patient-Controlled Transdermal System (PCTS). Effect of Current Magnitude and Multiple-Day Dosing and Comparison with IV Fentanyl Administration.* Clinical Pharmacokinetics, 2005. **44**: p. 7-15.
96. Gupta, S.K., et al., *Effects of application site and subject demographics on the pharmacokinetics of fentanyl HCl patient-controlled transdermal system (PCTS).* Clin Pharmacokinet, 2005. **44 Suppl 1**: p. 25-32.
97. Sathyan, G., et al., *The Effect of Dosing Frequency on the Pharmacokinetics of a Fentanyl HCl Patient-Controlled Transdermal System (PCTS).* Clinical Pharmacokinetics, 2005. **44**: p. 17-24.
98. Chelly, J.E., et al., *The Safety and Efficacy of a Fentanyl Patient-Controlled Transdermal System for Acute Postoperative Analgesia: A Multicenter, Placebo-Controlled Trial.* Anesth Analg, 2004. **98**(2): p. 427-433.
99. Viscusi, E.R., et al., *Patient-Controlled Transdermal Fentanyl Hydrochloride vs Intravenous Morphine Pump for Postoperative Pain: A Randomized Controlled Trial.* JAMA, 2004. **291**(11): p. 1333-1341.

100. Banga, A.K. and P.C. Panus, *Clinical Applications of Iontophoretic Devices in Rehabilitation Medicine.* Critical Reviews in Physical and Rehabilitation Medicine, 1998. **10**(2): p. 147-179.
101. Curdy, C., et al., *Piroxicam delivery into human stratum corneum in vivo: iontophoresis versus passive diffusion.* J Control Release, 2001. **76**(1-2): p. 73-9.
102. Tiwari, S.B. and N. Udupa, *Investigation into the potential of iontophoresis facilitated delivery of ketorolac.* International Journal of Pharmaceutics, 2003. **260**(1): p. 93-103.
103. Mathy, F.X., et al., *Study of the percutaneous penetration of flurbiprofen by cutaneous and subcutaneous microdialysis after iontophoretic delivery in rat.* J Pharm Sci, 2005. **94**(1): p. 144-52.
104. Singh, P. and M.S. Roberts, *Iontophoretic transdermal delivery of salicylic acid and lidocaine to local subcutaneous structures.* J Pharm Sci, 1993. **82**(2): p. 127-31.
105. Panus, P.C., et al., *Transdermal iontophoretic delivery of ketoprofen through human cadaver skin and in humans.* Journal of Controlled Release, 1997. **44**(2-3): p. 113-121.
106. Tashiro, Y., et al., *Iontophoretic transdermal delivery of ketoprofen: novel method for the evaluation of plasma drug concentration in cutaneous vein.* Biol Pharm Bull, 2000. **23**(5): p. 632-6.
107. Tashiro, Y., et al., *Iontophoretic transdermal delivery of ketoprofen: effect of iontophoresis on drug transfer from skin to cutaneous blood.* Biol Pharm Bull, 2000. **23**(12): p. 1486-90.
108. Panus, P.C., et al., *Ketoprofen tissue permeation in swine following cathodic iontophoresis.* Phys Ther, 1999. **79**(1): p. 40-9.
109. Fang, J., et al., *Passive and iontophoretic delivery of three diclofenac salts across various skin types.* Biol Pharm Bull, 2000. **23**(11): p. 1357-62.
110. Famaey, J.P., et al., *Ionisation with Voltaren. A multi-centre trial.* J Belge Med Phys Rehabil, 1982. **5**(2): p. 55-60.
111. Vecchini, L. and E. Grossi, *Ionization with diclofenac sodium in rheumatic disorders: a double-blind placebo-controlled trial.* J Int Med Res, 1984. **12**(6): p. 346-50.

112. Grossi, E., et al., *NSAID ionisation in the management of soft-tissue rheumatism: role played by the drug, electrical stimulation and suggestion.* Clin Exp Rheumatol, 1986. **4**(3): p. 265-7.
113. Garagiola, U., et al., *Iontophoretic administration of pirprofen or lysine soluble aspirin in the treatment of rheumatic diseases.* Clin Ther, 1988. **10**(5): p. 553-8.
114. Saggini, R., et al., *Comparison of electromotive drug administration with ketorolac or with placebo in patients with pain from rheumatic disease: a double-masked study.* Clinical Therapeutics, 1996. **18**(6): p. 1169-1174.
115. Demirtas, R.N. and C. Oner, *The treatment of lateral epicondylitis by iontophoresis of sodium salicylate and sodium diclofenac.* Clinical Rehabilitation, 1998. **12**(1): p. 23-29.
116. Chantraine, A., J.P. Ludy, and D. Berger, *Is cortisone iontophoresis possible?* Arch Phys Med Rehabil, 1986. **67**(1): p. 38-40.
117. Harris, P.R., *Iontophoresis: Clinical Research in Musculoskeletal Inflammatory Conditions.* The Journal of Orthopaedic and Sports Physical Therapy, 1982. **4**(2): p. 109-112.
118. Bertolucci, L.E., *Introduction of Antiinflammatory Drugs by Iontophoresis: Double Blind Study.* The Journal of Orthopaedic and Sports Physical Therapy, 1982. **4**(2): p. 103-108.
119. Hasson, S.M., et al., *Dexamethasone Iontophoresis: Effect on Delayed Muscle Soreness and Muscle Function.* Canadian Journal of Sport Sciences-Revue Canadienne Des Sciences Du Sport, 1992. **17**(1): p. 8-13.
120. Pellecchia, G.L., H. Hamel, and P. Behnke, *Treatement of Infrapatellar Tendinitis: A Combination of Modalities and Transverse Friction Massage Versus Iontophoresis.* Journal of Sport Rehabilitation, 1994. **3**: p. 135-145.
121. Banta, C.A., *A Prospective, Nonrandomized Study of Iontophoresis, Wrist Splinting, and Antiinflammatory Medication in the Treatment of Early-Mild Carpal-Tunnel Syndrome.* Journal of Occupational and Environmental Medicine, 1994. **36**(2): p. 166-173.

122. Reid, K.I., et al., *Evaluation of iontophoretically applied dexamethasone for painful pathologic temporomandibular joints.* Oral Surg Oral Med Oral Pathol, 1994. **77**(6): p. 605-9.
123. Li, L.C., et al., *The efficacy of dexamethasone iontophoresis for the treatment of rheumatoid arthritic knees: a pilot study.* Arthritis Care and Research, 1996. **9**(2): p. 126-132.
124. Schiffman, E.L., B.L. Braun, and B.R. Lindgren, *Temporomandibular joint iontophoresis: a double-blind randomized clinical trial.* J Orofac Pain, 1996. **10**(2): p. 157-65.
125. Gudeman, S.D., et al., *Treatment of plantar fasciitis by Iontophoresis of 0.4% dexamethasone - A randomized, double-blind, placebo-controlled study.* The American Journal of Sports Medicine, 1997. **25**(3): p. 312-316.
126. Runeson, L. and E. Haker, *Iontophoresis with cortisone in the treatment of lateral epicondylalgia (tennis elbow)--a double-blind study.* Scand J Med Sci Sports, 2002. **12**(3): p. 136-42.
127. Neeter, C., et al., *Iontophoresis with or without dexamethazone in the treatment of acute Achilles tendon pain.* Scand J Med Sci Sports, 2003. **13**(6): p. 376-82.
128. Nirschl, R.P., et al., *Iontophoretic administration of dexamethasone sodium phosphate for acute epicondylitis. A randomized, double-blinded, placebo-controlled study.* The American Journal of Sports Medicine, 2003. **31**(2): p. 189-195.
129. Gokoglu, F., et al., *Evaluation of iontophoresis and local corticosteroid injection in the treatment of carpal tunnel syndrome.* American Journal of Physical Medicine & Rehabilitation, 2005. **84**(2): p. 92-96.
130. James, M.P., R.M. Graham, and J. English, *Percutaneous iontophoresis of prednisolone--a pharmacokinetic study.* Clin Exp Dermatol, 1986. **11**(1): p. 54-61.
131. Wang, Y., et al., *Iontophoresis of hydrocortisone across hairless mouse skin: investigation of skin alteration.* J Pharm Sci, 1993. **82**(11): p. 1140-4.

132. Wang, Y., L.V. Allen, Jr., and L.C. Li, *Effect of sodium dodecyl sulfate on iontophoresis of hydrocortisone across hairless mouse skin.* Pharm Dev Technol, 2000. **5**(4): p. 533-42.
133. Glass, J.M., R.L. Stephen, and S.C. Jacobson, *The Quantity and Distribution of Radiolabeled Dexamethasone Delivered to Tissue by Iontophoresis.* International Journal of Dermatology, 1980. **19**(9): p. 519-525.
134. Petelenz, T.J., et al., *Iontophoresis of Dexamethasone - Laboratory Studies.* Journal of Controlled Release, 1992. **20**(1): p. 55-66.
135. Blackford, J., et al., *Iontophoresis of dexamethasone-phosphate into the equine tibiotarsal joint.* Journal of Veterinary Pharmacology and Therapeutics, 2000. **23**(4): p. 229-236.
136. Smutok, M.A., et al., *Failure to detect dexamethasone phosphate in the local venous blood postcathodic iontophoresis in humans.* Journal of Orthopaedic & Sports Physical Therapy, 2002. **32**(9): p. 461-468.
137. Nowicki, K.D., et al., *Effects of iontophoretic versus injection administration of dexamethasone.* Medicine and Science in Sports and Exercise, 2002. **34**(8): p. 1294-1301.
138. Kaneps, A.J., et al., *Iontophoretic administration of dexamethasone into the tarsocrural joint in horses.* Am J Vet Res, 2002. **63**(1): p. 11-14.
139. Anderson, C.R., et al., *Effects of iontophoresis current magnitude and duration on dexamethasone deposition and localized drug retention.* Physical Therapy, 2003. **83**(2): p. 161-170.
140. Anderson, C.R., et al., *Quantification of Total Dexamethasone Phosphate Delivery by Iontophoresis.* International Journal of Pharmaceutical Compounding, 2003. **7**(2): p. 155-159.
141. Leboulanger, B., R.H. Guy, and M.B. Delgado-Charro, *Reverse iontophoresis for non-invasive transdermal monitoring.* Physiol Meas, 2004. **25**(3): p. R35-50.
142. Rao, G., P. Glikfeld, and R.H. Guy, *Reverse iontophoresis: development of a noninvasive approach for glucose monitoring.* Pharm Res, 1993. **10**(12): p. 1751-5.
143. Rao, G., et al., *Reverse iontophoresis: noninvasive glucose monitoring in vivo in humans.* Pharm Res, 1995. **12**(12): p. 1869-73.

144. Potts, R.O., J.A. Tamada, and M.J. Tierney, *Glucose monitoring by reverse iontophoresis.* Diabetes Metab Res Rev, 2002. **18 Suppl 1**: p. S49-53.
145. Mize, N.K., et al., *Reverse iontophoresis: monitoring prostaglandin E2 associated with cutaneous inflammation in vivo.* Experimental Dermatology, 1997. **6**(6): p. 298-302.
146. Merino, V., et al., *Noninvasive sampling of phenylalanine by reverse iontophoresis.* J Control Release, 1999. **61**(1-2): p. 65-9.
147. Nixon, S., et al., *Reverse iontophoresis of L-lactate: In vitro and in vivo studies.* J Pharm Sci, 2007.
148. Wascotte, V., et al., *Monitoring of urea and potassium by reverse iontophoresis in vitro.* Pharm Res, 2007. **24**(6): p. 1131-7.
149. Delgado-Charro, M.B. and R.H. Guy, *Transdermal reverse iontophoresis of valproate: a noninvasive method for therapeutic drug monitoring.* Pharm Res, 2003. **20**(9): p. 1508-13.
150. Leboulanger, B., R.H. Guy, and M.B. Delgado-Charro, *Non-invasive monitoring of phenytoin by reverse iontophoresis.* Eur J Pharm Sci, 2004. **22**(5): p. 427-33.
151. Leboulanger, B., et al., *Reverse iontophoresis as a noninvasive tool for lithium monitoring and pharmacokinetic profiling.* Pharm Res, 2004. **21**(7): p. 1214-22.
152. Leboulanger, B., et al., *Lithium monitoring by reverse iontophoresis in vivo.* Clin Chem, 2004. **50**(11): p. 2091-100.
153. Wascotte, V., et al., *Assessment of the "skin reservoir" of urea by confocal Raman microspectroscopy and reverse iontophoresis in vivo.* Pharm Res, 2007. **24**(10): p. 1897-901.
154. Sieg, A., R.H. Guy, and M.B. Delgado-Charro, *Reverse iontophoresis for noninvasive glucose monitoring: the internal standard concept.* J Pharm Sci, 2003. **92**(11): p. 2295-302.
155. Sieg, A., R.H. Guy, and M.B. Delgado-Charro, *Noninvasive glucose monitoring by reverse iontophoresis in vivo: application of the internal standard concept.* Clin Chem, 2004. **50**(8): p. 1383-90.

156. Sieg, A., R.H. Guy, and M.B. Delgado-Charro, *Simultaneous extraction of urea and glucose by reverse iontophoresis in vivo.* Pharm Res, 2004. **21**(10): p. 1805-10.

157. Yan, G., et al., *Correlation of transdermal iontophoretic phenylalanine and mannitol transport: test of the internal standard concept under DC iontophoresis and constant resistance AC iontophoresis conditions.* J Control Release, 2004. **98**(1): p. 127-38.

Chapter 2. *In vitro* optimization of dexamethasone phosphate delivery by iontophoresis

In vitro optimization of dexamethasone phosphate delivery by iontophoresis

Jean-Philippe Sylvestre, M. Begoña Delgado-Charro and Richard H. Guy

Department of Pharmacy & Pharmacology, University of Bath, Claverton Down, Bath, BA2 7AY, UK.

Research paper to be submitted

Abstract

Purpose: To evaluate the effects of competing ions and electroosmosis on the transdermal iontophoresis of dexamethasone phosphate (Dex-Phos), and to identify the optimal conditions for its delivery.

Methods: The experiments were performed using pig skin, in side-by-side diffusion cells (0.78 cm^2), passing a constant current of 0.3 mA via Ag/AgCl electrodes. Dex-Phos transport was quantified for donor solutions (anodal and cathodal) containing different drug concentrations, with and without background electrolyte. Electrotransport of co-ion, citrate, and counter-ions, Na^+, K^+ and Ca^{2+}, was also quantified. The contribution of electroosmosis was evaluated by measuring the transport of the neutral marker, mannitol.

Results: Electromigration was the dominant mechanism of drug iontophoresis and reduction in electroosmotic flow directed against the cathodic delivery of Dex-Phos did not improve drug delivery. The Dex-Phos flux from the cathode was found to be optimal (transport number of ~0.012) when background electrolyte was excluded from the formulation. In this case, the transport of the drug is limited principally by the competition with counter-ions (mainly Na^+ with a transport number of ~0.8) and the mobility of the drug in the membrane.

Conclusion: Dex-Phos must be delivered from the cathode and formulated rationally, excluding mobile co-anions, to achieve optimal iontophoretic delivery.

1. Introduction

The use of corticosteroids for the treatment of a variety of musculoskeletal conditions is common practice [1-6]. Local administration of the drug by injection usually results in improved clinical outcome, at least temporarily, and limits the systemic effects associated with oral delivery [2-6]. However, while injections are generally safe, they present some disadvantages and risks (for example, postinjection pain and flare, infection, difficulty to place accurately the needle, and the need for an experienced health-care professional to perform the injection) [2, 3].

Alternatively, iontophoresis is also used in clinical practice to deliver locally corticosteroids [7-9]. Iontophoresis is a minimally invasive technique that enhances the transport of charged and highly polar molecules across the skin by the application of a small electrical current (with a current density < 0.5 mA/cm^2). The two main mechanisms of transport of this electrically enhanced method are electromigration and/or electroosmosis [8, 10, 11].

Electromigration originates from the direct interaction of the electrical field and the ions present in the formulation and the skin and will therefore enhance the transport of cationic drugs from the anode and, inversely, negatively charged drugs from the cathode. Conservation of charge requires that the sum of the electrical current carried by each ion equals the total electrical current supplied by the power source. Practically, as far as drug delivery is concerned, this means that the drug competes with all the other ions present in the system [10, 11]. The efficiency of transport, i.e., the fraction of the total charge transported by a given drug (its transport number, t_D), can be determined experimentally by measuring its flux (J_D) and applying the relation:

$$J_d = \frac{I \cdot t_d}{F \cdot z_d} \quad (eq.1)$$

where I is the total current passed, F is the Faraday's constant and z_d is the valence of the drug [12].

Electroosmosis has its origin in the fact that the skin is a negatively charged membrane at physiological pH. When an electrical potential is applied

across a membrane containing fixed charge, a bulk volume flow of solution occurs in the direction of the counterion movement [13]. This means that for the negatively charged skin, the electoosmotic flow is in the anode-to-cathode direction. This assists the transport of cations and retards that of anions. This flow of solvent carries through the skin any dissolved solute and is therefore the mechanism enhancing the transdermal delivery of neutral, polar, molecules. The electroosmotic flow is the dominant mechanism of transport for the delivery of larger molecules [11]. The drug flux due to the electroosmotic mechanism (J_D^{EO}) is proportional to the concentration (C_D) of the solute:

$$J_D^{EO} = \upsilon \cdot C_D \quad (eq.\ 2)$$

where υ is the solvent volume flow [14]. The pH and the ionic strength are the main parameters of the formulation that can be used to modulate electroosmosis by, respectively, modifying and screening the skin's charge [11, 15, 16].

Dexamethasone phosphate (Dex-Phos, MW: 472.4), a phosphorylated prodrug of dexamethasone (Dex), has undoubtedly been the most studied corticosteroid for iontophoretic delivery [8]. Its disodium salt, dexamethasone sodium phosphate (Dex-Na_2-Phos, MW 516.4), is water soluble and at physiological pH is present mainly in its dianionic form (pK_as: 1.9 and 6.4). The iontophoretic treatment of various musculoskeletal problems with Dex-Phos has been the subject of clinical studies [17-29], many of which have reported subjective beneficial effects [17-27]. However, improvement in the patient's condition is not always seen [28, 29], a fact due, perhaps, to the variety of iontophoretic conditions employed [8], and to the fact that the optimal conditions for Dex-Phos delivery have not been identified. Hence, there is a need to optimize the conditions for Dex-Phos iontophoresis.

The primary objective of this research was therefore to identify the optimal iontophoretic conditions to deliver Dex-Phos. It was a further goal to better understand the effects of: (1) the ions present in the formulation and/or in the subdermal compartment that are competing with Dex-Phos to transport the current, and (2) the electroosmotic flow, which normally occurs in the anode-to-

cathode direction; that is, against the electromigration of Dex-Phos delivered from the cathode.

2. Materials and methods

2.1. Materials

Dex (>98%) and Dex-Na_2-Phos (>98%) were purchased from Sigma-Aldrich Co. (Gillingham, UK). Solutions of injectable Dex-Na_2-Phos where obtained from American Regent (Shirley, NY) (equivalent to 4 mg/ml Dex-Phos), Faulding (Royal Leamington Spa, UK) (again equivalent to 4 mg/ml Dex-Phos) and Organon Laboratories Ltd (Cambridge, UK) (equivalent to 4.6 mg/ml of Dex-Phos). Topical lidocaine HCl 4% (Xylocaine® Topical 4%) was obtained from AstraZeneca (London, UK). Sodium chloride, potassium chloride, calcium chloride, Na_2HPO_4, KH_2PO_4, mannitol, phosphoric acid (85%) and methanesulfonic acid (99%) were from Acros (Geel, Belgium). Potassium citrate, methanol (HPLC grade), acetonitrile (far UV HPLC grade), ethyl acetate and hydrochloric acid 37% (w/w) were provided by Fisher Scientific (Loughborough, UK). NaOH 50% (ion chromatograpy eluent grade) was from Fluka (Buchs, Switzerland). Ag wire (> 99.99% purity) and AgCl (99.999%) were purchased from Sigma-Aldrich Co. (Gillingham, UK). All regents were at least analytical grade and all aqueous solutions were prepared using high purity deionized water (18.2 MΩ·cm, Barnstead Nanopure Diamond™, Dubuque, IA). The concentration of Dex-Na_2-Phos solutions are expressed in term of the Dex-Phos concentration. For example, a 0.4% Dex-Phos solution contains 4.4 mg/ml of Dex-Na_2-Phos.

2.2. Skin preparation

Porcine ears were obtained from a local piggery. Ears were cleaned under running cold water and the skin was dermatomed to a nominal thickness of 750 μm (Zimmer™ Electric Dermatome, Dover, OH). The pieces of tissue obtained (~9 cm^2) were wrapped individually in Parafilm™ and stored for no more than three months at -20°C until use.

2.3. Preparation of Dex-Phos solution at pH 4

In one experiment, a solution of Dex-Phos prepared in deionized water at pH 4 was used. To avoid the inclusion of extraneous anions inevitable when a strong acid is used to lower the pH of a Dex-Na_2-Phos solution prepared in water (typical pH = 7.5), an equimolar mixture of the diacid (dexamethasone-dihydrogen-phosphate – Dex-H_2-Phos) and its conjugate base (Dex-Na_2-Phos) was dissolved in water to obtain a final concentration of 0.4% of Dex-Phos. Dex-H_2-Phos was prepared from the disodium salt by adding one part of 37% w/w HCl to 3 parts of a solution of 25 mM Dex-Na_2-Phos in water. The insoluble dihydrogen acid precipitated and was recovered by liquid extraction using ethyl acetate. The ethyl acetate was evaporated, leaving a powder of Dex-H_2-Phos which contained only trace amounts of extraneous ions when assayed by ion chromatography.

2.4. Iontophoresis

In vitro iontophoresis experiments were performed in side-by-side diffusion cells (transport area = 0.78 cm^2). The skin was clamped between the two half cells, with the stratum corneum side facing the donor (drug-containing solution) chamber. In all experiments the subdermal compartment was filled with phosphate-buffered saline (PBS - 170 mM sodium, 1.4 mM potassium, 137 mM chloride and 18 mM phosphate) at pH 7.4. Both chambers held 3.5 ml of solution and were magnetically stirred. 30 minutes prior to iontophoresis, the cathodal chamber was filled with 3.5 ml of deionized water and the anodal chamber with 3.5 ml PBS in order to check for leaks. Both chambers were then emptied and refilled with the appropriate donor and receptor solutions before the experiment was started. In all experiments, a 0.3 mA constant current intensity (current density = 0.38 mA/cm^2) was applied for 6 hours via Ag/AgCl electrodes connected to a power source (Yokogawa 7651 Programmable DC source, Woodburn Green, UK). All experiments were performed at room temperature with a minimum of four replicates, using the skin from at least two different pigs. To measure the delivery of Dex-Phos, 1 ml of the subdermal compartment was collected and replaced by the same volume of PBS every hour for the first two hours and every half-hour thereafter. A 24-hour control

experiment, with no electrical current applied, was also performed using Dex-Phos 0.4% in water as donor solution.

Effect of delivery electrode polarity

First, the effect of the polarity of delivery electrode was verified for two formulations containing sufficient Cl^- to satisfy the electrochemistry at the anode: (i) Dex-Phos 0.4% in 0.9% NaCl, and (ii) a mixture containing one part of injectable Dex-Phos (Faulding) for two parts of lidocaine HCl.

Effect of donor composition

The Dex-Phos delivery from the cathode was measured for a variety of donor solutions described in Table 1. The effect of the concentration of the drug in absence of background electrolyte was verified for concentrations ranging from 0.2 to 0.8%. In one experiment, to ensure that the concentration of the Cl^- released by the Ag/AgCl electrode remained an order of magnitude lower than that of the drug in the donor solution (Dex-Phos 0.4% in H_2O), the latter was continuously perfused (15 ml/h), using a peristaltic pump, during the iontophoretic delivery.

Effect of electroosmosis

Two strategies to reduce electroosmosis against the delivery of Dex-Phos were then explored. The first involved pre-treatment of the skin with Ca^{2+} prior to the delivery of Dex-Phos. Calcium ions were delivered from the anode for two hours from a 100 mM $CaCl_2$ solution. The content of both chambers was then removed and the chambers and electrodes were rinsed with deionized water. Following this pre-treatment, the drug was delivered from the cathode as before from a donor solution now containing 0.4% Dex-Phos in water. The second approach involved delivery of 0.4 % Dex-Phos from a donor solution at pH 4.

In these two iontophoretic conditions and those described in Table 2, electroosmotic flow was assessed using mannitol (at 10 mM) as a marker. The flux of mannitol was evaluated in both anode-to-cathode and cathode-to-anode directions. In addition to sampling of the receptor chamber, 0.3 ml of the donor solution was also collected hourly. The passive diffusion of mannitol across the skin was also measured as a control.

Contribution of competing ions

Finally, the donor solution samples obtained in the study with mannitol, in the four cases described in Table 4, were assayed for the major competing counter-ions sodium, potassium and calcium. The concentration of the co-ion citrate in the receptor was also measured when Dex-Phos was formulated with this anion. From these values, the contributions of the main competing ions to the total current were determined.

2.5. Sample Analysis

The concentrations of Dex-Phos and Dex in the receptor chamber were assayed by high-performance liquid chromatography (ASI-100 automated sample injector, P680 pump, TCC-100 thermostated column compartment, PDA-100 diode array detector, Chromeleon software, Dionex, Sunnyvale, CA) under isocratic conditions. A mobile phase consisting of 30:70 (v:v) acetonitrile:phosphate buffer (0.15 M, pH 2) was pumped (0.75 ml/min) through a Lichrospher® 100 RP-18 (4 x 125 mm) reverse-phase column (HiChrom, Reading, UK) fitted with its guard column and thermostated at 25°C. Dexamethasone and dexamethasone phosphate concentrations were quantified via their UV absorbance at 240 nm using their respective calibration curves obtained from a minimum of five standard solutions (made from 500 ppm stock solutions in methanol appropriately diluted in PBS pH 7.4) covering the entire range of experimental concentrations. The retention times for Dex-Phos and Dex were ~3.5 and ~10.5 minutes, respectively; the detection limit for both was 0.02 µg/ml for a 25 µl injection and detection was linear up to 150 µg/ml (CV > 0.998).

Ion chromatography with suppressed conductivity detection (AS50 autosampler and thermal compartment, GP50 gradient pump, ED50 electrochemical detector, Dionex, Sunnyvale, CA) was used to measure the concentrations of sodium, potassium, calcium and citrate. For the quantification of cations, the 20 mM methanesulfonic acid eluent was pumped under isocratic conditions (1 ml/min) through an IonPac™ CS12A column (Dionex, 250 x 4 mm) thermostated at 30°C and a CSRS ULTRA II suppressor (Dionex, 4 mm) set at

a current of 62 mA. Concentrations of Na^+, K^+ and Ca^{2+} were measured against calibration curves obtained from standard solutions (at least five different concentrations) of their respective chloride salt. For the quantification of citrate anions in the receptor compartment, the 35 mM NaOH mobile phase was pumped under isocratic conditions (1 ml/min) through an IonPac™ AS16 column (Dionex, 250 x 4 mm) thermostated at 30°C and the ASRS ULTRA II suppressor (Dionex, 4 mm) set at a current of 90 mA. At least five potassium citrate solutions were used as standards.

Analysis of mannitol was performed using ion chromatography coupled with pulsed amperometric detection (Dionex, Sunnyvale, CA). The mobile phase (380 mM NaOH) was pumped (0.4 ml/min) through a CarboPac MA1 (250 x 4 mm, Dionex) column maintained at a temperature of 20°C. Again, the calibration curve was obtained from at least five standards of mannitol in PBS.

2.6. Data analysis and statistics

Linear regressions and statistics were performed using Graph Pad Prism V.4.00 (Graph Pad Software Inc., San Diego, CA). Statistical differences within multiple data sets was assessed by one-way ANOVA, followed by a Tukey's multiple comparison test. The level of statistical significance was fixed at $p < 0.05$. The fluxes were obtained from the slope of the cumulative amount delivered as a function of time for each replicate and are expressed as (mean ± SD). The reported Dex-Phos flux is the sum of the Dex-Phos and Dex fluxes into the receptor phase to account for the partial dephosphorylation of the prodrug that occurred during transdermal passage or in the receptor compartment. Transport numbers were calculated using these fluxes and equation 1. The valence used for Dex-Phos in the calculations was 2 unless otherwise stated.

3. Results

3.1. Passive diffusion control

The passive diffusion flux of Dex-Phos from a 0.4% solution in pure water after 6 hours was below the detection limit and only reached 0.13 ± 0.11 nmol/h at 24 hours. Considering that all iontophoresis experiments lasted 6 hours, the

contribution of passive diffusion could be assumed to be negligible compared to electrotransport.

3.2. Anodic vs cathodic delivery

As Dex-Phos is negatively charged (z ~ -2 at physiological pH), delivery from the cathode (with electromigration as the main driving force) was expected to be more efficient than that from the anode (electroosmosis being the only available driving force) [11]. Yet, many studies in the literature have used the anode to deliver Dex-Phos [17, 22, 30]. We therefore compared directly Dex-Phos delivery from the anode with that from the cathode. Two donor solutions, which contained sufficient Cl^- to assure good functioning of the Ag/AgCl electrode during anodic delivery, were tested: (i) 0.4% drug in normal saline, and (ii) a mixture of commercially available citrate-buffered injectable Dex-Phos (0.4% w/v, Faulding) and lidocaine HCl (4% w/v). In the former case, cathodal and anodal fluxes were 14 (± 4) and 0.3 (± 0.2) nmol/h, respectively; for the latter, the corresponding transport rates were 2.1 (± 0.6) nmol/h from the cathode and below the level of detection from the anode.

3.3. Effect of donor composition on cathodic delivery

The next logical step was to optimize delivery from the cathode. In the case of the negatively charged Dex-Phos, the efficiency of iontophoretic delivery will be reduced by the presence of competing anions in the donor solution [11]. Dex-Phos flux was therefore measured from different formulations, many of which had been used in clinical studies, containing a more or less constant concentration of the drug together with a range of background electrolytes. The Dex-Phos solutions tested, the drug's flux and the corresponding transport numbers are reported in Table 1. The pH of all solutions tested, except the mixture of Dex-Phos and lidocaine, was between 7.2 and 7.9 meaning that >85% of the drug carried a charge of -2. For the Dex-Phos/lidocaine formulation, the pH was 6.8 and only ~70% of the drug had a charge of -2. However, because in all cases the majority of the drug was doubly charged, the value for z in equation 1, which was used to determine the transport number from the flux, was assumed equal to 2.

Table 1: Effect of the donor solution composition on Dex-Phos fluxes and the derived transport numbers during cathodal iontophoresis.

Donor solution	Competing anions	Dex-Phos Flux [nmol/h]	100*Transport number
Inj. Dex-Phos 0.4% (Faulding) : Lidocaine 4% (Astra) (1:2)	Cl^- (~100 mM)[a] $Citrate^{3-}$ (~13 mM)[b]	2.1 ± 0.6	0.04 ± 0.01
Inj. Dex-Phos 0.4% (American Regent)	$Citrate^{3-}$ (~40 mM)[b]	8.8 ± 3.9	0.16 ± 0.07
Inj. Dex-Phos 0.4% (Faulding)	$Citrate^{3-}$ (~40 mM)[b]	7.5 ± 2.9	0.13 ± 0.05
Dex-Phos 0.4% in potassium citrate	$Citrate^{3-}$ (40 mM)	10 ± 5	0.18 ± 0.08
Dex-Phos 0.4% in 0.9% NaCl	Cl^- (154 mM)	14 ± 4	0.25 ± 0.07
Inj. Dex-Phos 0.5% (Organon)	None (glycerol for isotonicity)	81 ± 39	1.4 ± 0.7
Dex-Phos 0.4% in H_2O	None	69 ± 24	1.2 ± 0.4

[a]Deduced from the molar concentration of lidocaine HCl in the final solution.

[b]Determined by direct measurement with ion chromatography.

It is clear that the absence of background electrolyte (Dex-Phos in pure water and the injectable Dex-Phos formulation from Organon containing a neutral molecule, glycerol, for isotonicity) greatly improved drug delivery. These two solutions resulted in fluxes that were not significantly different.

The donor solution in 40 mM potassium citrate resulted in a Dex-Phos flux not significantly different than those from the commercially available Faulding and American Regent injectable solutions, which contain sodium citrate for isotonicity. When Dex-Phos was formulated with 0.9% (154 mM) NaCl rather than 40 mM sodium citrate, the drug flux was slightly increased ($P < 0.05$), but remained much smaller than that in the absence of background electrolyte.

Improving Dex-Phos delivery by varying the drug concentration in the donor solution in the absence of background electrolyte was then explored. In the case of cations, when no background electrolyte is present, the electromigration flux is rather independent of the drug concentration in the

donor [10, 11, 31]. For anions, however, when Ag/AgCl electrodes are used, there is Cl^- release from the electrode and the potential for competition to evolve over time [32]. Nevertheless, as shown in Figure 1, when the Dex-Phos concentration was varied by 4 fold (0.2 to 0.8% w/v), there was no significant difference in the drug flux measured after 6 hours of iontophoresis, and these values did not differ from that obtained when the donor solution was continuously perfused at the high rate of 15 ml/h to ensure that the Cl^- concentration never attained $1/10^{th}$ of that of Dex-Phos.

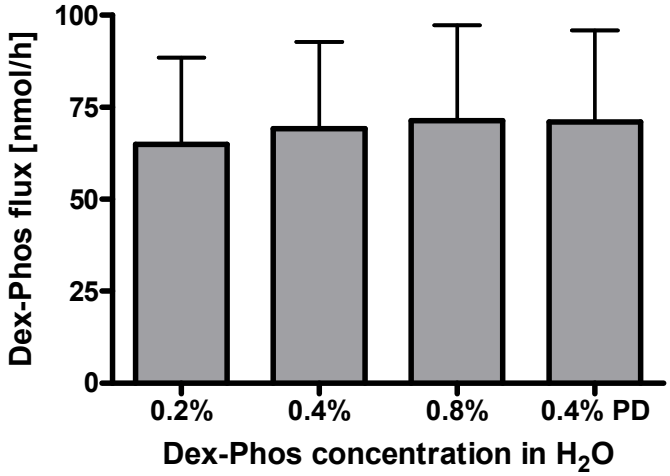

Figure 1: Dex-Phos iontophoretic flux as a function of concentration in deionized water. In the 0.4% PD experiment, the donor solution was continuously perfused with 0.4 % w/v Dex-Phos.

3.4. Effect of electroosmosis

To evaluate the effect of electroosmosis on the delivery of Dex-Phos, the flux of mannitol in the anode-to-cathode direction and its equivalent solvent flow was measured for four delivery conditions summarized in Table 2. The mannitol fluxes were also measured in the cathode-to-anode direction and were not significantly different than the negligible passive diffusion of the neutral marker (1.0 ± 0.6 nmol/h). Electroosmosis occurred against Dex-Phos delivery from the cathode. Solvent flow was maximal when no background electrolyte was present in the donor (Dex-Phos 0.4% in H_2O), the condition so far identified as 'optimal' for Dex-Phos delivery. Electroosmotic flow was significantly higher

when the background electrolyte was potassium citrate as compared to sodium chloride ($p < 0.05$). The presence of Dex-Phos in the anode, as opposed to the cathode, when normal saline acted as background electrolyte, did not significantly affect the level of electroosmotic flow.

Table 2: Mannitol flux in the anode-to-cathode direction and the corresponding solvent flow for the experimental Dex-Phos delivery conditions tested.

Dex-Phos delivery electrode	**Donor solution**	**Mannitol flux [nmol/h]**	**Solvent flow [µl/h]**
Cathode	**Dex-Phos 0.4% in H_2O**	52 ± 10	5.2 ± 1.0
Cathode	**Dex-Phos 0.4% in 40 mM potassium citrate**	40 ± 6	4.0 ± 0.6
Cathode	**Dex-Phos 0.4% in 0.9% NaCl**	24 ± 4	2.4 ± 0.4
Anode	**Dex-Phos 0.4% in 0.9% NaCl**	32 ± 9	3.2 ± 0.9

Two strategies were then explored to reduce (or reverse) the skin's negative charge, to decrease therefore the electroosmotic flow, and thereby enhance the delivery of the drug. First, Ca^{2+} cations (from a 100 mM $CaCl_2$ solution) were delivered into the skin from the anode for two hours; the donor compartment and electrodes were than washed with deionized water, before 0.4% Dex-Phos in H_2O was iontophoresed from the cathode across the Ca^{2+} loaded membrane. The rationale behind this approach was that Ca^{2+} would shield the fixed negative charges inside the skin and therefore reduce electroosmosis when the electrical field was re-applied [16]. Second, the Dex-Phos 0.4% in H_2O solution was prepared at pH 4 using a mixture of the diacid (Dex-H_2-Phos) and the disodium salt (Dex-Na_2-Phos). The idea, of course, was again to reduce the negative charge on the skin, the isoelectric point of which has been shown to be between 4 and 5 [33].

Table 3 summarizes the results obtained. Pre-treatment of skin by Ca^{2+} iontophoresis had no significant effect on Dex-Phos delivery, nor on solvent flow as measured by the electroosmotic transport of mannitol. At pH 4, on the other

hand, mannitol delivery was clearly reduced, and convective solvent flow decreased, but this had no impact on the electrotransport of Dex-Phos.

Table 3. Cathodal Dex-Phos flux, and anodal mannitol flux and the deduced electroosmotic flow when two strategies to reduce the skin's negative charge were examined.

Formulation	Dex-Phos flux [nmol/h]	Mannitol flux [nmol/h]	Solvent flow [µl/h]
Dex-Phos 0.4% in H_2O (control)	69 ± 24	52 ± 10	5.2 ± 1.0
Dex-Phos 0.4% in H_2O post-Ca^{2+}	43 ± 13	45 ± 5	4.5 ± 0.5
Dex-Phos 0.4% in H_2O at pH 4	65 ± 39	32 ± 6	3.2 ± 0.6

3.5. Transport numbers of main ionic species

Finally, the transport numbers of the main ionic species present in the different experimental conditions studied were measured (Table 4). It was clear that sodium was the major charge carrier across the skin contributing >70% in all cases. Only when the pH was reduced to 4 was the Na^+ transport lowered ($p < 0.05$) Calcium flux was significantly greater when $CaCl_2$ was iontophoresed before Dex-Phos suggesting that the pre-treatment did increase the presence of this cation in the skin (the subdermal compartment contained no external source of Ca^{2+}). Lastly, although all donor solutions eliminated Cl^-, the Ag/AgCl electrochemistry resulted in the progressive release of this anion into the donor solution such that a significant contribution to the movement of charge could be deduced for this anion.

Table 4. Transport numbers (%) of main ionic species during iontophoretic delivery of Dex-Phos from different donor solutions.

Donor / Ion	Dex-Phos 0.4% in H_2O	Dex-Phos 0.4% in H_2O, pH4	Dex-Phos 0.4% in H_2O post Ca^{2+}	Dex-Phos 0.4% in 40mM potassium citrate
Dex-Phos	1.2 ± 0.4	0.6 ± 0.4 (z = 1)	0.8 ± 0.2	0.18 ± 0.08
Na^+	81 ± 7	72 ± 4	86 ± 5	87 ± 2
K^+	1.7 ± 0.2	1.4 ± 0.3	1.4 ± 0.2	N.D.[b]
Ca^{2+}	0.11 ± 0.04	0.17 ± 0.04	0.6 ± 0.3	N.D.[b]
$Citrate^{3-}$	-	-	-	3.5 ± 0.3
$^{(a)}Cl^-$	17	26	11	9

[a]The Cl^- transport number was deduced from {100 – (the sum of all measured transport numbers)}.

[b]Not determined

4. Discussion

4.1. Electroosmosis

Dex-Phos delivery from the cathode proceeded against electroosmotic flow. The latter increased when the background electrolyte was removed from the drug solution in good agreement with previous reports [13, 15].

When Ca^{2+} was 'pre-delivered' into the skin, no impact on the subsequent electrotransport of mannitol was observed; an earlier report had indicated that electroosmosis was reduced during Ca^{2+} iontophoresis [16]. Lowering the pH of the Dex-Phos donor solution to 4 reduced the electroosmotic flow in the anode-to-cathode direction as previously observed [15, 33]. Consistent with the reduction of electroosmotic flow, the transport number of Na^+ was significantly smaller as well, reflecting a change in skin's permselectivity. However, the lower pH in the donor solution failed to improve drug delivery, suggesting that the altered electroosmotic flow has a negligible effect on the electrotransport of the drug.

Dex-Phos delivery from the anode was really inefficient and should therefore be avoided in the clinic. This conclusion contradicts an early study, in which the drug was iontophoresed *in vivo*, in a monkey, from the anode and resulted in measurable levels in deep underlying structures [30]. While the exact reasons for this discrepancy are still unclear, two comments on the latter study can be made in that respect: (i) a relatively important drug concentration (>2 µg/g) in subdermal structures (depth >3 mm) was observed after a short application of the drug (20 minutes) in absence of current, which raises the question whether the skin barrier in this animal model was compromised; and (ii) the current density used (0.94 mA/cm^2) is nearly twice the maximum tolerable level in man (0.5 mA/cm^2) [34], and could have altered the skin barrier.

4.2. Ionic competition

Not all commercially available Dex-Phos solutions are equivalent for iontophoresis. The ideal donor solution contains no background electrolyte to compete with the drug to carry charge across the skin. Trends similar to those observed in this study had been observed, but to a lesser extent due to a much higher passive diffusion contribution, when Dex-Phos was iontophoresed across an artificial membrane [35]. The Dex-Phos/lidocaine formulation resulted in a Dex-Phos flux much less than those from all other formulations, due to the high levels of chloride and citrate present. Although lidocaine hydrochloride increases the buffer capacity of the donor solution [9], this is not necessary when Ag/AgCl electrodes are used because problems associated with pH changes are avoided [32]. In fact, in the experiments reported here, the pH of the donor solution never varied by more than 0.2 pH unit over the 6 hours of iontophoresis.

Even in optimal delivery conditions, the transport number of Dex-Phos was relatively small with values just over 0.01. This is most probably due to the rather poor mobility of the drug inside the membrane resulting from its relatively large molecular weight. Similarly, the transport numbers of cations was found to fall-off rapidly with molecular weight, with values approaching zero at 400-500 Da [36]. The principal ionic species carrying electrical current during delivery of Dex-Phos from water was the subdermal counter-ion Na^+. Even when citrate

was present, the transport number of sodium was >80%. This value is in good agreement with the transport number of sodium previously observed when the competing counter-ion was gluconate, an anion with a molecular weight very similar to that of citrate [37]. Interestingly, the release of Cl^- from the Ag/AgCl cathode during iontophoresis of Dex-Phos from water did not impact significantly on drug transport over the period of experiment. Given the amount of Cl^- produced (~67 µmol corresponding to a concentration of ~19 mM), it is surprising (and, for the moment, not fully understood) that the Dex-Phos flux did not decrease somewhat after 6 hours of current passage. From a practical standpoint, however, this is a positive result as it means that an iontophoretic delivery device for Dex-Phos would not require complex characteristics, such as an ion-exchange membrane to sequester Cl^- [32].

4.3. Other practical issues

The steady-state flux of Dex-Phos from water (~70 nmol/h at a current of 0.3 mA, or ~2 µg/mA·min) translates to the delivery of about 0.16 mg from a typical current 'dose' of 80 mA·min. While this is rather less than that administered via injection (1 ml of a 0.4% w/v solution contains 4 mg), it is significantly greater than that resulting from iontophoresis of the Dex-Phos formulations containing citrate (~0.02 mg) and lidocaine (again, ~0.02 mg), as reported previously [9].

In vivo, the current 'dose' is typically delivered over 20 minutes and it seems unlikely that a steady-state flux is achieved in this time-span (in the experiments reported here (data not shown), a lag-time of about 30-60 minutes was observed). The kinetics of transport and uptake *in vivo* are typically more rapid than those seen *in vitro* due to the presence of a fully functional microcirculation which can 'clear' drug to the underlying tissue and, ultimately, the systemic circulation. Further, it is known that *in vivo* uptake and absorption can be significantly influenced by, for example, local vasoconstriction [38].

Obviously, the simple *in vitro* model used in this study cannot perfectly replicate the much more complex *in vivo* situation in man. Porcine skin is however a good model for human skin [33, 39] and it is expected that the trends observed here should still apply *in vivo*. Ultimately, well designed *in vivo* studies

will be necessary to demonstrate the efficiency of iontophoresis to deliver clinically relevant corticosteroid doses in soft tissues, and the results presented here should be of particular importance for their design.

5. Acknowledgements

This research was supported by the US National Institutes of Health (EB–001420). Injectable Dex-Phos 0.4% (American Regent) was kindly provided by the NISMAT (NY, USA). J.-P. S. thanks BIJAB, NSERC, FQRNT and Universities UK for funding.

6. References

1. Harmon, K.G. and C. Hawley, *Physician prescribing patterns of oral corticosteroids for musculoskeletal injuries.* J Am Board Fam Pract, 2003. **16**(3): p. 209-12.
2. Cole, B.J. and H.R. Schumacher, Jr., *Injectable corticosteroids in modern practice.* J Am Acad Orthop Surg, 2005. **13**(1): p. 37-46.
3. Ines, L.P. and J.A. da Silva, *Soft tissue injections.* Best Pract Res Clin Rheumatol, 2005. **19**(3): p. 503-27.
4. Bell, A.D. and D. Conaway, *Corticosteroid injections for painful shoulders.* Int J Clin Pract, 2005. **59**(10): p. 1178-86.
5. Schumacher, H.R. and L.X. Chen, *Injectable corticosteroids in treatment of arthritis of the knee.* Am J Med, 2005. **118**(11): p. 1208-14.
6. Goodyear-Smith, F. and B. Arroll, *What can family physicians offer patients with carpal tunnel syndrome other than surgery? A systematic review of nonsurgical management.* Ann Fam Med, 2004. **2**(3): p. 267-73.

7. Hamann, H., M. Hodges, and B. Evans, *Effectiveness of iontophoresis of anti-inflammatory medications in the treatment of common musculoskeletal inflammatory conditions: a systematic review.* Physical Therapy Reviews, 2006. **11**: p. 190-194.

8. Banga, A.K. and P.C. Panus, *Clinical Applications of Iontophoretic Devices in Rehabilitation Medicine.* Critical Reviews in Physical and Rehabilitation Medicine, 1998. **10**(2): p. 147-179.

9. Petelenz, T.J., et al., *Iontophoresis of Dexamethasone - Laboratory Studies.* Journal of Controlled Release, 1992. **20**(1): p. 55-66.

10. Kalia, Y.N., et al., *Iontophoretic drug delivery.* Adv Drug Deliv Rev, 2004. **56**(5): p. 619-58.

11. Delgado-Charro, M.B., Guy, R.H., *Transdermal iontophoresis for controlled drug delivery and non-invasive monitoring.* S.T.P. Pharma Sciences, 2001. **11**(6): p. 403-414.

12. Phipps, J.B., Gyory, J. R., *Transdermal ion migration.* Adv Drug Deliv Rev, 1992. **9**: p. 137-176.

13. Pikal, M.J., *The role of electroosmotic flow in transdermal iontophoresis.* Adv Drug Deliv Rev, 2001. **46**(1-3): p. 281-305.

14. Pikal, M.J. and S. Shah, *Transport mechanisms in iontophoresis. III. An experimental study of the contributions of electroosmotic flow and permeability change in transport of low and high molecular weight solutes.* Pharm Res, 1990. **7**(3): p. 222-9.

15. Santi, P. and R.H. Guy, *Reverse iontophoresis -- Parameters determining electroosmotic flow: I. pH and ionic strength.* Journal of Controlled Release, 1996. **38**(2-3): p. 159-165.

16. Santi, P. and R.H. Guy, *Reverse iontophoresis -- parameters determining electro-osmotic flow. II. Electrode chamber formulation.* Journal of Controlled Release, 1996. **42**(1): p. 29-36.

17. Harris, P.R., *Iontophoresis: Clinical Research in Musculoskeletal Inflammatory Conditions.* The Journal of Orthopaedic and Sports Physical Therapy, 1982. **4**(2): p. 109-112.

18. Bertolucci, L.E., *Introduction of Antiinflammatory Drugs by Iontophoresis: Double Blind Study.* The Journal of Orthopaedic and Sports Physical Therapy, 1982. **4**(2): p. 103-108.

19. Pellecchia, G.L., H. Hamel, and P. Behnke, *Treatement of Infrapatellar Tendinitis: A Combination of Modalities and Transverse Friction Massage Versus Iontophoresis.* Journal of Sport Rehabilitation, 1994. **3**: p. 135-145.

20. Banta, C.A., *A Prospective, Nonrandomized Study of Iontophoresis, Wrist Splinting, and Antiinflammatory Medication in the Treatment of Early-Mild Carpal-Tunnel Syndrome.* Journal of Occupational and Environmental Medicine, 1994. **36**(2): p. 166-173.

21. Schiffman, E.L., B.L. Braun, and B.R. Lindgren, *Temporomandibular joint iontophoresis: a double-blind randomized clinical trial.* J Orofac Pain, 1996. **10**(2): p. 157-65.

22. Hasson, S.M., et al., *Dexamethasone Iontophoresis: Effect on Delayed Muscle Soreness and Muscle Function.* Canadian Journal of Sport Sciences-Revue Canadienne Des Sciences Du Sport, 1992. **17**(1): p. 8-13.

23. Neeter, C., et al., *Iontophoresis with or without dexamethazone in the treatment of acute Achilles tendon pain.* Scand J Med Sci Sports, 2003. **13**(6): p. 376-82.

24. Nirschl, R.P., et al., *Iontophoretic administration of dexamethasone sodium phosphate for acute epicondylitis. A randomized, double-blinded, placebo-controlled study.* The American Journal of Sports Medicine, 2003. **31**(2): p. 189-195.

25. Gokoglu, F., et al., *Evaluation of iontophoresis and local corticosteroid injection in the treatment of carpal tunnel syndrome.* American Journal of Physical Medicine & Rehabilitation, 2005. **84**(2): p. 92-96.

26. Li, L.C., et al., *The efficacy of dexamethasone iontophoresis for the treatment of rheumatoid arthritic knees: a pilot study.* Arthritis Care and Research, 1996. **9**(2): p. 126-132.

27. Gudeman, S.D., et al., *Treatment of plantar fasciitis by Iontophoresis of 0.4% dexamethasone - A randomized, double-blind, placebo-controlled study.* The American Journal of Sports Medicine, 1997. **25**(3): p. 312-316.

28. Reid, K.I., et al., *Evaluation of iontophoretically applied dexamethasone for painful pathologic temporomandibular joints.* Oral Surg Oral Med Oral Pathol, 1994. **77**(6): p. 605-9.

29. Runeson, L. and E. Haker, *Iontophoresis with cortisone in the treatment of lateral epicondylalgia (tennis elbow)--a double-blind study.* Scand J Med Sci Sports, 2002. **12**(3): p. 136-42.

30. Glass, J.M., R.L. Stephen, and S.C. Jacobson, *The Quantity and Distribution of Radiolabeled Dexamethasone Delivered to Tissue by Iontophoresis.* International Journal of Dermatology, 1980. **19**(9): p. 519-525.

31. Marro, D., et al., *Contributions of electromigration and electroosmosis to iontophoretic drug delivery.* Pharm Res, 2001. **18**(12): p. 1701-8.

32. Scott, E.R., Phipps, B., Gyory, R., Padmanabhan, R.V., *Electrotransport System for Transdermal Delivery: A Practical Implementation of Iontophoresis*, in *Handbook of Pharmaceutical Controlled Release Technology*, D.L. Wise, Editor. 2000, Marcel Dekker: New York. p. 617-659.

33. Marro, D., R.H. Guy, and M.B. Delgado-Charro, *Characterization of the iontophoretic permselectivity properties of human and pig skin.* J Control Release, 2001. **70**(1-2): p. 213-7.

34. Ledger, P.W., *Skin biological issues in electrically enhanced transdermal delivery.* Adv Drug Deliv Rev, 1992. **9**: p. 289-307.

35. Anderson, C.R., et al., *Quantification of Total Dexamethasone Phosphate Delivery by Iontophoresis.* International Journal of Pharmaceutical Compounding, 2003. **7**(2): p. 155-159.

36. Mudry, B., et al., *Quantitative structure-permeation relationship for iontophoretic transport across the skin.* J Control Release, 2007. **122**(2): p. 165-72.

37. Mudry, B., R.H. Guy, and M.B. Delgado-Charro, *Electromigration of ions across the skin: determination and prediction of transport numbers.* J Pharm Sci, 2006. **95**(3): p. 561-9.

38. Roberts, M.S., Lai, P.M., Cross, S.E., Yoshida, N.H., *Solute Structure as a Determinant of Iontophoresic Transport*, in *Mechanisms of Transdermal Drug Delivery*, R.O. Potts, Guy, R.H., Editor. 1997, Marcel Dekker Inc.: New York. p. 291-349.

39. Mudry, B., R.H. Guy, and M.B. Delgado-Charro, *Prediction of iontophoretic transport across the skin.* J Control Release, 2006. **111**(3): p. 362-7.

Chapter 3. Iontophoresis of dexamethasone phosphate: competition with chloride ions

Iontophoresis of dexamethasone phosphate: competition with chloride ions

Jean-Philippe Sylvestre, Cristina Díaz-Marín, M. Begoña Delgado-Charro and Richard H. Guy

Department of Pharmacy & Pharmacology, University of Bath, Claverton Down, Bath, BA2 7AY, UK.

Research paper to be submitted

Abstract

Purpose: To study the competition effect of chloride released from a Ag/AgCl cathode on the iontophoretic delivery of dexamethasone phosphate (Dex-Phos).
Methods: The effect of Cl^- in the donor solution was studied during iontophoretic delivery of Dex-Phos in side-by-side diffusion cells (0.78 cm^2) across pig skin. A 0.3 mA constant current was applied via Ag/AgCl electrodes. The amount of Dex-Phos and dexamethasone (Dex) was also quantified in the stratum corneum (SC), using tape stripping, after iontophoresis and compared to a passive diffusion control. The profiles of Dex-Phos and Dex, as a function of the position in the SC, were deduced.
Results: The delivery of Dex-Phos from pure water was unaffected by the accumulation of Cl^- released by the donor cathode when the drug's concentration was 0.2 to 0.8% w/v. At 0.04%, however, Cl^- competition was significant and the drug flux was significantly reduced. Formulation of the drug in the presence of Cl^- resulted in a non-linear dependence of flux on the molar fraction of the drug. Tape stripping experiments confirmed the enhanced delivery of Dex-Phos by iontophoresis relative to passive diffusion, with Dex-Phos concentration greater inside the barrier post-iontophoresis than that in the donor. On the other hand, the total amount of drug in the SC after iontophoresis was considerably smaller than that crossing the skin per hour.

Conclusion: The iontophoretic delivery of Dex-Phos from the cathode is relatively robust to the inclusion of Cl^- in the donor solution. An increase of the drug's concentration in the SC relative to that in the donor post-iontophoresis could possibly explain this phenomenon.

1. Introduction

Iontophoresis is a technique used to enhance the transdermal passage of charged and polar molecules by the application of a small electrical current (<0.5 mA/cm^2) [1, 2]. Its symmetrical nature means that both drug delivery and clinical monitoring applications are possible [1-3]. The two principal mechanisms of transdermal iontophoretic transport are electromigration and electroosmosis. Electroosmosis refers to the net solvent flow taking place in the anode-to-cathode direction during the application of the electrical current and has its origin in the fact that the skin possesses a net negative charge at physiological pH [1, 4]. It is the dominant transport mechanism for neutral, polar molecules and ions of relatively large molecular weight [1, 2]. Electromigration, on the other hand, is the result of the direct interaction of the electrical field with the ions present in the formulation and inside the skin. The iontophoretic flux (J_d) of a drug "d" transported by electromigration is directly proportional to the intensity of the current (I) applied in agreement with Faraday's law:

$$J_d = \frac{t_d \cdot I}{F \cdot z_d} \quad (eq.1)$$

where t_d is the transport number of the drug, z_d its valence and F is Faraday's constant [5].

The drug's transport number is the fraction of the electrical current applied which is transported across the skin by the drug. The drug competes with all other ions present in the system to carry the charge and it follows that to optimize electromigration the amount of all other ions should be minimized. Ideally, co-ions are absent from the formulation, such that only the endogenous counter-ions can compete with the drug, the transport number of which is then maximized [6, 7]. When competing co-ions are present, the transport number of the drug usually depends upon its molar fraction rather than its absolute concentration [5, 8, 9].

Electrodes are critical components of an iontophoretic system as they transfer the electrical current supplied by the external circuit into ion migration across the skin [10]. Electrodes should meet a variety of performance,

compatibility and physical requirements and importantly, they should not substantially alter the delivery conditions, meaning that they should not contain or release competing ions of the same charge of the drug being delivered [10, 11]. Ag/AgCl electrodes are commonly used for iontophoretic delivery as they are biocompatible and their electrochemistry is driven at a sufficiently low potential insuring that unwanted secondary reactions are unlikely. The reactions occurring at the anode and the cathode are respectively:

$$(Anode) \quad Ag_{(M)} + Cl^-_{(aq)} \rightarrow AgCl_{(S)} + e^- \quad (eq.\,2a)$$

$$(Cathode) \quad AgCl_{(S)} + e^- \rightarrow Ag_{(M)} + Cl^-_{(aq)} \quad (eq.\,2b)$$

Importantly, compared to electrodes made of inert materials (platinum, stainless steel and glassy carbon for example), water is not hydrolyzed and pH shifts are avoided. Ag/AgCl electrodes are well adapted for the delivery of cationic drugs available as chloride salts provided there is a sufficient quantity of chloride in the donor to satisfy the electrochemistry at the anode. However, when negatively charged drugs are iontophoresed from the cathode, chloride ions released by the electrode will compete to transport the current and reduce the efficiency of delivery [12-15]. Strategies to circumvent this phenomenon have been described in the patent literature [16-18].

Previously, we observed that the iontophoretic delivery of dexamethasone phosphate (Dex-Phos) from the cathode was minimally affected by the release of Cl^- when the drug was present in the donor solution at concentrations between 0.2 and 0.8% w/v in water [Chapter 2]. The objective of this study was therefore to better understand the effects of chloride anions released from the Ag/AgCl cathode on the delivery of Dex-Phos. To this end, the iontophoresis of Dex-Phos was investigated systematically as a function of the amount of Cl^- present. In addition, tape stripping experiments were performed post-iontophoresis to assess the accumulation of the drug in the membrane.

2. Materials and methods

2.1. Materials

Dexamethasone (Dex) (>98%) and dexamethasone sodium phosphate (Dex-Na_2-Phos) (>98%) were purchased from Sigma-Aldrich Co. (Gillingham, UK). Sodium chloride, Na_2HPO_4, KH_2PO_4 and phosphoric acid (85%) were from Acros (Geel, Belgium). Potassium citrate, methanol (HPLC grade), acetonitrile (far UV HPLC grade) were from Fisher Scientific (Loughborough, UK). NaOH 50% (ion chromatography eluent grade) was from Fluka (Buchs, Switzerland). Ag wire (> 99.99% purity) and AgCl (99.999%) were purchased from Sigma-Aldrich Co. (Gillingham, UK). All regents were at least analytical grade unless stated otherwise and all aqueous solutions were prepared using high purity deionized water (18.2 MΩ·cm, Barnstead Nanopure Diamond™, Dubuque, IA). The concentration of Dex-Na_2-Phos solutions are expressed in term of the Dex-Phos concentration. For example, a 0.4% Dex-Phos solution contains 4.4 mg/ml of Dex-Na_2-Phos.

2.2. Skin preparation

Porcine ears were obtained from a local piggery. Ears were cleaned under running cold water and the skin was dermatomed to a nominal thickness of 750 μm (Zimmer™ Electric Dermatome, Dover, OH). The pieces of tissue obtained (~9 cm^2) were wrapped individually in Parafilm™ and stored for no more than three months at -20°C until use.

2.3. Iontophoresis

Iontophoresis experiments were performed *in vitro* in side-by-side diffusion cells (transport area = 0.78 cm^2) with the stratum corneum side facing the donor (drug containing solution) chamber. In all experiments the subdermal compartment was filled with phosphate-buffered saline (PBS - 170 mM sodium, 1.4 mM potassium, 137 mM chloride and 18 mM phosphate) at pH 7.4. Both chambers held 3.5 ml of solution and were magnetically stirred. In all experiments, a 0.3 mA constant current (0.38 mA/cm^2) was applied for 6 hours via Ag/AgCl electrodes connected to a power source (Yokogawa 7651

Programmable DC source, Woodburn Green, UK). All experiments were performed at room temperature with a minimum of five replicates, using skin from at least two different pigs. Every hour for the first two hours and every half-hour for the remaining 4 hours of the experiment, 1 ml of the receptor compartment was collected and replaced by the same volume of PBS.

Two series of solutions were tested. In the first set, the donor solution consisted of Dex-Phos solutions with a concentration of 0.04% w/v (0.85 mM), 0.2% (4.25 mM), 0.4% (8.5 mM) or 0.8% (17 mM) in pure water. When the donor solution was 0.4% Dex-Phos in water, in addition to sampling of the receptor chamber, 0.3 ml of the donor solution was also collected every hour and assayed for chloride. In one specific experiment, the donor solution (Dex-Phos 0.4% in H_2O) was continuously perfused (15 ml/h) through a 1.5 ml donor compartment, using a peristaltic pump, during iontophoresis. This ensured that the concentration of Cl^- never attained $1/10^{th}$ of the drug's concentration. In the second set of experiments, the donor solutions consisted in 0.4% Dex-Phos containing 0.06% w/v (10.3 mM), 0.3% (51 mM), 0.6% (103 mM) or 0.9% (154 mM) NaCl as background electrolyte.

In three experiments, for which the donor solution was Dex-Phos 0.4% in water, the amount of drug in the stratum corneum (SC) was assessed by tape stripping following (a) passive diffusion for 3h (n = 4), (b) iontophoresis for 30 minutes (n = 5), and (c) iontophoresis for 3 hours (n = 7).

At the end of the experiment, any solution remaining on the skin surface was removed using absorbent paper. The skin was then pinned to a dissecting board and a polypropylene foil template with a circular aperture (8 mm diameter) was positioned over the treated area. The SC was then removed by repeated adhesive tape-stripping (Scotch Book Tape, 3M, St. Paul, MN). Between 15 and 28 tapes were required to completely ablate the barrier. Each tape was weighed before and after stripping on a 0.1-µg precision balance (Satorius SE2-F, Epsom, UK) to determine the mass and thickness of the SC layer removed [19, 20]. Dex and Dex-Phos were completely extracted from the tapes by overnight shaking with 1 ml of 30:70 acetonitrile: pH 2 phosphate buffer. Validation of the extraction procedure involved spiking tape-stripped

samples of untreated skin with a known amount of Dex and/or Dex-Phos; recovery was (98 ± 2)% (n = 6).

2.5. Sample Analysis

The concentrations of Dex-Phos and Dex in the receptor chamber and tape extracts were assayed by high-performance liquid chromatography (ASI-100 automated sample injector, P680 pump, TCC-100 thermostated column compartment, PDA-100 diode array detector, Dionex, Sunnyvale, CA) under isocratic conditions. A mobile phase consisting of 30:70 (v:v) acetonitrile:phosphate buffer (0.15 M, pH 2) was pumped (0.75 ml/min) through a Lichrospher® 100 RP-18 (4 x 125 mm) reverse-phase column (HiChrom, Reading, UK) fitted with its guard column and thermostated at 25°C. Dex-Phos and Dex concentrations were quantified via their UV absorbance at 240 nm using their respective linear calibration curves (CV > 0.998) obtained from a minimum of five standard solutions (made from 500 ppm stock solutions in methanol appropriately diluted in PBS pH 7.4) covering the entire range of experimental concentrations. The retention times for Dex-Phos and Dex were ~3.5 and ~10.5 minutes respectively; the detection limit for both was 0.02 µg/ml for a 25 µl sample injection (used for analysis in receptor compartment) and 0.01 µg/ml for a 50 µl sample injection (used for the analysis of tape extracts).

Ion chromatography (AS50 autosampler and thermal compartment, GP50 gradient pump, ED50 electrochemical detector, Chromeleon software, Dionex, Sunnyvale, CA) was used to measure the concentrations of chloride. The 35 mM NaOH mobile phase was pumped under isocratic conditions (1 ml/min) through an IonPac™ AS16 column (Dionex, 250 x 4 mm) thermostated at 30°C and the ASRS ULTRA II suppressor (Dionex, 4 mm) set at a current of 90 mA. Here, at least five sodium chloride solutions were used as standards.

2.6. Data analysis and statistics

Linear regressions, Lowess curves and statistics were performed using Graph Pad Prism V.4.00 (Graph Pad Software Inc., San Diego, CA, USA). Statistical differences within multiple data sets was assessed by one-way ANOVA, followed by a Tukey's multiple comparison test. The level of statistical

significance was fixed at $p < 0.05$. The fluxes were obtained from the slope of the cumulative amount delivered as a function of time for each replicate and are expressed as (mean ± SD). The reported Dex-Phos flux is the sum of the Dex-Phos and Dex fluxes into the receptor phase to account for the partial dephosphorylation of the prodrug that occurred during transdermal passage or in the receptor phase. Transport numbers were calculated using these fluxes and equation 1. The valence used for Dex-Phos in the calculations was 2 in all cases since the pH of the donor solution was >7.2, meaning that at least 85% of the Dex-Phos in solution was in its dianionic form.

3. Results and discussion

3.1. Effect of Cl^-

Cl^- ions are released from the Ag/AgCl electrode into the cathode compartment at a constant rate determined by the electrical current flowing in the circuit (eq. 2b). Hence, the concentration of the competing co-ion will gradually increase in the donor solution even when it initially only contained Dex-Phos in water. Figure 1 compares the theoretical evolution of the Cl^- concentration in the 3.5 ml donor solution, as a function of time, for a current of 0.3 mA, assuming that all the chloride formed remains in the electrode compartment, with the experimentally measured values when the Dex-Phos concentration was 0.4%. The figure also shows the Cl^- concentrations predicted (dashed line) when 20% of the charge is carried by these ions liberated at the cathode. The measured values suggest that when Dex-Phos is present at a reasonably high concentration in water, the contribution of Cl^- to the transport of current is relatively modest and is less than 20% as it had been previously deduced from the measurement of the transport of the counter-ions [Chapter 2].

Earlier results showed that the Dex-Phos fluxes from 0.2%, 0.4% and 0.8% solutions in water were statistically indistinguishable, despite the fact that the times and current doses at which the Cl^- concentration reached an equivalent level to that of Dex-Phos were quite different. Respectively, these can be read from Figure 1: for 0.2% Dex-Phos, Cl^- reached the same concentration at ~80 minutes (current dose of about 24 mA·min); for 0.4% at

160 minutes (48 mA·min); for 0.8% at 320 minutes (96 mA·min). The same was true when the 0.4% Dex-Phos in water was perfused continuously to maintain the level of Cl^- at $1/10^{th}$ of this concentration (Figure 2). Only for 0.04% is the Dex-Phos flux markedly lower (see Table 1 and Figure 2); in this case Cl^- matches the Dex-Phos level after 16 minutes (4.8 mA·min).

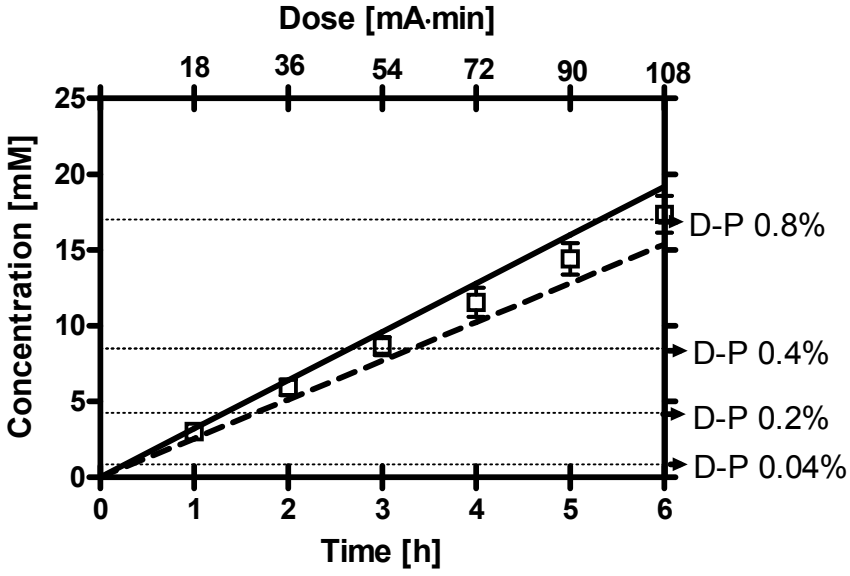

Figure 1. Theoretical evolution of Cl^- concentration in the cathode compartment either when all the ions remain in the donor (solid line) or when 20% are subsequently 'delivered' across the skin (dashed line). Experimentally measured values when the donor solution was initially 0.4% Dex-Phos in water (mean ± SD, n = 11) are shown for comparison. Also shown, are the different Dex-Phos donor concentrations in water (dotted lines).

The impact of Cl^- in the drug formulation was systematically studied and the combined results of the new experiments reported here together with those from before are summarized in Figure 2 and Table 1. Clearly, the transport of the drug is progressively hampered by an increase in the presence of the competing halide.

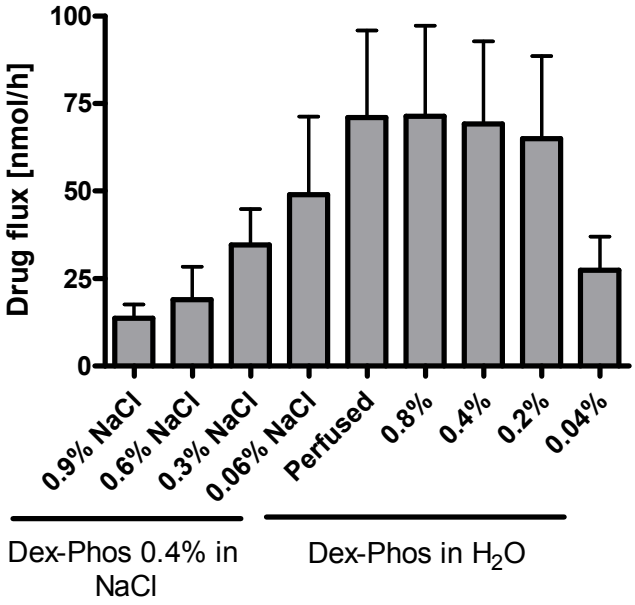

Figure 2. Dex-Phos fluxes from a donor solution containing 0.4% of the drug in various concentrations of saline, compared to those obtained when the drug was dissolved in water alone.

Table 1. Dex-Phos fluxes and transport numbers under various conditions. The initial molar fractions of the drug in the donor solutions and their evolution with the duration of iontophoresis (t) are also shown.

Experimental condition	Dex-Phos flux [nmol/h]	100*Transport number	Dex-Phos molar fraction			
			t = 0	t = 1h	t = 3h	t = 6h
Dex-Phos 0.4% in 0.9% NaCl	14 ± 4	0.25 ± 0.07	0.05	0.05	0.05	0.05
Dex-Phos 0.4% in 0.6% NaCl	19 ± 9	0.34 ± 0.16	0.08	0.07	0.07	0.07
Dex-Phos 0.4% in 0.3% NaCl	37 ± 10	0.66 ± 0.18	0.14	0.13	0.12	0.11
Dex-Phos 0.4% in 0.06% NaCl	49 ± 22	0.88 ± 0.39	0.45	0.39	0.30	0.22
Dex-Phos 0.4% in H_2O Perfused	73 ± 25	1.3 ± 0.4	1	> 0.9	> 0.9	> 0.9
Dex-Phos 0.8% in H_2O	71 ± 26	1.3 ± 0.4	1	0.84	0.64	0.47
Dex-Phos 0.4% in H_2O	69 ± 24	1.2 ± 0.4	1	0.73	0.47	0.31
Dex-Phos 0.2% in H_2O	65 ± 24	1.2 ± 0.4	1	0.57	0.31	0.18
Dex-Phos 0.04% in H_2O	27 ± 10	0.48 ± 0.18	1	0.21	0.08	0.04

Table 1 also includes the theoretically calculated molar fractions of Dex-Phos as a function of the time of iontophoresis assuming that all Cl^- released from the cathode remained in the donor solution. It is apparent that, whenever the drug's molar fraction was less than 50% after 1 hour of current passage, the Dex-Phos flux was compromised. In some cases, it is worth noting, the molar fraction of drug dropped precipitately during the 6 hours of iontophoresis; for example, from 1 to 0.18 and to 0.04, respectively, for 0.2% and 0.04% Dex-Phos in water. Nevertheless, it is intriguing to note that, despite the decreasing Dex-Phos molar fraction, the drug's iontophoretic flux over the 6-hours duration of the experiment first increased over the initial period of current passage before remaining relatively constant. This phenomenon is illustrated in Figure 3 for the two donor solutions mentioned above. In other words, the anticipated falling-off of the flux with increasing time (as has been observed for other anions, such as amino acids and peptides [12, 13], piroxicam [14] and diclofenac [15] under similar conditions) was not observed.

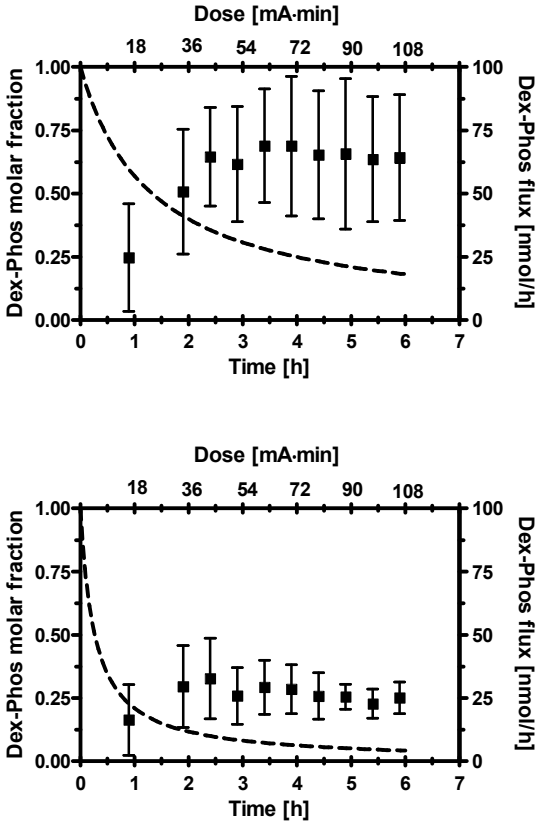

Figure 3. Measured Dex-Phos fluxes as a function of time of iontophoresis (square symbols, mean ± SD) compared to the calculated change in the molar fraction of the drug in the donor solution (dotted line) (upper panel: 0.2% Dex-Phos in water; lower panel 0.04% Dex-Phos in water).

The transport numbers reported for Dex-Phos in Table 1 do not vary linearly with the initial molar fraction of Dex-Phos in the donor solution (Figure 4). In this respect, the results diverge from those reported for small cations (Na^+, K^+, Li^+ and NH_4^+), and for drugs like lidocaine [8], but parallel those seen for quinine and propanolol, two relatively lipophilic cations believed to interact significantly with the fixed charge on the skin and to change its permselective properties [7]. The results reported here raise the question, therefore, as to whether Dex-Phos is perhaps altering the membrane in some way and/or accumulating in the tissue.

In attempting to predict the effect of co-ion competition, Phipps and Gyory derived an expression for the transport number of a drug across a

homogeneous uncharged membrane as a function of its molar fraction in the donor solution [5]:

$$t_d = \frac{\frac{t_d^0}{1-t_d^0}}{\frac{t_d^0}{1-t_d^0} + \frac{BZX}{1-t_a^0} + 1} \quad (eq.\,3)$$

where $t^0{}_d$ and $t^0{}_a$ are the transport numbers of the drug and the co-anion (Cl^-) when they are the only species present (the single anion situation), B is a proportionality constant that relates the ratio of the anion concentrations in the membrane to that in the donor solution, Z is the valence ratio of the anions and X their molar fraction ratio in the donor solution. In practice, this approach has found little practical use because there is no validated method to predict the value of the parameter B [8]. In theory, when B = 1, the concentration ratio of the co-anion and the drug is conserved inside the membrane; a value of B <1 suggests a higher concentration of the drug in the membrane relative to that of the co-anion when compared to the donor solution. The data from the experiments described here were fitted to the model assuming $t^0{}_a$ = 0.4, the reported transport number of Cl^- in the single ion situation [6] . The B value resulting in the fit was 0.3 (Figure 4) suggesting that the apparent concentration of the drug relative to Cl^- inside the skin is more important relative to that in the donor solution.

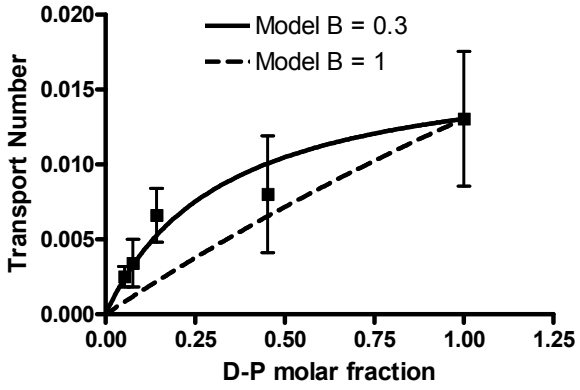

Figure 4. Transport numbers of Dex-Phos as a function of its initial molar fraction in the donor solution compared to predictions of the Phipps and Gyory model [5].

3.2. Tape-stripping

Tape-stripping experiments were performed to test directly whether Dex-Phos accumulated in the stratum corneum (SC) during iontophoretic delivery from a donor solution containing Dex-Phos 0.4% in water. Both Dex-Phos and the dephosphorylated, uncharged Dex were quantified. The results are in Table 2. When no current was applied (passive control), the amount of drug present in the SC was an order of magnitude less than that achieved post-iontophoresis. The duration of current passage influenced the amount of drug (Dex-Phos + Dex) uptake into the SC, with about 70% more being found in the SC after 3 hours compared to 30 minutes. The higher level of Dex recovered accounted for nearly all of this difference. However, the absolute drug level in the SC, even with iontophoresis, was small compared to the measured flux (~69 nmol/h) implying that “accumulation” was not a significant factor.

Table 2. Dex-Phos, Dex and {Dex-Phos + Dex} uptake into the SC after 3 hours of passive diffusion and 30 minutes and 3 hours of iontophoresis.

	Iontophoresis 3 hours	**Iontophoresis 30 minutes**	**Passive diffusion 3 hours**
Dex-Phos in SC [nmol]	4.9 ± 2.0	4.6 ± 0.9	0.41 ± 0.17
Dex in SC [nmol]	5.0 ± 1.6	1.4 ± 0.2	0.28 ± 0.06
Dex-Phos + Dex [nmol]	9.9 ± 3.3	6.0 ± 1.1	0.69 ± 0.24

As the tape-stripping experiment involved individual analysis of drug on all the strips, and quantification of the amount of SC removed (achieved gravimetrically as previously described [19]), it was possible to derive concentration profiles of Dex-Phos and Dex across the SC after passive diffusion and following either 30 minutes or 3 hours of iontophoresis (Figure 5). When no current was applied, the profiles decayed rapidly from the skin surface, intercepting the concentration axis at a level similar to that of Dex-Phos in the donor solution (8.5 mM). With iontophoresis, on the other hand, while the surface level of the drug was similar, its concentration (and that of Dex as well) then increased over the first one-third or so of the SC, before falling off towards the inner boundary of the barrier (although not always returning to zero). Dex-

Phos levels were obviously higher than Dex at 30 minutes but had become quite similar (as well as of greater absolute magnitude) by 3 hours of current passage.

The pattern observed in Figure 5 has been predicted theoretically from the Nernst-Plank equation (with the electroneutrality assumption) [21, 22], and shows that iontophoresis can enhance a drug's concentration in the membrane relative to that in the delivery formulation. Whether the increased level of Dex-Phos can account for the negligible impact of Cl^- released from the cathode in some of the experiments reported here cannot be unambiguously deduced. Certainly, it could be argued that an elevated presence of anions inside the already negatively-charged membrane would be more likely to raise the transport number of Na^+ (moving from the receiver solution into the cathode chamber) and disadvantage the migration of Cl^-, at least over the relatively short duration of these experiments.

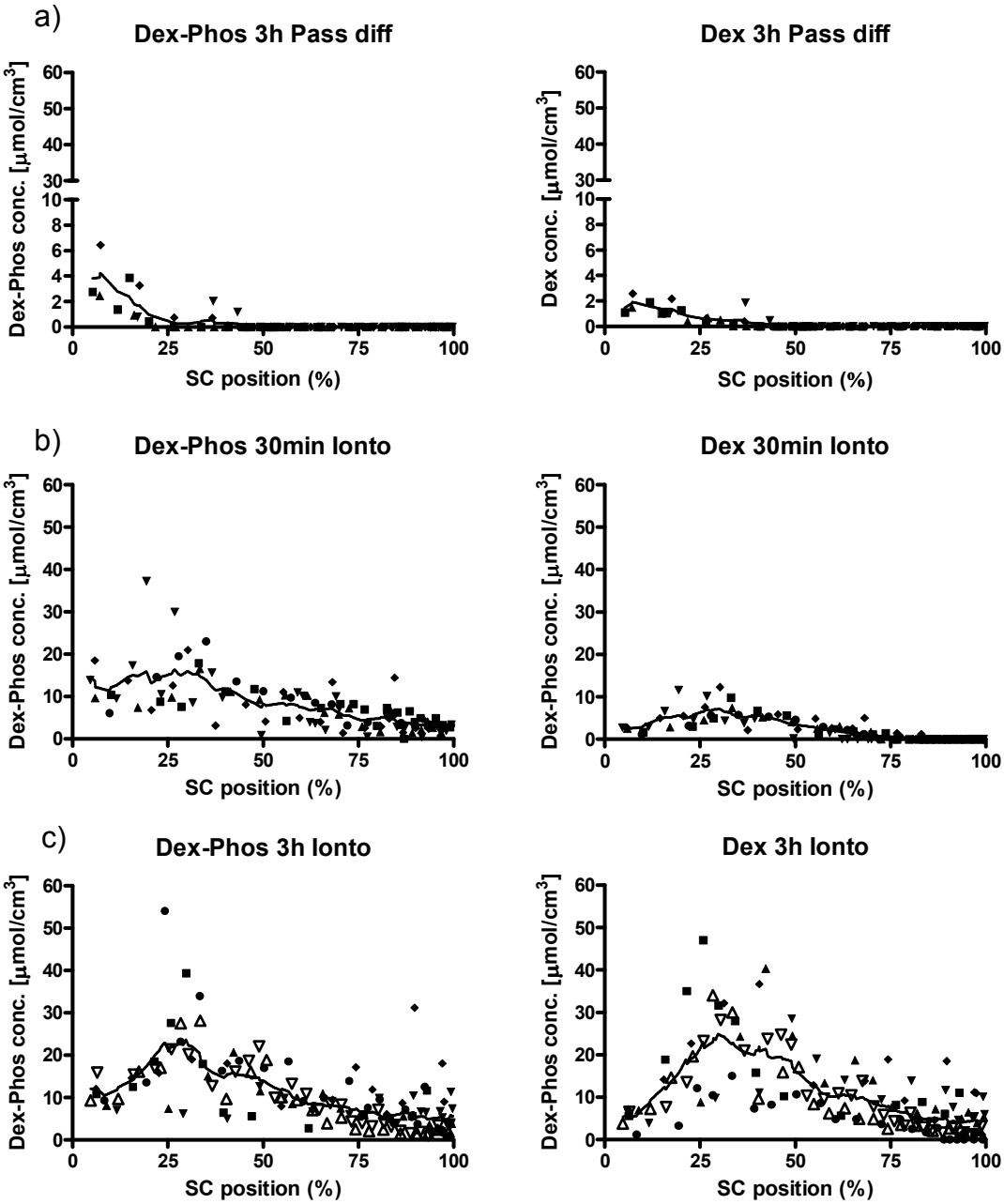

Figure 5. Dex-Phos (left panel) and Dex (right panel) concentration profiles as a function of relative position in the stratum cornum for a) 3h of passive diffusion (n = 4), b) 30 min of iontophoresis (n = 5) and c) 3h of iontophoresis (n = 7) of a solution of 0.4% Dex-Phos in H_2O. Each piece of skin is represented by a different symbol and the full line tracks the trend of the data without following a specific model (Lowess curve).

4. Conclusions

In summary, the results presented here demonstrate that the delivery of Dex-Phos from a Ag/AgCl cathode is relatively robust to the presence of Cl^- in the donor solution. From a practical standpoint, the results suggest that optimal delivery of the drug should be obtained if the cathode compartment contains sufficient Dex-Phos to ensure that its molar fraction remains >50% for the first ~20 mA·min of the dose. The exact reasons for this phenomenon are still unclear, but quantification of the drug in the SC by tape-tripping revealed that it was not due to an important absolute accumulation of the drug in this barrier. The concentration profile of the Dex-Phos inside the SC could, on the other hand, bring some new insight to this problem.

5. Acknowledgements

This research was supported by the US National Institutes of Health (EB–001420). J.-P. S. thanks BIJAB, NSERC, FQRNT and Universities UK for funding.

6. References

1. Delgado-Charro, M.B., Guy, R.H., *Transdermal iontophoresis for controlled drug delivery and non-invasive monitoring.* S.T.P. Pharma Sciences, 2001. **11**(6): p. 403-414.
2. Kalia, Y.N., et al., *Iontophoretic drug delivery.* Adv Drug Deliv Rev, 2004. **56**(5): p. 619-58.
3. Leboulanger, B., R.H. Guy, and M.B. Delgado-Charro, *Reverse iontophoresis for non-invasive transdermal monitoring.* Physiol Meas, 2004. **25**(3): p. R35-50.
4. Pikal, M.J., *The role of electroosmotic flow in transdermal iontophoresis.* Adv Drug Deliv Rev, 2001. **46**(1-3): p. 281-305.

5. Phipps, J.B., Gyory, J. R., *Transdermal ion migration.* Adv Drug Deliv Rev, 1992. **9**: p. 137-176.

6. Mudry, B., R.H. Guy, and M.B. Delgado-Charro, *Electromigration of ions across the skin: determination and prediction of transport numbers.* J Pharm Sci, 2006. **95**(3): p. 561-9.

7. Marro, D., et al., *Contributions of electromigration and electroosmosis to iontophoretic drug delivery.* Pharm Res, 2001. **18**(12): p. 1701-8.

8. Mudry, B., R.H. Guy, and M.B. Delgado-Charro, *Prediction of iontophoretic transport across the skin.* J Control Release, 2006. **111**(3): p. 362-7.

9. Mudry, B., R.H. Guy, and M.B. Delgado-Charro, *Transport numbers in transdermal iontophoresis.* Biophys J, 2006. **90**(8): p. 2822-30.

10. Scott, E.R., Phipps, B., Gyory, R., Padmanabhan, R.V., *Electrotransport System for Transdermal Delivery: A Practical Implementation of Iontophoresis*, in *Handbook of Pharmaceutical Controlled Release Technology*, D.L. Wise, Editor. 2000, Marcel Dekker: New York. p. 617-659.

11. Cullander, C., Rao, G., Guy, R.H., ed. *Why silver/silver chloride? Criteria for iontophoresis electrodes*. Prediction of Percutaneous Penetration, ed. V.J.J. K.R. Brain, K.A. Walters. Vol. 3b. 1993, STS Publishing: Cardiff. 381-390.

12. Green, P.G., et al., *Iontophoretic delivery of amino acids and amino acid derivatives across the skin in vitro.* Pharm Res, 1991. **8**(9): p. 1113-20.

13. Green, P.G., et al., *Iontophoretic delivery of a series of tripeptides across the skin in vitro.* Pharm Res, 1991. **8**(9): p. 1121-7.

14. Gay, C.L., et al., *Iontophoretic delivery of piroxicam across the skin in vitro.* Journal of Controlled Release, 1992. **22**(1): p. 57-67.

15. Hui, X., et al., *Pharmacokinetic and local tissue disposition of [14C]sodium diclofenac following iontophoresis and systemic administration in rabbits.* J Pharm Sci, 2001. **90**(9): p. 1269-76.

16. Untereker, D.F., Phipps, J.B., Cahalan, P.T., Brennan, K.R., *Iontophoresis electrode*, 1990, U.S. Patent 5,395,310.

17. Phipps, J.B., Moodie, L.C., Gyory, J.R., Theeuwes, F., *Electrotransport system with ion exchange material competitive ion capture*, 1999, U.S. Patent 6,289,249 B1.

18. Haak, R.P., *Electrotransport device having improved cathodic electrode assembly*, 1994, U.S. Patent 5,503,632.

19. Kalia, Y.N., F. Pirot, and R.H. Guy, *Homogeneous transport in a heterogeneous membrane: water diffusion across human stratum corneum in vivo.* Biophys. J., 1996. **71**(5): p. 2692-2700.

20. Herkenne, C., et al., *Pig ear skin ex vivo as a model for in vivo dermatopharmacokinetic studies in man.* Pharm Res, 2006. **23**(8): p. 1850-6.

21. Li, S.K., et al., *Influence of asymmetric donor-receiver ion concentration upon transscleral iontophoretic transport.* Journal of Pharmaceutical Sciences, 2005. **94**(4): p. 847-860.

22. Kasting, G.B., *Theoritical models for iontophoretic delivery.* Adv Drug Deliv Rev, 1992. **9**: p. 177-199.

Chapter 4. Amino acids in the stratum corneum: quantification and extraction *in vitro* by tape-stripping and reverse iontophoresis

Amino acids in the stratum corneum: quantification and extraction *in vitro* by tape-stripping and reverse iontophoresis

Camille C. Bouissou, Jean-Philippe Sylvestre, M. Begoña Delgado-Charro and Richard H. Guy

Department of Pharmacy & Pharmacology, University of Bath, Claverton Down, Bath, BA2 7AY, UK.

Research paper to be submitted

Abstract

Purpose: The skin's natural moisturizing factor (NMF) comprises a complex mixture of chemicals including most of the naturally-occurring amino acids (AAs). The quantity and distribution of these compounds are relevant to the maintenance of the barrier's hydration and general health. The goal of this research, therefore, was to characterize the AAs in the stratum corneum (SC) using tape-stripping and reverse iontophoresis.

Methods: Experiments were performed *in vitro* using porcine skin, a good model for the human membrane. Repetitive tape-stripping, solvent extraction of the layers removed and subsequent analysis by ion chromatography permitted the amounts and distribution (as a function of position or depth in the SC) of 13 AAs to be determined. These data were compared with the relatively non-invasive extraction of the same compounds by passive diffusion and by the use of reverse iontophoresis.

Results: The AAs were relatively homogeneously distributed across the SC and broadly divided into three groups (high, medium, low) in terms of total amount present. Extraction via passive diffusion or reverse iontophoresis was facile and initially rapid. As the time of extraction increased, superior quantities were recovered at the cathode (primarily carried by the electroosmotic flow) relative to those at the anode, or measured passively.

Conclusion: Overall, both tape-stripping and reverse iontophoresis provided information about the amount of AAs in the SC; the former enables a full distribution profile to be deduced, while the latter can characterize and quantify non-destructively the levels present in the horny layer.

1. Introduction

The passive loss of water across human skin is impressively regulated by the stratum corneum (SC) [1, 2]. Key to the control of skin hydration is natural moisturizing factor (NMF), a complex mixture of low molecular weight humectants. More precisely, NMF is composed primarily of free amino acids (AAs) which are derived from filaggrin [3]. Originally, profilaggrin, the precursor of filaggrin, is expressed in the keratinocytes of the granular layer [4]. As these cells differentiate into corneocytes in the SC, profilaggrin undergoes proteolysis to filaggrin. The latter is ultimately degraded into free AAs, some of which are further transformed into pyrrolidone carboxylic acid, urocanic acid, citrulline and urea [5, 6]. The constituents of NMF are very hygroscopic and can retain a large amount of water even at relatively low humidity. In effect, the skin responds to environmental changes in relative humidity by constantly rectifying the level of NMF. For example, at low relative humidity, profilaggrin expression has been reported to increase, presumably to enhance skin hydration [7]. It follows that the correct control of NMF is vital to maintain homeostasis, and also to provide the skin its natural elasticity through the plasticizing effect of water.

When NMF is compromised, the skin becomes dry and scaly and transepidermal water loss increases significantly. Equally, ichthyosis vulgaris and psoriasis vulgaris are skin disorders characterised by alteration of profilaggrin and filaggrin expression, and involve clear changes in the quality of barrier function [8, 9]. Correct and early diagnosis of filaggrin-related disorders is not straightforward, and it is interesting to ask whether the monitoring of AAs in the SC might be helpful in this regard [10]. Similarly, from a simply cosmetic viewpoint, a non-invasive tool with which to evaluate skin hydration and the overall ‘health’ of the barrier would be valuable.

Iontophoresis enhances the transfer of molecules through the skin via the application of a low electrical current (<0.5 mA/cm^2) [11]. Two transport mechanisms are operative: electromigration and electroosmosis [12]. Because iontophoresis is a symmetric process, it can be used to enhance delivery into the skin and also to extract substances from within and below the barrier to the skin surface, as exemplified by the GlucoWatch® Biographer for non-invasive

glucose monitoring in diabetics [13]. It is logical to hypothesise, therefore, that the components of NMF might also be sampled using reverse iontophoresis. This study examines this idea *in vitro* and compares the results obtained with the levels of AAs measured in the SC by extraction and analysis of repetitive tape-stripping of the barrier.

2. Materials and methods

2.1. Materials

Sodium chloride, Na_2HPO_4, KH_2PO_4 and phosphoric acid (85% w/w) were purchased from Acros (Geel, Belgium). Sodium azide, Ag wire (>99.99% purity) and AgCl (99.99%), a standard amino acids solution (17 primary amino acids in 0.1 N HCl), L-glutamine, L-asparagine, L-tryptophan and D-glucose were from Sigma-Aldrich Co. (Gillingham, UK). NaOH 50% (ion chromatography eluent grade) was obtained from Fluka (Buchs, Switzerland). Anhydrous sodium acetate (electrochemical grade) was purchased from Dionex (Sunnyvale, CA), and glacial acetic acid (HPLC grade) from Fisher Scientific (Loughborough, UK). Deionized water (18.2 MΩ·cm) was used for all aqueous solutions (Barnstead Nanopure Diamond^{TM}, Dubuque, IA).

2.2 Skin

Pig skin was gently washed under running cold water and dermatomed to a nominal 750 μm thickness (Zimmer^{TM} Electric Dermatome, Dover, OH) post-sacrifice at a local abattoir. The pieces of tissue obtained (~50 cm^2) were wrapped individually in Parafilm^{TM} and stored for no more than three months at −20°C until use. All experiments were repeated 6 times using skin from 2 different pigs and different body sites (ear and abdomen). A single piece of skin was cut into 3 smaller pieces: one used for reverse iontophoresis, the second for passive diffusion, and the third for tape-stripping.

2.3. Reverse iontophoresis

Reverse iontophoresis was performed in vertical cells, previously described [14], with a single subdermal compartment and an upper chamber divided into cathode and anode compartments. Skin was carefully clamped in place with the surface facing the electrode chambers. The latter were filled with 20 mM NaCl in 10 mM phosphate buffer at pH 7.4. The subdermal compartment contained phosphate-buffered saline (137 mM NaCl and 18 mM phosphate) at pH 7.4, which was continuously stirred throughout the experiment. Once the cell had been prepared, a constant current of 0.3 mA (0.38 mA/cm^2) was applied to Ag/AgCl electrodes from a power-supply (Yokogawa 7651 Programmable DC source, Woodburn Green, UK). The total duration of current passage was 6 hours. At 0.25, 0.5, 1, 2, 3, 4, 5, and 6 hours, the current was stopped, and the cathodal and anodal solutions were removed for analysis. The two chambers were then replenished with fresh buffer and the current was restarted.

2.4. Passive diffusion

Identical experiments to those involving reverse iontophoresis were performed except that no current was applied and that Franz cells (2 cm^2 surface area) were used.

2.5. Tape stripping

Layers of SC were progressively removed by consecutively applying and removing 20 adhesive tapes (Scotch Book Tape, 3M, St. Paul, MN). To ensure that SC was removed from the same location, a 2 cm diameter template was used. Each tape (2.5 x 2.5 cm) was weighed before and after stripping on a 0.1-µg precision balance (Sartorius SE2-F, Epsom, UK), and the thickness of SC on each tape was then determined from its mass, the area stripped, and the known density of the tissue (1 g/cm^3) [15, 16]. Finally, each tape was extracted by shaking overnight in 1 ml of an aqueous solution of sodium azide (20 mg/l).

2.6. Sample analysis

All sample solutions (from the electrode chambers, passive diffusion experiments, and the tape-strips) were passed through nylon syringe filters prior

to analysis (0.45 µm, Nalgene, Thorn Business Park, UK) by ion chromatography with integrated pulsed-amperometric detection (IC-IPAD). This approach was preferred to high-performance liquid chromatography as sample derivatization was unnecessary and good sensitivity, accuracy and reproducibility for primary and secondary amino acids was demonstrated [17, 18]. The IC-IPAD system comprised three modules: a GP50 gradient pump, an AS50 autosampler, and an ED50 electrochemical detector (Dionex, Sunnyvale, CA). AAA-certified™ disposable gold working electrodes (Dionex) were used for amino acid detection, and data acquisition was performed with Chromeleon software (Dionex). The improved gradient method for the separation of amino acids and carbohydrates was followed [19]. Briefly, a complex gradient of 4 solutions (10 mM NaOH, 250 mM NaOH, 1 mM sodium acetate in 10 mM NaOH, and 100 mM acetic acid) was pumped at a constant flow rate of 0.25 ml/min, and separation was performed on an anion exchange column (AminoPac PA10, 2 x 250 mm analytical column and 2 x 50 mm guard column, Dionex) kept at 33°C. The run time for one sample was 92 minutes (including column washing and equilibration for subsequent sample) and included an 8 minute isocratic period at 10 mM NaOH at the beginning of each run. A complex potential waveform (AAA-direct™ waveform, Dionex) versus a combination pH/Ag/AgCl reference electrode was applied at the detector to measure current at the surface of the electrode.

2.7. Data analysis and statistics

The extraction fluxes were determined for each sampling interval. The term ‘cathodal fluxes’ refers to the extractions collected from cathodal compartments. Data manipulation, linear regressions and statistics were performed using Graph Pad Prism V.4.00 (Graph Pad Software Inc., CA). When data were compared, the level of statistical significance was fixed at $p < 0.05$. Unless stated otherwise, all values are expressed as mean ± standard deviation (SD).

3. Results and discussion

3.1. Analysis of AAs by IC-IPAD

It was possible to detect and quantify 13 AAs accurately: glycine (Gly), alanine (Ala), valine (Val), leucine (Leu), isoleucine (Ile), phenylalanine (Phe), tryptophan (Trp), proline (Pro), serine (Ser), threonine (Thr), tyrosine (Tyr), asparagine (Asn) and histidine (His).

3.2. Distribution of AAs across the SC determined by tape-stripping

The average concentrations and the total amounts of the 13 AAs determined from the SC tape-stripping experiments are collected in Table 1. The results can be divided into three clear groups: (1) AAs present at high levels (ranging from 23 ± 6 to 40 ± 11 mmol/kg): Ser, Gly, Ala and His; (2) those at moderate concentrations (ranging from 7.7 ± 1.8 to 10 ± 3 mmol/kg): Thr, Pro and Leu; and (3) the rest which were the least abundant (ranging from 0.6 ± 0.1 to 3.5 ± 0.7 mmol/kg): Val, Ile, Tyr, Phe, Asn and Trp. Representative distribution profiles of an illustrative AA from each group are shown in Figure 1. All of the substances measured were homogenously distributed across the SC, with no significant difference between the levels found at the outer and inner surfaces of the barrier.

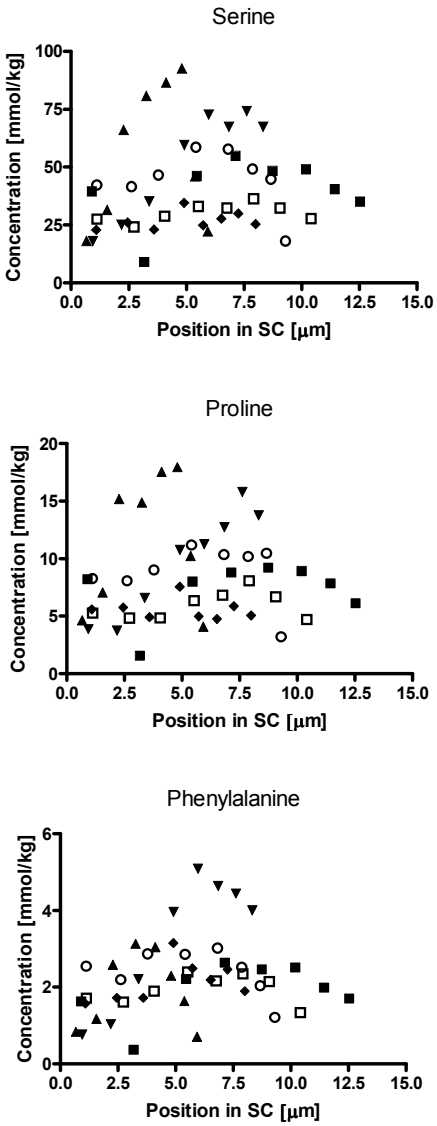

Figure 1. Concentration profiles of Ser, Pro, and Phe across the SC illustrating the behaviours of the three groups of AAs (high, medium and low concentrations) present in the barrier. Each symbol corresponds to a different piece of skin.

3.3. Passive and reverse iontophoretic extraction of AAs from the SC

The quantities of AAs extracted passively and during reverse iontophoresis were measured as a function of time. The total amounts recovered in the absence of current and found in the cathode and anode compartments, for each AA are summarized in Table 1. The rates of extraction (i.e., the instantaneous

fluxes) for the same three illustrative analytes are in Figure 2. The pattern of behaviours observed was the same regardless of the absolute level of AA in the SC. Initial fluxes were high but then settled to lower values at longer times. At 15 minutes, no differences (except for histidine – see below) between the quantities extracted iontophoretically (cathode and anode) or passively were found. With increasing time, however, for all AAs, extraction to the cathode eventually and significantly exceeded that at the anode and removed passively.

Under the conditions of the reverse iontophoretic experiments performed (pH 7.4), the AAs studied would have been essentially (>94%) zwitterionic. Preferential extraction to the cathode via electroosmosis was anticipated, therefore, and was clearly seen when the amounts recovered at 6 hours in the cathode and anode chambers were compared (Table 1). Histidine is a weakly basic AA (pK_a of side chain = 6.0 [20]) and could be partially present in the cationic form inside the SC, at least at the beginning of the experiment, due to the slightly acidic nature of the membrane [21]; the more exaggerated enhancement of extraction at the cathode for the AA is, therefore, most probably due to an increased contribution from electromigration. Indeed, for this AA, the 6-hour ratio of cathodal to anodal extraction was, on average, nearly 4 whereas, for all other species, the ratio never exceeded 2.

Passive extraction of AAs from the SC was quite efficient (and no different from that to the anode when current was applied (with the exception of His)) suggesting that the compounds were able to diffuse readily from the SC when the surface was contacted with an aqueous solution. The ‘release’ process followed $t^{1/2}$ kinetics quite closely for the whole duration of the experiment.

The origin of the AAs extracted in these experiments remains unclear. As mentioned earlier, free AAs, which form part of the NMF, are believed to result from the degradation of filaggrin in the cytosol of corneocytes. The immediate and high extraction of AAs during passive diffusion would imply that these molecules have diffused through the cornified envelope, the corneocyte lipid envelope and finally the extracellular lipid matrix relatively quickly. This is in contradiction with the generally accepted idea that the predominant route of transport through the SC is via the intercellular spaces [22]. The results suggest therefore that at least some AAs of the NMF must be present in these regions. It

has been proposed that NMF compounds could remain in the extracellular lipid matrix, but no specific reference to AAs has been made [23]. Clearly, more work is necessary to elucidate the origin of the water extractable AAs.

Table 1. Quantities of AAs in skin determined by tape-stripping, passive extraction and reverse iontophoresis (mean ± SD; n = 6).

AA	[AA] in SC from tape-stripping (mmol/kg)	AA removed from SC by tape stripping (nmol/cm^2)	AA extracted:		
			at cathode (nmol/cm^2)	at anode (nmol/cm^2)	by passive diffusion (nmol/cm^2)
Ser	40 ± 11	37 ± 9	68 ± 15	45 ± 12	47 ± 12
Gly	25 ± 6	23 ± 6	53 ± 16	38 ± 14	34 ± 7
Ala	24 ± 8	22 ± 4	39 ± 8	25 ± 8	26 ± 6
His	23 ± 6	21 ± 4	37 ± 5	10 ± 4	23 ± 6
Thr	10 ± 3	10 ± 2	16 ± 4	10 ± 3	10 ± 3
Pro	7.9 ± 2.3	7.3 ± 1.5	14 ± 3	8.5 ± 2.1	8.5 ± 2.7
Leu	7.7 ± 1.8	7.3 ± 2.1	12 ± 3	7.2 ± 2.6	9.4 ± 2.8
Val	3.5 ± 0.7	3.4 ± 1.0	7.3 ± 2.2	3.6 ± 1.2	4.7 ± 1.2
Ile	3.2 ± 0.6	3.0 ± 0.8	5.8 ± 1.7	3.4 ± 1.0	4.5 ± 1.5
Tyr	3.4 ± 0.5	3.2 ± 0.6	4.0 ± 1.2	2.5 ± 0.6	3.0 ± 0.9
Phe	2.2 ± 0.4	2.1 ± 0.5	3.1 ± 1.3	1.9 ± 0.4	2.3 ± 0.8
Asn	1.9 ± 0.5	1.8 ± 0.6	2.9 ± 1.2	1.8 ± 0.8	2.4 ± 1.0
Trp	0.6 ± 0.1	0.5 ± 0.2	0.6 ± 0.3	0.3 ± 0.1	0.4 ± 0.2
Glucose	1.7 ± 1.4	1.4 ± 0.7	3.6 ± 3.0	1.4 ± 0.8	1.0 ± 0.8

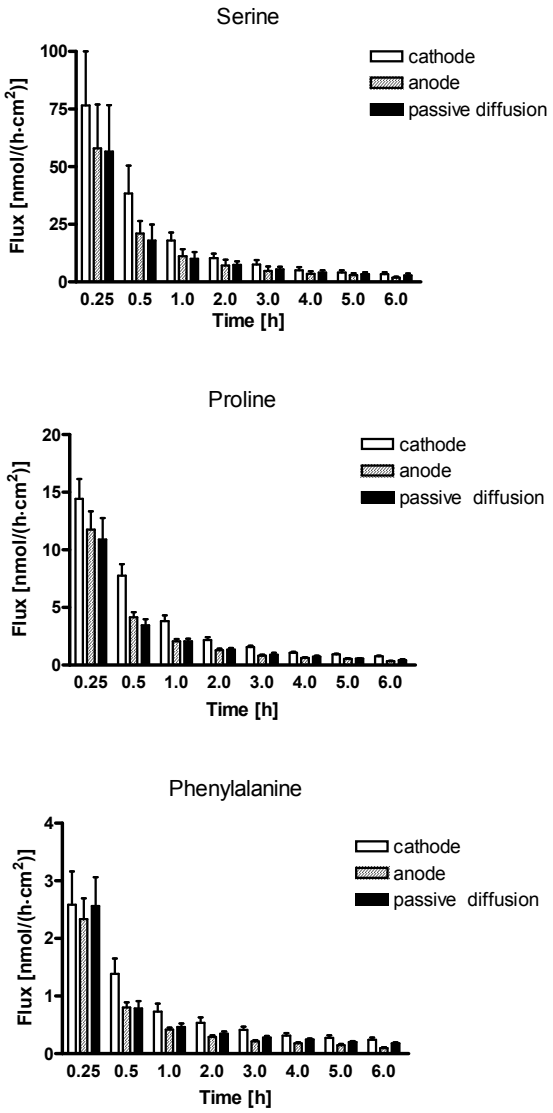

Figure 2. Passive and reverse iontophoretic (cathode and anode) extraction fluxes as a function of time of Ser, Pro and Phe illustrating the behaviours of the three groups of AAs (high, medium and low concentrations) present in the barrier.

Perhaps not surprisingly, the total amounts of AAs extracted passively correlated well with the quantities recovered from the tape-stripping experiments (Figure 3). With increasing time of extraction, the slope of the regression with the passive data approached a value of 1 suggesting that the non-invasive extraction had depleted the SC reservoir of AAs. Cathodal extraction proved to be more efficient in extracting AAs from the skin (Table 1), suggesting that reverse iontophoresis may be able to sample sites deeper than the SC. This possibility becomes more evident when the extraction fluxes from 3 to 6 hours are compared (Table 2). It is observed, for 11 out of 13 AAs, that the ratio of average cathodal to passive fluxes significantly exceeded unity. Further, when the cumulative amounts extracted as a function of time are compared, and are also considered relative to the mean amounts (±SD) of the quantities recovered from the tape-stripping experiments, the enhanced efficiency of reverse iontophoresis to the cathode is apparent (Figure 4). The extent to which this finding might be exploited further is addressed in a subsequent paper [Chapter 5].

Parenthetically, Figure 5 illustrates the cumulative amounts of His extracted by reverse iontophoresis to the cathode and by passive diffusion. In contrast to Figure 4, the almost immediate differentiation between with and without current is striking for the reason already discussed and the ability of iontophoresis to continue to pull the AA from the tissue is evident.

Passive diffusion

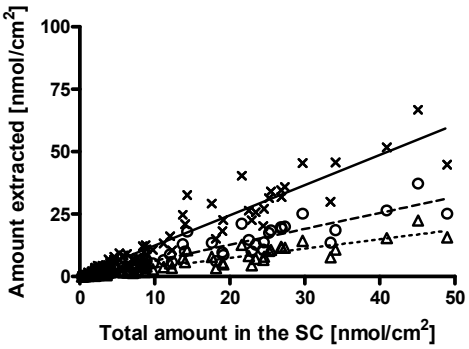

Cathode

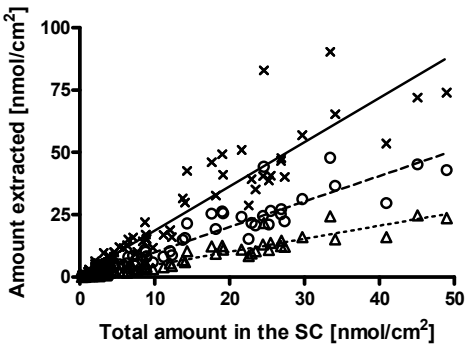

Figure 3. Correlation between the amounts of AAs extracted passively, and by reverse iontophoresis to the cathode, after 15 minutes (triangles), 1 hour (circles), and 6 hours (crosses), with the quantities removed in the SC tape-stripping experiments. Linear regressions through the data are shown.

Table 2. Comparison of average cathodal extraction fluxes and passive diffusion between 3 and 6 hours (mean ± SD, n = 6).

AA	Flux to cathode [nmol/(h·cm^2)]	Passive flux [nmol/(h·cm^2)]	Ratio of cathodal to passive fluxes
Ser	4.1 ± 1.2	3.4 ± 1.0	1.2
Gly	3.7 ± 1.2	2.3 ± 0.6	1.6
Ala	2.7 ± 0.6	1.7 ± 0.5	1.6
His	1.8 ± 0.4	1.8 ± 0.5	1.0
Thr	1.1 ± 0.3	0.8 ± 0.2	1.4
Pro	0.9 ± 0.2	0.6 ± 0.2	1.5
Leu	1.1 ± 0.3	0.8 ± 0.3	1.4
Val	0.6 ± 0.3	0.4 ± 0.1	1.5
Ile	0.5 ± 0.2	0.4 ± 0.1	1.3
Tyr	0.4 ± 0.1	0.3 ± 0.1	1.3
Phe	0.3 ± 0.1	0.2 ± 0.1	1.5
Asn	0.2 ± 0.1	0.2 ± 0.1	1.0
Trp	0.05 ± 0.03	0.03 ± 0.01	1.7
Glucose	0.4 ± 0.3	0.06 ± 0.05	6.7

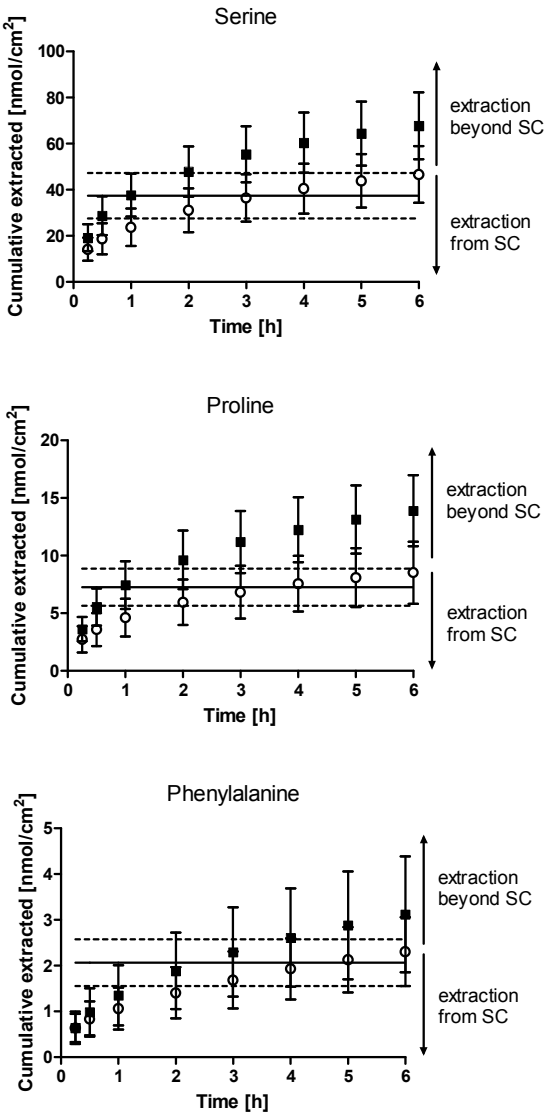

Figure 4. Cumulative extraction of Ser, Pro and Phe as a function of time by reverse-iontophoresis at the cathode (filled squares) and by passive diffusion (open circles). The quantities of the AAs present in the SC determined by tape-stripping (mean = solid line; ±SD = dashed lines) are shown for comparison.

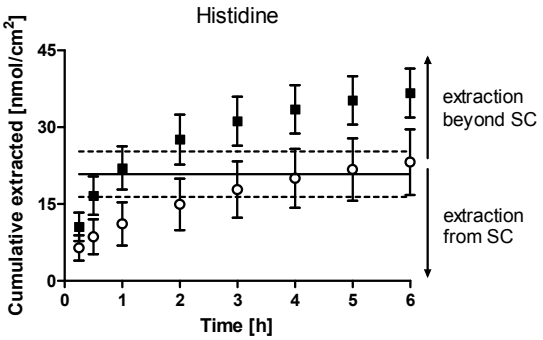

Figure 5. Cumulative extraction of histidine as a function of time by reverse-iontophoresis at the cathode (filled squares) and by passive diffusion (open circles). The quantity of the AA present in the SC determined by tape-stripping (mean = solid line; ±SD = dashed lines) is shown for comparison.

Finally, it is also appropriate to comment on the data obtained for glucose in these experiments. The presence of glucose in the SC has been demonstrated [24], and the need to deplete this reservoir for the application of non-invasive monitoring of blood sugar by reverse iontophoresis has been recognized in the development of the GlucoWatch® Biographer. From the results in Table 1 and 2, the store of glucose in the SC is confirmed and the efficiency of iontophoresis to then pull the analyte from the deeper tissues is very obvious: the cathodal flux from 3 to 6 hours surpassed the corresponding passive transport rate by nearly 7-fold.

4. Conclusions

This investigation shows that AA sampling from the skin can be accomplished by tape-stripping, by passive extraction and by reverse iontophoresis. Tools to examine quantitatively the key components of NMF, and hence the SC's hydration status, are suggested therefore. The advantage of tape-stripping is that it samples uniquely the SC and can produce a full concentration profile of the AAs across the barrier. The procedure, on the other hand is relatively invasive. Passive extraction is a benign procedure and also reveals the quantities of the analytes in the SC (but without the distribution profiles);

however, 6 hours are needed to pull out all the AAs which are present in the SC. Reverse iontophoresis to the cathode is more efficient and can shorten the time needed to fully sample the SC to only ~3 hours for zwitterionic AAs, even less for only partially charged species like His (see Figures 4 and 5, respectively). Furthermore, reverse iontophoresis can also “interrogate” deeper into the skin, and this represents an opportunity worthy of further exploration.

5. Acknowledgements

This research was supported by the US National Institutes of Health (EB–001420). J.-P. S. thanks BIJAB, NSERC, FQRNT and Universities UK for funding.

6. References

1. Rawlings, A.V., et al., *Stratum corneum moisturization at the molecular level.* J Invest Dermatol, 1994. **103**(5): p. 731-41.
2. Madison, K.C., *Barrier function of the skin: "La Raison d'Etre" of the epidermis.* Journal of Investigative Dermatology, 2003. **121**(2): p. 231-241.
3. Horii, I., et al., *Histidine-rich protein as a possible origin of free amino acids of stratum corneum.* Current problems in dermatology, 1983. **11**: p. 301-315.
4. Dale, B.A., et al., *Characterization of two monoclonal antibodies to human epidermal keratohyalin: reactivity with filaggrin and related proteins.* Journal of Investigative Dermatology, 1987. **88**(3): p. 306-313.
5. Scott, I.R., C.R. Harding, and J.G. Barrett, *Histidine-rich protein of the keratohyalin granules : Source of the free amino acids, urocanic acid and pyrrolidone carboxylic acid in the stratum corneum.* Biochimica et Biophysica Acta (BBA) - General Subjects, 1982. **719**(1): p. 110-117.

6. Marstein, S., E. Jellum, and L. Eldjarn, *The concentration of pyroglutamic acid (2-pyrrolidone-5-carboxylic acid) in normal and psoriatic epidermis, determined on a microgram scale by gas chromatography.* Clin Chim Acta, 1973. **49**(3): p. 389-95.

7. Scott, I.R. and C.R. Harding, *Filaggrin breakdown to water binding compounds during development of the rat stratum corneum is controlled by the water activity of the environment.* Developmental Biology, 1986. **115**(1): p. 84-92.

8. Sybert, V.P., B.A. Dale, and K.A. Holbrook, *Ilchthyosis vulgaris: identification of a defect in synthesis of filaggrin correlated with an absence of keratohyaline granules.* Journal of Investigative Dermatology, 1985. **84**(3): p. 191-194.

9. Ghadially, R., J.T. Reed, and P.M. Elias, *Stratum corneum structure and function correlates with phenotype in psoriasis.* Journal of Investigative Dermatology, 1996. **107**(4): p. 558-564.

10. Denda, M., et al., *Stratum corneum sphingolipids and free amino acids in experimentally-induced scaly skin.* Arch Dermatol Res, 1992. **284**(6): p. 363-7.

11. Kalia, Y.N., et al., *Iontophoretic drug delivery.* Advanced Drug Delivery Reviews, 2004. **56**(5): p. 619-658.

12. Leboulanger, B., R.H. Guy, and M.B. Delgado-Charro, *Reverse iontophoresis for non-invasive transdermal monitoring.* Physiological Measurement, 2004. **25**(3): p. R35-R50.

13. Potts, R.O., J.A. Tamada, and M.J. Tierney, *Glucose monitoring by reverse iontophoresis.* Diabetes Metab Res Rev, 2002. **18 Suppl 1**: p. S49-53.

14. Glikfeld, P., et al., *A new system for in vitro studies of iontophoresis.* Pharm Res, 1988. **5**(7): p. 443-6.

15. Kalia, Y.N., F. Pirot, and R.H. Guy, *Homogeneous transport in a heterogeneous membrane: water diffusion across human stratum corneum in vivo.* Biophys. J., 1996. **71**(5): p. 2692-2700.

16. Herkenne, C., et al., *Pig ear skin ex vivo as a model for in vivo dermatopharmacokinetic studies in man.* Pharm Res, 2006. **23**(8): p. 1850-6.

17. Hanko, V.P. and J.S. Rohrer, *Determination of amino acids in cell culture and fermentation broth media using anion-exchange chromatography with integrated pulsed amperometric detection.* Anal Biochem, 2004. **324**(1): p. 29-38.

18. Jandik, P., J. Cheng, and N. Avdalovic, *Analysis of amino acid-carbohydrate mixtures by anion exchange chromatography and integrated pulsed amperometric detection.* J Biochem Biophys Methods, 2004. **60**(3): p. 191-203.

19. *An Improved Gradient Method for the AAA-Direct™ Separation of Amino Acids and Carbohydrates in Cmplex Sample Matrices*. 2006, Dionex corporation: Sunnyvale, CA. p. 12.

20. Murray, R.K., Granner, D.K., Mayes, P.A., Rodwell, V.W., *Harper's Biochemistry*. 25th ed. 2000, Stamford, CT: Appleton&Lange. 927.

21. Schmid-Wendtner, M.H. and H.C. Korting, *The pH of the skin surface and its impact on the barrier function.* Skin Pharmacol Physiol, 2006. **19**(6): p. 296-302.

22. Hadgraft, J., *Skin deep.* Eur J Pharm Biopharm, 2004. **58**(2): p. 291-9.

23. Rawlings, A.V., *Sources and role of stratum corneum hydration*, in *Skin barrier*, P.M. Elias and K.R. Feingold, Editors. 2006, Taylor & Francis: New York. p. 399-425.

24. Rao, G., et al., *Reverse iontophoresis: noninvasive glucose monitoring in vivo in humans.* Pharm Res, 1995. **12**(12): p. 1869-73.

Chapter 5. Reverse iontophoresis of amino acids: identification and separation of stratum corneum and subdermal sources *in vitro*

Reverse iontophoresis of amino acids: identification and separation of stratum corneum and subdermal sources *in vitro*

Jean-Philippe Sylvestre, Camille C. Bouissou, M. Begoña Delgado-Charro and Richard H. Guy

Department of Pharmacy & Pharmacology, University of Bath, Claverton Down, Bath, BA2 7AY, UK.

Research paper to be submitted

Abstract

Purpose: To apply reverse iontophoresis as a minimally-invasive tool to determine amino acid (AA) content in the stratum corneum (SC) and subdermally.

Methods: *In vitro* experiments were performed in which electrode compartments, initially containing a simple buffer were separated by excised porcine skin from a subdermal chamber containing a mixture of 14 amino acids (at concentrations of 0.1, 0.25 and 0.5 mM) and glucose (at 1, 2.5 and 5 mM) in a buffered electrolyte at pH 7.4. Iontophoresis at 0.3 mA (0.38 mA/cm^2) was applied and the extraction of the analytes to the anode and cathode was measured as a function of time.

Results: As expected, extraction to the cathode for the essentially neutral analytes involved was more efficient. Initial samples obtained during the first hour or two of iontophoresis primarily extracted the amino acids from the SC. The fluxes observed in the latter half of the 6-hour experiment, on the other hand, correlated well with the corresponding subdermal concentrations.

Conclusion: Once the 'reservoir' of amino acids in the SC has been depleted, reverse iontophoresis can be used to monitor the subdermal concentrations of the analytes. The procedure appears to be most useful for compounds which are present at lower quantities in the SC.

1. Introduction

Amino acids (AAs) are the constituents of myriad proteins responsible for a diverse array of vital functions essential to life [1]. Genetic defects affecting the metabolism of AAs, such as phenylketonuria, can result in severe problems if undetected and/or left untreated. In neonates, therefore, the levels of AAs are often measured in a blood sample to screen for such hereditary disorders [1, 2]. Free AAs are also involved in important metabolic processes. For example, tryptophan and glutamate are precursors of the neurotransmitters serotonin (5-HT) and γ-aminobutyrate (GABA), respectively. Moreover, changes in AA blood levels have been linked to fatigue in athletes [3, 4] and post-operative patients [5]. It follows that there is potential to explore the development of a minimally-invasive (i.e., needle-free) method to monitor free AA levels in blood.

Reverse iontophoresis is such an approach that enhances the extraction of (charged and polar) substances through the skin by the application of a small electrical current (< 0.5 mA/cm^2) [6]. The method has been successfully employed in the GlucoWatch® Biographer [7] to continuously monitor blood glucose.

The flux of a solute extracted by reverse iontophoresis (J_s) is the sum of the contributions of passive diffusion (J_P), electromigration (J_{EM}) and electroosmosis (J_{EO}):

$$J_s = J_P + J_{EM} + J_{EO} \quad (eq.1)$$

Electromigration results from the direct interaction between a charged solute and the electrical field. Electroosmosis arises from the fact that the skin is negatively charged under normal physiological conditions; application of an electrical field therefore induces a net solvent (water) flow in the anode-to-cathode direction [8]. The solute flux of electroosmotic origin (J_{EO}) is proportional, at least to a first approximation, to the solute's subdermal concentration (C_s):

$$J_s^{EO} = \upsilon \cdot C_s \quad (eq.2)$$

where υ is the solvent volume flow [9]. The third, passive contribution (J_P) is typically small relative to J_{EM} and J_{EO}.

The application of reverse iontophoresis to the skin provokes molecular transport towards the cathode by all three mechanisms. In the case of zwitterionic amino acids and glucose, the first molecules to reach the skin surface originate from the outermost layer of the membrane, the stratum corneum (SC). AAs form an important part (>50%) of the SC's natural moisturizing factor (NMF) [10-12] and the initial extraction of this source of analytes is highly significant, whether an iontophoretic current is applied or not [Chapter 4]. Nevertheless, previous *in vitro* experiments have shown that, with increasing time of current passage, the SC "reservoir" of the AAs is depleted and that subsequent extraction is 'pulling' molecules from deeper within the skin [Chapter 4]. It follows that the technique has the potential to sample AAs (just as it has with glucose) which are in equilibrium with systemic levels.

The goal of this work, therefore, was to validate this hypothesis and to verify that the extraction rates of AAs as iontophoresis proceeds are correlated with their subdermal concentrations. Glucose extraction was used as a positive control. At the same time, the experiments performed served to differentiate the SC and subdermal sources of the extracted AAs and provided guidance, therefore, on the manner in which the technique might be used to probe these different compartments.

2. Materials and methods

2.1. Chemicals

Sodium chloride, sodium phosphate (dibasic), potassium phosphate (monobasic) and phosphoric acid (85%) were from Acros (Geel, Belgium). Sodium hydroxide (50%, ion chromatography eluent grade) was from Fluka (Buchs, Switzerland). Sodium azide, D-glucose, silver wire (> 99.99% purity) and silver chloride (99.999%) were purchased from Sigma-Aldrich Co. (Gillingham, UK). The 20 primary AAs in powder form and the AA standard solution (containing 17 primary amino acids in 0.1 N HCl) were from Sigma (Gillingham, UK). Sodium acetate (anhydrous, electrochemical grade) was from Dionex (Sunnyvale, CA) and glacial acetic acid (HPLC grade) from Fisher Scientific (Loughborough, UK). All chemicals were at least of reagent grade

unless stated otherwise and all aqueous solutions were prepared using high-purity deionized water (18.2 MΩ·cm, Barnstead Nanopure Diamond™, Dubuque, IA).

2.2. Skin preparation

Pig skin was gently washed under running cold water post-sacrifice at a local abattoir. The skin was then dermatomed to a nominal thickness of 750 μm (Zimmer™ Electric Dermatome, Dover, OH). The tissue samples obtained (~9 cm^2) were wrapped individually in Parafilm™ and stored for no more than three months at -20°C until use.

2.3. Reverse iontophoresis

Experiments were performed in vertical cells, described elsewhere [13], having the two electrode chambers on epidermal side of the skin. The area of skin exposed in each chamber was 0.8 cm^2. The subdermal compartment volume was ~7 ml. A constant current (Yokogawa 7651 Programmable DC source, Woodburn Green, UK) of 0.3 mA (0.38 mA/cm^2) was applied via Ag/AgCl electrodes. The extraction solution was 20 mM NaCl in 10 mM phosphate buffer at pH 7.4.

The magnetically stirred subdermal compartment contained a solution of the 20 primary AAs at concentrations of 0.1, 0.25 or 0.5 mM and glucose at 1, 2 or 5 mM in either (a) phosphate-buffered saline (PBS, 137 mM NaCl and 18 mM phosphate) at pH 7.4, or (b) phosphate buffer (PB) alone at the same pH. The anodal and cathodal chambers were filled with 0.8 ml of the extraction solution and current was applied for 6 hours in total. Every hour, the entire contents of the electrode compartments were removed for analysis and replenished with fresh solution. Samples were filtered with 0.45 μm nylon syringe filters (Nalgene, Thorn Business Park, UK) and stored at -20°C.

2.4. Analytical method

Extraction samples were analyzed for amino acids and glucose using ion chromatography coupled with integrated pulsed-amperometric detection (IC-IPAD) as previously described [Chapter 4] (AminoPac PA10 column set, AS50

autosampler and thermal compartment, GP50 gradient pump, ED50 electrochemical detector, Chromeleon software (Dionex, Sunnyvale, CA)). The improved gradient method for the separation of amino acids and carbohydrates was followed [14-18]. The run time for one sample was 92 minutes (including column washing and equilibration for the subsequent sample) and included an 8-minute isocratic period with 10 mM NaOH at the beginning of each run. Integrated pulsed amperometric detection at the surface of a AAA-certified™ disposable gold working electrode (Dionex) was performed by the application of the AAA-direct™ waveform versus a combination pH/Ag/AgCl reference electrode.

2.5. Data analysis and statistics

Extraction fluxes were determined for each sampling interval. The equivalent volume flow (υ) was calculated from the flux and the subdermal concentration using equation 2. Data manipulation, linear regressions and statistics were performed using Graph Pad Prism V.4.00 (Graph Pad Software Inc., San Diego, CA). Linear regressions were tested for significance by ANOVA. When data were compared, the level of statistical significance was fixed at $p < 0.05$. Unless stated otherwise, all values are expressed as mean ± standard deviation (SD) of six replicates obtained using skin (from the abdomen or ears) from two pigs.

3. Results and discussion

3.1. Reverse iontophoresis

Of the 20 primary AAs and glucose, 15 molecules were successfully quantified: glucose, asparagine (Asn), alanine (Ala), threonine (Thr), glycine (Gly), valine (Val), seronine (Ser), proline (Pro), isoleucine (Ile), leucine (Leu), methionine (Met), histidine (His), phenylalanine (Phe), tyrosine (Tyr) and tryptophan (Trp). Arginine, glutamine and cysteine coeluted with other substances and could not be assessed, while lysine, aspartate and glutamate were detected with insufficient precision to be quantified. All compounds measured, therefore, were essentially neutral (zwitterionic in the case of the AAs) at pH 7.4 and transported to the skin surface by electroosmosis and passive diffusion.

The behaviour observed, in terms of the rate and extent of extraction, was the same for both background electrolytes used in the subdermal compartment. The saline-free buffer allowed for a higher electroosmotic flow as anticipated when the ionic strength was reduced [8, 19].

The extraction fluxes of three representative AAs (Ser, Pro and Phe, illustrating examples of those present in the SC at high, medium and low levels [Chapter 4]), as a function of time and of subdermal concentration, are shown in Figure 1. For all AAs measured, and for glucose, extraction to the cathode was significantly higher than that to the anode (paired t-test, $p < 0.05$), in accord with a cation-permselective membrane.

For the AAs, which are most abundant in the SC (Ser, Gly, Ala, His), the extracted fluxes were not very sensitive to the subdermal levels, suggesting that the 'reservoir' of these compounds, requires a significant period to be fully depleted (as indicated in an earlier study in which no AAs were added to the subdermal solution) [Chapter 4]. The extraction was initially very high and then decayed over time, consistent with classic release behaviour from a membrane initially loaded with solute [20].

In contrast, the AAs least present in the SC (Phe, Trp, Met, Asn, Tyr, Ile, Val) as well as glucose, revealed a clear relationship between extraction flux and subdermal concentration over the entire duration of the extraction. In this case, the relatively small SC 'reservoir' of these compounds is quickly depleted and reverse iontophoresis samples the subdermal space. At the highest AA concentrations, there is no obvious drop-off in the extraction flux with increasing time of current passage, implying that even at the earliest times, the contribution of the SC source of AAs is negligible relative to that originating from the subdermal space.

Logically, the behaviour of the AAs present in the SC at intermediate levels (Pro, Thr, Leu) fall between the two extremes just described, with the extraction fluxes becoming more obviously sensitive to the subdermal levels at higher concentrations and longer times of current passage.

For all AAs, replacement of PBS with PB in the subdermal chamber enhanced the fluxes observed by roughly a factor of four except for the earliest periods of extraction of the AAs most abundant in the SC.

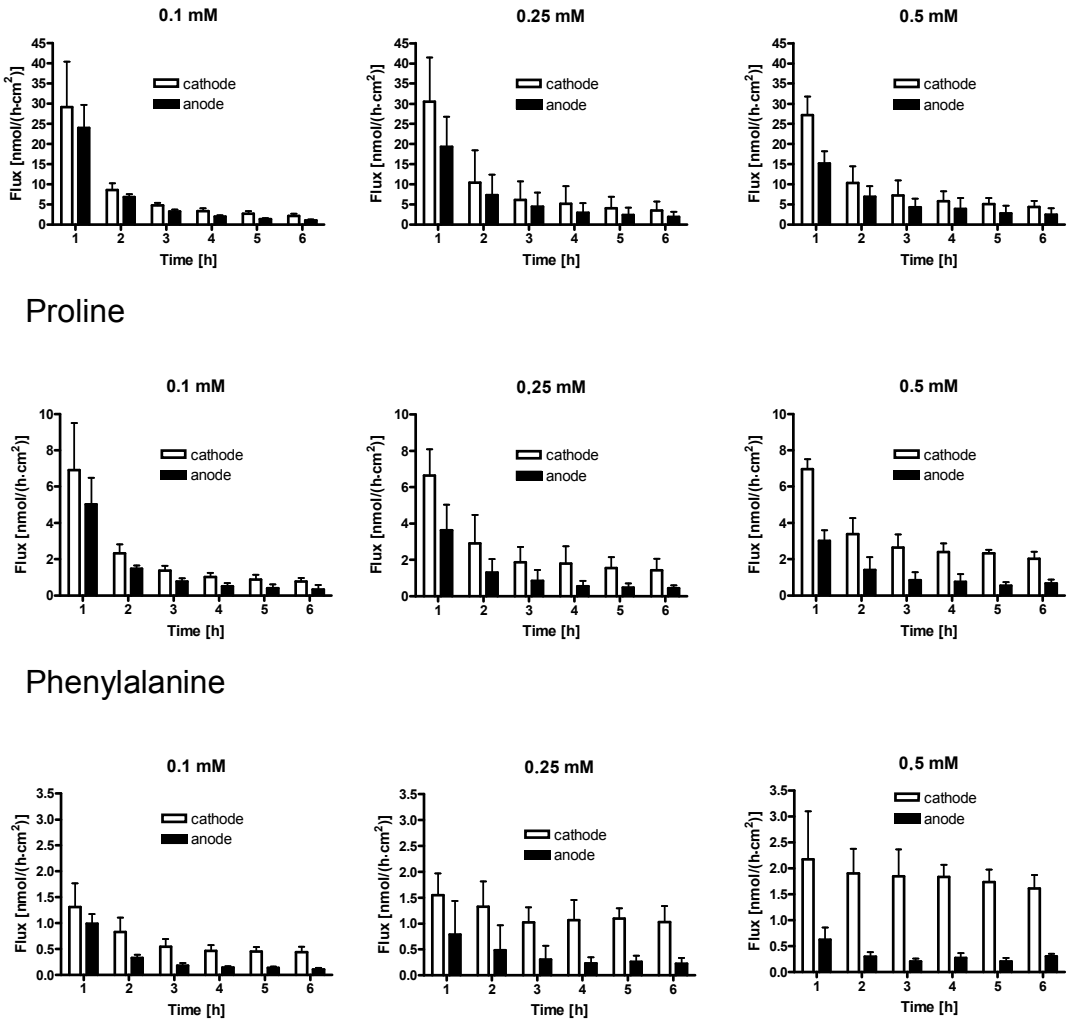

Figure 1. Iontophoretic extraction fluxes at the cathode and anode as a function of time and subdermal concentrations of Ser, Pro and Phe, when the subdermal electrolyte was PBS at pH 7.4.

3.2. Apparent electroosmotic solvent flow

For all AAs, at the three subdermal concentrations tested and for both PBS and PB background electrolytes, the extraction fluxes to the anode during the 3-6 hour period of current passage were relatively constant. When these values were normalized by the corresponding subdermal concentration, an apparent electroosmotic flow was determined in accord with equation 2. The results for the PBS experiments are collected in Figure 2 (those obtained with PB as

background electrolyte are substantially similar except that the apparent convective flows are about 4-fold higher); also shown for comparison are the amounts of AAs determined in the SC by tape-striping [Chapter 4]. The normalized fluxes were evaluated relative to those measured for glucose, the electroosmotic extraction of which after 3 hours of iontophoresis is known to originate uniquely from the subdermal compartment (the skin depot having been completely cleared by this time).

Clearly, the AAs, which are most abundant in the SC, demonstrated normalized fluxes which were significantly higher than those for glucose, signalling that these extractions included an important contribution from the SC 'reservoir'. These relative contributions became smaller as the subdermal concentrations increased. For the least present AAs in the SC, on the other hand, their normalized fluxes were comparable to that of glucose, indicating that their extraction was originating exclusively from the subdermal space.

From a practical standpoint, the results imply that while reverse iontophoretic monitoring of systemic AA levels may be possible in theory, there are clearly some important limitations. First, for the most abundant AAs in the SC, the time necessary to deplete this depot is more than 6 hours and the probability, therefore, that useful information can be obtained from the subdermal compartment is negligible. Second, for AAs which are present at low levels in the SC, although the approach looks more promising (in that it is possible to show a correlation between extraction flux and the subdermal concentration), the actual *in vivo* concentration ranges of these species in the systemic compartment is often less than 0.1 mM. There is an issue of assay sensitivity as a result, as well as a concern that even the low SC levels of these AAs may overwhelm the contribution to the extracted flux from the systemic source. The greatest potential value of the approach concerns AAs, which are at low concentrations in the SC and in the plasma, but which show large positive deviations in the latter compartment when a pathology exists. For example, in phenylketonuria, plasma concentrations can exceed 1 mM [21], a dramatic increase over the normal range of 35-80 μM [22]. A monitoring system in children afflicted with this metabolic disease may represent, therefore, a practically useful device.

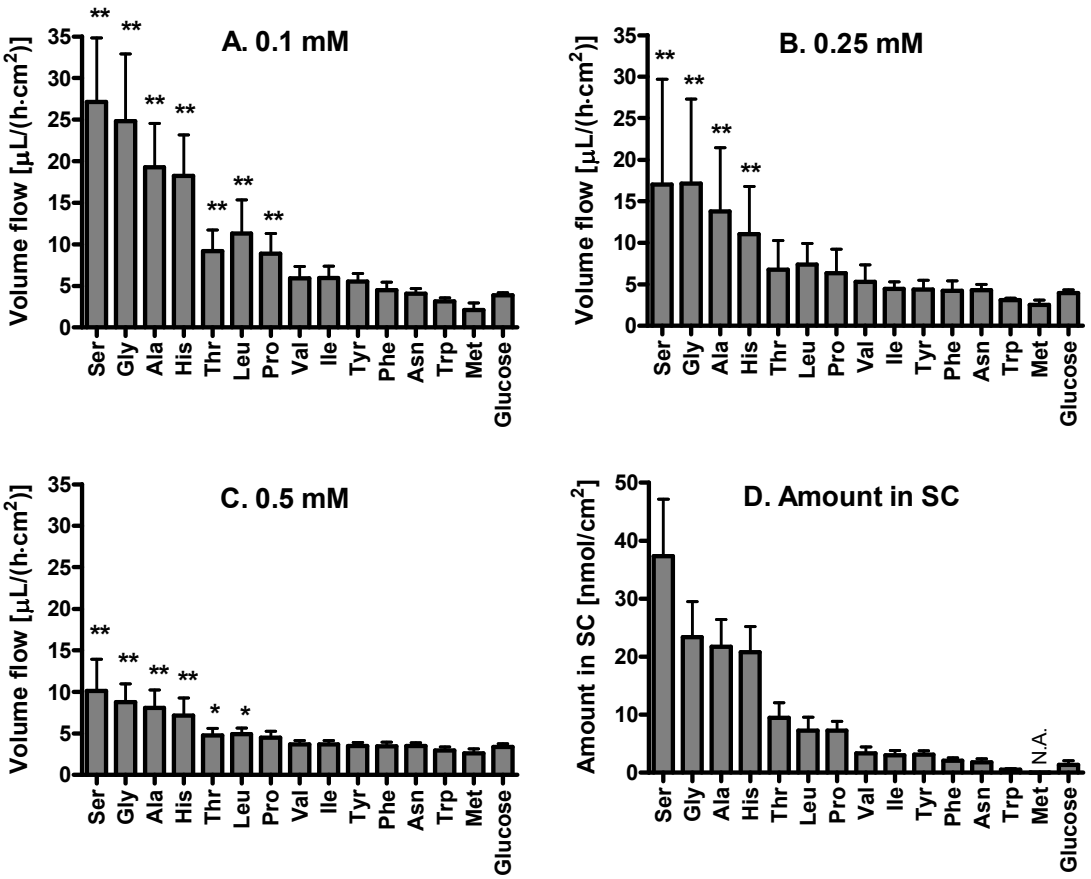

Figure 2. Panels A, B, C – AA and glucose cathodal extraction fluxes (during the 3-6 hour period) normalized by the subdermal concentration (mean ± SD) in PBS background electrolyte. Values significantly different from that for glucose (Anova followed by a Dunnett's test) are indicated with asterisks (** $p < 0.01$, * $p < 0.05$). Panel D displays the previously measured amounts of the AAs in the SC (mean ± SD) form tape-stripping experiments [Chapter 4]. Amount of Met in SC was below quantification limit.

3.3. Separating SC and subdermal sources of AAs

Figure 3 shows that the AAs extracted to the cathode in the first hour of iontophoresis correlated very well with the corresponding amounts measured in the SC in a previously reported tape-stripping experiment (see Panel D of Figure 2) [Chapter 4]. Regardless of the subdermal concentration of the AAs, almost all the individual data points fell within the 95% confidence interval of the regression obtained (slope = 0.88 ± 0.05) when no AAs were introduced into the solution beneath the skin. This means that the ratio of the amounts extracted by reverse iontophoresis to those measured in the tape-stripping did not deviate

appreciably from unity and demonstrates that the initial period of current passage is sampling, to all intents and purposes, only the SC. The contrast to glucose, in that case, is striking. When the subdermal concentrations of glucose are set at 1, 2.5 and 5 mM, respectively, the amounts extracted at the cathode in the first hour are ~4, 6 and 12 times greater than the quantity recovered from the SC by tape-stripping.

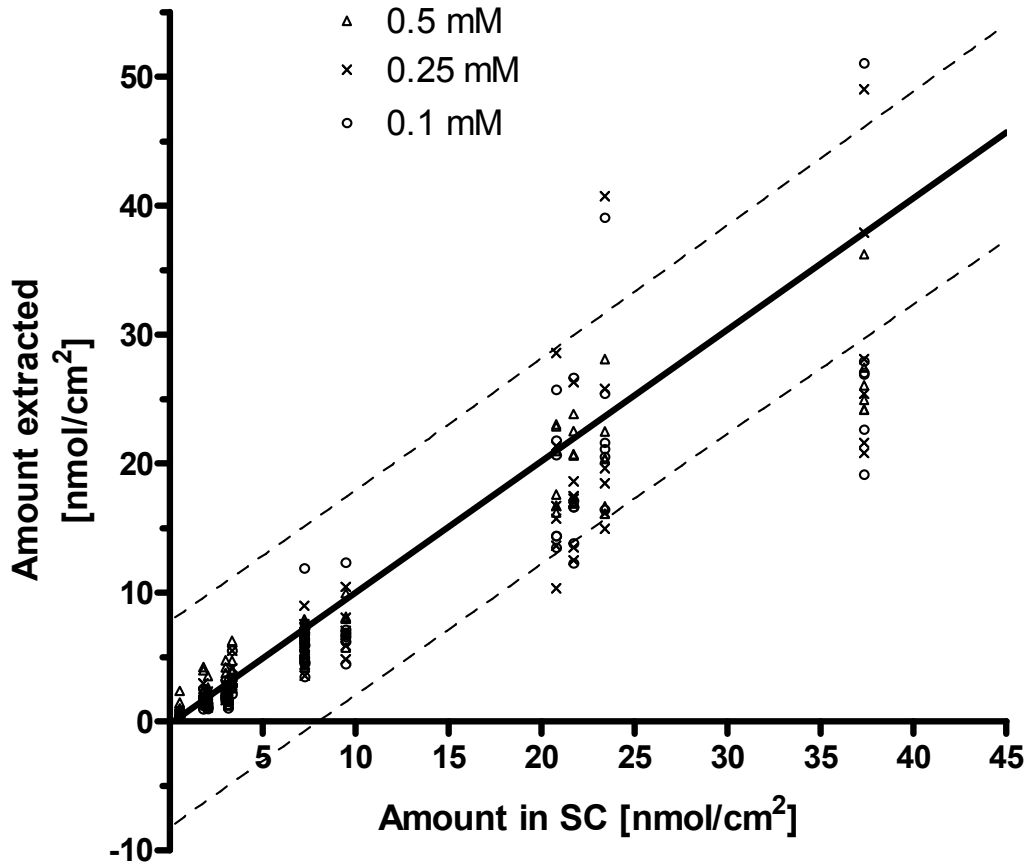

Figure 3. AAs extracted at the cathode in the first hour of reverse iontophoresis when their subdermal concentration was 0.1, 0.25 or 0.5 mM plotted as a function of the corresponding levels in the SC determined by tape-stripping [Chapter 4]. The solid and dashed lines show the regression obtained previously (± 95% confidence interval) when no AAs were added to the subdermal solution. Note that the values for Met are not included as the amount in the SC was not determined for this AA.

The evolution of the extraction process as a function of time for different examples of the AAs studied is illustrated in Figure 4. As already explained, the first hour of iontophoresis samples primarily the SC and is insensitive to the subdermal level. In the case of an AA which is abundantly present in the SC, such as Ser, and even Pro, 6 hours of current passage are insufficient to unambiguously demonstrate that the SC 'depot' has been fully depleted. On the other hand, for AAs which are less concentrated in the SC, like phenylalanine and tryptophan, reverse iontophoresis effectively 'clears' the SC reservoir within a couple of hours of current passage and the extraction is then very sensitive to the presence (or not) of the AA in the subdermal compartment.

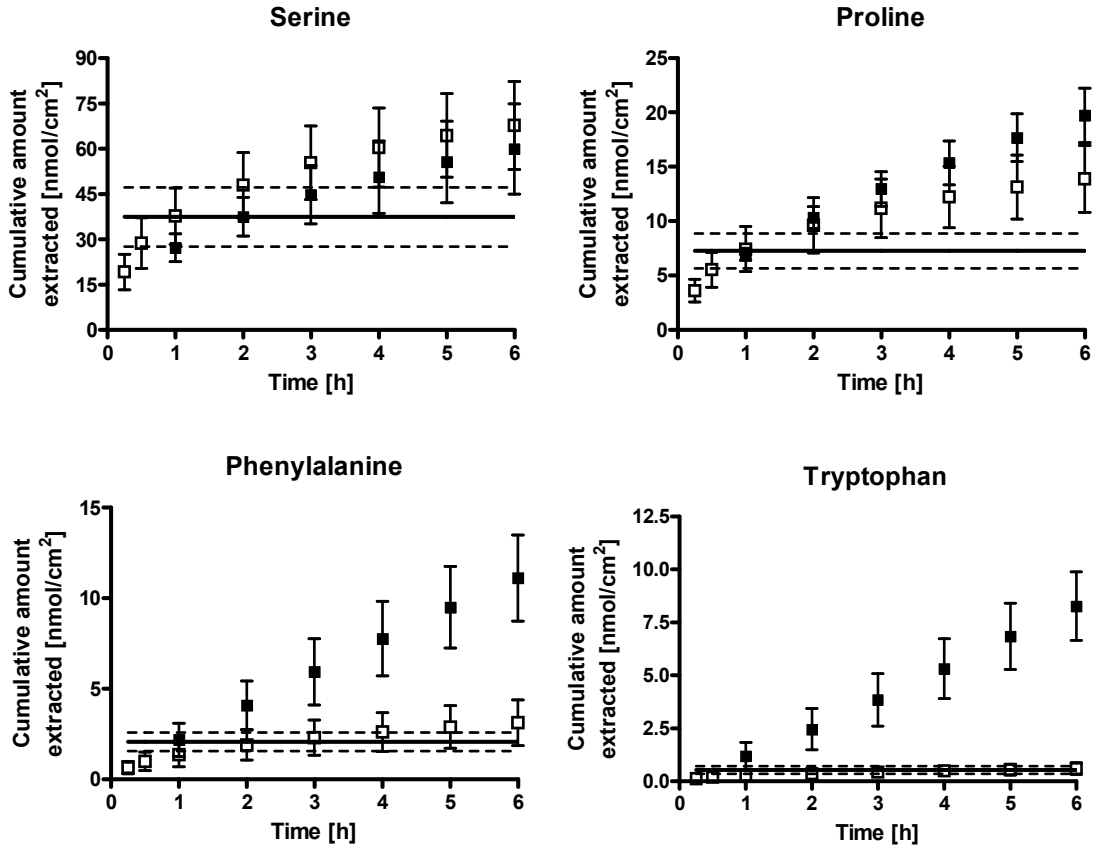

Figure 4. Cumulative extraction of 4 AAs by reverse iontophoresis as a function of time when initially present in the subdermal compartment at either 0 (open squares) or 0.5 mM (filled squares). The solid and dashed lines represent, respectively, the mean amount, and the ±SD, of the AAs recovered in the SC by tape-stripping [Chapter 4].

4. Conclusions

The results reported in this paper confirm that a relatively short period of reverse iontophoresis (~1 hour) is an effective, minimally-invasive method with which to determine the levels of many AAs within the skin. When the period of current passage is prolonged, the levels of AAs collected at the cathode are correlated with their subdermal concentrations for those compounds having relatively small SC reservoirs (e.g., phenylalanine). Fluctuations in the systemic concentrations of such AAs, as a result, for example, of a metabolic disorder, may therefore be usefully monitored by reverse iontophoresis.

5. Acknowledgements

This research was supported by the US National Institutes of Health (EB–001420). J.-P. S. thanks BIJAB, NSERC, FQRNT and Universities UK for funding.

6. References

1. Murray, R.K., Granner, D.K., Mayes, P.A., Rodwell, V.W., *Harper's Biochemistry*. 25th ed. 2000, Stamford, CT: Appleton&Lange. 927.
2. Bender, D.A., *Amino Acid Metabolism*. 2nd ed. ed. 1985, Chichester: John Wiley & Sons. 263.
3. Blomstrand, E., *Amino acids and central fatigue.* Amino Acids, 2001. **20**(1): p. 25-34.
4. Blomstrand, E., *A role for branched-chain amino acids in reducing central fatigue.* J Nutr, 2006. **136**(2): p. 544S-547S.
5. McGuire, J., et al., *Biochemical markers for post-operative fatigue after major surgery.* Brain Res Bull, 2003. **60**(1-2): p. 125-30.

6. Leboulanger, B., R.H. Guy, and M.B. Delgado-Charro, *Reverse iontophoresis for non-invasive transdermal monitoring.* Physiol Meas, 2004. **25**(3): p. R35-50.

7. Pitzer, K.R., et al., *Detection of hypoglycemia with the GlucoWatch biographer.* Diabetes Care, 2001. **24**(5): p. 881-5.

8. Pikal, M.J., *The role of electroosmotic flow in transdermal iontophoresis.* Adv Drug Deliv Rev, 2001. **46**(1-3): p. 281-305.

9. Pikal, M.J. and S. Shah, *Transport mechanisms in iontophoresis. III. An experimental study of the contributions of electroosmotic flow and permeability change in transport of low and high molecular weight solutes.* Pharm Res, 1990. **7**(3): p. 222-9.

10. Rawlings, A.V., *Sources and Role of Stratum Corneum Hydration*, in *Skin Barrier*, P.M. Elias, Feingold, K.R., Editor. 2006, Taylor & Francis. p. 399-425.

11. Rawlings, A.V. and P.J. Matts, *Stratum corneum moisturization at the molecular level: an update in relation to the dry skin cycle.* J Invest Dermatol, 2005. **124**(6): p. 1099-110.

12. Rawlings, A.V., et al., *Stratum corneum moisturization at the molecular level.* J Invest Dermatol, 1994. **103**(5): p. 731-41.

13. Glikfeld, P., et al., *A new system for in vitro studies of iontophoresis.* Pharm Res, 1988. **5**(7): p. 443-6.

14. *An Improved Gradient Method for the AAA-Direct™ Separation of Amino Acids and Carbohydrates in Cmplex Sample Matrices*. 2006, Dionex corporation: Sunnyvale, CA. p. 12.

15. *Determination of Amino Acids in Cell Cultures and Fermentation Broths*. 2003, Dionex corporation: Sunnyvale, CA.

16. Jandik, P., J. Cheng, and N. Avdalovic, *Analysis of amino acid-carbohydrate mixtures by anion exchange chromatography and integrated pulsed amperometric detection.* J Biochem Biophys Methods, 2004. **60**(3): p. 191-203.

17. Hanko, V.P. and J.S. Rohrer, *Determination of amino acids in cell culture and fermentation broth media using anion-exchange chromatography with integrated pulsed amperometric detection.* Anal Biochem, 2004. **324**(1): p. 29-38.

18. Ding, Y., H. Yu, and S. Mou, *Direct determination of free amino acids and sugars in green tea by anion-exchange chromatography with integrated pulsed amperometric detection.* J Chromatogr A, 2002. **982**(2): p. 237-44.

19. Santi, P. and R.H. Guy, *Reverse iontophoresis -- Parameters determining electroosmotic flow: I. pH and ionic strength.* Journal of Controlled Release, 1996. **38**(2-3): p. 159-165.

20. Rao, G., et al., *Reverse iontophoresis: noninvasive glucose monitoring in vivo in humans.* Pharm Res, 1995. **12**(12): p. 1869-73.

21. Stegink, L.D., et al., *Plasma amino acid concentrations and amino acid ratios in normal adults and adults heterozygous for phenylketonuria ingesting a hamburger and milk shake meal.* Am J Clin Nutr, 1991. **53**(3): p. 670-5.

22. Lepage, N., et al., *Age-specific distribution of plasma amino acid concentrations in a healthy pediatric population.* Clin Chem, 1997. **43**(12): p. 2397-402.

Chapter 6. Amino acids in human stratum corneum *in vivo* determined by tape-stripping and reverse iontophoresis

Amino acids in human stratum corneum *in vivo* determined by tape-stripping and reverse iontophoresis

Jean-Philippe Sylvestre, Camille C. Bouissou, M. Begoña Delgado-Charro and Richard H. Guy

Department of Pharmacy & Pharmacology, University of Bath, Claverton Down, Bath, BA2 7AY, UK.

Research paper to be submitted

Abstract

Purpose: To examine the application of stratum corneum (SC) tape-stripping and reverse iontophoresis as minimally invasive tools for the analysis of amino acids (AAs) within the skin, and subdermally, in man.

Methods: AAs in the SC were determined following repetitive tape-stripping, extraction and analysis. At distinct skin sites, reverse iontophoresis and passive diffusion were also employed to extract AAs to the skin surface over a 4-hour period; a subsequent tape-stripping procedure evaluated the residual presence of these substances in the skin's outermost layer. Plasma concentrations were also measured for comparison with the levels extracted. In all samples obtained, glucose concentrations were evaluated as a positive control.

Results: SC concentrations of 13 essentially zwitterionic AAs were approximately two orders of magnitude higher than their respective plasma levels. Passive and reverse iontophoretic extraction for 4 hours did not deplete the SC depot of AAs, a fact reinforced by post-extraction tape-stripping, which revealed that AAs remained in the SC at this time. In contrast, glucose was much less abundant in the SC and was fully and relatively quickly extracted by reverse iontophoresis.

Conclusion: Reverse iontophoresis is not practical for the routine monitoring of AA plasma concentrations (as it is, in contrast, for glucose, the skin reservoir of which is much smaller). On the contrary, the data obtained in this way are highly

correlated with the levels measured in the SC by tape-stripping. It is questionable, however, if the improvement in extraction efficiency of the method is sufficient to justify its used compared to the more simple passive diffusion.

1. Introduction

Amino acids (AAs) are substances essential for life [1], and imbalances in their systemic levels, due to genetic defects or metabolic problems, may have serious consequences [1, 2]. The importance of AAs is further reinforced by their role as neurotransmitter precursors, and as markers of central fatigue and stress [2-5]. In addition, within the skin, AAs make up a significant part of the so-called "natural moisturising factor" (NMF), originating (primarily) from the breakdown of filaggrin, and responsible for the maintenance of hydration in the outermost barrier layer of the membrane, the stratum corneum (SC) [6-8]. Changes in NMF levels are correlated with abnormally dry and scaly skin [8-11], and considerable dermatological and cosmetic effort is directed at resolving this condition.

It follows that there is a rationale for the development of tools with which to monitor the presence of AAs both systemically and in the skin. In previous investigations [Chapters 4 and 5], the applications of reverse iontophoresis and SC tape-stripping have been examined *in vitro* for the interrogation of AA levels in the subdermal 'compartment' beneath the skin and in the SC. Reverse iontophoresis uses a small electrical current to enhance molecular transport across a membrane [12], and is a technique employed in a recently developed, minimally-invasive glucose monitoring device, the GlucoWatch® Biographer [13]. For glucose, and for the zwitterionic AAs, which are the subjects of this study, imposition of an electric field results in their extraction to the skin surface by passive diffusion and by electroosmosis [14]. The former mechanism dominates at early times, as the 'reservoir' of the analytes in the SC is emptied. Thereafter, convective solvent flow to the cathode begins to make a progressively more important contribution (especially for those substances which are least abundant in the SC) [15-17]. Tape-stripping is a simple procedure by which the SC can be progressively and completely removed; extraction and analysis of the contents of the strips allows an unequivocal estimation of the levels of AAs in the membrane and provides details on their spatial distribution [Chapter 4]. The amounts present have been correlated with those extracted from the skin by passive diffusion and by reverse iontophoresis,

and have permitted delineation of the SC and subdermal origins of the analytes [Chapter 5].

The objective of the experiments presented here was to extend the earlier *in vitro* studies (which were conducted using porcine skin) to measurements *in vivo* in human volunteers. Specific goals were to determine whether levels of AAs in the SC were correlated with amounts extracted by relatively short periods of either passive diffusion or reverse iontophoresis, and to examine whether the latter techniques can ultimately be used to sample subdermal (i.e., systemic) concentrations. Concurrent analyses of glucose [18, 19] were also undertaken as a positive control.

2. Materials and methods

2.1. Chemicals

Sodium chloride, Na_2HPO_4, KH_2PO_4 and phosphoric acid (85%) were from Acros (Geel, Belgium). NaOH 50% (ion chromatography eluent grade) was obtained from Fluka (Buchs, Switzerland). Sodium azide, D-glucose, Ag wire (>99.99% purity) and AgCl (99.999%) were purchased from Sigma-Aldrich Co. (Gillingham, UK). An amino acid standard solution (containing 17 primary amino acids in 0.1 N HCl), L-glutamine, L-asparagine, and L-tryptophan were from Sigma (Gillingham, UK). Sodium acetate (anhydrous, electrochemical grade) was acquired from Dionex (Sunnyvale, CA), and glacial acetic acid (HPLC grade) was from Fisher Scientific (Loughborough, UK). All chemicals were at least reagent grade unless stated otherwise and all aqueous solutions were prepared using high purity deionized water (18.2 MΩ·cm, Barnstead Nanopure Diamond^{TM}, Dubuque, IA).

2.2. Human subjects

Four healthy volunteers (2 males, 2 females, aged between 20 and 30 years) with no history of skin disease participated in the study, which was approved by the Bath Local Research Ethics Committee, and provided written consent. Experiments were performed in the morning on the ventral forearm on two separate occasions at least four weeks apart. The volunteers fasted overnight

and were allowed only water until the experiments were completed. The ventral forearm surface was first cleaned gently with an isopropyl alcohol swab. Then, in the first component of the study, samples for AA and glucose analysis were obtained by reverse iontophoresis and tape-stripping (at an adjacent site). In the second part, sampling involved passive diffusion and tape-stripping (again, at an adjacent site). On both occasions, capillary blood samples were obtained from the finger-tips during and/or at the end of the extraction periods.

2.3. Reverse iontophoresis extraction

Two glass cells (internal diameter of 1.6 cm, extraction surface 2 cm^2) separated by ~7 cm were fixed to the ventral forearm of the subjects with silicone grease and medical grade tape (Curafix® H, Lohmann & Rauscher, Rengsdorf, Germany). Both cells were filled with 1.6 ml of 20 mM NaCl in 10 mM phosphate buffer at pH 7.4. A direct current of 0.6 mA (i.e., 0.3 mA/cm^2) was applied from a Phoresor II Auto (Iomed, Salt Lake City, UT) via Ag/AgCl electrodes. The entire contents of the anode and cathode chambers were collected and replaced by an equal volume of extraction solution at 15 and 30 minutes and then every half-hour thereafter for a total extraction time of 4 hours. The collected samples were passed through a sterile syringe filter (Millex-GV, 0.22 µm, 13 mm diameter, Millipore, Watford, UK) and stored in the freezer at -20°C until analysis.

2.4. Passive diffusion extraction

One glass cell (extraction surface = 2 cm^2) was adhered to the skin as before and was filled with 1.6 ml of the same extraction solution used in the reverse iontophoresis experiment. Identical sample collection, filtration and storage procedures were followed.

2.5. Tape-stripping

Tape-stripping was performed at skin sites adjacent to the reverse iontophoresis and passive extraction sites. The SC was progressively removed by the repeated application and removal of adhesive tape-strips (Scotch Book Tape, 3M, St. Paul, MN). A polypropylene foil template with a central hole was

first fixed to the skin with self-adhesive medical tape (Micropore, 3M, St. Paul, MN) to ensure that all tape-strips were taken from exactly the same site. The tapes (2.5 x 2.5 cm) were applied with pressure from a weighted roller and then removed. Up to 25 strips were taken, but the SC was never completely removed. Instead, transepidermal water loss (TEWL) measurements were taken (AquaFlux V4.7, Biox Systems Ltd., London, UK) before and during the stripping procedure, which was stopped when TEWL reached ~4-fold the baseline value, at which point approximately 75% of the SC had been removed [20]. Each tape was weighed before and after stripping on a 0.1-µg precision balance (Sartorius SE2-F, Epsom, UK) to determine the mass (and hence the thickness [21]) of the SC layer removed. AAs and glucose present in SC on the tape-strips were subsequently extracted with an aqueous solution of sodium azide (20 mg/l). The first and second tapes were extracted individually into 1 ml, while the remaining tapes were extracted in groups of three into 3 ml of solution. The extracts were filtered (0.45 µm, Nalgene, Thorn Business Park, UK) and stored at -20°C until analysis.

2.6. Capillary blood samples

Capillary blood samples were obtained from the finger-tips of the volunteers after 2, 3 and 4 hours of iontophoresis and after 4 hours of passive diffusion. The finger-tip was disinfected with an isopropyl alcohol swab prior to pricking with a BD Genie™ Lancet (Becton Dickinson, Oxford, UK) (1.5 mm width and 1.5 mm depth). The first drop of blood was analyzed for blood glucose (Accu-Chek® Compact Plus, Roche); subsequently, 200-400 µL of blood was collected in heparin-coated tubes (BD Microtainer™ LH). Plasma was separated by centrifugation (Boeco U-32, Hamburg, Germany) at 2000x g for 3 minutes, and then diluted 5-fold in a solution containing 20 mM NaCl, 10mM phosphate buffer at pH 7.4, and 20 mg/l sodium azide before deproteination by ultrafiltration (Centrifree® Micropartition Devices, Millipore, Watford, UK) at 1000x g for 35 minutes. The resulting sample was further diluted by 4-fold and stored at -20°C until analysis.

2.7. Sample Analysis

Except for glucose in plasma, all samples were analyzed for amino acids and glucose using ion chromatography coupled with integrated pulsed-amperometric detection (IC-IPAD) as previously described (Dionex, Sunnyvale, CA) [22] (see Chapters 4 and 5).

2.8. Data analysis and statistics

AA and glucose concentrations in the SC were expressed in terms of amount per mass of tissue, and their profiles across the barrier were deduced from the tape-stripping data as previously described [23]. Extraction fluxes were calculated by dividing the amounts removed during a sampling interval by the duration of that collection period. Data manipulation and statistics were performed using Graph Pad Prism V.4.00 (Graph Pad Software Inc., San Diego, CA). When datasets were compared, the level of statistical significance was fixed at $p < 0.05$. All results were expressed as mean ± standard deviation (SD).

3. Results and discussion

Thirteen essentially zwitterionic AAs and glucose were successfully quantified. Other AAs were detected but could not be quantified (aspartic and glutamic acids, lysine, methionine) while the chromatographic peaks of arginine, cystine, citrulline and glutamine either co-eluted or could not be sufficiently separated to allow their quantification.

3.1. Tape-stripping

The levels of AAs and glucose in human SC *in vivo* determined by tape-stripping are in Table 1 and are compared with the results previously reported for pig SC *ex vivo* [Chapter 4]. Significantly greater amounts (up to 10-fold) of the AAs were found in the human barrier; in contrast, the levels of glucose in human and pig SC were not significantly different.

Figure 1 illustrates the concentration profiles of the AAs as a function of position in the SC for serine (in abundant presence), proline (moderately

abundant) and phenylalanine (a lesser presence); the glucose profile is also shown for comparison. The pattern of the AAs distribution is consistant, being negligible at the skin surface (believed to be due to regular washing [8, 24]) before increasing to relatively constant levels; the glucose profile, on the other hand, shows no obvious trend.

Table 1. Amounts and concentrations of AAs and glucose (mean ± SD) in human (n = 8) and pig (n = 6) SC.

Compound	Human		Pig		Concentration ratio human/pig
	[nmol/cm^2]	[mmol/kg]	[nmol/cm^2]	[mmol/kg]	
Ser	370 ± 80	386 ± 53	37 ± 9	40 ± 11	9.7
Gly	250 ± 53	260 ± 33	23 ± 6	25 ± 6	10.4
Ala	184 ± 39	194 ± 45	22 ± 4	24 ± 8	8.1
His	101 ± 34	104 ± 28	21 ± 4	23 ± 6	4.5
Thr	84 ± 19	88 ± 15	10 ± 2	10 ± 3	8.8
Pro	42 ± 11	44 ± 12	7.3 ± 1.5	7.9 ± 2.3	5.6
Leu	20 ± 4	21 ± 2	7.3 ± 2.1	7.7 ± 1.8	2.7
Val	30 ± 7	31 ± 6	3.4 ± 1.0	3.5 ± 0.7	8.9
Ile	13 ± 5	13 ± 4	3.0 ± 0.8	3.2 ± 0.6	4.1
Tyr	21 ± 5	21 ± 3	3.2 ± 0.6	3.4 ± 0.5	6.2
Phe	8.5 ± 3.5	8.7 ± 2.3	2.1 ± 0.5	2.2 ± 0.4	4.0
Asn	14 ± 5	15 ± 4	1.8 ± 0.6	1.9 ± 0.5	7.9
Trp	8.8 ± 2.0	9.2 ± 0.9	0.5 ± 0.2	0.6 ± 0.1	15.3
Glucose	1.2 ± 0.3	1.3 ± 0.4	1.4 ± 0.7	1.7 ± 1.4	0.8

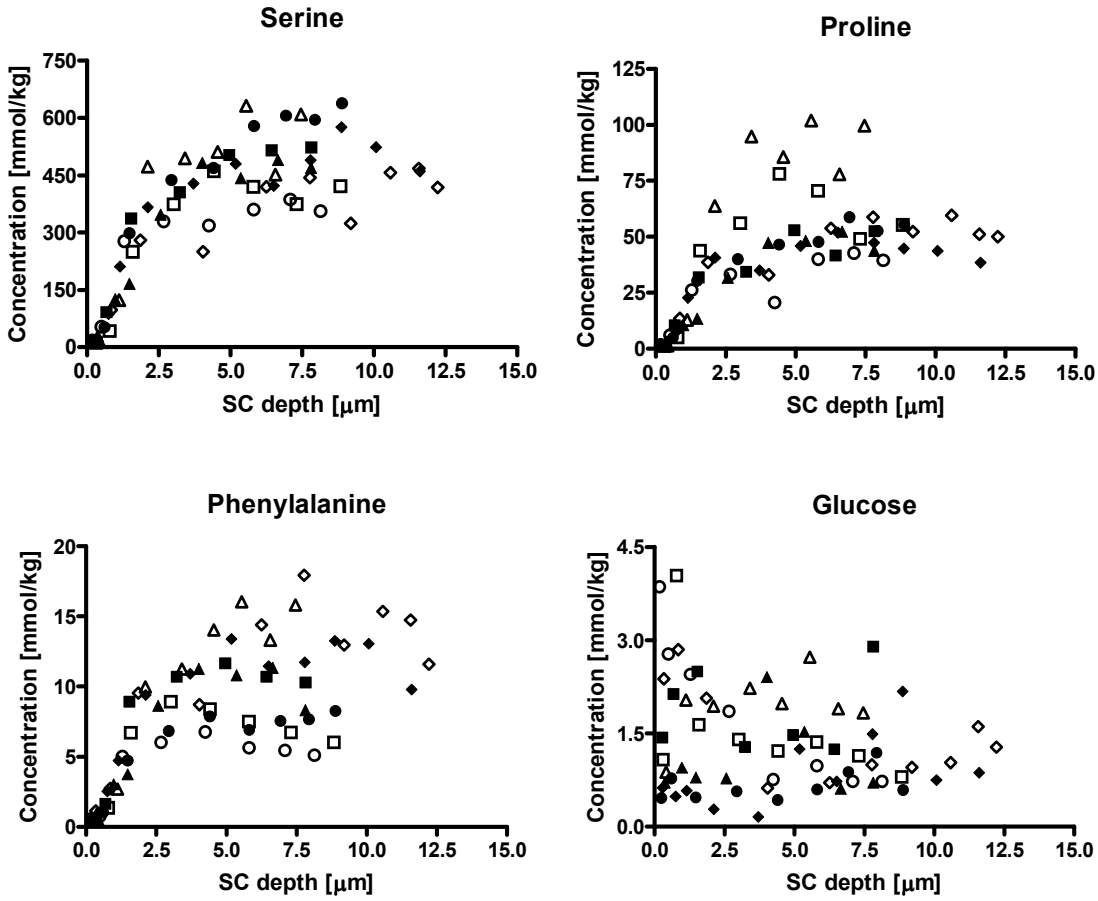

Figure 1. Concentration profiles of serine, proline, phenylalanine and glucose as a function of position in the SC in 4 human volunteers (subject 1, open and closed squares; subject 2, open and closed circles; subject 3, open and closed triangles; subject 4, open and closed diamonds).

3.2. Systemic concentrations

The pooled values of the systemic levels of the AAs (plasma) and glucose (blood) of the three measurements made during reverse iontophoresis are reported in Table 2. The concentrations measured at the end of the passive extraction experiment were similar. The results, for the most part, fall within the normal ranges [1, 25, 26]. Only tryptophan is consistently lower than usual, probably because of its known, strong binding to plasma proteins [27] which were removed by ultrafiltration during sample preparation.

It is noteworthy that the AA concentrations in plasma fall in the range of 10-350 µM, whereas those in the SC are much higher (5-400 mM, assuming a SC density of ~1 g/ml). The SC/plasma ratio ranges from 150 for valine to

>1000 for serine and glycine. Conversely, the concentrations of glucose in the SC and in the blood were of the same order of magnitude.

Table 2. AA plasma levels and blood glucose concentrations (μM) in 4 volunteers (mean ± SD; n = 3 for subjects 1, 3, 4; n = 2 for subject 2).

Molecule	Subject 1	Subject 2	Subject 3	Subject 4	Normal range[a]
Ser	219 ± 22	265 ± 4	160 ± 7	274 ± 26	90-290
Gly	206 ± 11	187 ± 6	184 ± 3	230 ± 14	100-330
Ala	306 ± 8	251 ± 2	168 ± 3	184 ± 2	150-450
His	121 ± 4	110 ± 2	79 ± 2	92 ± 3	30-150
Thr	114 ± 4	163 ± 6	82 ± 1	91 ± 3	70-220
Pro	242 ± 6	148 ± 6	99 ± 6	138 ± 9	85-290
Leu	119 ± 3	97 ± 1	95 ± 1	118 ± 4	65-220
Val	235 ± 11	157 ± 6	181 ± 9	235 ± 2	90-300
Ile	93 ± 4	81 ± 2	80 ± 2	99 ± 4	26-100
Tyr	60 ± 8	42 ± 1	32 ± 1	43 ± 3	30-120
Phe	66 ± 3	54 ± 5	40 ± 2	53 ± 2	35-100
Asn	55 ± 2	56 ± 2	48 ± 3	48 ± 2	35-80
Trp	20 ± 1	15.5 ± 0.5	15.3 ± 0.3	11.2 ± 0.2	30-80
Glucose	5000 ± 200	4200 ± 120	4150 ± 50	4270 ± 50	3600-6100

[a]From reference [25] except for Asn [26] and glucose [1].

3.3. Extraction by reverse iontophoresis and passive diffusion

Iontophoresis was well tolerated by all subjects. As observed before [12, 15, 18, 19, 28], only minor tingling sensations, more noticeable at the anode, were reported during the first 30 minutes of the experiment. The iontophoretic sites were slightly erythematous after the experiment, a situation that resolved within 24 hours after termination of current.

Iontophoretic extraction fluxes at the cathode and anode were compared to those resulting from passive diffusion. Figure 2 illustrates the results for serine, proline, phenylalanine and glucose. For all AAs, initial fluxes were high, then fell rapidly over the first 60 minutes before becoming relatively constant during the last 2 hours of the experiment. In general, reverse iontophoresis to

the cathode was significantly higher than that to the anode and greater than passive diffusion (repeated measures ANOVA followed by Tukey's post-test); exept for glucose and isoleucine, passive extaction was not significantly different from reverse iontophoresis to the anode. When a nonparametric Friedman test was performed followed by Dunn's post-test instead, the cathode was again found more efficient than the anode for all molecules except isoleucine and glucose, and more efficient than passive diffusion for all molecules except histidine and tyrosine. In the last 2 hours of extraction, the trend in AAs fluxes and that of glucose was cathodal > passive > anodal, although not all differences were significant. The higher extraction rate to the cathode is consistent with the anticipated direction of the convective solvent (electroosmotic) flow [14]. Except for glucose, however, the improvement of extraction efficiency at the cathode compared to passive diffusion was rather small.

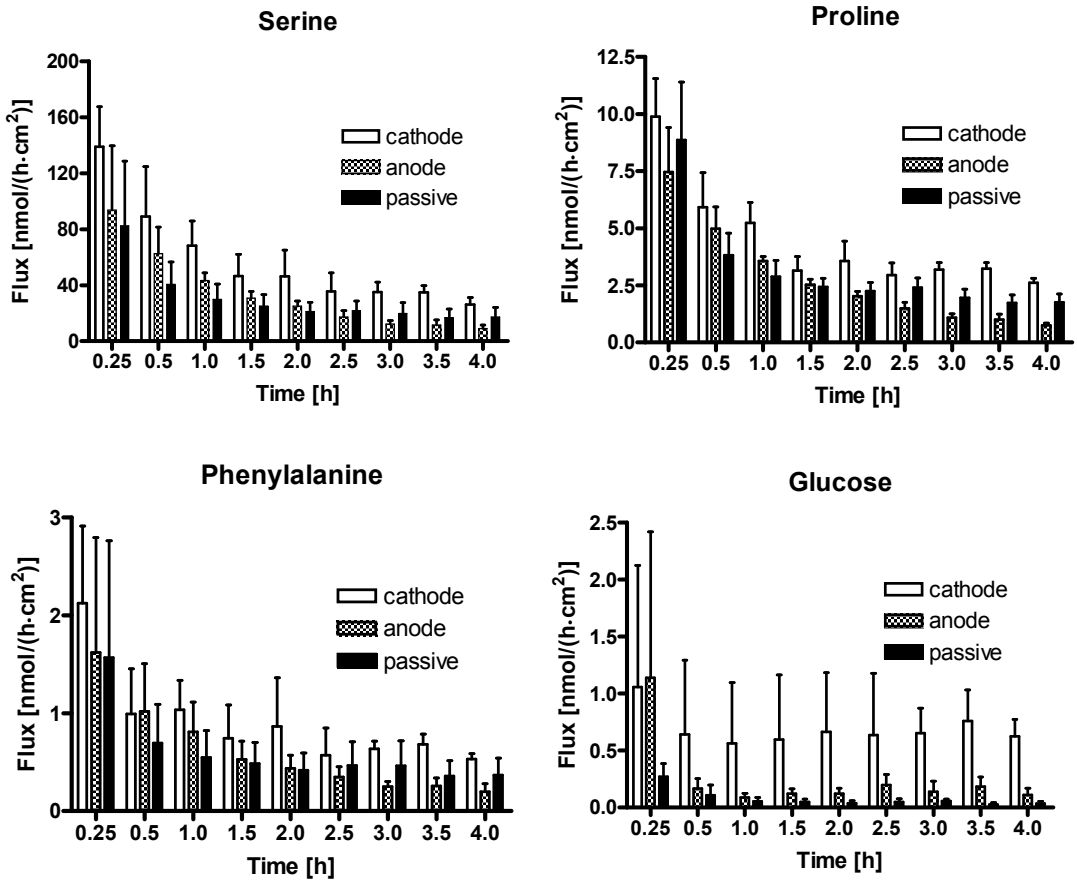

Figure 2. Reverse iontophoretic (to the cathode and to the anode) and passive diffusion extraction fluxes of three AAs and glucose *in vivo* in human volunteers as a function of time.

3.4. Origin of the substances extracted

Figure 3 compares graphically the amounts of serine, histidine and glucose extracted from the skin over 4 hours by passive diffusion and by reverse iontophoresis at the cathode. Also shown on these graphs are the average amounts of these same substances (± SD) measured at adjacent SC sites by tape-stripping. Table 3 collects the corresponding data for all the compounds assayed in this study.

For all zwitterionic AAs (as illustrated by serine in Figure 3), reverse iontophoresis extraction at the cathode, which exceeded that at the anode and that extracted passively, failed to empty the SC 'depot'. Only for histidine, which may have been present to a greater extent in its cationic form [Chapter 4], was the amount extracted iontophoretically not significantly different from that in the

SC as measured by tape-stripping. In other words, for all AAs, the non-invasive sampling procedure only interrogated the SC and did not provide any information about the levels beneath this skin layer. For glucose, in contrast, the SC reservoir was already depleted by 2-3 hours of current passage, at which point subdermal sampling was taking place [15]. The cumulative amount of glucose extracted iontophoretically at the end of the experiment was increasing linearly with time as expected. On the other hand, the profiles for the AAs showed initially higher fluxes which then dropped off at longer times. Indeed, the behaviour closely followed a square root of time dependence ($r^2 > 98$) (Figure 4), characteristic of the classic “burst” effect from an initially full reservoir being depleted of solute [15], a further indication that electroosmosis contributed only slightly to the extraction of AAs from the SC.

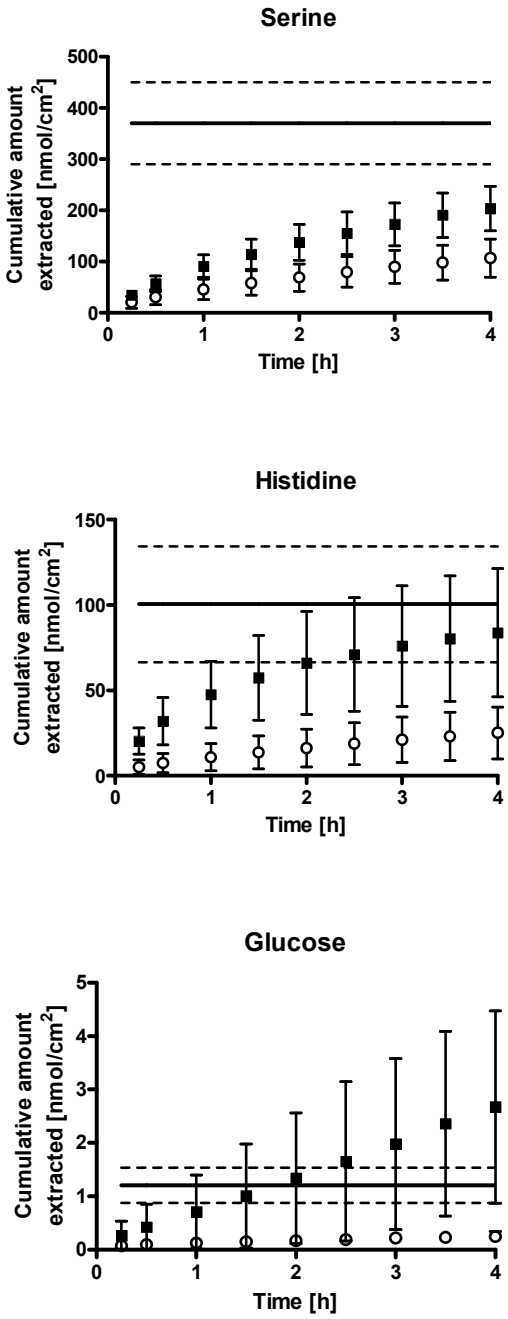

Figure 3. Cumulative amounts (mean ± SD, n = 4) of serine, histidine and glucose extracted passively (open circles) and by reverse iontophoresis (filled squares) as a function of time. The solid and dashed lines represent the mean and the ±SD, respectively, of the substances measured in the SC by tape stripping.

Table 3. Amounts of AAs and glucose in the SC determined by tape-stripping compared to the quantities extracted in 4 hours by reverse iontophoresis and by passive diffusion.

Molecule	SC [nmol/cm^2]	Iontophoresis - cathode [nmol/cm^2]	Iontophoresis - anode [nmol/cm^2]	Passive diffusion [nmol/cm^2]
Ser	370 ± 80	204 ± 43	114 ± 17	107 ± 37
Gly	250 ± 53	138 ± 33	69 ± 8	82 ± 27
Ala	184 ± 39	99 ± 25	50 ± 7	59 ± 19
His	101 ± 34	84 ± 38	14 ± 6	25 ± 15
Thr	84 ± 19	38 ± 10	21 ± 3	24 ± 8
Pro	42 ± 11	16 ± 4	9.4 ± 1.9	11 ± 4
Leu	20 ± 4	11 ± 2	5.5 ± 1.8	4.5 ± 0.8
Val	30 ± 7	14 ± 3	8.2 ± 1.0	7.8 ± 3.1
Ile	13 ± 5	7.5 ± 1.5	4.6 ± 1.1	3.0 ± 0.8
Tyr	21 ± 5	7.1 ± 1.5	4.5 ± 0.7	5.4 ± 1.8
Phe	8.5 ± 3.5	3.3 ± 1.0	2.1 ± 0.7	2.1 ± 1.0
Asn	14 ± 5	4.5 ± 1.5	3.2 ± 0.8	2.6 ± 1.3
Trp	8.8 ± 2.0	3.1 ± 0.6	2.3 ± 0.4	2.0 ± 0.6
Glucose	1.2 ± 0.3	2.7 ± 1.8	0.8 ± 0.3	0.2 ± 0.1

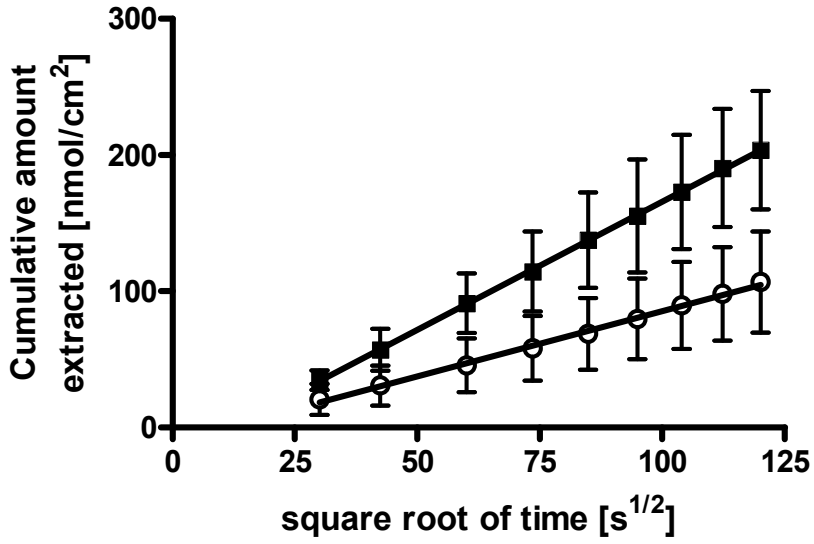

Figure 4. Cumulative amounts (mean ± SD, n = 4) of serine extracted passively (open circles) and by reverse iontophoresis (filled squares) as a function of the square root of time. Linear regressions through the data are shown.

The amounts of AAs extracted by reverse iontophoresis and passive diffusion during the first hour of the experiment were highly correlated ($r^2 > 0.79$) with the amounts recovered from the SC by tape-stripping (Figure 5, upper panels). The slopes of the regressions were 0.23 (± 0.02) for iontophoresis compared to 0.14 (± 0.01) for passive transport, showing that the imposition of current had improved the extraction efficiency slightly by about 50%. However, the fact that the gradients were much less than unity demonstrated that the SC reservoir of the analytes was far from depleted in one hour. When extraction fluxes during the final two hours of the experiment were plotted against the amounts in the SC, a strong correlation ($r^2 > 0.9$) was again observed (Figure 4, lower graphs); once more, reverse iontophoresis extraction showed a modest improvement in extraction compared to passive diffusion with a ratio of the slopes of the lines in the lower graphs of Figure 4 being ~1.45. It is questionable, therefore, whether this relatively small improvement in extraction justifies the use of a more complex device over passive diffusion.

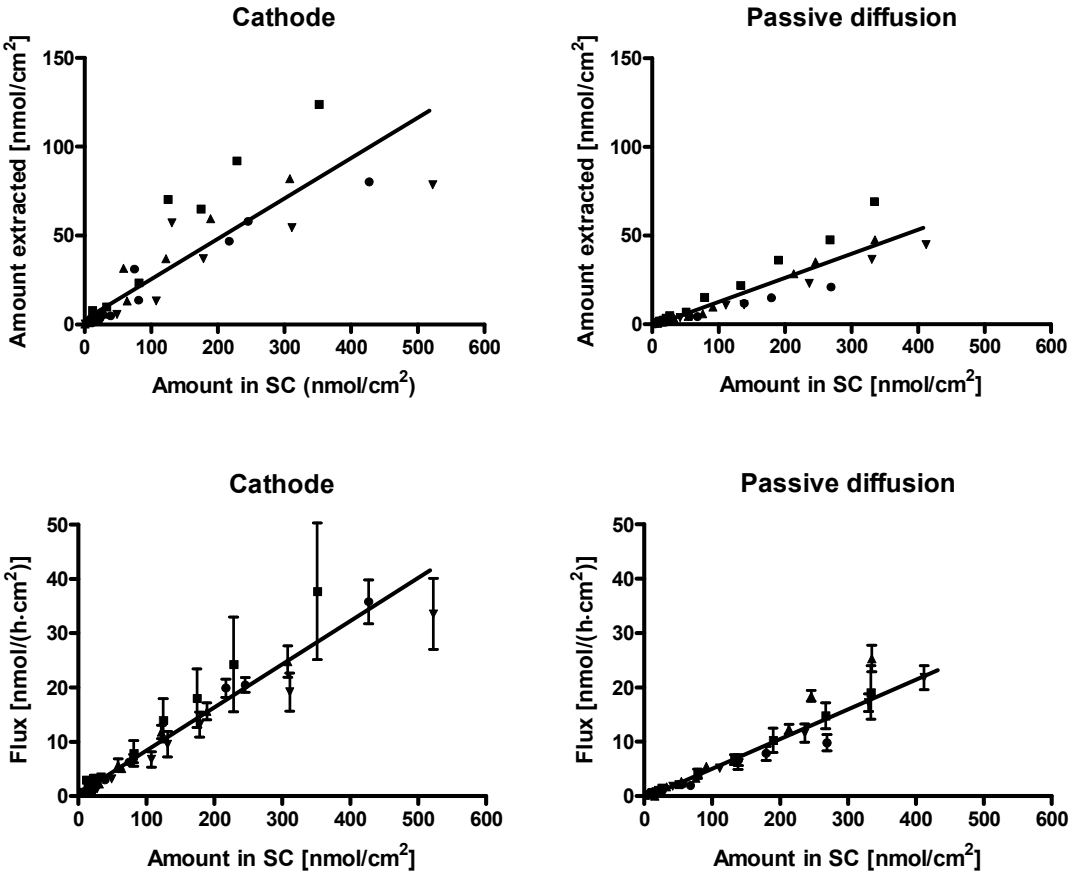

Figure 5. Correlations between the quantities of AAs extracted by reverse iontophoresis at the cathode (left panels) and by passive diffusion (right panels) after 1h of transport (upper graphs) and the corresponding extraction fluxes during the final two hours of the experiment (lower graphs), with the amounts measured in the SC by tape-stripping. The four symbols corresponds to the different subjects studied; error bars represent SDs for n = 4, and lines of linear regression have been drawn through the data.

To further emphasise, *in vivo* in man, that the non-invasive extraction procedure during a 4-hour experiment was not able to sample the subdermal 'compartment', Figure 6 displays the ratio of the AAs reverse iontophoresis extraction fluxes (2-4 hour average) to the measured plasma concentrations. If the technique was indeed interrogating the tissue beneath the SC, these ratios should correspond to the electroosmotic flow induced across the skin by the applied electric field (i.e., $\upsilon = J_{AA}/C_{AA}$) and should be approximately equal. In fact, the values are highly divergent, ranging from 8 (±2) $\mu L \cdot hr^{-1} \cdot cm^{-2}$ for leucine to 146 (± 36) $\mu L \cdot hr^{-1} \cdot cm^{-2}$ for serine. It follows that the SC reservoir of AAs *in vivo* in humans is significantly greater than that observed in porcine skin *in vitro*, and that the opportunity to sample systemic AA levels using reverse iontophoresis will be limited either to experiments of rather long duration, or to situations in which metabolic diseases (e.g., phenylketonuria) cause a substantial increase in blood levels over those found normally.

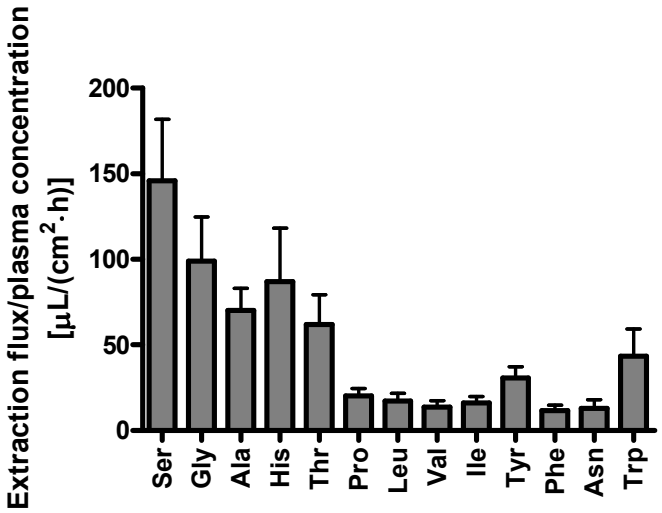

Figure 6. Reverse iontophoresis extraction fluxes of AAs to the cathode during the last 2 hours of the experiment normalized by the corresponding plasma concentrations (mean ± SD; n = 4)

Finally, when the SC was tape-stripped at the end of the 4-hour passive extraction experiment, it was possible to perform a “mass balance” and show that for each AA the amount extracted in 4 hours added to that which remained equalled (more or less) the quantity measured previously in the SC which had not been subjected to extraction (Table 4). Unfortunately, because of the 4-hour hydration period, the removal of the SC was a much less uniform process and it was difficult, therefore, to generate reproducible concentration profiles to compare with those observed pre-extraction (Figure 1).

Table 4. AA mass balance in SC (mean ± SD; n = 4).

Molecule	**Unextracted SC [nmol/cm^2]**	**Extracted by passive diffusion [nmol/cm^2]**	**Extracted from SC post-passive diffusion [nmol/cm^2]**
Ser	338 ± 51	107 ± 32	211 ± 106
Gly	256 ± 54	82 ± 24	161 ± 83
Ala	194 ± 36	59 ± 16	113 ± 55
His	104 ± 32	25 ± 13	61 ± 33
Thr	84 ± 20	24 ± 7	55 ± 28
Pro	47 ± 12	11 ± 4	29 ± 16
Leu	18 ± 2	4.5 ± 0.7	8.4 ± 3.1
Val	30 ± 8	7.8 ± 2.7	19 ± 11
Ile	9 ± 2	3.0 ± 0.7	5.6 ± 2.2
Tyr	21 ± 5	5.4 ± 1.6	14 ± 7
Phe	9 ± 4	2.1 ± 0.8	5.2 ± 3.0
Asn	13 ± 5	2.6 ± 1.2	7.7 ± 5.3
Trp	9 ± 2	2.0 ± 0.5	5.3 ± 2.9
Glucose	1.4 ± 0.1	0.24 ± 0.08	1.1 ± 0.1

4. Conclusions

AAs are abundantly present in human SC *in vivo*. Although depleted near the skin surface by normal daily washing routines, their concentrations are relatively constant across the rest of the SC. A 4-hour period of extraction either with iontophoresis, or simply passively, only removes part of the SC reservoir of AAs and does not allow interrogation of subdermal levels (as is possible with reverse iontophoresis for glucose, on the other hand). AA amounts extracted passively or with current are highly correlated with the quantities in the SC measured by an invasive tape-stripping procedure. It follows that minimally-invasive tools are available, therefore, with which to probe various analytes which are relevant to maintenance of the skin's hydration state *in vivo*. While iontophoresis has the additional advantage of being able to extract the AAs at a slightly higher (~50%) efficiency relative to passive diffusion, it is questionable if the increased complexity of the device for the former method justifies its use over the latter.

5. Acknowledgements

We thank the four subjects who participated in this study. This research was supported by the US National Institutes of Health (EB–001420). J.-P. S. thanks BIJAB, NSERC, FQRNT and Universities UK for funding.

6. References

1. Murray, R.K., Granner, D.K., Mayes, P.A., Rodwell, V.W., *Harper's Biochemistry*. 25th ed. 2000, Stamford, CT: Appleton&Lange. 927.
2. Bender, D.A., *Amino Acid Metabolism*. 2nd ed. ed. 1985, Chichester: John Wiley & Sons. 263.
3. Blomstrand, E., *Amino acids and central fatigue.* Amino Acids, 2001. **20**(1): p. 25-34.

4. Blomstrand, E., *A role for branched-chain amino acids in reducing central fatigue.* J Nutr, 2006. **136**(2): p. 544S-547S.

5. McGuire, J., et al., *Biochemical markers for post-operative fatigue after major surgery.* Brain Res Bull, 2003. **60**(1-2): p. 125-30.

6. Rawlings, A.V., *Sources and Role of Stratum Corneum Hydration*, in *Skin Barrier*, P.M. Elias, Feingold, K.R., Editor. 2006, Taylor & Francis. p. 399-425.

7. Rawlings, A.V. and P.J. Matts, *Stratum corneum moisturization at the molecular level: an update in relation to the dry skin cycle.* J Invest Dermatol, 2005. **124**(6): p. 1099-110.

8. Rawlings, A.V., et al., *Stratum corneum moisturization at the molecular level.* J Invest Dermatol, 1994. **103**(5): p. 731-41.

9. Marstein, S., E. Jellum, and L. Eldjarn, *The concentration of pyroglutamic acid (2-pyrrolidone-5-carboxylic acid) in normal and psoriatic epidermis, determined on a microgram scale by gas chromatography.* Clin Chim Acta, 1973. **49**(3): p. 389-95.

10. Horii, I., et al., *Stratum corneum hydration and amino acid content in xerotic skin.* Br J Dermatol, 1989. **121**(5): p. 587-92.

11. Denda, M., et al., *Stratum corneum sphingolipids and free amino acids in experimentally-induced scaly skin.* Arch Dermatol Res, 1992. **284**(6): p. 363-7.

12. Leboulanger, B., R.H. Guy, and M.B. Delgado-Charro, *Reverse iontophoresis for non-invasive transdermal monitoring.* Physiol Meas, 2004. **25**(3): p. R35-50.

13. Pitzer, K.R., et al., *Detection of hypoglycemia with the GlucoWatch biographer.* Diabetes Care, 2001. **24**(5): p. 881-5.

14. Pikal, M.J., *The role of electroosmotic flow in transdermal iontophoresis.* Adv Drug Deliv Rev, 2001. **46**(1-3): p. 281-305.

15. Rao, G., et al., *Reverse iontophoresis: noninvasive glucose monitoring in vivo in humans.* Pharm Res, 1995. **12**(12): p. 1869-73.

16. Wascotte, V., et al., *Assessment of the "skin reservoir" of urea by confocal Raman microspectroscopy and reverse iontophoresis in vivo.* Pharm Res, 2007. **24**(10): p. 1897-901.

17. Nixon, S., et al., *Reverse iontophoresis of L-lactate: In vitro and in vivo studies.* J Pharm Sci, 2007.

18. Sieg, A., R.H. Guy, and M.B. Delgado-Charro, *Noninvasive glucose monitoring by reverse iontophoresis in vivo: application of the internal standard concept.* Clin Chem, 2004. **50**(8): p. 1383-90.

19. Sieg, A., R.H. Guy, and M.B. Delgado-Charro, *Simultaneous extraction of urea and glucose by reverse iontophoresis in vivo.* Pharm Res, 2004. **21**(10): p. 1805-10.

20. Kalia, Y.N., et al., *Normalization of stratum corneum barrier function and transepidermal water loss in vivo.* Pharm Res, 2000. **17**(9): p. 1148-50.

21. Kalia, Y.N., F. Pirot, and R.H. Guy, *Homogeneous transport in a heterogeneous membrane: water diffusion across human stratum corneum in vivo.* Biophys. J., 1996. **71**(5): p. 2692-2700.

22. *An Improved Gradient Method for the AAA-Direct™ Separation of Amino Acids and Carbohydrates in Complex Sample Matrices*. 2006, Dionex corporation: Sunnyvale, CA. p. 12.

23. Kalia, Y.N., et al., *Assessment of topical bioavailability in vivo: the importance of stratum corneum thickness.* Skin Pharmacol Appl Skin Physiol, 2001. **14 Suppl 1**: p. 82-6.

24. Caspers, P.J., et al., *In vivo confocal Raman microspectroscopy of the skin: noninvasive determination of molecular concentration profiles.* J Invest Dermatol, 2001. **116**(3): p. 434-42.

25. Kingsbury, K.J., L. Kay, and M. Hjelm, *Contrasting plasma free amino acid patterns in elite athletes: association with fatigue and infection.* Br J Sports Med, 1998. **32**(1): p. 25-32; discussion 32-3.

26. Lepage, N., et al., *Age-specific distribution of plasma amino acid concentrations in a healthy pediatric population.* Clin Chem, 1997. **43**(12): p. 2397-402.

27. *Preparing Physiological Samples for Amino Acid Analysis*. 2000, Millipore Inc.: Bedford, MA. p. 4.

28. Ledger, P.W., *Skin biological issues in electrically enhanced transdermal delivery.* Adv Drug Deliv Rev, 1992. **9**: p. 289-307.

Conclusion and perspectives

In this thesis, the use of transdermal iontophoresis in sports medicine was investigated. More specifically, the objectives were to: (1) optimize the local delivery of the corticosteroid dexamethasone phosphate (Dex-Phos) by iontophoresis for the treatment of musculoskeletal inflammation, and (2) evaluate reverse iontophoresis as a mean to extract systemic amino acids (AAs), possible markers of fatigue in athletes.

1. Iontophoretic delivery of Dex-Phos

Iontophoresis represents an interesting alternative to the needle for the local delivery of corticosteroids, such as Dex-Phos, to treat injury-related inflammation of soft tissues. The optimal conditions for the electrotransport of Dex-Phos have, however, not been clearly identified yet. The iontophoretic delivery of Dex-Phos was therefore studied, *in vitro* using pig skin as a model, in order to evaluate the effects of competing ions and electroosmosis, and identify the optimal conditions for its delivery.

The negatively charged Dex-Phos was best delivered by electromigration from the cathode in absence of background electrolyte in the drug solution. In this situation, the Dex-Phos transport occurs against the electroosmotic solvent flow, which was found to have negligible effect on the efficiency of the drug the delivery. Iontophoresis of Dex-Phos is limited principally by the small mobility of the drug inside the membrane and the competition with counter-ions (mainly Na^+) present subdermally. As expected, the presence of competing co-ions, such as chloride or citrate, in the drug solution results in decreased Dex-Phos delivery.

In that respect, the effect of the accumulation of Cl^-, released by the Ag/AgCl cathode in the drug solution during current passage, was studied in detail. The Dex-Phos delivery was relatively robust to the release of Cl^- from the cathode in the donor solution, and remained optimal as long as the molar fraction of the drug in the first hour of current passage remained >50%. Tape-stripping experiments, performed after Dex-Phos iontophoresis, confirmed that the amount of the drug present in the stratum corneum (SC) was more abundant than that obtained after passive diffusion. The absolute amount of the

drug found in the membrane after iontophoresis could not explain the limited effect of Cl^- release by the cathode. It is possible, however, that the increased Dex-Phos concentration measured in the membrane compared to that in the donor solution, could bring insight to this phenomenon.

The results obtained in these *in vitro* studies will ultimately have to be verified *in vivo*. Clinical studies using the optimal delivery conditions should be conducted in order to demonstrate that the method is effective for the treatment of musculoskeletal injuries. Ideally, the drug's concentration in the (targeted) structures underlying the delivery electrode after iontophoresis should also be assessed to verify that sufficient drug is present to obtain a clinical effect. Such a quantitative study in human subjects could, however, be problematic as invasive methods (e.g., biopsy, microdialysis) would be required. One possible approach would be to deliver iontophoretically Dex-Phos, pre-surgery, in volunteers requiring a surgical repair of injured tissues. The tissues could then be sampled during the intervention and assayed for Dex-Phos.

2. Reverse iontophoresis of AAs

The AAs glutamine, tryptophan, isoleucine, leucine and valine are possible markers of overtraining in athletes. It was hypothesised that reverse iontophoresis could be used to monitor these molecules minimally-invasively. As the monitoring of AAs could find many other applications in medicine, the targeted molecules were extended to the 14 primary AAs that could be quantified by the analytical method used. The iontophoretic extraction of AAs from the skin was first evaluated *in vitro*, using pig skin as a model. The findings were then verified in a group of human subjects. Extraction of glucose was also measured as a positive control in both situations.

As expected, the extraction of essentially zwitterionic AAs from the skin was more efficient from the cathode, than from the anode or by passive diffusion. The iontophoretic extraction of the AAs was highly influenced by their presence in the outermost layer of the skin, the stratum corneum (SC). The AAs are indeed present in high quantity in the SC as they are major constituents of natural moisturizing factor (NMF), important to keep the skin hydrated. In pig skin, extraction by passive diffusion sampled only the AAs present in the SC. This was evidenced by the excellent agreement found between the amounts

extracted passively in 6 hours and those recovered in the tape-strips used to sample the SC. Iontophoretic extraction at the cathode permitted a quicker (~3 hours) extraction of the AAs 'reservoir'. Furthermore, the amounts of AAs extracted iontophoretically in a short extraction period (1 hour) were not influenced significantly by their sudermal concentration and correlated with their abundance in the SC. This demonstrated that iontophoresis could be used to assess the SC content in AAs, which could be useful for applications in dermatology and cosmetology. Once this 'reservoir' was emptied, the subdermal compartment could be sampled, suggesting that iontophoresis could also be used to monitor systemic levels of AAs.

The experiments in human volunteers revealed, however, that a 4-hour iontophoretic extraction period was insufficient to deplete the AAs 'reservoir'. The AAs were indeed much more abundant in human SC than in pig, meaning that a longer extraction period is required to deplete the SC 'depot'. It follows that the method can be used, *in vivo* in man, to evaluate the abundance of zwitterionic AAs in the SC, but is unpractical for the clinical monitoring of systemic levels. Since all the AAs identified as potential biological markers of fatigue in athletes are zwitterions, reverse iontophoresis is therefore not a viable option for their clinical monitoring. Reverse iontophoresis of neutral analytes remains, however, an interesting avenue for clinical monitoring when the molecule of interest, such as glucose for example, has a similar or higher systemic concentration than that found in the SC.

Finally, comparing the amount of a compound extracted by iontophoresis to that present in the SC determined by tape-stripping was an effective method to evaluate the ability of iontophoresis to pull molecules from beyond the SC reservoir. It would be interesting to apply this method to other compounds, such as the negatively charged lactate for example, another potential marker of fatigue in athletes, whose extraction *in vivo* was not clearly related to the blood levels.

Annexes

ANNEX I. Analytical method for the detection of amino acids and glucose

Amino acids and glucose were analyzed using ion chromatography combined with integrated pulsed amperometric detection (IC-IPAD). The 'improved' gradient method for the *AAA-Direct*™ separation of amino acids and carbohydrates in complex samples was used (Application Update 152, Dionex). As the separation is performed with an anion exchange column at high pH, amino acids and carbohydrates can be separated in the same run. The electrochemical detection has some advantages compared to other detection methods available for the quantification of amino acids. Compared to spectroscopic detection methods (i.e. UV absorption or fluorescence) no derivatization of the molecules is required and the method is more sensitive. The electrochemical detection has a similar sensitivity to mass spectroscopy and is much less sensitive to the presence of ions in the matrix of the samples to analyze. Indeed, the sensitivity of mass spectroscopy deceases dramatically when sodium is present in the solution of amino acids to analyze (Nagy et al., 2003, Rapid Commun Mass Specrom, 17, 983). As the extraction solution used for iontophoresis contained 20 mM NaCl, IC-IPAD seemed as the most convenient method to analyze amino acids (and glucose) as no sample preparation was necessary before analysis.

Equipment:

- gradient pump GP-50
- autosampler with column oven AS-50
- electrochemical detector ED-50
- Chromeleon software
- combination pH/Ag/AgCl reference electrode
- *AAA-Certified*™ disposable Au working electrode
- AminoPac PA10 analytical column + AminoPac PA10 guard column

Conditions:

Temperature: 33°C (to improve separation between Ser and Pro)

Flow rate: 0.25 mL/min

Injection volume: 25 µL (the volume of sample required is 100 µL)

Eluent: (A) 10 mM NaOH (2 litres)

(B) 250 mM NaOH (2 litres)

(C) 1 M sodium acetate + 25 mM NaOH (1 litre)

(D) 100 mM acetic acid (1litre)

All solutions were prepared from deionised water (18.2 MΩ·cm). The solutions were degassed with helium (He) for 10 minutes and kept under He pressure afterwards to avoid contamination from air. The sodium acetate was of electrochemical grade and bought from Dionex. 50% NaOH (electrochemical grade) was used to avoid inclusion of carbonates.

Table 1. *AAA-Direct* waveform applied for the detection at the gold surface

Time (s)	Potential vs pH reference (V)	Integration
0.00	+0.13	Off
0.04	+0.13	Off
0.05	+0.13	Off
0.21	+0.33	On
0.22	+0.55	On
0.46	+0.55	On
0.47	+0.33	On
0.56	+0.33	On
0.57	-1.67	Off
0.58	-1.67	Off
0.59	+0.93	Off
0.60	+0.13	Off

Table 2. Gradient method

Time (minutes)	Curve type	Solution			
		%A	%B	%C	%D
0.0	5	100.0	0.0	0.0	0.0
8.0	5	100.0	0.0	0.0	0.0
14.0	8	66.7	33.3	0.0	0.0
17.0	5	66.7	33.3	0.0	0.0
24.0	8	1.0	89.0	10.0	0.0
27.0	5	1.0	89.0	10.0	0.0
30.0	8	0.0	80.0	20.0	0.0
32.0	5	0.0	80.0	20.0	0.0
34.0	8	40.0	30.0	30.0	0.0
36.0	5	40.0	30.0	30.0	0.0
38.0	8	30.0	30.0	40.0	0.0
40.0	5	30.0	30.0	40.0	0.0
42.0	8	20.0	30.0	50.0	0.0
44.0	5	20.0	30.0	50.0	0.0
46.0	8	10.0	30.0	60.0	0.0
48.0	5	10.0	30.0	60.0	0.0
50.0	8	0.0	30.0	70.0	0.0
62.0	5	0.0	30.0	70.0	0.0
62.1	8	0.0	0.0	0.0	100.0
64.1	5	0.0	0.0	0.0	100.0
64.2	8	20.0	80.0	0.0	0.0
66.2	5	20.0	80.0	0.0	0.0
66.3	5	100.0	0.0	0.0	0.0
92.0	5	100.0	0.0	0.0	0.0

Results

As previously mentioned, it is possible to separate amino acids and carbohydrates with the IC-IPAD method. As glucose is known to be present in samples obtained by reverse iontophoresis (e.g., the GlucoWatch), it was important to make sure that this compound would not interfere with the detection of the amino acids. An initial concentration of 10 mM NaOH at the beginning of the gradient permits a quick elution of glucose (and most of other carbohydrates) compared to all primary amino acids except arginine and lysine (Application Note 150, Dionex). The inconvenient of this low initial NaOH concentration is a loss in sensitivity for some amino acids (mainly lysine, glutamine and asparagine), and was one of the reasons why lysine could not be quantified (Table 3).

Glutamine, a potential biomarker of fatigue in athletes, was found to co-elute with citrulline (Table 3) with the gradient method used (Table 2). Several variations of the gradient (e.g. vary the initial isocratic period, vary the curve type of initial gradient) were tried in order to increase the resolution between these two molecules, but none improved their separation. It was therefore decided to concentrate our efforts on the separation of the other amino acids with potential interest in sports medicine (tryptophan, isoleucine, leucine and valine) and those constituting natural moisturizing factor (NMF).

Using the recommended column temperature of 30°C resulted in a poor separation of serine and proline. Different temperatures (25-35°C) were therefore tested to optimize the separation of these two abundant compounds in NMF and a temperature of 33°C was chosen for that purpose.

Figure 1 is an example of chromatogram obtained with the conditions used. The following molecules were analysed in unknown samples: glucose, asparagine, alanine, threonine, glycine, valine, serine, proline, isoleucine, leucine, methionine, histidine, phenylalanine, tyrosine, tryptophan. In Table 3, the amino acids that could not be quantified are presented with the reasons for their exclusion. Finally, the linearity range, precision and repeatability for each amino acid quantified are summarized in Table 4.

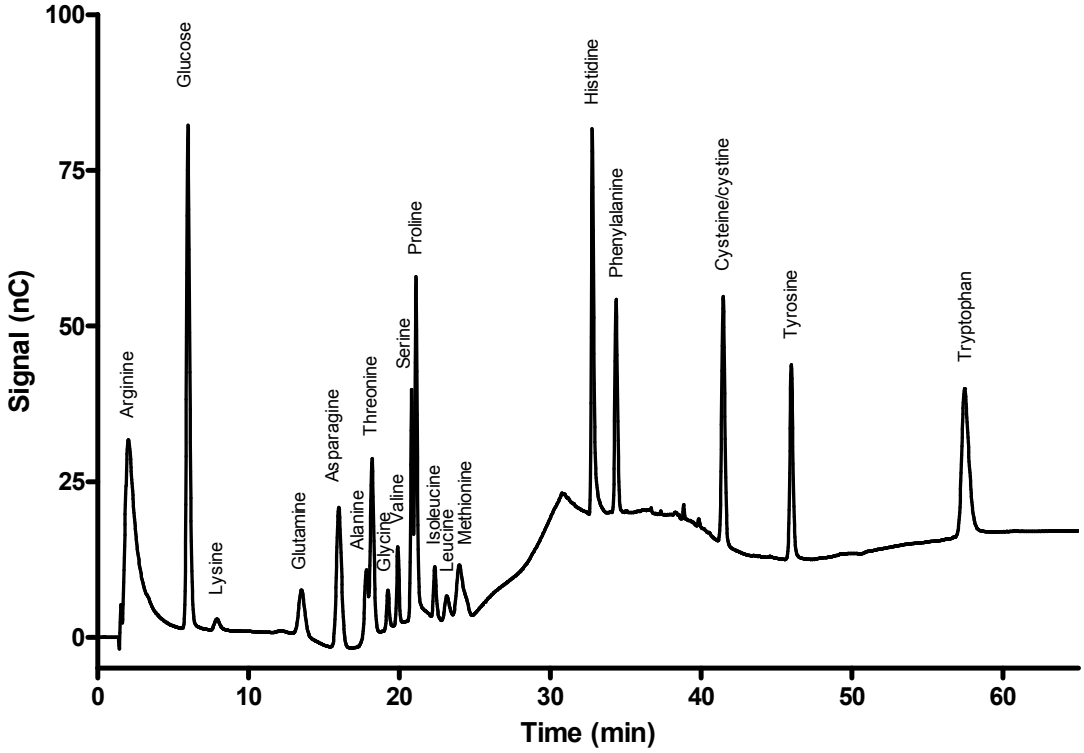

Figure 1. Example of chromatogram obtained for a standard solution containing 5 µM of each of the 20 primary amino acids and glucose.

Table 3. Molecules not analyzed in samples and reason for exclusion.

Molecule	Reason for exclusion
Arginine	Co-elution with urea + other unidentified molecules
Lysine	Poor sensitivity + co-elution with unidentified molecules
Glutamine	Co-elution with citrulline
Aspartate	Poor sensitivity
Glutamate	Poor sensitivity
Cysteine	Co-elution with cystine and other unidentified molecules

Table 4. Linearity range (r > 0.99), precision (at 1µM) and repeatability (at 1µM) of the method for the molecules analyzed using the above mentioned conditions.

Molecule	Linearity range (µM)	Precision (n = 4) (%)	Repeatability (n = 4) (%)
Glucose	0.05 - 50	97	1
Asparagine	0.1 – 5.0	113	6
Alanine	0.5 – 25	112	6
Threonine	0.25 - 25	97	4
Glycine	0.25 - 25	101	6
Valine	0.25 - 25	92	7
Serine	0.1 – 50	99	2
Proline	0.1 – 10	95	5
Isoleucine	0.1 – 10	95	4
Leucine	0.1 – 10	96	8
Methionine	0.25 – 10	94	5
Histidine	0.1 – 10	101	9
Phenylalanine	0.1 – 10	101	9
Tyrosine	0.1 - 10	97	7
Tryptophan	0.05 - 10	89	6

ANNEX II. Complements to Chapter 4

1. Concentration profiles of AAs and glucose in pig SC

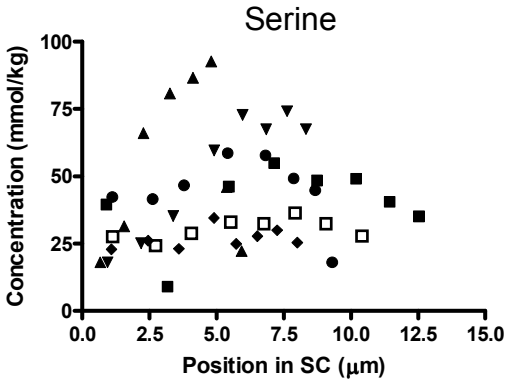

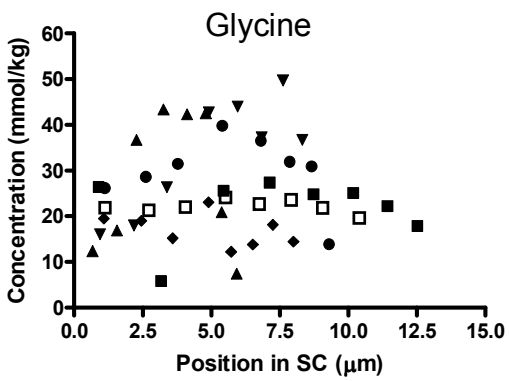

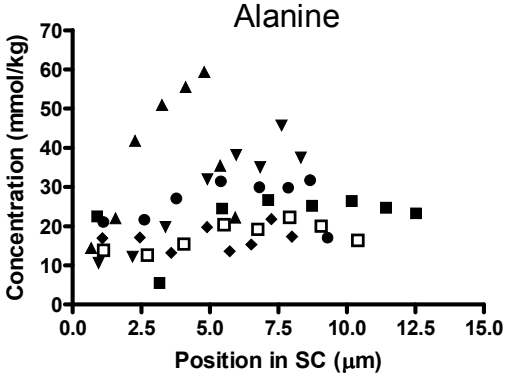

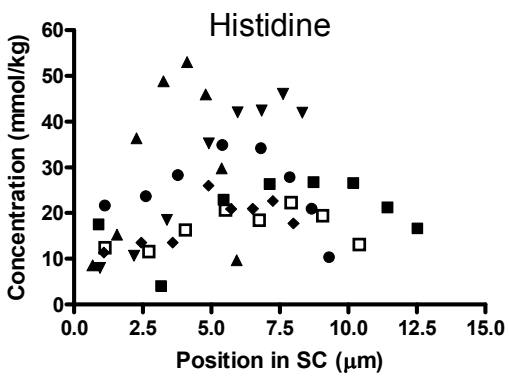

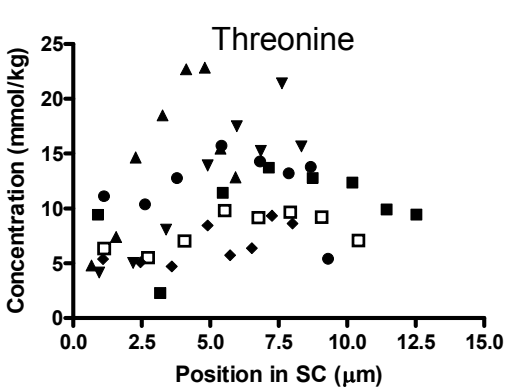

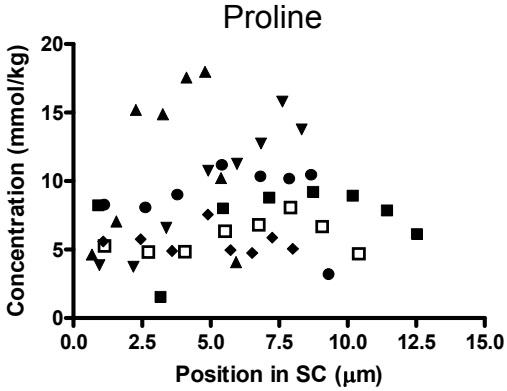

1. Concentration profiles of amino acids and glucose in pig SC (continued)

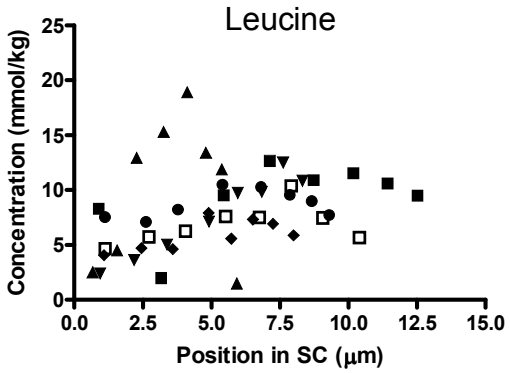

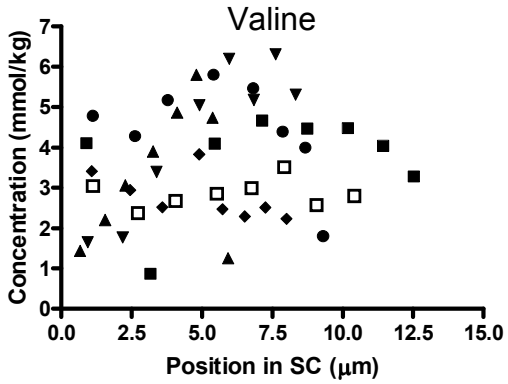

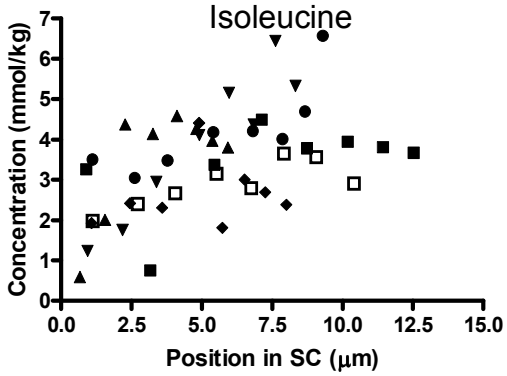

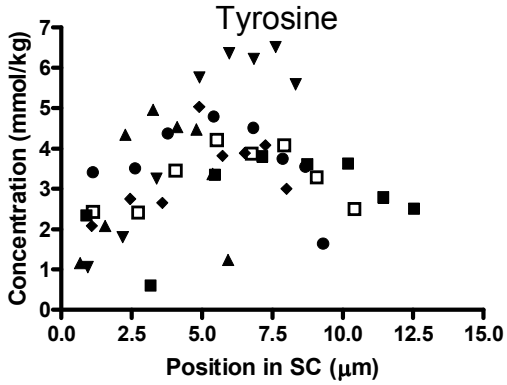

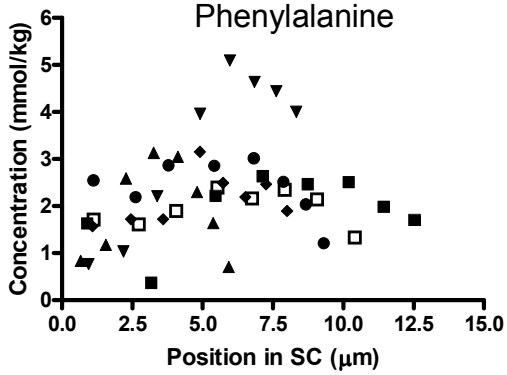

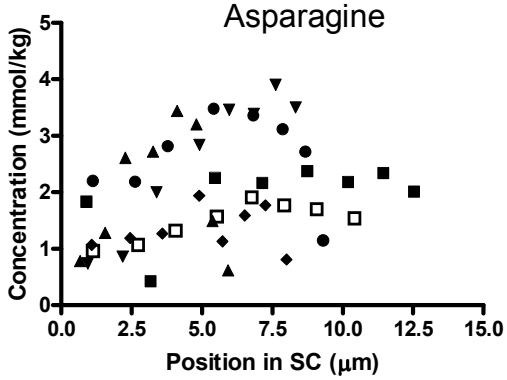

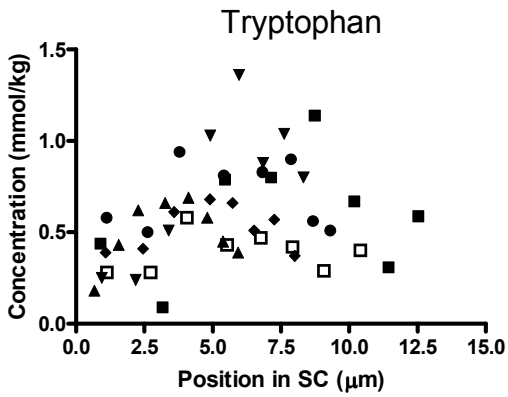

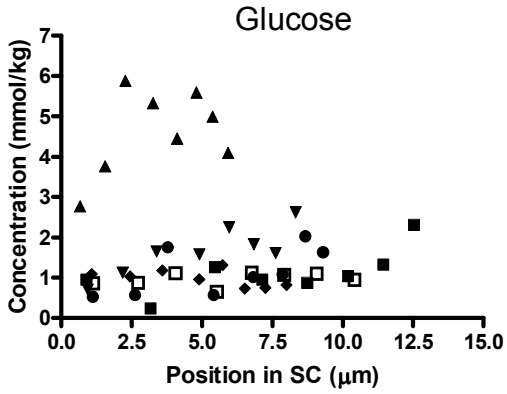

2. Fluxes at the cathode, anode and passive diffusion for amino acids and glucose as a function of time

Molecule	Compartment	Extraction fluxes ± SD (n = 6) at [nmol/(h·cm^2)]							
		0.25 h	0.5 h	1 h	2 h	3 h	4 h	5 h	6 h
Serine	Cathode	76.5 ± 23.4	38.3 ± 12.1	17.9 ± 3.5	10.2 ± 2.0	7.5 ± 2.0	5.0 ± 1.3	4.0 ± 1.0	3.3 ± 0.8
	Anode	57.9 ± 19.0	21.0 ± 5.4	11.0 ± 3.2	7.0 ± 2.6	4.7 ± 1.9	3.5 ± 1.1	2.8 ± 0.9	1.8 ± 0.5
	Passive	56.5 ± 20.1	18.0 ± 6.8	10.1 ± 2.8	7.4 ± 1.5	5.5 ± 1.1	4.1 ± 1.0	3.3 ± 0.9	2.8 ± 0.8
Glycine	Cathode	57.9 ± 16.1	30.5 ± 12.8	13.0 ± 2.7	7.5 ± 2.7	5.6 ± 1.7	4.1 ± 1.1	3.6 ± 1.2	3.3 ± 1.3
	Anode	49.7 ± 17.4	18.7 ± 5.6	9.6 ± 4.5	5.2 ± 2.3	3.9 ± 1.9	3.1 ± 1.0	2.3 ± 0.8	1.7 ± 0.5
	Passive	42.5 ± 9.7	15.1 ± 4.4	7.7 ± 1.8	5.1 ± 0.7	3.6 ± 0.6	2.7 ± 0.5	2.2 ± 0.5	1.9 ± 0.5
Alanine	Cathode	40.2 ± 9.2	21.8 ± 7.2	10.4 ± 2.3	5.9 ± 1.0	4.3 ± 0.9	3.0 ± 0.6	2.6 ± 0.6	2.4 ± 0.7
	Anode	34.2 ± 13.4	12.4 ± 4.7	6.2 ± 2.2	3.5 ± 1.2	2.3 ± 1.0	1.8 ± 0.4	1.6 ± 0.3	1.0 ± 0.3
	Passive	32.0 ± 11.0	11.5 ± 3.6	6.4 ± 1.1	4.0 ± 0.6	2.9 ± 0.6	2.3 ± 0.5	1.6 ± 0.4	1.3 ± 0.3
Histidine	Cathode	42.2 ± 11.2	24.2 ± 4.6	10.8 ± 2.5	5.6 ± 1.0	3.6 ± 0.3	2.3 ± 0.1	1.8 ± 0.1	1.4 ± 0.1
	Anode	19.1 ± 7.7	5.0 ± 1.8	2.1 ± 0.8	1.1 ± 0.4	0.7 ± 0.3	0.4 ± 0.3	0.3 ± 0.2	0.2 ± 0.1
	Passive	25.6 ± 9.9	8.6 ± 3.7	5.1 ± 1.7	3.8 ± 0.8	2.9 ± 0.7	2.2 ± 0.5	1.7 ± 0.5	1.4 ± 0.4
Threonine	Cathode	15.7 ± 5.3	8.4 ± 3.3	4.2 ± 1.0	2.6 ± 0.4	1.9 ± 0.6	1.3 ± 0.3	1.0 ± 0.3	0.9 ± 0.2
	Anode	12.3 ± 4.8	4.3 ± 1.4	2.4 ± 0.8	1.5 ± 0.6	1.0 ± 0.6	0.8 ± 0.3	0.6 ± 0.2	0.3 ± 0.1
	Passive	11.9 ± 5.2	4.0 ± 1.9	2.2 ± 0.6	1.7 ± 0.4	1.2 ± 0.3	1.0 ± 0.2	0.7 ± 0.2	0.6 ± 0.2
Proline	Cathode	14.4 ± 4.2	7.7 ± 2.5	3.8 ± 1.3	2.2 ± 0.6	1.6 ± 0.2	1.1 ± 0.2	0.9 ± 0.2	0.7 ± 0.1
	Anode	11.7 ± 3.9	4.1 ± 1.1	2.1 ± 0.5	1.3 ± 0.3	0.8 ± 0.2	0.6 ± 0.1	0.5 ± 0.1	0.3 ± 0.1
	Passive	10.9 ± 4.5	3.4 ± 1.3	2.0 ± 0.6	1.3 ± 0.4	0.9 ± 0.4	0.7 ± 0.1	0.5 ± 0.2	0.4 ± 0.2
Leucine	Cathode	10.0 ± 3.4	5.4 ± 1.8	3.2 ± 1.0	1.9 ± 0.5	1.5 ± 0.5	1.3 ± 0.3	1.0 ± 0.3	1.0 ± 0.4
	Anode	8.8 ± 5.4	3.2 ± 0.9	1.6 ± 0.7	1.1 ± 0.4	0.7 ± 0.2	0.7 ± 0.2	0.5 ± 0.1	0.4 ± 0.1
	Passive	10.0 ± 4.7	4.2 ± 1.3	2.0 ± 0.6	1.2 ± 0.3	1.1 ± 0.3	0.9 ± 0.2	0.9 ± 0.4	0.7 ± 0.2

2. Fluxes at the cathode, anode and passive diffusion for amino acids and glucose as a function of time (continued)

Molecule	Compartment	Extraction fluxes ± SD (n = 6) at [nmol/(h·cm^2)]							
		0.25 h	0.5 h	1 h	2 h	3 h	4 h	5 h	6 h
Valine	Cathode	6.8 ± 3.0	3.6 ± 1.4	2.1 ± 0.6	1.1 ± 0.2	0.9 ± 0.3	0.7 ± 0.4	0.5 ± 0.2	0.4 ± 0.2
	Anode	5.1 ± 2.2	1.8 ± 0.9	0.8 ± 0.2	0.5 ± 0.2	0.3 ± 0.1	0.25 ± 0.03	0.23 ± 0.08	0.15 ± 0.04
	Passive	5.8 ± 2.1	1.7 ± 0.7	1.0 ± 0.3	0.7 ± 0.2	0.5 ± 0.1	0.4 ± 0.1	0.4 ± 0.1	0.3 ± 0.1
Isoleucine	Cathode	5.0 ± 1.7	2.6 ± 0.8	1.5 ± 0.6	0.9 ± 0.3	0.7 ± 0.2	0.7 ± 0.2	0.5 ± 0.1	0.4 ± 0.1
	Anode	4.1 ± 1.8	1.6 ± 0.6	0.7 ± 0.1	0.5 ± 0.2	0.3 ± 0.1	0.3 ± 0.1	0.2 ± 0.1	0.2 ± 0.1
	Passive	4.8 ± 2.5	1.8 ± 0.5	0.9 ± 0.3	0.6 ± 0.2	0.5 ± 0.2	0.5 ± 0.1	0.4 ± 0.2	0.4 ± 0,1
Tyrosine	Cathode	3.1 ± 1.5	1.7 ± 0.7	0.9 ± 0.3	0.7 ± 0.2	0.5 ± 0.1	0.4 ± 0.1	0.4 ± 0.1	0.3 ± 0.1
	Anode	2.7 ± 1.2	1.1 ± 0.3	0.6 ± 0.1	0.4 ± 0.1	0.3 ± 0.1	0.2 ± 0.1	0.2 ± 0.1	0.1 ± 0.1
	Passive	3.0 ± 1.4	1.0 ± 0.4	0.6 ± 0.2	0.5 ± 0.1	0.4 ± 0.1	0.3 ± 0.1	0.3 ± 0.1	0.1 ± 0.1
Phenylalanine	Cathode	2.6 ± 1.4	1.4 ± 0.6	0.7 ± 0.3	0.5 ± 0.2	0.4 ± 0.1	0.3 ± 0.1	0.3 ± 0.1	0.2 ± 0.1
	Anode	2.3 ± 0.9	0.8 ± 0.2	0.4 ± 0.1	0.3 ± 0.1	0.2 ± 0.1	0.17 ± 0.04	0.15 ± 0.05	0.09 ± 0.04
	Passive	2.6 ± 1.2	0.8 ± 0.3	0.5 ± 0.1	0.3 ± 0.1	0.3 ± 0.1	0.24 ± 0.04	0.2 ± 0.1	0.18 ± 0.04
Asparagine	Cathode	2.8 ± 1.5	1.5 ± 0.5	0.7 ± 0.3	0.5 ± 0.2	0.3 ± 0.1	0.2 ± 0.1	0.2 ± 0.1	0.2 ± 0.1
	Anode	2.3 ± 1.3	0.7 ± 0.4	0.4 ± 0.2	0.2 ± 0.1	0.2 ± 0.1	0.1 ± 0.1	0.09 ± 0.04	0.06 ± 0.05
	Passive	2.9 ± 1.5	0.9 ± 0.5	0.5 ± 0.2	0.4 ± 0.1	0.3 ± 0.1	0.2 ± 0.1	0.2 ± 0.1	0.1 ± 0.1
Tryptophan	Cathode	0.5 ± 0.3	0.2 ± 0.1	0.2 ± 0.1	0.09 ± 0.05	0.08 ± 0.03	0.06 ± 0.03	0.05 ± 0.03	0.05 ± 0.03
	Anode	0.4 ± 0.2	0.2 ± 0.1	0.06 ± 0.03	0.03 ± 0.02	0.03 ± 0.02	0.02 ± 0.01	0.01 ± 0.01	0.01 ± 0.01
	Passive	0.5 ± 0.2	0.2 ± 0.1	0.08 ± 0.04	0.07 ± 0.03	0.06 ± 0.02	0.04 ± 0.02	0.04 ± 0.02	0.03 ± 0.02
Glucose	Cathode	2.5 ± 2.0	1.5 ± 1.3	0.9 ± 0.9	0.6 ± 0.5	0.5 ± 0.4	0.4 ± 0.3	0.4 ± 0.3	0.4 ± 0.3
	Anode	2.4 ± 1.5	0.5 ± 0.3	0.2 ± 0.1	0.1 ± 0.1	0.1 ± 0.1	0.1 ± 0.1	0.1 ± 0.1	0.2 ± 0.2
	Passive	1.8 ± 1.1	0.4 ± 0.3	0.2 ± 0.1	0.1 ± 0.1	0.1 ± 0.1	0.1 ± 0.1	0.05 ± 0.04	0.05 ± 0.04

3. Cumulative amount of amino acids and glucose (mean ± SD, n = 6) extracted as a function of time at the cathode and by passive diffusion. The quantities in the SC determined by tape-stripping are shown for comparison.

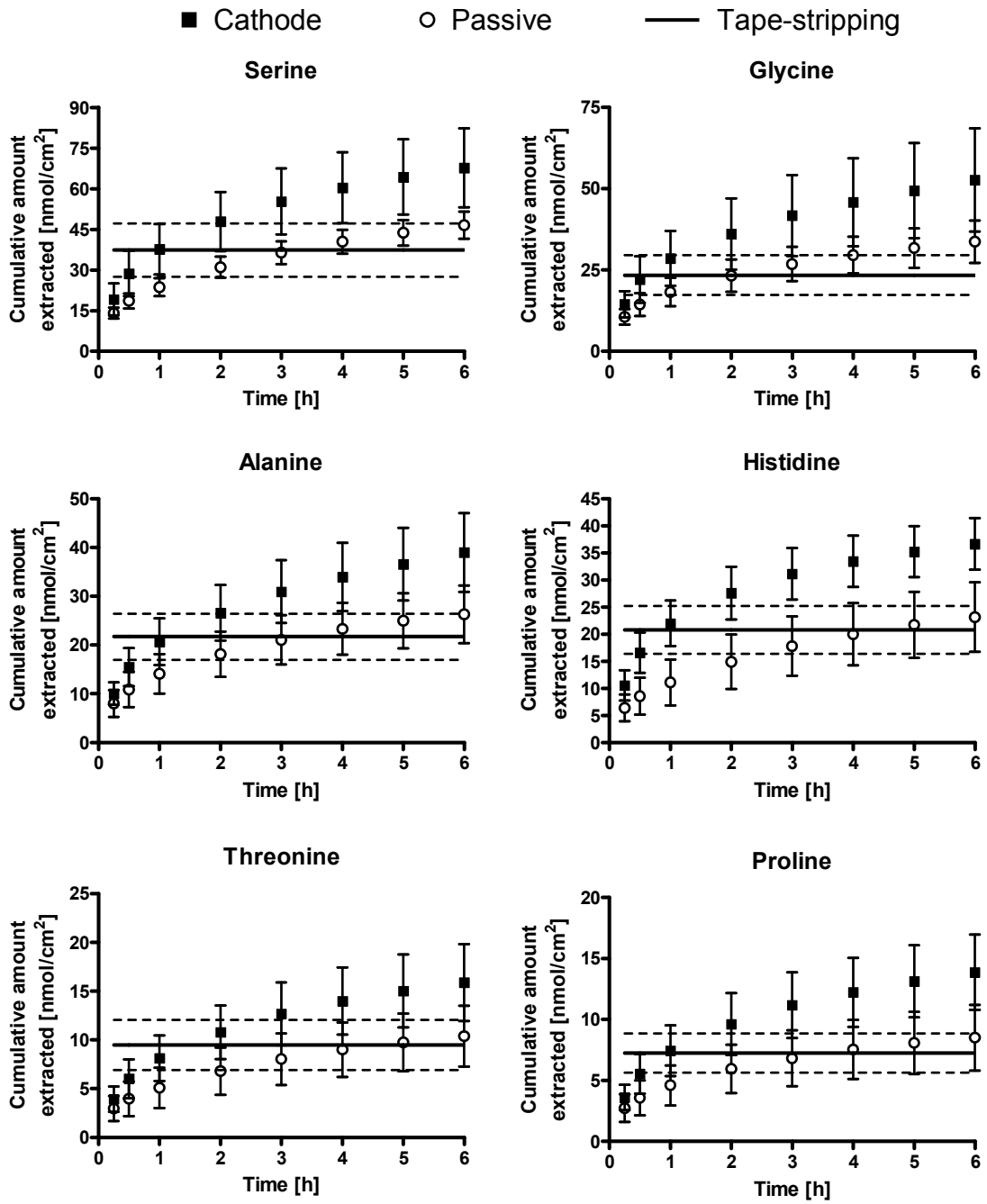

3. Cumulative amount of amino acids and glucose (mean ± SD, n = 6) extracted as a function of time at the cathode and by passive diffusion. The quantities in the SC determined by tape-stripping are shown for comparison. (continued)

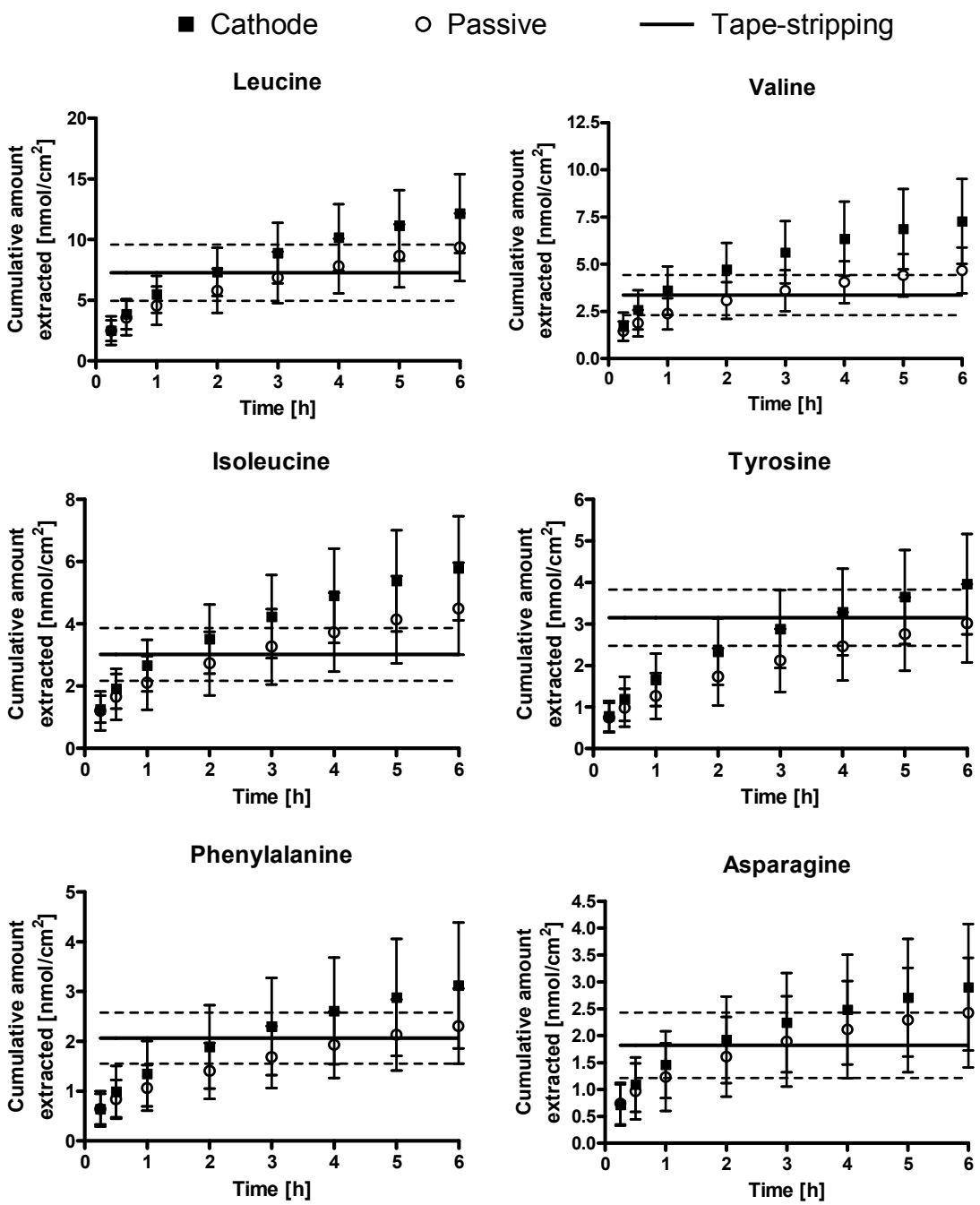

3. Cumulative amount of amino acids and glucose (mean ± SD, n = 6) extracted as a function of time at the cathode and by passive diffusion. The quantities in the SC determined by tape-stripping are shown for comparison. (continued)

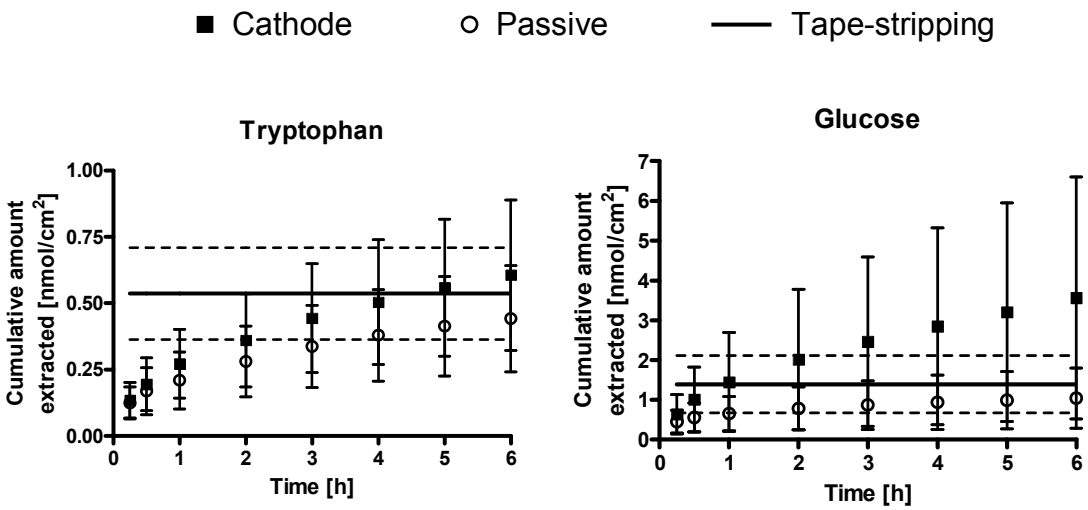

ANNEX III. Complements to Chapter 5

1. Iontophoretic extraction fluxes at the cathode and anode as a function of time and subdermal concentration of AAs and glucose when the subdermal electrolyte was PBS.

Serine fluxes (± SD, n = 6) for experiments in PBS [nmol/(h·cm^2)]

Time (h)	0.1 mM		0.25 mM		0.5 mM	
	Cathode	Anode	Cathode	Anode	Cathode	Anode
1	29.1 ± 11.3	24.0 ± 5.7	30.5 ± 11.0	19.6 ± 6.7	27.2 ± 4.6	15.2 ± 3.0
2	8.6 ± 1.7	6.8 ± 0.7	10.4 ± 8.1	7.2 ± 4.5	10.3 ± 4.2	6.9 ± 2.7
3	4.7 ± 0.7	3.3 ± 0.4	6.1 ± 4.6	4.2 ± 3.2	7.2 ± 3.7	4.3 ± 2.2
4	3.3 ± 0.7	2.0 ± 0.3	5.2 ± 4.3	2.9 ± 2.4	5.8 ± 2.4	3.9 ± 2.7
5	2.7 ± 0.6	1.4 ± 0.2	4.1 ± 2.8	2.3 ± 1.8	5.0 ± 1.6	2.8 ± 1.9
6	2.1 ± 0.5	1.0 ± 0.2	3.5 ± 2.3	1.9 ± 1.3	4.3 ± 1.5	2.5 ± 1.6

Glycine fluxes (± SD, n = 6) for experiments in PBS [nmol/(h·cm^2)]

Time (h)	0.1 mM		0.25 mM		0.5 mM	
	Cathode	Anode	Cathode	Anode	Cathode	Anode
1	24.0 ± 7.9	20.3 ± 3.0	22.6 ± 9.6	16.5 ± 7.0	20.7 ± 4.4	12.4 ± 2.9
2	6.6 ± 2.0	5.1 ± 0.9	7.7 ± 5.2	5.5 ± 3.8	7.5 ± 2.8	4.8 ± 2.0
3	3.9 ± 1.0	2.6 ± 1.0	5.4 ± 3.7	3.1 ± 2.6	5.5 ± 1.9	2.9 ± 1.9
4	3.0 ± 0.8	1.8 ± 0.9	4.8 ± 3.2	2.2 ± 1.6	4.7 ± 1.4	2.6 ± 1.7
5	2.4 ± 0.8	1.5 ± 1.1	4.1 ± 2.3	2.0 ± 1.4	4.5 ± 0.9	2.0 ± 1.2
6	2.1 ± 0.7	1.4 ± 1.1	3.9 ± 2.4	1.7 ± 1.1	3.9 ± 1.0	2.1 ± 1.0

Alanine fluxes (± SD, n = 6) for experiments in PBS [nmol/(h·cm^2)]

Time (h)	0.1 mM		0.25 mM		0.5 mM	
	Cathode	Anode	Cathode	Anode	Cathode	Anode
1	17.2 ± 5.0	13.5 ± 2.3	17.6 ± 4.9	12.0 ± 3.8	20.3 ± 2.8	10.9 ± 2.4
2	5.2 ± 0.9	3.8 ± 0.4	6.7 ± 3.6	4.3 ± 2.0	7.3 ± 3.0	4.5 ± 2.2
3	2.9 ± 0.6	1.9 ± 0.4	4.6 ± 2.8	2.5 ± 1.5	5.3 ± 2.2	2.7 ± 1.7
4	2.3 ± 0.4	1.3 ± 0.5	4.0 ± 2.4	1.8 ± 0.9	4.5 ± 1.4	2.3 ± 1.5
5	1.9 ± 0.5	1.0 ± 0.6	3.2 ± 1.8	1.5 ± 0.6	4.1 ± 0.9	1.4 ± 0.7
6	1.6 ± 0.5	0.9 ± 0.7	3.1 ± 1.7	1.3 ± 0.5	3.5 ± 0.9	1.7 ± 0.7

Histidine fluxes (± SD, n = 6) for experiments in PBS [nmol/(h·cm^2)]

Time (h)	0.1 mM		0.25 mM		0.5 mM	
	Cathode	Anode	Cathode	Anode	Cathode	Anode
1	18.4 ± 5.0	8.0 ± 2.3	17.7 ± 6.4	5.1 ± 2.0	19.6 ± 3.1	3.3 ± 1.1
2	5.9 ± 0.8	2.1 ± 0.9	6.4 ± 4.2	1.9 ± 0.7	6.8 ± 2.4	1.0 ± 0.4
3	3.2 ± 0.5	1.0± 0.3	3.7 ± 1.9	0.9 ± 0.3	4.8 ± 1.7	0.6 ± 0.4
4	2.1 ± 0.4	0.5 ± 0.2	3.2 ± 2.1	0.5 ± 0.1	4.2 ± 1.4	0.6 ± 0.4
5	1.8 ± 0.5	0.4 ± 0.2	2.7 ± 0.9	0.4 ± 0.1	3.6 ± 0.8	0.4 ± 0.3
6	1.5 ± 0.5	0.2 ± 0.1	2.4 ± 1.1	0.3 ± 0.1	3.0 ± 0.6	0.4 ± 0.3

Threonine fluxes (± SD, n = 6) for experiments in PBS [nmol/(h·cm^2)]

Time (h)	0.1 mM		0.25 mM		0.5 mM	
	Cathode	Anode	Cathode	Anode	Cathode	Anode
1	7.2 ± 2.7	5.2 ± 0.9	7.1 ± 1.9	4.7 ± 1.8	7.6 ± 1.5	3.3 ± 0.5
2	2.5 ± 0.6	1.6 ± 0.1	3.2 ± 1.8	1.9 ± 1.1	3.5 ± 0.9	1.5 ± 0.5
3	1.4 ± 0.3	0.8 ± 0.2	2.1 ± 1.2	1.0 ± 0.8	2.9 ± 0.9	1.0 ± 0.4
4	1.1 ± 0.2	0.5 ± 0.1	2.0 ± 1.2	0.8 ± 0.5	2.5 ± 0.5	0.9 ± 0.6
5	0.9 ± 0.2	0.4 ± 0.1	1.6 ± 0.8	0.6 ± 0.3	2.5 ± 0.4	0.7 ± 0.3
6	0.8 ± 0.2	0.3 ± 0.1	1.5 ± 0.7	0.5 ± 0.2	2.2 ± 0.3	0.7 ± 0.3

Proline fluxes (± SD, n = 6) for experiments in PBS [nmol/(h·cm^2)]

Time (h)	0.1 mM		0.25 mM		0.5 mM	
	Cathode	Anode	Cathode	Anode	Cathode	Anode
1	6.9 ± 2.6	5.0 ± 1.4	6.6 ± 1.5	4.2 ± 1.8	7.0 ± 0.6	3.0 ± 0.6
2	2.3 ± 0.5	1.5 ± 0.2	2.9 ± 1.6	1.5 ± 0.8	3.4 ± 0.9	1.4 ± 0.7
3	1.4 ± 0.3	0.8 ± 0.2	1.9 ± 0.8	0.8 ± 0.5	2.6 ± 0.7	0.8 ± 0.4
4	1.0 ± 0.2	0.5 ± 0.2	1.8 ± 1.0	0.5 ± 0.3	2.4 ± 0.5	0.8 ± 0.4
5	0.9 ± 0.3	0.4 ± 0.2	1.5 ± 0.6	0.5 ± 0.2	2.3 ± 0.2	0.5 ± 0.2
6	0.8 ± 0.2	0.3 ± 0.2	1.4 ± 0.6	0.4 ± 0.2	2.0 ± 0.4	0.7 ± 0.2

Leucine fluxes (± SD, n = 6) for experiments in PBS [nmol/(h·cm^2)]

Time (h)	0.1 mM		0.25 mM		0.5 mM	
	Cathode	Anode	Cathode	Anode	Cathode	Anode
1	5.5 ± 1.7	3.9 ± 1.3	5.2 ± 1.1	3.2 ± 2.0	5.8 ± 1.5	5.1 ± 6.2
2	2.4 ± 0.7	1.4 ± 0.3	2.7 ± 1.4	1.4 ± 0.8	3.1 ± 0.4	1.6 ± 1.3
3	1.3 ± 0.3	0.7 ± 0.2	1.8 ± 0.5	0.7 ± 0.4	2.5 ± 0.6	0.9 ± 0.2
4	1.2 ± 0.4	0.5 ± 0.2	1.7 ± 0.9	0.5 ± 0.2	2.5 ± 0.4	0.9 ± 0.4
5	1.2 ± 0.5	0.4 ± 0.1	1.8 ± 0.3	0.6 ± 0.2	2.5 ± 0.2	0.7 ± 0.2
6	1.0 ± 0.4	0.3 ± 0.1	2.0 ± 0.6	0.5 ± 0.2	2.4 ± 0.4	0.7 ± 0.2

Valine fluxes (± SD, n = 6) for experiments in PBS [nmol/(h·cm^2)]

Time (h)	0.1 mM		0.25 mM		0.5 mM	
	Cathode	Anode	Cathode	Anode	Cathode	Anode
1	3.2 ± 1.2	2.5 ± 0.4	3.6 ± 1.1	2.1 ± 1.2	4.1 ± 1.3	1.5 ± 0.5
2	1.5 ± 0.4	0.6 ± 0.1	2.0 ± 1.0	0.9 ± 0.6	2.4 ± 0.4	0.6 ± 0.1
3	0.9 ± 0.3	0.4 ± 0.1	1.4 ± 0.7	0.5 ± 0.4	2.0 ± 0.4	0.4 ± 0.2
4	0.6 ± 0.2	0.3 ± 0.2	1.5 ± 0.6	0.4 ± 0.2	1.9 ± 0.2	0.4 ± 0.2
5	0.6 ± 0.1	0.2 ± 0.1	1.3 ± 0.5	0.4 ± 0.2	2.0 ± 0.1	0.2 ± 0.1
6	0.5 ± 0.1	0.1 ± 0.2	1.2 ± 0.5	0.4 ± 0.1	1.7 ± 0.2	0.5 ± 0.1

Isoleucine fluxes (± SD, n = 6) for experiments in PBS [nmol/(h·cm^2)]

Time (h)	0.1 mM		0.25 mM		0.5 mM	
	Cathode	Anode	Cathode	Anode	Cathode	Anode
1	2.2 ± 0.6	1.4 ± 0.3	2.2 ± 0.4	1.7 ± 1.5	3.3 ± 1.1	1.0 ± 0.3
2	1.1 ± 0.3	0.4 ± 0.2	1.5 ± 0.6	0.7 ± 0.5	2.1 ± 0.3	0.5 ± 0.1
3	0.7 ± 0.1	0.3 ± 0.1	1.1 ± 0.3	0.3 ± 0.2	1.9 ± 0.4	0.3 ± 0.1
4	0.6 ± 0.2	0.21 ± 0.04	1.1 ± 0.3	0.3 ± 0.1	1.9 ± 0.2	0.4 ± 0.1
5	0.6 ± 0.1	0.2 ± 0.1	1.1 ± 0.1	0.3 ± 0.1	1.9 ± 0.2	0.3 ± 0.1
6	0.6 ± 0.1	0.2 ± 0.1	1.1 ± 0.2	0.2 ± 0.1	1.7 ± 0.3	0.4 ± 0.1

Tyrosine fluxes (± SD, n = 6) for experiments in PBS [nmol/(h·cm^2)]

Time (h)	0.1 mM		0.25 mM		0.5 mM	
	Cathode	Anode	Cathode	Anode	Cathode	Anode
1	1.6 ± 0.5	0.9 ± 0.3	1.8 ± 0.4	1.5 ± 1.3	2.2 ± 0.8	0.9 ± 0.2
2	1.1 ± 0.2	0.7 ± 0.2	1.4 ± 0.5	0.8 ± 0.6	1.9 ± 0.5	0.5 ± 0.1
3	0.7 ± 0.1	0.4 ± 0.2	1.1 ± 0.3	0.5 ± 0.3	1.9 ± 0.4	0.4 ± 0.1
4	0.6 ± 0.1	0.2 ± 0.2	1.1 ± 0.4	0.4 ± 0.2	1.8 ± 0.2	0.4 ± 0.1
5	0.6 ± 0.1	0.2 ± 0.1	1.1 ± 0.2	0.3 ± 0.2	1.8 ± 0.2	0.3 ± 0.1
6	0.5 ± 0.1	0.1 ± 0.1	1.1 ± 0.3	0.3 ± 0.2	1.6 ± 0.2	0.3 ± 0.1

Phenylalanine fluxes (± SD, n = 6) for experiments in PBS [nmol/(h·cm^2)]

Time (h)	0.1 mM		0.25 mM		0.5 mM	
	Cathode	Anode	Cathode	Anode	Cathode	Anode
1	1.3 ± 0.5	1.0 ± 0.2	1.5 ± 0.4	1.3 ± 1.3	2.2 ± 0.9	0.6 ± 0.2
2	0.8 ± 0.3	0.3 ± 0.1	1.3 ± 0.5	0.6 ± 0.5	1.9 ± 0.5	0.3 ± 0.1
3	0.5 ± 0.1	0.18 ± 0.04	1.0 ± 0.3	0.3 ± 0.2	1.8 ± 0.5	0.2 ± 0.1
4	0.5 ± 0.1	0.15 ± 0.02	1.1 ± 0.4	0.2 ± 0.1	1.8 ± 0.2	0.3 ± 0.1
5	0.4 ± 0.1	0.13 ± 0.03	1.1 ± 0.2	0.3 ± 0.1	1.7 ± 0.2	0.2 ± 0.1
6	0.4 ± 0.1	0.10 ± 0.03	1.0 ± 0.3	0.2 ± 0.1	1.6 ± 0.3	0.3 ± 0.1

Asparagine fluxes (± SD, n = 6) for experiments in PBS [nmol/(h·cm^2)]

Time (h)	0.1 mM		0.25 mM		0.5 mM	
	Cathode	Anode	Cathode	Anode	Cathode	Anode
1	1.5 ± 0.6	0.9 ± 0.1	1.7 ± 0.6	1.4 ± 1.3	2.8 ± 1.1	0.7 ± 0.1
2	0.7 ± 0.2	0.29 ± 0.05	1.2 ± 0.4	0.6 ± 0.6	1.8 ± 0.3	0.3 ± 0.1
3	0.5 ± 0.1	0.17 ± 0.04	1.1 ± 0.3	0.3 ± 0.3	1.8 ± 0.3	0.2 ± 0.1
4	0.4 ± 0.1	0.13 ± 0.06	1.1 ± 0.2	0.2 ± 0.1	1.8 ± 0.1	0.2 ± 0.1
5	0.4 ± 0.1	0.11 ± 0.03	1.1 ± 0.1	0.2 ± 0.1	1.8 ± 0.2	0.20 ± 0.03
6	0.4 ± 0.1	0.10 ± 0.03	1.0 ± 0.2	0.2 ± 0.1	1.7 ± 0.2	0.3 ± 0.1

Tryptophan fluxes (± SD, n = 6) for experiments in PBS [nmol/(h·cm^2)]

Time (h)	0.1 mM		0.25 mM		0.5 mM	
	Cathode	Anode	Cathode	Anode	Cathode	Anode
1	0.4 ± 0.1	0.21 ± 0.05	0.6 ± 0.1	0.62 ± 1.02	1.2 ± 0.7	0.26 ± 0.13
2	0.3 ± 0.1	0.12 ± 0.04	0.7 ± 0.1	0.32 ± 0.40	1.3 ± 0.3	0.16 ± 0.06
3	0.3 ± 0.1	0.08 ± 0.02	0.7 ± 0.1	0.13 ± 0.07	1.4 ± 0.3	0.11 ± 0.03
4	0.3 ± 0.1	0.05 ± 0.01	0.8 ± 0.1	0.11 ± 0.03	1.5 ± 0.2	0.13 ± 0.04
5	0.3 ± 0.1	0.05 ± 0.02	0.8 ± 0.1	0.09 ± 0.02	1.5 ± 0.3	0.11 ± 0.03
6	0.3 ± 0.1	0.04 ± 0.02	0.8 ± 0.1	0.09 ± 0.04	1.4 ± 0.2	0.13 ± 0.05

Methionine fluxes (± SD, n = 6) for experiments in PBS [nmol/(h·cm^2)]

Time (h)	0.1 mM		0.25 mM		0.5 mM	
	Cathode	Anode	Cathode	Anode	Cathode	Anode
1	0.6 ± 0.2	0.18 ± 0.16	0.8 ± 0.2	0.21 ± 0.23	1.8 ± 0.8	0.27 ± 0.16
2	0.4 ± 0.1	0.09 ± 0.02	0.7 ± 0.1	0.14 ± 0.17	1.4 ± 0.3	0.08 ± 0.04
3	0.3 ± 0.1	0.04 ± 0.02	0.56 ± 0.04	0.07 ± 0.03	1.3 ± 0.3	0.08 ± 0.02
4	0.2 ± 0.1	0.04 ± 0.04	0.6 ± 0.1	0.07 ± 0.04	1.4 ± 0.3	0.13 ± 0.10
5	0.2 ± 0.1	0.05 ± 0.01	0.7 ± 0.1	0.09 ± 0.04	1.4 ± 0.3	0.10 ± 0.04
6	0.2 ± 0.1	0.04 ± 0.03	0.6 ± 0.2	0.05 ± 0.02	1.2 ± 0.3	0.13 ± 0.05

Glucose fluxes (± SD, n = 6) for experiments in PBS [nmol/(h·cm^2)]

Time (h)	0.1 mM		0.25 mM		0.5 mM	
	Cathode	Anode	Cathode	Anode	Cathode	Anode
1	5.1 ± 2.4	1.5 ± 1.6	8.3 ± 3.0	8.1 ± 14.3	16.2 ± 7.9	1.6 ± 2.1
2	4.1 ± 0.8	0.4 ± 0.4	9.1 ± 1.4	3.1 ± 5.2	15.6 ± 3.4	0.5 ± 0.4
3	3.9 ± 0.4	0.3 ± 0.3	9.0 ± 1.0	1.3 ± 1.4	16.6 ± 2.9	0.5 ± 0.2
4	3.8 ± 0.2	0.4 ± 0.3	10.0 ± 1.0	0.7 ± 0.5	17.1 ± 2.3	0.6 ± 0.2
5	3.9 ± 0.5	0.5 ± 0.4	9.8 ± 1.0	0.9 ± 0.7	17.4 ± 2.1	0.8 ± 0.3
6	3.9 ± 0.3	0.5 ± 0.4	9.9 ± 1.2	1.1 ± 0.7	16.1 ± 1.8	1.5 ± 0.7

2. Iontophoretic extraction fluxes at the cathode and anode as a function of time and subdermal concentration of AAs and glucose when the subdermal electrolyte was PB.

Serine fluxes (± SD, n = 6) for experiments in PB [nmol/(h·cm^2)]

Time (h)	0.1 mM		0.25 mM		0.5 mM	
	Cathode	Anode	Cathode	Anode	Cathode	Anode
1	45.1 ± 18.2	34.5 ± 16.0	39.1 ± 6.5	28.5 ± 4.9	47.5 ± 13.6	28.3 ± 12.5
2	15.0 ± 4.0	12.2 ± 5.2	15.4 ± 2.7	10.3 ± 3.8	20.4 ± 4.4	9.3 ± 3.3
3	9.6 ± 3.1	6.0 ± 2.6	10.7 ± 2.2	7.0 ± 2.9	14.8 ± 3.5	5.7 ± 2.2
4	7.4 ± 2.6	3.1 ± 1.3	8.9 ± 1.4	4.3 ± 1.7	12.9 ± 1.7	3.6 ± 2.4
5	5.6 ± 1.7	1.8 ± 0.7	8.1 ± 1.8	3.1 ± 1.3	11.7 ± 2.5	3.7 ± 1.6
6	5.3 ± 1.6	1.7 ± 1.1	7.1 ± 1.2	2.0 ± 0.8	12.0 ± 2.5	1.9 ± 1.0

Glycine fluxes (± SD, n = 6) for experiments in PB [nmol/(h·cm^2)]

Time (h)	0.1 mM		0.25 mM		0.5 mM	
	Cathode	Anode	Cathode	Anode	Cathode	Anode
1	27.5 ± 7.4	24.0 ± 6.5	20.6 ± 10.3	18.6 ± 5.8	29.5 ± 8.5	18.6 ± 6.8
2	11.2 ± 3.6	7.3 ± 2.2	8.8 ± 3.1	6.1 ± 3.0	13.6 ± 2.3	5.8 ± 2.7
3	6.9 ± 2.1	3.5 ± 1.7	6.9 ± 2.9	4.1 ± 2.0	11.4 ± 2.3	3.8 ± 2.3
4	6.4 ± 2.0	2.0 ± 1.0	6.3 ± 1.6	2.6 ± 1.5	10.1 ± 2.3	2.6 ± 2.3
5	5.6 ± 2.0	0.9 ± 0.3	5.5 ± 2.1	1.9 ± 1.1	9.4 ± 1.5	2.8 ± 1.0
6	4.7 ± 0.9	0.9 ± 0.8	5.3 ± 1.5	1.4 ± 0.9	9.4 ± 1.3	1.8 ± 0.9

Alanine fluxes (± SD, n = 6) for experiments in PB [nmol/(h·cm^2)]

Time (h)	0.1 mM		0.25 mM		0.5 mM	
	Cathode	Anode	Cathode	Anode	Cathode	Anode
1	19.0 ± 3.6	13.7 ± 3.3	17.2 ± 7.0	14.4 ± 4.4	19.7 ± 5.3	11.4 ± 3.9
2	8.0 ± 1.8	5.2 ± 1.3	8.3 ± 2.6	4.8 ± 2.4	11.4 ± 2.6	4.0 ± 1.8
3	5.7 ± 1.1	2.7 ± 0.8	6.7 ± 2.2	3.1 ± 1.5	9.9 ± 1.0	2.6 ± 1.7
4	4.8 ± 1.3	1.6 ± 0.4	5.7 ± 0.8	1.9 ± 1.0	8.7 ± 0.9	1.7 ± 1.9
5	4.2 ± 0.8	1.2 ± 0.4	5.6 ± 1.5	1.4 ± 0.5	8.9 ± 0.9	1.6 ± 1.0
6	4.4 ± 0.7	1.1 ± 0.3	5.0 ± 0.8	1.0 ± 0.5	8.6 ± 1.0	1.2 ± 0.5

Histidine fluxes (± SD, n = 6) for experiments in PB [nmol/(h·cm^2)]

Time (h)	0.1 mM		0.25 mM		0.5 mM	
	Cathode	Anode	Cathode	Anode	Cathode	Anode
1	18.1 ± 3.7	5.4 ± 2.9	16.9 ± 4.0	4.9 ± 1.5	21.2 ± 6.5	5.6 ± 2.0
2	7.9 ± 1.8	1.4 ± 0.9	8.9 ± 2.7	1.1 ± 0.2	14.0 ± 3.3	1.6 ± 0.6
3	5.8 ± 2.2	0.6 ± 0.5	7.6 ± 2.7	0.5 ± 0.2	12.9 ± 2.6	0.8 ± 0.2
4	4.9 ± 1.9	0.3 ± 0.2	7.1 ± 1.9	0.3 ± 0.1	10.1 ± 1.4	0.4 ± 0.1
5	4.0 ± 1.1	0.2 ± 0.1	6.2 ± 1.9	0.3 ± 0.1	9.4 ± 1.2	0.5 ± 0.2
6	4.2 ± 0.9	0.2 ± 0.1	5.4 ± 0.8	0.2 ± 0.1	9.4 ± 0.9	0.2 ± 0.1

Threonine fluxes (± SD, n = 6) for experiments in PB [nmol/(h·cm^2)]

Time (h)	0.1 mM		0.25 mM		0.5 mM	
	Cathode	Anode	Cathode	Anode	Cathode	Anode
1	10.8 ± 4.3	7.5 ± 3.7	10.6 ± 2.3	7.0 ± 1.4	13.1 ± 3.1	6.4 ± 2.5
2	4.5 ± 1.0	2.8 ± 1.4	5.6 ± 0.6	2.6 ± 0.9	8.7 ± 1.5	2.3 ± 0.7
3	3.3 ± 1.1	1.4 ± 0.6	4.9 ± 1.4	1.9 ± 0.8	8.3 ± 1.6	1.5 ± 0.5
4	2.9 ± 0.9	0.7 ± 0.3	4.6 ± 0.9	1.2 ± 0.5	7.9 ± 1.0	1.0 ± 0.6
5	2.5 ± 0.6	0.5 ± 0.2	4.5 ± 1.5	0.8 ± 0.3	8.0 ± 1.1	0.9 ± 0.4
6	2.5 ± 0.3	0.4 ± 0.2	4.1 ± 1.0	0.6 ± 0.2	8.5 ± 2.0	0.6 ± 0.2

Proline fluxes (± SD, n = 6) for experiments in PB [nmol/(h·cm^2)]

Time (h)	0.1 mM		0.25 mM		0.5 mM	
	Cathode	Anode	Cathode	Anode	Cathode	Anode
1	9.8 ± 3.9	5.5 ± 2.4	9.2 ± 2.9	4.6 ± 1.9	12.4 ± 2.8	5.6 ± 2.5
2	4.0 ± 1.1	1.9 ± 0.9	4.8 ± 1.3	1.6 ± 0.5	8.7 ± 1.6	1.8 ± 0.7
3	2.9 ± 1.1	0.9 ± 0.4	4.1 ± 1.3	1.1 ± 0.3	7.9 ± 1.7	1.1 ± 0.4
4	2.6 ± 0.9	0.5 ± 0.2	3.9 ± 1.3	0.6 ± 0.2	7.6 ± 1.1	0.7 ± 0.4
5	2.1 ± 0.4	0.2 ± 0.1	3.7 ± 1.7	0.5 ± 0.1	6.9 ± 1.0	0.7 ± 0.2
6	2.1 ± 0.3	0.2 ± 0.1	3.4 ± 1.4	0.3 ± 0.1	8.0 ± 1.4	0.4 ± 0.2

Leucine fluxes (± SD, n = 6) for experiments in PB [nmol/(h·cm^2)]

Time (h)	0.1 mM		0.25 mM		0.5 mM	
	Cathode	Anode	Cathode	Anode	Cathode	Anode
1	7.9 ± 4.4	5.3 ± 2.5	12.5 ± 2.5	6.2 ± 1.5	10.0 ± 3.2	5.0 ± 2.3
2	4.2 ± 1.2	2.2 ± 1.1	5.8 ± 0.9	2.4 ± 0.8	8.2 ± 1.8	2.0 ± 0.4
3	3.5 ± 1.5	1.3 ± 0.7	4.8 ± 0.8	1.9 ± 1.0	7.6 ± 2.1	1.6 ± 0.4
4	2.4 ± 0.5	0.7 ± 0.3	4.5 ± 1.0	1.2 ± 0.6	6.7 ± 1.1	0.9 ± 0.3
5	1.7 ± 0.2	0.5 ± 0.2	3.9 ± 1.3	1.0 ± 0.4	8.0 ± 1.3	1.0 ± 0.5
6	2.0 ± 0.3	0.5 ± 0.1	3.8 ± 1.4	1.0 ± 0.3	7.6 ± 1.5	0.8 ± 0.2

Valine fluxes (± SD, n = 6) for experiments in PB [nmol/(h·cm^2)]

Time (h)	0.1 mM		0.25 mM		0.5 mM	
	Cathode	Anode	Cathode	Anode	Cathode	Anode
1	5.5 ± 1.6	3.1 ± 1.4	5.8 ± 1.8	3.1 ± 1.1	7.7 ± 1.7	2.5 ± 0.9
2	2.9 ± 0.9	0.8 ± 0.5	3.8 ± 0.7	1.0 ± 0.5	6.6 ± 0.9	0.9 ± 0.4
3	2.1 ± 0.7	0.4 ± 0.3	3.6 ± 1.0	0.8 ± 0.4	6.7 ± 1.2	0.6 ± 0.3
4	1.9 ± 0.6	0.2 ± 0.2	3.5 ± 0.5	0.5 ± 0.3	6.9 ± 0.9	0.3 ± 0.3
5	1.7 ± 0.4	0.1 ± 0.1	3.3 ± 1.1	0.3 ± 0.2	6.5 ± 0.5	0.4 ± 0.1
6	1.5 ± 0.2	0.1 ± 0.1	3.2 ± 0.8	0.2 ± 0.2	7.3 ± 1.2	0.3 ± 0.1

Isoleucine fluxes (± SD, n = 6) for experiments in PB [nmol/(h·cm^2)]

Time (h)	0.1 mM		0.25 mM		0.5 mM	
	Cathode	Anode	Cathode	Anode	Cathode	Anode
1	4.5 ± 1.5	2.1 ± 0.9	6.5 ± 1.6	2.8 ± 0.8	6.9 ± 1.8	2.8 ± 1.3
2	2.6 ± 1.0	0.7 ± 0.3	3.8 ± 0.7	1.1 ± 0.4	6.7 ± 1.3	1.0 ± 0.3
3	2.1 ± 1.1	0.4 ± 0.3	3.8 ± 1.0	0.9 ± 0.5	6.8 ± 1.1	0.8 ± 0.3
4	1.8 ± 0.6	0.2 ± 0.1	3.5 ± 0.7	0.6 ± 0.3	6.6 ± 1.0	0.5 ± 0.2
5	1.5 ± 0.2	0.2 ± 0.1	3.4 ± 1.1	0.4 ± 0.2	6.6 ± 0.8	0.6 ± 0.2
6	1.7 ± 0.2	0.2 ± 0.1	3.2 ± 1.1	0.3 ± 0.2	6.6 ± 1.3	0.5 ± 0.2

Tyrosine fluxes (± SD, n = 6) for experiments in PB [nmol/(h·cm^2)]

Time (h)	0.1 mM		0.25 mM		0.5 mM	
	Cathode	Anode	Cathode	Anode	Cathode	Anode
1	3.1 ± 1.1	2.0 ± 1.1	4.1 ± 1.7	2.2 ± 0.7	5.8 ± 1.6	1.8 ± 0.5
2	2.0 ± 0.5	0.8 ± 0.3	3.3 ± 1.0	1.1 ± 0.3	5.8 ± 1.3	1.2 ± 0.6
3	1.9 ± 0.7	0.5 ± 0.3	3.4 ± 1.1	0.8 ± 0.3	6.4 ± 0.9	1.0 ± 0.4
4	1.8 ± 0.6	0.3 ± 0.1	3.4 ± 1.0	0.5 ± 0.2	6.0 ± 0.6	0.6 ± 0.2
5	1.6 ± 0.3	0.2 ± 0.1	3.2 ± 1.1	0.4 ± 0.1	6.4 ± 0.6	0.5 ± 0.1
6	1.7 ± 0.2	0.2 ± 0.1	3.1 ± 1.0	0.3 ± 0.1	6.9 ± 1.0	0.4 ± 0.1

Phenylalanine fluxes (± SD, n = 6) for experiments in PB [nmol/(h·cm^2)]

Time (h)	0.1 mM		0.25 mM		0.5 mM	
	Cathode	Anode	Cathode	Anode	Cathode	Anode
1	2.8 ± 1.1	1.6 ± 0.8	3.4 ± 1.3	1.3 ± 0.4	5.3 ± 1.6	1.4 ± 0.6
2	1.8 ± 0.6	0.6 ± 0.2	2.7 ± 0.8	0.6 ± 0.2	5.8 ± 1.4	0.6 ± 0.2
3	1.9 ± 1.0	0.4 ± 0.2	2.7 ± 0.9	0.5 ± 0.1	6.3 ± 1.3	0.4 ± 0.1
4	1.7 ± 0.8	0.2 ± 0.1	2.7 ± 0.7	0.3 ± 0.1	6.0 ± 1.3	0.3 ± 0.1
5	1.4 ± 0.3	0.2 ± 0.0	2.6 ± 0.9	0.2 ± 0.1	6.4 ± 1.2	0.4 ± 0.1
6	1.6 ± 0.2	0.2 ± 0.1	2.5 ± 0.8	0.2 ± 0.1	6.9 ± 1.2	0.3 ± 0.1

Asparagine fluxes (± SD, n = 6) for experiments in PB [nmol/(h·cm^2)]

Time (h)	0.1 mM		0.25 mM		0.5 mM	
	Cathode	Anode	Cathode	Anode	Cathode	Anode
1	2.8 ± 0.7	1.7 ± 0.6	3.7 ± 1.4	1.7 ± 0.5	6.2 ± 2.1	1.4 ± 0.5
2	1.8 ± 0.3	0.6 ± 0.2	2.4 ± 0.6	0.6 ± 0.2	6.0 ± 1.3	0.5 ± 0.2
3	1.8 ± 0.5	0.3 ± 0.1	2.8 ± 0.7	0.4 ± 0.2	6.4 ± 1.2	0.4 ± 0.1
4	1.9 ± 0.6	0.2 ± 0.1	2.8 ± 0.3	0.3 ± 0.1	6.3 ± 1.7	0.3 ± 0.2
5	1.8 ± 0.3	0.2 ± 0.1	2.9 ± 0.7	0.2 ± 0.1	6.7 ± 1.6	0.4 ± 0.1
6	1.9 ± 0.3	0.1 ± 0.1	2.8 ± 0.5	0.2 ± 0.1	7.3 ± 1.6	0.4 ± 0.1

Tryptophan fluxes (± SD, n = 6) for experiments in PB [nmol/(h·cm^2)]

Time (h)	0.1 mM		0.25 mM		0.5 mM	
	Cathode	Anode	Cathode	Anode	Cathode	Anode
1	1.1 ± 0.5	0.13 ± 0.09	1.7 ± 0.9	0.10 ± 0.03	3.7 ± 1.6	0.20 ± 0.12
2	1.2 ± 0.4	0.06 ± 0.03	2.3 ± 0.9	0.08 ± 0.04	5.0 ± 1.1	0.10 ± 0.07
3	1.2 ± 0.4	0.04 ± 0.03	2.5 ± 0.9	0.05 ± 0.03	6.0 ± 0.9	0.07 ± 0.02
4	1.2 ± 0.4	0.02 ± 0.02	2.7 ± 0.7	0.04 ± 0.02	5.8 ± 0.9	0.06 ± 0.06
5	1.2 ± 0.3	0.01 ± 0.01	2.7 ± 0.8	0.03 ± 0.01	6.3 ± 0.7	0.03 ± 0.02
6	1.3 ± 0.2	0.01 ± 0.01	2.8 ± 0.7	0.02 ± 0.01	7.1 ± 1.0	0.02 ± 0.02

Methionine fluxes (± SD, n = 6) for experiments in PB [nmol/(h·cm^2)]

Time (h)	0.1 mM		0.25 mM		0.5 mM	
	Cathode	Anode	Cathode	Anode	Cathode	Anode
1	1.4 ± 0.8	0.5 ± 0.2	2.3 ± 0.6	0.3 ± 0.2	3.8 ± 1.6	0.3 ± 0.2
2	1.3 ± 0.4	0.15 ± 0.08	2.0 ± 0.4	0.12 ± 0.02	5.0 ± 1.2	0.12 ± 0.08
3	1.2 ± 0.7	0.07 ± 0.06	2.21 ± 0.61	0.09 ± 0.05	5.3 ± 1.6	0.12 ± 0.09
4	1.0 ± 0.3	0.05 ± 0.02	2.3 ± 0.5	0.05 ± 0.05	5.2 ± 1.6	0.07 ± 0.05
5	0.9 ± 0.2	0.06 ± 0.03	2.1 ± 0.7	0.03 ± 0.01	5.1 ± 0.7	0.06 ± 0.03
6	1.0 ± 0.2	0.04 ± 0.02	2.0 ± 0.8	0.05 ± 0.03	5.9 ± 1.0	0.06 ± 0.03

Glucose fluxes (± SD, n = 6) for experiments in PB [nmol/(h·cm^2)]

Time (h)	0.1 mM		0.25 mM		0.5 mM	
	Cathode	Anode	Cathode	Anode	Cathode	Anode
1	15.3 ± 9.0	1.6 ± 1.7	24.4 ± 13.6	1.7 ± 1.9	40.4 ± 19.4	0.7 ± 0.4
2	13.1 ± 4.5	0.4 ± 0.2	25.2 ± 9.4	0.9 ± 1.1	48.1 ± 11.0	0.2 ± 0.1
3	14.5 ± 4.9	0.2 ± 0.1	29.3 ± 8.7	0.5 ± 0.1	56.1 ± 11.2	0.3 ± 0.2
4	14.6 ± 4.8	0.2 ± 0.1	31.1 ± 7.1	0.4 ± 0.1	56.1 ± 10.0	0.5 ± 0.3
5	14.1 ± 3.2	0.18 ± 0.04	31.0 ± 8.2	0.5 ± 0.2	60.4 ± 7.5	1.1 ± 0.5
6	15.4 ± 2.4	0.24 ± 0.04	30.4 ± 6.2	0.5 ± 0.3	69.0 ± 11.3	0.9 ± 0.5

3. Extraction fluxes (mean ± SD) at the cathode for the 3-6 hour period as a function of subdermal concentration for 14 AAs and glucose when the background electrolyte was PBS pH 7.4. Values obtained in absence of the analytes are also included [Chapter 4].

Molecule	Extraction fluxes [nmol/(h·cm^2)] for subdermal concentration in PBS			
	0 mM	0.1 mM AAs 1 mM glucose	0.25 mM AAs 2.5mM glucose	0.5 mM AAs 5 mM glucose
Serine	4.1 ± 1.2	2.7 ± 0.8	4.3 ± 3.2	5.1 ± 1.9
Glycine	3.7 ± 1.2	2.5 ± 0.8	4.3 ± 2.5	4.4 ± 1.1
Alanine	2.7 ± 0.6	1.9 ± 0.5	3.4 ± 1.9	4.0 ± 1.1
Histidine	1.8 ± 0.4	1.8 ± 0.5	2.8 ± 1.4	3.6 ± 1.1
Threonine	1.1 ± 0.3	0.9 ± 0.3	1.7 ± 0.9	2.4 ± 0.4
Proline	0.9 ± 0.2	0.9 ± 0.2	1.6 ± 0.7	2.3 ± 0.4
Leucine	1.1 ± 0.3	1.1 ± 0.4	1.9 ± 0.6	2.5 ± 0.4
Valine	0.6 ± 0.3	0.6 ± 0.1	1.3 ± 0.5	1.9 ± 0.2
Isoleucine	0.5 ± 0.2	0.6 ± 0.1	1.1 ± 0.2	1.8 ± 0.2
Tyrosine	0.4 ± 0.1	0.6 ± 0.1	1.1 ± 0.3	1.7 ± 0.2
Phenylalanine	0.3 ± 0.1	0.5 ± 0.1	1.1 ± 0.3	1.7 ± 0.2
Asparagine	0.2 ± 0.1	0.4 ± 0.1	1.1 ± 0.2	1.8 ± 0.2
Tryptophan	0.05 ± 0.03	0.31 ± 0.04	0.8 ± 0.1	1.5 ± 0.2
Methionine	N.A.	0.2 ± 0.1	0.6 ± 0.1	1.3 ± 0.3
Glucose	0.4 ± 0.3	3.9 ± 0.3	9.9 ± 1.0	16.9 ± 2.0

4. Extraction fluxes (mean ± SD) at the cathode for the 3-6 hour period as a function of subdermal concentration for 14 AAs and glucose when the background electrolyte was PB pH 7.4.

Molecule	Extraction fluxes [nmol/(h·cm^2)] for subdermal concentration in PB		
	0.1 mM AAs 1 mM glucose	**0.25 mM AAs 2.5mM glucose**	**0.5 mM AAs 5 mM glucose**
Serine	6.1 ± 2.1	8.0 ± 1.6	12.2 ± 2.2
Glycine	5.6 ± 1.8	5.7 ± 1.7	9.6 ± 1.7
Alanine	4.5 ± 0.9	5.4 ± 1.1	8.7 ± 0.9
Histidine	4.4 ± 1.3	6.2 ± 1.7	9.6 ± 1.2
Threonine	2.6 ± 0.6	4.4 ± 1.1	8.1 ± 1.4
Proline	2.3 ± 0.6	3.7 ± 1.4	7.5 ± 1.2
Leucine	2.1 ± 0.5	4.1 ± 1.2	7.4 ± 1.4
Valine	1.7 ± 0.4	3.4 ± 0.6	6.9 ± 0.9
Isoleucine	1.7 ± 0.4	3.4 ± 0.9	6.6 ± 1.0
Tyrosine	1.7 ± 0.4	3.2 ± 1.0	6.4 ± 0.8
Phenylalanine	1.6 ± 0.5	2.6 ± 0.7	6.4 ± 1.2
Asparagine	1.8 ± 0.4	2.8 ± 0.5	6.8 ± 1.6
Tryptophan	1.2 ± 0.3	2.7 ± 0.7	6.4 ± 1.0
Methionine	1.0 ± 0.2	2.1 ± 0.6	5.4 ± 1.2
Glucose	14.7 ± 3.4	30.9 ± 6.8	61.8 ± 10.7

5. Linear regressions of the average fluxes of the 3-6 hour extraction period at the cathode as a function of subdermal concentration for 14 AAs and glucose. The slopes (± SE (r^2)), which represent apparent electroosmotic flows, when either PBS or PB was the background electrolyte are presented. The amount of each compound in the SC as determined by tape-stripping [Chapter 4] is also presented.

Molecule	Slope PBS [μL/(h·cm^2)]	Slope PB [μL/(h·cm^2)]	Amount in SC [nmol/cm^2]
Serine	3.1 ± 1.3 (0.08)	15 ± 2 (0.63)	37 ± 9
Glycine	2.6 ± 1.0 (0.08)	11 ± 2 (0.49)	23 ± 6
Alanine	3.5 ± 0.8 (0.23)	11 ± 1 (0.77)	22 ± 4
Histidine	3.8 ± 0.6 (0.37)	13 ± 1 (0.71)	21 ± 4
Threonine	3.0 ± 0.3 (0.51)	14 ± 1 (0.83)	10 ± 2
Proline	2.9 ± 0.3 (0.61)	13 ± 1 (0.80)	7.3 ± 1.5
Leucine	3.0 ± 0.3 (0.61)	13 ± 1 (0.82)	7.3 ± 2.1
Valine	2.8 ± 0.2 (0.71)	13 ± 1 (0.91)	3.4 ± 1.0
Isoleucine	2.8 ± 0.1 (0.87)	12 ± 1 (0.87)	3.0 ± 0.8
Tyrosine	2.9 ± 0.1 (0.89)	12 ± 1 (0.87)	3.2 ± 0.6
Phenylalanine	3.0 ± 0.1 (0.88)	12 ± 1 (0.83)	2.1 ± 0.5
Asparagine	3.2 ± 0.1 (0.94)	13 ± 1 (0.80)	1.8 ± 0.6
Tryptophan	2.9 ± 0.1 (0.95)	13 ± 1 (0.90)	0.5 ± 0.2
Methionine	2.5 ± 0.1 (0.88)	11 ± 1 (0.85)	N.A.
Glucose	3.3 ± 0.1 (0.96)	12 ± 1 (0.88)	1.4 ± 0.7

The slopes in each group (PBS and PB) are not significantly different one another and the pooled slopes are 3.3 and 12 (μL/cm^2·h)) respectively.

6. AA and glucose cathodal extraction fluxes (during the 3-6 hour period) normalized by the subdermal concentration (mean ± SD) when the background electrolyte is PB. Values significantly different from that for glucose (ANOVA followed by Dunnett's test) are indicated by asterisks (p<0.01, *p<0.05).**

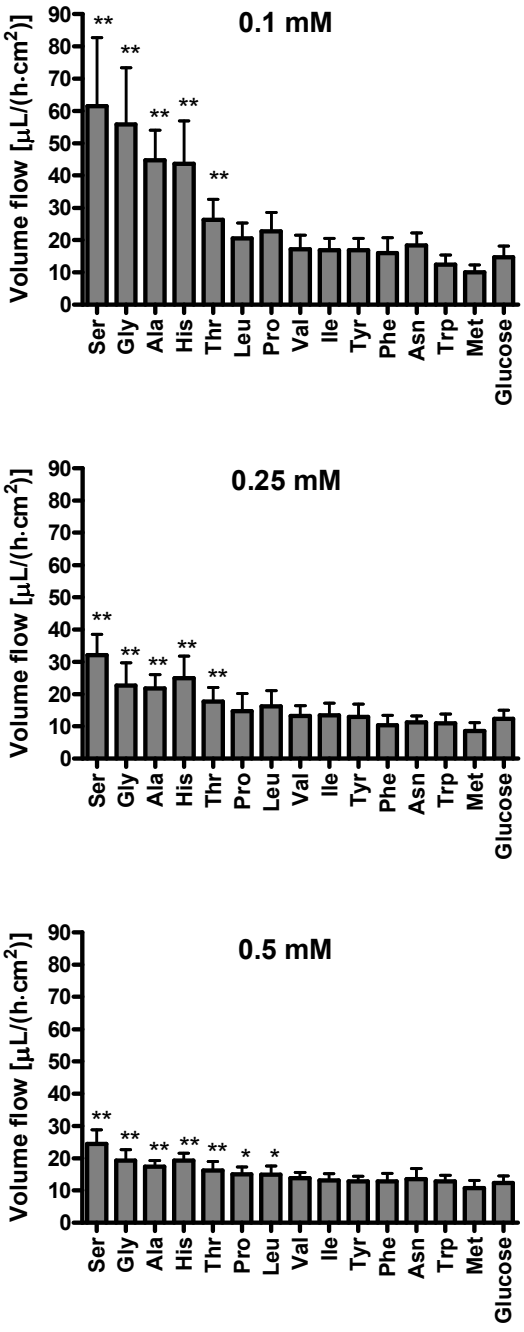

7. Amount extracted at the cathode in the 1st hour normalized by the mean amount found in the SC for 13 AAs and glucose for the different subdermal concentration tested (PBS and PB).

Molecule	Subdermal concentration in PBS			Subdermal concentration in PB		
	0.1 mM AAs 1 mM glucose	0.25 mM AAs 2.5 mM glucose	0.5 mM AAs 5 mM glucose	0.1 mM AAs 1 mM glucose	0.1 mM AAs 1 mM glucose	0.5 mM AAs 5 mM glucose
Serine	0.8 ± 0.3	0.8 ± 0.3	0.7 ± 0.1	1.1 ± 0.5	1.0 ± 0.2	1.2 ± 0.3
Glycine	1.0 ± 0.3	1.0 ± 0.4	0.9 ± 0.2	1.1 ± 0.3	0.8 ± 0.4	1.2 ± 0.3
Alanine	0.8 ± 0.2	0.8 ± 0.2	0.9 ± 0.1	0.8 ± 0.2	0.7 ± 0.3	0.8 ± 0.2
Histidine	0.9 ± 0.2	0.9 ± 0.3	0.9 ± 0.1	0.8 ± 0.2	0.7 ± 0.2	0.9 ± 0.3
Threonine	0.8 ± 0.3	0.8 ± 0.2	0.8 ± 0.2	1.1 ± 0.4	1.0 ± 0.2	1.3 ± 0.3
Proline	1.0 ± 0.4	0.9 ± 0.2	1.0 ± 0.1	1.2 ± 0.5	1.2 ± 0.4	1.6 ± 0.4
Leucine	0.8 ± 0.2	0.7 ± 0.1	0.8 ± 0.2	1.0 ± 0.6	1.6 ± 0.3	1.3 ± 0.4
Valine	1.0 ± 0.3	1.1 ± 0.3	1.2 ± 0.4	1.6 ± 0.5	1.7 ± 0.5	2.2 ± 0.5
Isoleucine	0.7 ± 0.2	0.7 ± 0.1	1.1 ± 0.4	1.4 ± 0.5	2.0 ± 0.5	2.2 ± 0.6
Tyrosine	0.5 ± 0.2	0.6 ± 0.1	0.7 ± 0.2	0.9 ± 0.3	1.2 ± 0.5	1.7 ± 0.5
Phenylalanine	0.6 ± 0.2	0.7 ± 0.2	1.1 ± 0.4	1.3 ± 0.5	1.5 ± 0.6	2.4 ± 0.7
Asparagine	0.8 ± 0.3	0.9 ± 0.3	1.5 ± 0.6	1.5 ± 0.3	1.9 ± 0.7	3.2 ± 1.1
Tryptophan	0.7 ± 0.2	1.1 ± 0.2	2.2 ± 1.2	2.0 ± 0.9	3.0 ± 1.6	6.6 ± 2.9
Glucose	3.6 ± 1.7	6.0 ± 2.1	11.7 ± 5.7	9.1 ± 5.4	14.5 ± 8.1	24.0 ± 11.5

8. Cumulative amount extracted at the cathode as a function of time when the subdermal compartment was 0.5 mM AAs and 5 mM glucose in PBS when no analytes were added in the subdermal compartment (Blank). The amounts found in the SC by tape-stripping are also presented [Chapter 4].

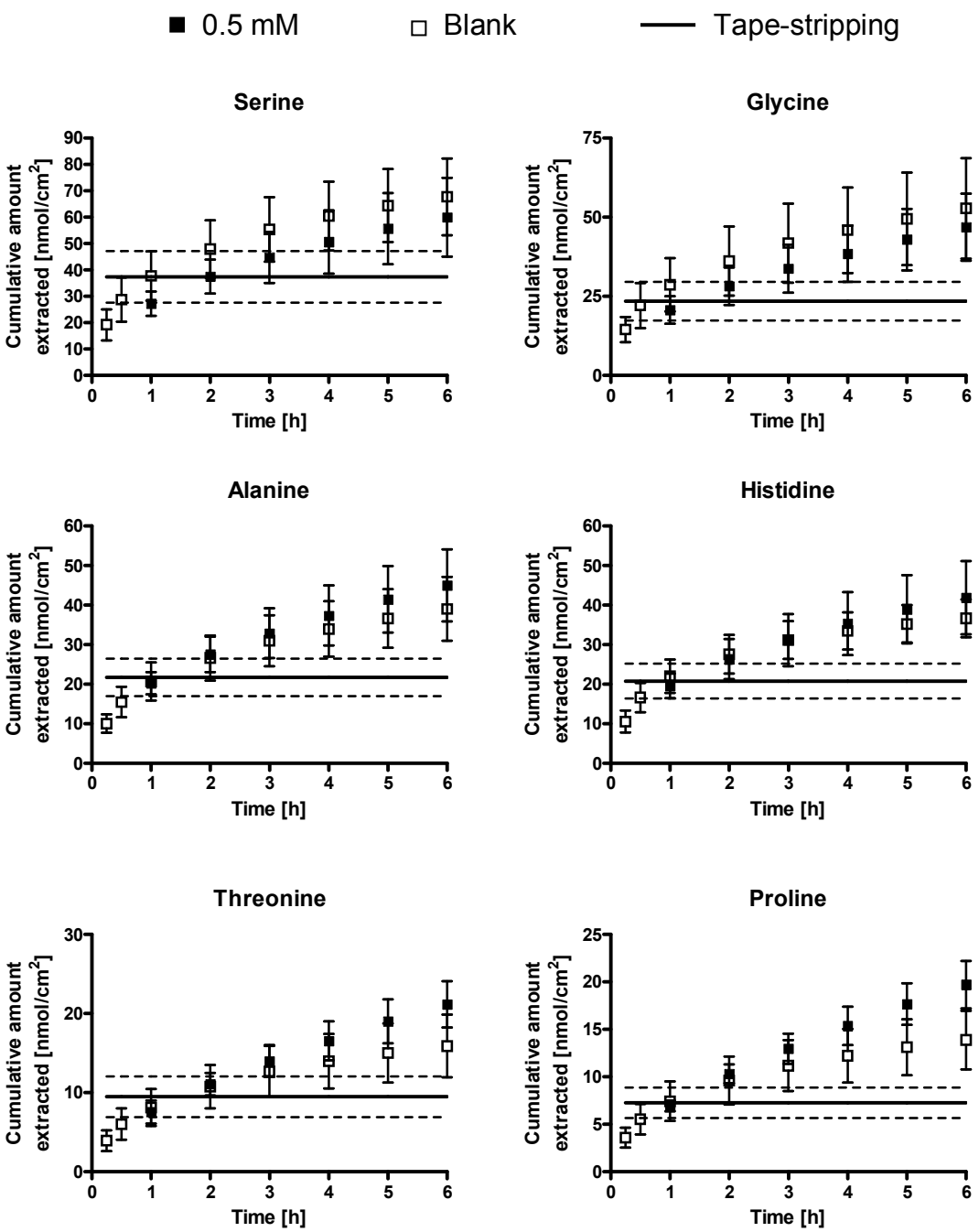

8. Cumulative amount extracted at the cathode as a function of time when the subdermal compartment was 0.5 mM AAs and 5 mM glucose in PBS when no analytes were added in the subdermal compartment (Blank). The amounts found in the SC by tape-stripping are also presented [Chapter 4]. (continued)

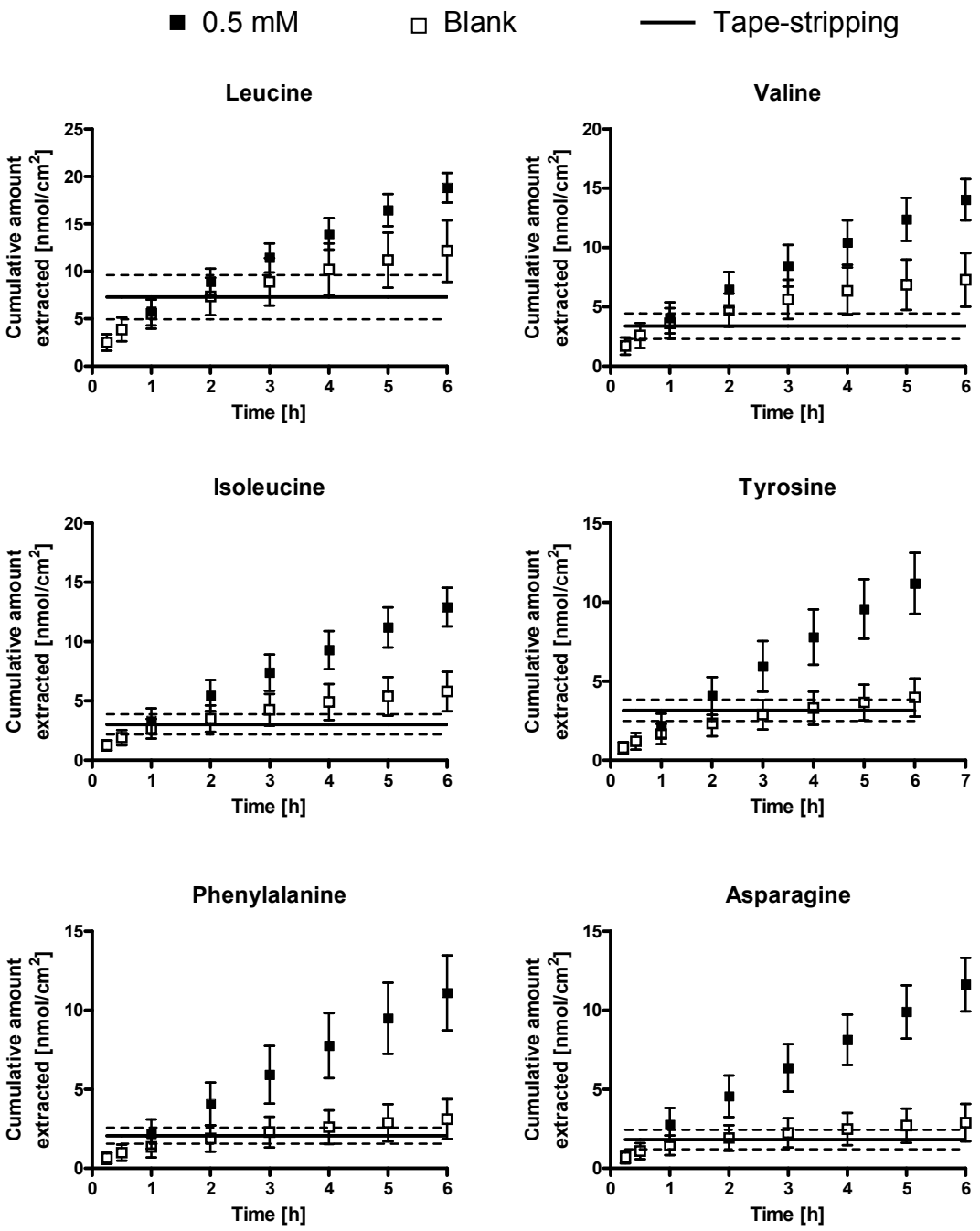

8. Cumulative amount extracted at the cathode as a function of time when the subdermal compartment was 0.5 mM AAs and 5 mM glucose in PBS when no analytes were added in the subdermal compartment (Blank). The amounts found in the SC by tape-stripping are also presented [Chapter 4]. (continued)

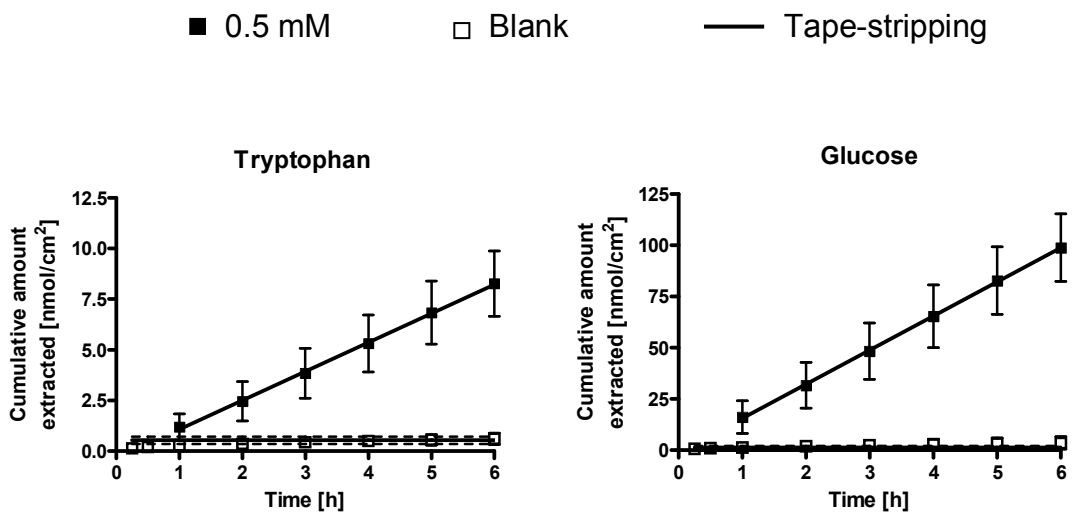

ANNEX IV. Complements to Chapter 6

1. Concentration profiles of 13 AAs and glucose in the SC in the four subjects measured on two occasions.

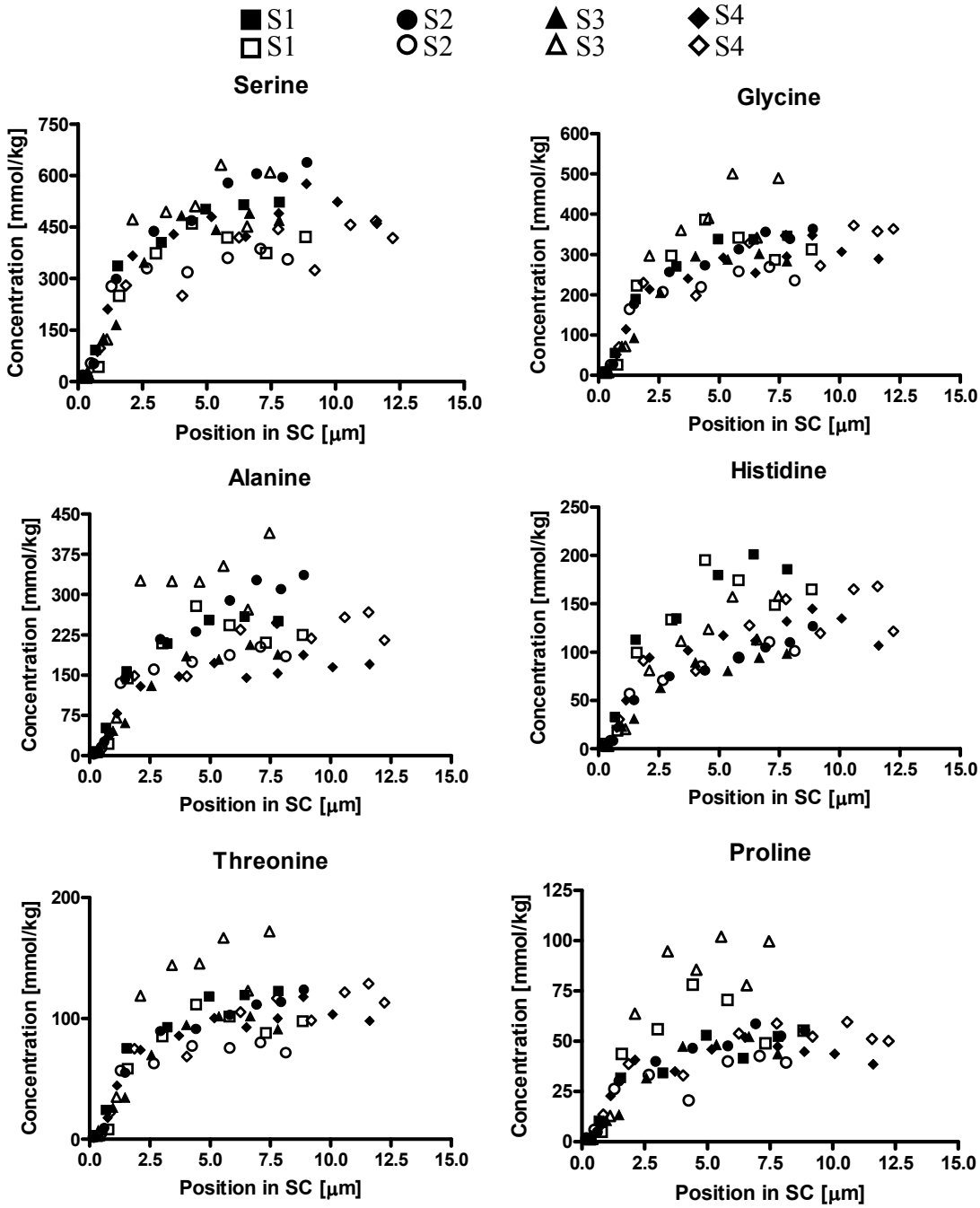

1. Concentration profiles of 13 AAs and glucose in the SC in the four subjects measured on two occasions. (continued)

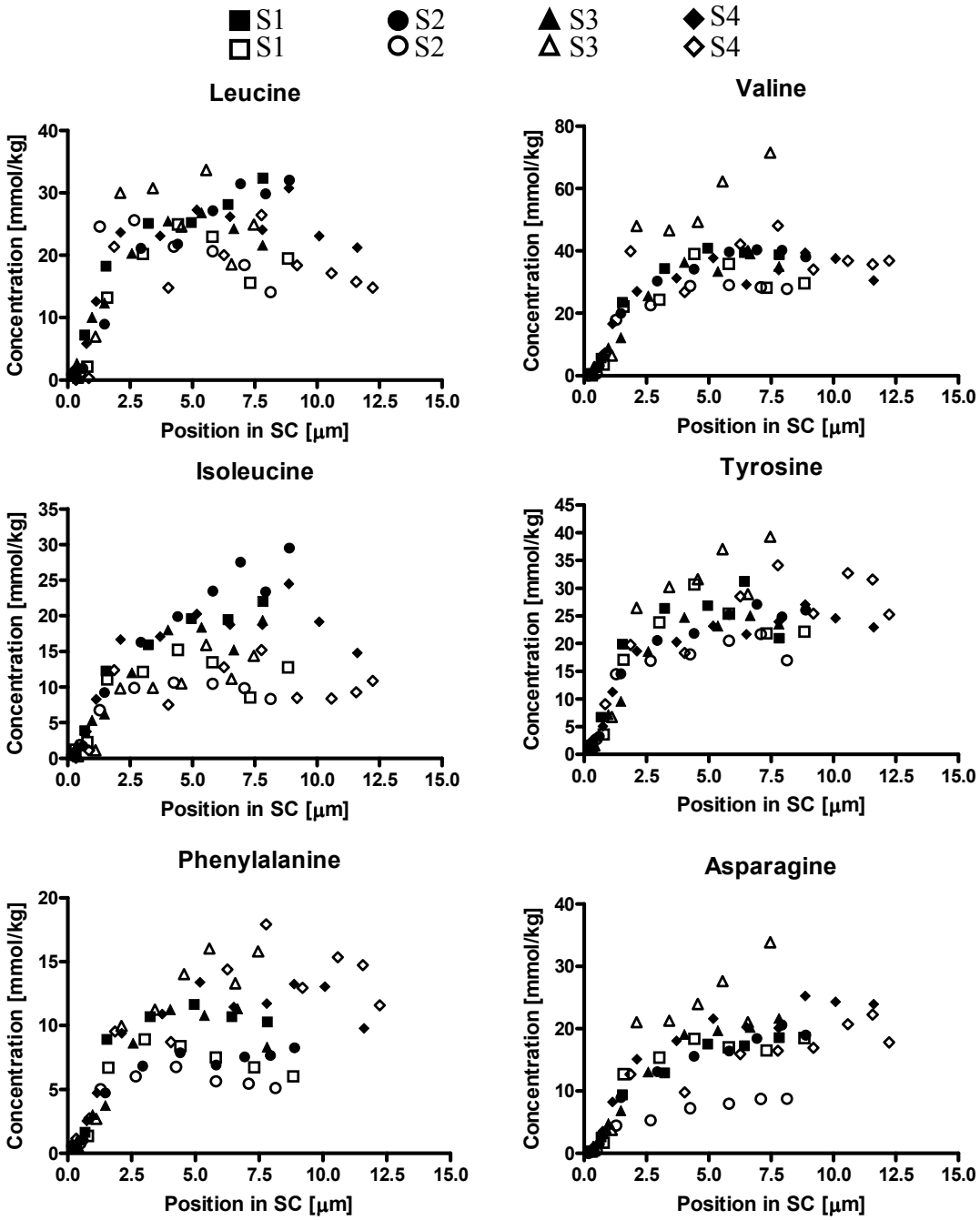

1. Concentration profiles of 13 AAs and glucose in the SC in the four subjects measured on two occasions. (continued)

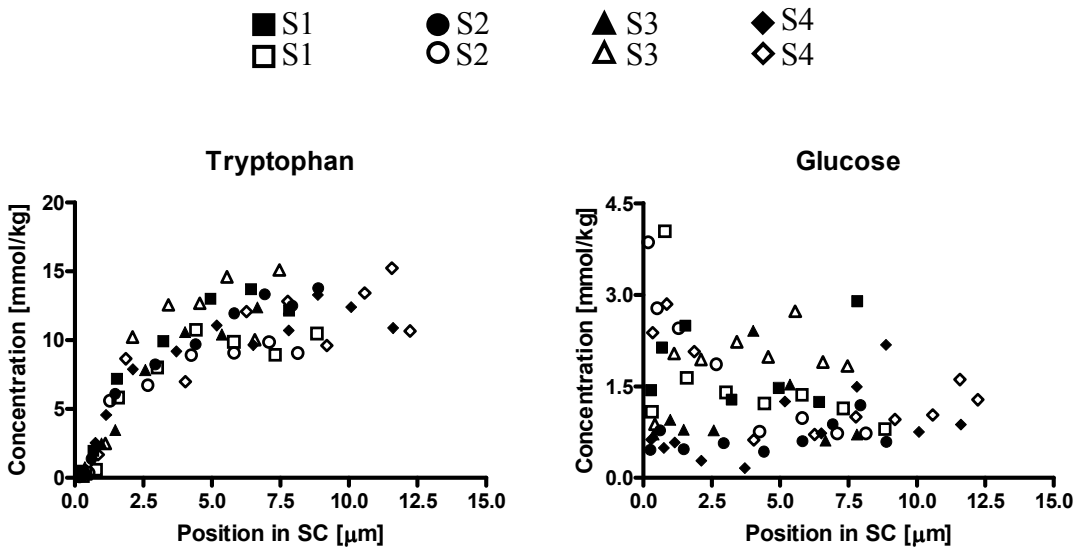

2. Plasma levels of 13 AAs and blood glucose in the four subjects studied during the passive diffusion experiment. The blood sample was obtained after 4 hours of extraction.

Molecule	S1 (µM)	S2 (µM)	S3 (µM)	S4 (µM)	Usual range (µM)
Serine	175	239	208	237	90-290
Glycine	192	234	276	205	100-330
Alanine	321	285	234	154	150-450
Histidine	115	112	92	121	30-150
Threonine	85	130	93	141	70-220
Proline	222	137	139	145	85-290
Leucine	123	116	82	145	65-220
Valine	234	190	162	185	90-300
Isoleucine	91	100	87	81	26-100
Tyrosine	69	44	40	52	30-120
Phenylalanine	55	54	45	68	35-100
Asparagine	36	38	39	28	40-90
Tryptophan	13	19	11	15	30-80
Glucose	5000	4400	4600	4700	4000-5500

3. Fluxes at the cathode, anode and by passive diffusion for 13 AAs and glucose as a function of time

AA or Glucose	Compart-ment	Extraction fluxes ± SD (n = 4) at [nmol/(h·cm^2)]								
		0.25 h	0.5 h	1 h	1.5 h	2 h	2.5 h	3 h	3.5 h	4 h
Ser	Cathode	139 ± 28	89.1 ± 35.7	68.3 ± 17.5	46.6 ± 18.9	46.3 ± 18.9	35.4 ± 13.4	35.1 ± 7.2	35.0 ± 4.7	26.3 ± 4.9
	Anode	93.7 ± 45.9	62.4 ± 19.1	43.3 ± 5.5	30.7 ± 4.8	25.2 ± 3.4	17.4 ± 4.5	12.3 ± 2.6	11.7 ± 3.7	9.0 ± 2.6
	Passive	82.5 ± 46.3	40.6 ± 16.1	29.9 ± 11.1	24.9 ± 8.5	21.3 ± 6.5	21.9 ± 6.9	19.9 ± 7.8	16.8 ± 6.3	17.4 ± 6.6
Gly	Cathode	102 ± 24	68.6 ± 26.9	46.6 ± 11.8	32.6 ± 10.8	30.7 ± 12.0	23.2 ± 8.9	20.6 ± 3.4	20.2 ± 2.4	15.5 ± 2.3
	Anode	53.8 ± 15.8	36.1 ±9.9	24.6 ± 3.1	17.7 ± 3.0	16.0 ± 3.1	11.5 ± 3.0	8.8 ± 1.8	8.4 ± 2.4	6.2 ± 2.1
	Passive	57.4 ± 26.4	31.6 ± 14.7	22.8 ± 8.4	19.7 ± 6.2	18.2 ± 5.4	16.6 ± 4.7	14.3 ± 4.7	13.6 ± 4.9	13.8 ± 4.9
Ala	Cathode	70.8 ± 18.4	46.6 ± 19.1	33.4 ± 10.2	22.6 ± 7.6	21.3 ± 6.6	16.9 ± 6.3	16.5 ± 3.9	16.3 ± 3.5	13.2 ± 4.4
	Anode	40.3 ± 14.5	26.7 ± 6.1	18.1 ± 4.4	13.5 ± 1.4	11.5 ± 1.6	8.1 ± 2.4	5.8 ± 1.6	5.7 ± 2.1	4.3 ± 1.5
	Passive	44.5 ± 23.6	22.7 ± 9.0	16.3 ± 5.7	14.7 ± 5.5	11.9 ± 3.9	11.7 ± 2.7	10.8 ± 3.0	9.1 ± 2.6	9.3 ± 2.6
His	Cathode	81.3 ± 30.8	46.8 ± 29.2	31.1 ± 12.0	19.7 ± 10.9	17.3 ± 11.6	9.9 ± 6.6	9.9 ± 4.3	8.7 ± 2.7	7.0 ± 2.0
	Anode	8.5 ± 4.4	7.2 ± 2.6	5.4 ± 1.8	4.2 ± 2.6	3.3 ± 2.2	2.5 ± 2.0	1.6 ± 1.2	1.8 ± 1.6	1.2 ± 1.2
	Passive	20.1 ± 17.1	9.8 ± 6.0	6.7 ± 4.7	5.7 ± 3.5	5.1 ± 2.9	5.0 ± 2.7	4.7 ± 2.3	3.9 ± 1.7	4.2 ± 2.2
Thr	Cathode	23.8 ± 6.5	15.9 ± 7.6	12.0 ± 3.7	8.5 ± 3.3	8.5 ± 3.8	6.9 ± 2.9	7.1 ± 1.2	7.0 ± 0.9	5.6 ± 1.0
	Anode	17.4 ± 8.7	11.3 ± 3.5	8.2 ± 0.9	5.9 ± 1.0	4.9 ± 0.9	3.3 ± 0.9	2.4 ± 0.7	2.3 ± 0.8	1.7 ± 0.6
	Passive	19.0 ± 10.5	8.9 ± 3.9	6.3 ± 2.5	5.6 ± 2.0	4.6 ± 1.6	4.6 ± 1.3	4.4 ± 1.7	3.8 ± 1.4	4.1 ± 1.6
Pro	Cathode	9.9 ± 3.4	5.9 ± 3.0	5.2 ± 1.8	3.1 ± 1.3	3.6 ± 1.7	3.0 ± 1.1	3.2 ± 0.6	3.2 ± 0.5	2.6 ± 0.4
	Anode	7.5 ± 3.9	5.0 ± 1.9	3.6 ± 0.4	2.5 ± 0.5	2.0 ± 0.4	1.5 ± 0.5	1.1 ± 0.3	1.0 ± 0.5	0.8 ± 0.2
	Passive	8.9 ± 5.1	3.8 ± 1.9	2.9 ± 1.4	2.4 ± 0.8	2.2 ±0.8	2.4 ±0.9	2.0 ± 0.8	1.7 ± 0.7	1.8 ± 0.8
Leu	Cathode	6.0 ± 0.5	5.3 ± 1.3	3.2 ± 0.7	2.7 ± 0.9	2.1 ± 0.8	1.8 ± 0.8	1.9 ± 0.5	2.1 ± 0.7	1.6 ± 0.2
	Anode	4.8 ± 2.5	2.6 ± 1.4	1.7 ± 0.5	1.3 ± 0.4	1.2 ± 0.3	1.0 ± 0.5	0.8 ± 0.4	0.7 ± 0.3	0.7 ± 0.3
	Passive	3.2 ± 1.2	2.0 ± 0.6	1.1 ± 0.3	1.0 ± 0.2	0.9 ± 0.2	0.9 ± 0.1	0.9 ± 0.2	0.8 ± 0.1	0.9 ± 0.1

3. Fluxes at the cathode, anode and passive diffusion for 13 AAs and glucose as a function of time (continued)

AA or Glucose	Compart-ment	Extraction fluxes ± SD (n = 4) at [nmol/(h·cm^2)]								
		0.25 h	0.5 h	1 h	1.5 h	2 h	2.5 h	3 h	3.5 h	4 h
Val	Cathode	8.4 ± 1.9	5.7 ± 2.4	4.4 ± 1.2	3.3 ± 1.0	3.3 ± 1.6	2.4 ± 1.0	2.9 ± 0.6	3.0 ± 0.3	2.6 ± 0.8
	Anode	6.9 ± 2.5	4.1 ± 1.4	3.3 ± 0.7	2.2 ± 0.4	1.8 ± 0.3	1.2 ± 0.4	0.8 ± 0.3	0.8 ± 0.3	0.7 ± 0.2
	Passive	6.4 ± 3.7	2.9 ± 1.4	2.0 ± 1.0	1.8 ± 0.8	1.5 ± 0.6	1.7 ± 0.7	1.4 ± 0.4	1.3 ± 0.5	1.3 ± 0.5
Ile	Cathode	4.3 ± 0.9	2.6 ± 1.1	2.3 ± 0.6	1.6 ± 0.7	1.8 ± 0.5	1.5 ± 0.6	1.4 ± 0.3	1.5 ± 0.1	1.2 ± 0.2
	Anode	4.0 ± 2.2	2.3 ± 0.7	1.7 ± 0.5	1.1 ± 0.2	1.0 ± 0.2	0.7 ± 0.2	0.6 ± 0.1	0.5 ± 0.1	0.4 ± 0.1
	Passive	2.1 ± 0.7	1.4 ± 0.5	0.9 ± 0.4	0.7 ± 0.3	0.7 ± 0.2	0.6 ± 0.2	0.5 ± 0.1	0.5 ± 0.1	0.4 ± 0.1
Tyr	Cathode	4.0 ± 0.8	2.4 ± 0.6	2.0 ± 0.3	1.8 ± 0.9	2.0 ± 1.1	1.2 ± 0.4	1.4 ± 0.2	1.4 ± 0.1	1.2 ± 0.2
	Anode	3.3 ± 1.8	2.4 ± 0.8	1.8 ± 0.4	1.3 ± 0.4	0.9 ± 0.2	0.7 ± 0.2	0.5 ± 0.1	0.6 ± 0.2	0.4 ± 0.2
	Passive	4.2 ± 2.1	2.1 ± 0.8	1.4 ± 0.6	1.2 ± 0.4	1.1 ± 0.3	1.1 ± 0.4	1.0 ± 0.4	0.9 ± 0.3	0.9 ± 0.3
Phe	Cathode	2.1 ± 0.8	1.0 ± 0.5	1.0 ± 0.3	0.7 ± 0.3	0.9 ± 0.5	0.6 ± 0.3	0.6 ± 0.1	0.7 ± 0.1	0.5 ± 0.1
	Anode	1.6 ± 1.2	1.0 ± 0.5	0.8 ± 0.3	0.5 ± 0.2	0.4 ± 0.1	0.3 ± 0.1	0.2 ± 0.1	0.3 ± 0.1	0.2 ± 0.1
	Passive	1.6 ± 1.2	0.7 ± 0.4	0.5 ± 0.3	0.5 ± 0.3	0.4 ± 0.2	0.5 ± 0.2	0.5 ± 0.2	0.4 ± 0.2	0.4 ± 0.2
Asn	Cathode	3.5 ± 1.4	1.9 ± 0.8	1.5 ± 0.4	1.1 ± 0.3	1.1 ± 0.8	0.7 ± 0.2	0.7 ± 0.3	0.7 ± 0.2	0.5 ± 0.1
	Anode	2.7 ± 1.1	1.9 ± 0.8	1.2 ± 0.4	0.9 ± 0.3	0.7 ± 0.2	0.5 ± 0.1	0.35 ± 0.04	0.29 ± 0.05	0.22 ± 0.02
	Passive	2.1 ± 1.3	1.1 ± 0.5	0.8 ± 0.4	0.7 ± 0.4	0.5 ± 0.3	0.5 ± 0.3	0.5 ± 0.2	0.4 ± 0.2	0.4 ± 0.2
Trp	Cathode	2.0 ± 0.5	1.3 ± 0.3	1.1 ± 0.2	0.7 ± 0.3	0.8 ± 0.4	0.6 ± 0.2	0.7 ± 0.2	0.7 ± 0.1	0.6 ± 0.1
	Anode	1.6 ± 0.9	1.3 ± 0.5	0.9 ± 0.2	0.7 ± 0.1	0.5 ± 0.1	0.4 ± 0.1	0.3 ± 0.1	0.2 ± 0.1	0.2 ± 0.1
	Passive	1.5 ± 0.7	0.7 ± 0.3	0.5 ± 0.2	0.4 ± 0.1	0.4 ± 0.1	0.4 ± 0.1	0.4 ± 0.2	0.3 ± 0.1	0.3 ± 0.1
Glucose	Cathode	1.1 ± 1.1	0.6 ± 0.7	0.6 ± 0.5	0.6 ± 0.6	0.7 ± 0.5	0.6 ± 0.5	0.7 ± 0.2	0.8 ± 0.3	0.6 ± 0.1
	Anode	1.1 ± 1.3	0.2 ± 0.1	0.09 ± 0.04	0.12 ± 0.04	0.12 ± 0.05	0.2 ± 0.1	0.1 ± 0.1	0.2 ± 0.1	0.1 ± 0.1
	Passive	0.3 ± 0.1	0.1 ± 0.1	0.05 ± 0.03	0.05 ± 0.03	0.04 ± 0.02	0.05 ± 0.03	0.06 ± 0.01	0.03 ± 0.02	0.03 ± 0.02

4. Fluxes of AAs and glucose of the final 2-hour period of extraction at the cathode and by passive diffusion normalized by systemic levels and the quantities in the SC.

Molecule	Cathode/ systemic [µL/(h·cm^2)]	Cathode/SC [h^{-1}]	Passive diffusion/ SC [h^{-1}]
Ser	146 ± 36	0.08 ± 0.02	0.06 ± 0.02
Gly	99 ± 26	0.08 ± 0.02	0.06 ± 0.01
Ala	70 ± 13	0.09 ± 0.02	0.05 ± 0.01
His	87 ± 31	0.09 ± 0.02	0.04 ± 0.01
Thr	62 ± 17	0.08 ± 0.02	0.05 ± 0.01
Pro	17 ± 4	0.08 ± 0.02	0.04 ± 0.01
Leu	8 ± 2	0.09 ± 0.03	0.05 ± 0.01
Val	14 ± 4	0.09 ± 0.02	0.05 ± 0.01
Ile	13 ± 3	0.09 ± 0.03	0.05 ± 0.01
Tyr	30 ± 7	0.07 ± 0.01	0.05 ± 0.01
Phe	11 ± 3	0.08 ± 0.02	0.05 ± 0.01
Asn	13 ± 5	0.04 ± 0.01	0.03 ± 0.01
Trp	42 ± 17	0.07 ± 0.01	0.04 ± 0.01
Glucose	0.15 ± 0.05	0.67 ± 0.23	0.03 ± 0.02

5. Cumulative amount of 13 amino acids and glucose extracted in the four subjects (mean ± SD) at the cathode and by passive diffusion as a function of time. The quantities in the SC determined by tape-stripping are shown for comparison.

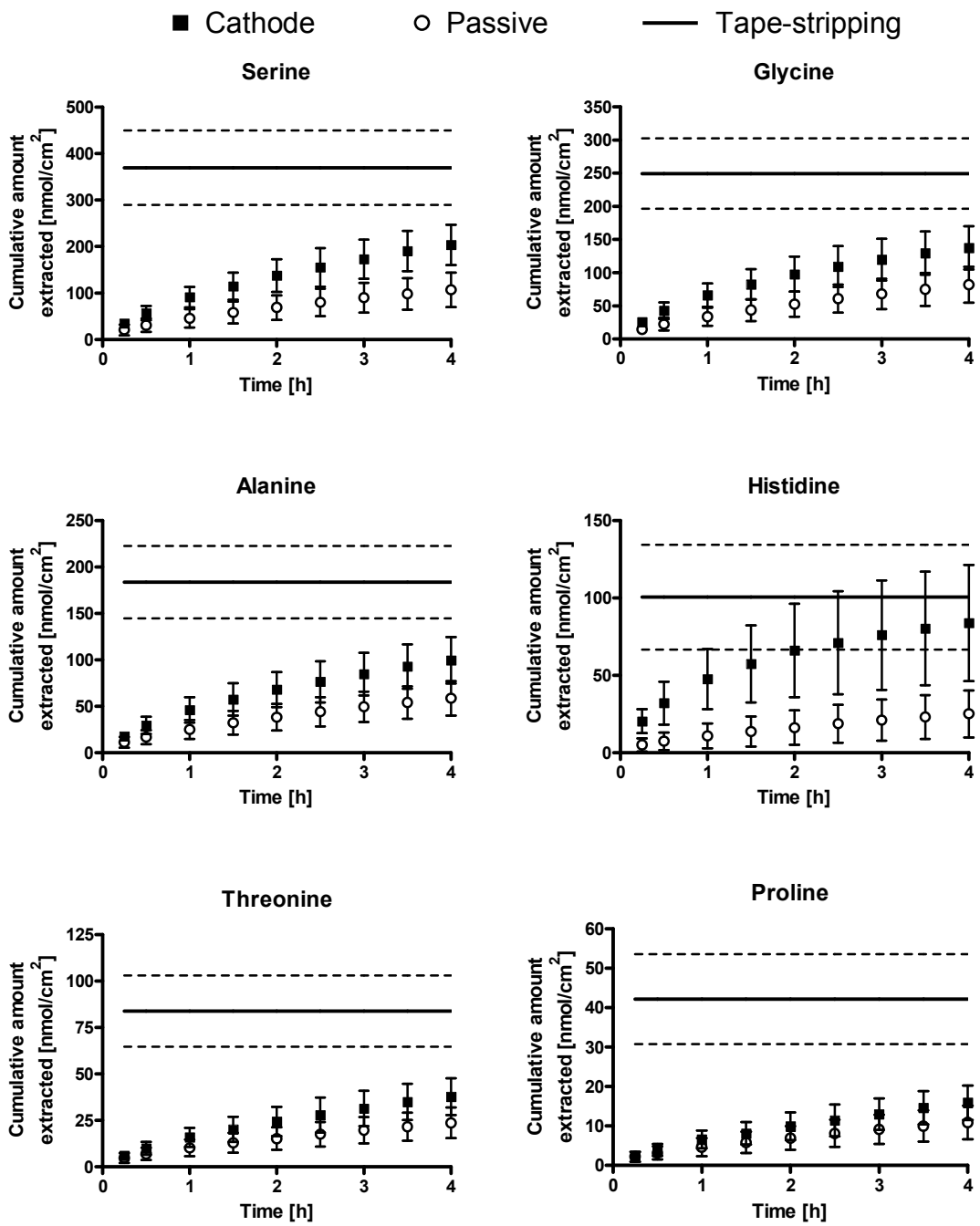

5. Cumulative amount of 13 amino acids and glucose extracted in the four subjects (mean ± SD) at the cathode and by passive diffusion as a function of time. The quantities in the SC determined by tape-stripping are shown for comparison. (continued)

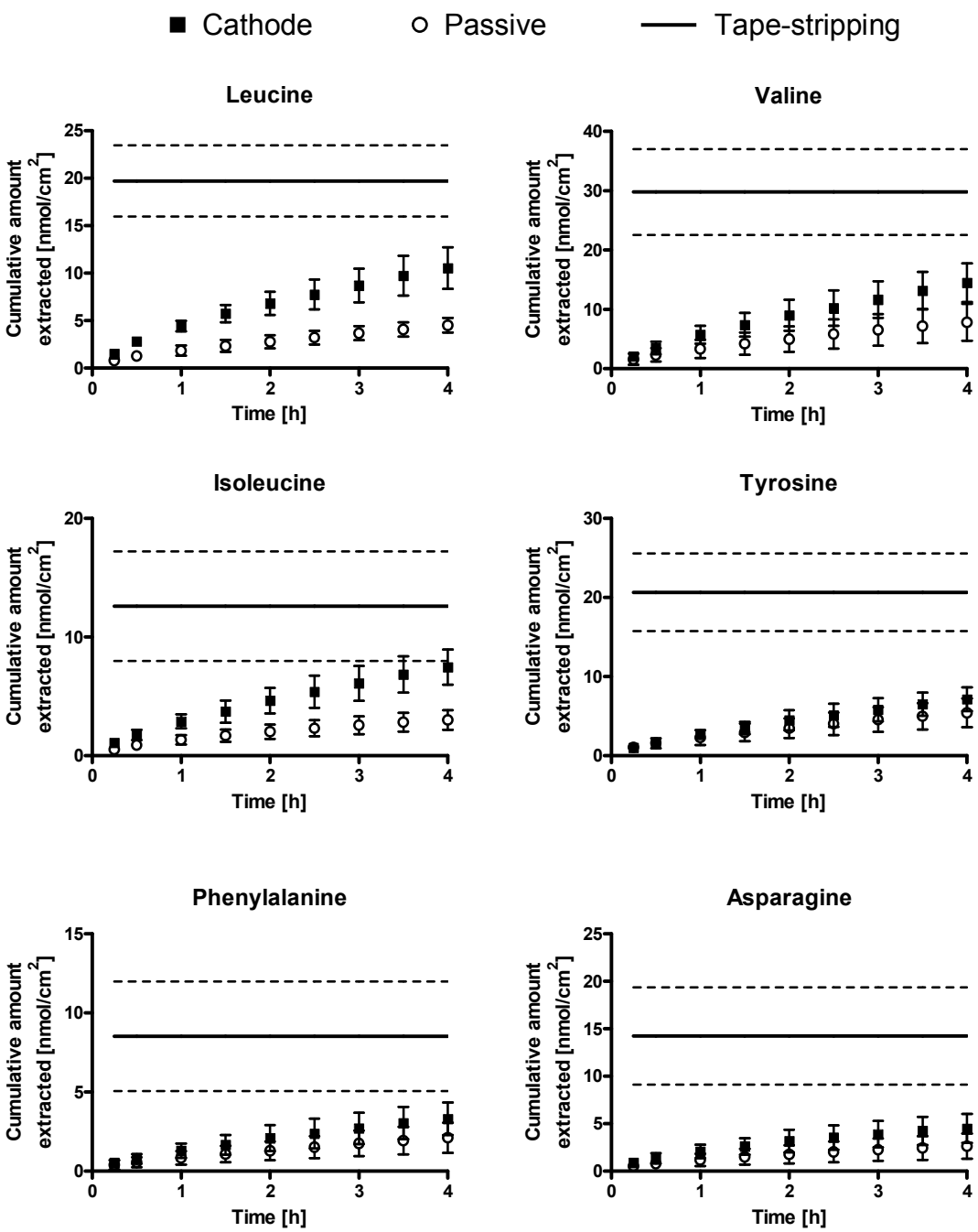

5. Cumulative amount of 13 amino acids and glucose extracted in the four subjects (mean ± SD) at the cathode and by passive diffusion as a function of time. The quantities in the SC determined by tape-stripping are shown for comparison. (continued)